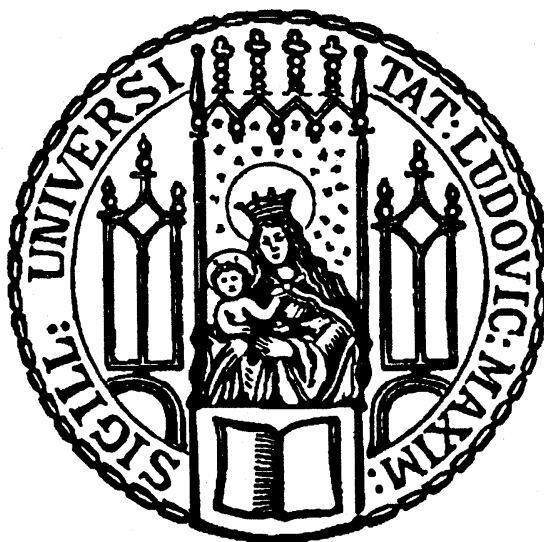


Dissertation

zur Erlangung des Doktorgrades
der Fakultät für Chemie und Pharmazie der
Ludwig-Maximilians-Universität München

**Crystalline Monoclonal Antibodies:
Development of stable crystals for drying and
sustained release formulations**



Christian Hildebrandt

aus Berlin, Deutschland

2014

Erklärung

Diese Dissertation wurde im Sinne von § 7 der Promotionsordnung vom
28. November 2011 von Herrn Prof. Dr. Gerhard Winter betreut.

Eidesstattliche Versicherung

Diese Dissertation wurde eigenständig und ohne unerlaubte Hilfe erarbeitet.

München, 21.09.2014

(Christian Hildebrandt)

Dissertation eingereicht am: 30.05.2014
1. Gutachter: Prof. Dr. Gerhard Winter
2. Gutachter: Prof. Dr. Wolfgang Frieß
Mündliche Prüfung am: 10.07.2014

Terms used in this publication might be protected by copyright law even if not marked as such.

Für Laura
in Liebe und Dankbarkeit

Acknowledgments

The present thesis was prepared between June 2010 and December 2013 at the Department of Pharmacy, Pharmaceutical Technology and Biopharmaceutics at the Ludwig-Maximilians-University (LMU) in Munich under the supervision of Prof. Dr. Gerhard Winter.

First, I want to express my deepest gratitude to my supervisor Prof. Dr. Gerhard Winter for offering me the possibility to become a member of his research group and for supervising the present thesis. In particular I would like to thank him for his dedicated scientific guidance and outstanding, trustful and professional advice throughout this project. I want to highlight his ambition to support my scientific as well as my personal development.

The present thesis was supervised in collaboration with Dr. Rainer Saedler from AbbVie Deutschland GmbH & Co. KG. I also want to express my deepest gratitude to Rainer for his excellent guidance and support from the first day of our project. I profited in many ways from his outstanding scientific expertise. I will really miss the intensive time we spent together in scientific and personal manner.

I further want to thank Dr. Hans-Jürgen Krause, Dr. Carsten Weber and Dr. Markus Tschöepe from AbbVie Deutschland GmbH & Co. KG for her support and valuable scientific discussion during the route of the project. Special thanks go to Dr. Jessica Wohlgemuth, from AbbVie Deutschland GmbH & Co. KG, for her indispensable support and expertise.

I want to thank Prof. Dr. Wolfgang Frieß for interesting discussions as well as the scientific input over the last years and for his effort in organizing scientific and social events together with Prof. Gerhard Winter. Thereby, an excellent personal and working atmosphere was created. Events such as the excursion to Basel, the hiking and skiing trips were great!

My tremendous gratitude is expressed to all my companions from the research groups from Prof. Winter and Prof. Frieß. I very much enjoyed the scientific and personal support from each of you: Dr. Gerhard Simon, Dr. Julia Enget, Dr. Madlen Hubert, Dr. Ahmed Besheer, Dr. Sarah Küchler, Dr. Alexandra Mössland, Alice Hirschmann, Imke

Leitner, Dr. Raimund Geidobler, Dr. Angelika Freitag, Dr. Yibin Deng, Dr. Sarah Claus, Dr. Julia Kasper, Dr. Eva Maria Ruberg, Dr. Sarah Zölls, Dr. Gerhard Sax, Sebastian Hertel, Kerstin Höger, Ayla Tekbudak, Elsa Ettl, Madeleine Witting, Kay Strüver, Cihad Anamur, Laura Engelke, Ilona Konrad, Moritz Vollrath, Angela Schoch, Randy Wanner, Elisa Agostini, Matthias Lucke, Philipp Matthias, Tim Menzen, Ellen Köpf, Verena Saller, Christoph Korpus, Stefanie Funke and Kerstin Hoffman.

In particular, special thanks are given to the “HESchen Stall”, namely Dr. Matthäus Noga, Dr. Erlisabeth Härtel and Christian Neuhofer for the great time and scientific discussion we had together.

I want to thank Lea Joos for always being there in all circumstances and just for becoming a friend.

My deepest gratitude goes to my “L-Lab”: Marie-Paule Even, Robert Liebner and Roman Mathäs. I will never forget the great and funny time we spent together. I will always remember the trustful atmosphere and the “adventures” we lived through together.

Special thanks go to Dr. Markus Hofer for his indispensable scientific and personal advice. I really met a friend in you.

Many thanks are expressed to the master students Benjamin Werner who become a valuable companion afterwards and Bistra Nikolaeva Rainova. You really did an excellent job.

My deepest gratitude goes to my parents and my brothers for all the support they gave me over all the years and to Laura for her love and always being on my side.

Table of contents

Crystalline Monoclonal Antibodies: Development of stable crystals for drying and sustained release formulations.....	I
Acknowledgments	V
Table of contents	VII
List of Abbreviations	XII
Chapter 1	1
1 Introduction.....	2
1.1 General Introduction	2
1.2 Macromolecular crystallization.....	6
1.2.1 The mechanism of protein crystallization	7
1.2.1.1 Growth rate	7
1.2.1.2 Crystallization agents.....	9
1.2.2 Protein crystal properties	11
1.3 Crystallization of mAb1 and mAb2: The achievements of a preliminary study on mAb crystallization and process up-scaling.....	13
1.3.1 mAb1 lead crystallization conditions (preliminary study)	14
1.3.2 mAb2 lead crystallization conditions (preliminary study)	14
1.3.3 Stability of antibody crystals (preliminary study).....	15
1.3.3.1 mAb1 stability during crystallization and storage (preliminary study).....	16
1.3.3.2 mAb2 stability during crystallization and storage (preliminary study).....	16
1.4 Objectives of the thesis.....	17
1.5 References	19
Chapter 2	27
2 Case study: From protein bulk crystallization towards dry protein products	28
2.1 Abstract	28
2.2 Introduction	29
2.3 Materials and Methods	31
2.3.1 Materials	31
2.3.2 Methods.....	31
2.3.2.1 Crystallization of lysozyme	31
2.3.3 Drying of lysozyme crystals	31
2.3.3.1 Inert gas drying	31
2.3.3.2 Freeze Drying.....	32
2.3.3.3 Test for mechanical properties.....	32
2.3.3.4 Transferability and handling properties.....	32
2.3.3.5 Solvent screening.....	33
2.3.3.6 Protein yield determination	33
2.3.3.7 Microscopic examination	33
2.3.3.8 Determination of residual moisture.....	33
2.3.3.9 Size exclusion high performance liquid chromatography (SE-HPLC).....	34
2.3.3.10 Nephelometry.....	34
2.3.3.11 Gas Chromatography (GC).....	34
2.3.3.12 Particle counting	35
2.3.3.13 Determination of lysozyme activity.....	35
2.4 Results	36
2.4.1 Polymorph-screening	36
2.4.2 Crystal properties dependent on the polymorphic form.....	37

2.4.2.1	<i>Handling and mechanical properties</i>	37
2.4.2.2	<i>Solubility and stability during organic liquid exposure</i>	38
2.4.3	<i>Hot-Air drying</i>	39
2.4.4	<i>Comparative study assessing the suitability of freeze drying to obtain dry and stable protein crystal products</i>	40
2.4.5	<i>Assessment of crystal and protein integrity during the hot-air drying procedure</i>	41
2.5	<i>Discussion</i>	44
2.6	<i>Conclusion</i>	47
2.7	<i>References</i>	48
Chapter 3		51
3	<i>Drying of mAb crystals</i>	52
3.1	<i>Introduction</i>	52
3.1.1	<i>Freeze drying (lyophilization)</i>	52
3.1.2	<i>Vacuum drying</i>	53
3.1.3	<i>Spray drying</i>	53
3.1.4	<i>Spray-freeze drying</i>	54
3.1.5	<i>Alternative drying methods suitable for protein crystals</i>	54
3.1.6	<i>Stabilizing agents</i>	55
3.1.7	<i>Cryoprotectants</i>	55
3.1.8	<i>Lyoprotectants</i>	55
3.1.9	<i>Chances of dry protein crystal material and challenges in producing it</i>	55
3.2	<i>Materials and Methods</i>	58
3.2.1	<i>Materials</i>	58
3.2.2	<i>Methods</i>	58
3.2.2.1	<i>Crystallization of mAb1</i>	58
3.2.2.2	<i>Crystallization of mAb2</i>	58
3.2.2.3	<i>Solvent screening</i>	59
3.2.2.4	<i>Drying of protein crystals</i>	59
3.2.2.5	<i>Assessment of crystal and protein integrity</i>	60
3.3	<i>Results</i>	62
3.3.1	<i>mAb1 and mAb2 crystal properties</i>	62
3.3.2	<i>Reproducibility of the vacuum drying approach for mAb1 crystals</i>	63
3.3.3	<i>Solvent screening for mAb1 and mAb2 crystals</i>	65
3.3.4	<i>Hot-Air drying of mAb1 crystals</i>	69
3.3.5	<i>Freeze drying</i>	69
3.4	<i>Discussion</i>	72
3.5	<i>Conclusion</i>	74
3.6	<i>References</i>	75
Chapter 4		79
4	<i>Different strategies to obtain mAb crystal polymorphs with higher stability</i> .	80
4.1	<i>Introduction</i>	80
4.2	<i>Materials and Methods</i>	82
4.2.1	<i>Materials</i>	82
4.2.2	<i>Methods</i>	82
4.2.2.1	<i>Crystallization of mAb1</i>	82
4.2.2.2	<i>Crystallization of mAb2</i>	82
4.2.2.3	<i>Alteration of crystallization conditions</i>	82
4.2.2.4	<i>High hydrostatic pressure</i>	83
4.2.2.5	<i>Size exclusion high performance liquid chromatography (SE-HPLC)</i>	85
4.2.2.6	<i>Microscopic examination</i>	85
4.2.2.7	<i>Nephelometry</i>	85

4.2.2.8	Total subvisible particle count	86
4.3	Results	87
4.3.1	Reproducibility of mAb1 and mAb2 crystallization lead conditions	87
4.3.2	Alteration of mAb1 and mAb2 crystal morphology by variations in the crystallization lead conditions	88
4.3.2.1	Agitation and alternative crystallization temperatures	88
4.3.2.2	Additives, pH shifts and PEG of higher molecular weight	91
4.3.3	High hydrostatic pressure	94
4.3.3.1	mAb1 and mAb2 crystal stability at elevated pressure levels	95
4.3.3.2	The effect of high hydrostatic pressure on the mAb crystal morphology	96
4.3.3.3	The effect of high hydrostatic pressure on mAb crystallization and the protein integrity	99
4.3.3.4	Reduction of the aggregate contents of mAb crystal suspensions by application of elevated pressure levels	102
4.3.3.5	The impact of high hydrostatic pressure on the protein integrity of differently concentrated mAb solutions	105
4.3.3.6	Dissociation of mAb aggregates through high pressure	108
4.4	Discussion	113
4.5	Conclusion	117
4.6	References	118
Chapter 5	123
5	The mechanisms behind the aggregate formation in mAb1 and mAb2 crystal suspensions	124
5.1	Introduction	124
5.1.1	Chemical instability	124
5.1.1.1	Deamidation	124
5.1.1.2	Oxidation	124
5.1.1.3	Cross-linking	125
5.1.1.4	Fragmentation	125
5.1.2	Physical instability	125
5.1.2.1	Denaturation	125
5.1.2.2	Aggregation	126
5.1.3	Strategies to maintain protein stability	127
5.1.3.1	Formulation pH	127
5.1.3.2	Surfactants	128
5.1.3.3	Antioxidants	128
5.1.3.4	Amino acids and Polyols	128
5.1.3.5	Salts	128
5.1.4	Protein stability in the crystalline state	129
5.2	Materials and Methods	131
5.2.1	Materials	131
5.2.2	Methods	131
5.2.2.1	Crystallization of mAb1	131
5.2.2.2	Crystallization of mAb2	131
5.2.2.3	mAb1 labelling	132
5.2.2.4	Supernatant exchange (mAb1)	132
5.2.2.5	Assessment of crystal and protein integrity	132
5.2.2.6	Ion exchange chromatography (IEC)	133
5.2.2.7	Confocal laser scanning microscopy (CLSM)	133
5.2.2.8	Flow cytometry (FACS)	133
5.3	Results	135
5.3.1	The initial state of mAb1 and mAb2 crystal stability	135
5.3.2	Aggregate characterization	136
5.3.2.1	SDS-PAGE	136

5.3.2.2	<i>Isoelectric focusing (IEF)</i>	137
5.3.3	<i>Investigation of critical crystallization formulation parameters</i>	139
5.3.3.1	<i>mAb1: Investigation of the instability pathway</i>	140
5.3.3.2	<i>mAb2: Investigation of the aggregate formation</i>	152
5.4	<i>Discussion</i>	155
5.5	<i>Conclusion</i>	160
5.6	<i>References</i>	161
Chapter 6		165
6	Case study: Sustained release formulations containing mAb crystals	166
6.1	<i>Introduction</i>	166
6.2	<i>Materials and Methods</i>	170
6.2.1	<i>Materials</i>	170
6.2.2	<i>Methods</i>	170
6.2.2.1	<i>Crystallization of mAb1</i>	170
6.2.2.2	<i>Crystallization of mAb2</i>	171
6.2.2.3	<i>Crystallization of lysozyme</i>	171
6.2.2.4	<i>Drying of protein crystals</i>	171
6.2.2.5	<i>Preliminary screening approaches</i>	172
6.2.2.6	<i>Preparation of in situ forming depot devices (mAb1, mAb2)</i>	173
6.2.2.7	<i>Depot characterization</i>	174
6.2.2.8	<i>Preparation of lipid implants (mAb1)</i>	175
6.2.2.9	<i>Release study for SAIB based in situ precipitating lysozyme depots</i>	175
6.3	<i>Results</i>	176
6.3.1	<i>In situ precipitating depot formulations for mAb1 and mAb2 crystals</i>	176
6.3.1.1	<i>Preliminary screening approaches</i>	176
6.3.1.2	<i>In vitro drug release</i>	181
6.3.1.3	<i>Influence of degradation on pH</i>	187
6.3.1.4	<i>Depot characteristics</i>	190
6.3.2	<i>Lipid implants</i>	194
6.3.3	<i>SAIB depots containing dried lysozyme crystals</i>	196
6.4	<i>Discussion</i>	198
6.5	<i>Conclusion</i>	203
6.6	<i>References</i>	204
Chapter 7		209
7	Quality control of protein crystal suspensions using micro flow imaging and flow cytometry	210
7.1	<i>Abstract</i>	210
7.2	<i>Introduction</i>	211
7.3	<i>Materials and Methods</i>	212
7.3.1	<i>Materials</i>	212
7.3.2	<i>Methods</i>	212
7.3.2.1	<i>Amorphous precipitation of insulin</i>	212
7.3.2.2	<i>Light microscopy</i>	212
7.3.2.3	<i>Scanning electron microscopy (SEM)</i>	212
7.3.2.4	<i>Particle counting (LO)</i>	212
7.3.2.5	<i>Micro flow Imaging (MFI)</i>	213
7.3.2.6	<i>Flow cytometry (FACS)</i>	213
7.4	<i>Results</i>	214
7.5	<i>Discussion</i>	219

7.6	<i>Conclusion</i>	221
7.7	<i>References</i>	222
Chapter 8	225
8	Final summary of the thesis	226

List of Abbreviations

CLSM	Confocal laser scanning microscopy
DTT	Dithiothreitol
EDTA	Ethylenediaminetetraacetic
EMA	European Medicines Agency
EtAc	Ethyl acetate
EtOH	Ethanol
FSC	forward scatter detector
IEC	Ion exchange chromatography
IEF	Isoelectric focusing
FACS	Fluorescence-activated cell sorting
FDA	US Food and Drug Administration
FNU	Formazine Nephelometric Units
IgG	Immunoglobulin G
LC-MS	Liquid chromatography–mass spectrometry
LO	Light obscuration – particle counting
mAb	Monoclonal antibody
PBS	Phosphate buffer saline
PEG	Poly(ethylene glycol)
Ph Eur	Pharmacopoea Europaea
PLGA	Poly(D, L- lactide-co-glycolide)
RT	Ambient temperature
SAIB	Sucrose acetate isobutyrate
SDS-PAGE	Sodium dodecyl sulphate polyacrylamide gel electrophoresis

SE-HPLC	Size exclusion high performance liquid chromatography
SSC	Side scatter detector
TAP	Total acidic protein
USP	United States Pharmacopeia
WHO	World Health Organization

Chapter 1

1 Introduction

1.1 General Introduction

More than three decades ago the field of therapeutic drugs was extended by a new class of pharmaceuticals: therapeutic proteins. Proteins are defined as macromolecules which consist of at least 100 proteinogenic amino acids ^{1,2}. Nowadays, this class is represented by approximately 200 marketed products which are mainly therapeutic proteins besides a few diagnostic proteins and vaccines which differ in their pharmacologic activity ³. Biopharmaceutics can be grouped into drugs which a) can be used to replace deficient or morbid natural proteins, b) can be used to augment existing pathways, c) allow to enter new pathways of drug action which cannot be induced by small molecule drugs, d) offer extremely high specificity and affinity to molecules or organisms, or e) deliver radionuclides, cytotoxics or effectors ⁴. Other classifications include enzymes, hormones, engineered scaffolds, growth factors, interferons, interleukins and antibody-based drugs ^{1-3,5}. Within these groups, antibody therapeutics represent the fastest growing segment with around 30 drugs already marketed either in the US or EU, and further 30 molecules in late stage clinical trials ^{6,7}. This success dates back to 1950s when the development of monoclonal antibodies started following the discovery that DNA encodes for proteins ⁸. However, it took around 25 years until Kohler and Milstein developed an efficient procedure to prepare monoclonal antibodies ⁹. Another 15 years later, Winter and Milstone discovered a method to clone antibody genes which then allowed to obtain recombinant versions of any antibody from diverse cell lines. Additionally, they were able to optimize their product antibodies according to their needs ¹⁰. Further advancement in pharmaceutical and biopharmaceutical technology, molecular biology, protein engineering, life sciences and genomics allowed to establish antibodies as successful drugs with a remarkable value in the pharmaceutical market ^{6,11,12}.

In 2010, the market value for pharmaceuticals was already about 597 billion USD with around 75% of this sum represented by small therapeutic drug molecules. Recombinant proteins without antibodies counted for 10%, while antibodies alone had a total market value of about 7% ⁶. This commercial value makes antibodies an attractive field for research and development for biotec and pharmaceutical companies.

Antibodies are characterized by their ability to bind and eliminate antigens with extremely high specificity. It is envisioned to develop an infinite number of different tailor-made antibodies against any target ¹³.

In contrast to small therapeutic drug molecules, antibodies are characterized by a highly ordered three-dimensional structure and a large amount of functional groups. Additionally, proteins are naturally unstable, and this instability includes not only chemical degradation such as deamination, oxidation and others, but also physical denaturation ^{11,14}. The latter one refers to alterations of the antibody molecule, such as partial or complete unfolding of its native confirmation, even without chemical mutations which most often results in a loss of biological activity ¹⁵. In addition, unfolded species tend to interact with each other by forming protein aggregates of different sizes ¹⁶⁻¹⁸. Such antibody aggregates are considered as a serious risk to induce immunogenicity ¹⁹⁻²². Hence, scientists are faced with a number of challenges when it comes to formulation of antibodies, which usually result in high development costs ^{11,16,23-26}. All these concerns should be addressed by an appropriate quality control of the final product including the quality itself as well as the monitoring of product stability during storage and release ²¹.

In addition to these stability issues, routes of administration are limited for antibodies due to enzymatic degradation in the gastrointestinal tract. Therefore, most proteins are usually administered by the intravenous or subcutaneous route ^{27,28}. Alternative routes of administration such as oral, nasal or transdermal applications are currently under development but remain hardly feasible ^{27,29-33}. Furthermore, certain clinical needs may also limit the choice of route how the protein can be applied. Especially administration of antibody formulations remains challenging due to large quantities (often > 100 mg up to 1 g per dose) required for therapeutic use ³⁴. Stable antibody solutions rarely exceed concentrations of 50 mg/mL and are therefore applied by infusion ³⁴⁻³⁶. This way of administration is one of the most unpopular methods for the patient since a clinical setting is needed, costs are high and patient compliance is rather poor ^{35,37}. On this account, development of subcutaneous injections is of high interest ³⁴. However, volumes that can be administered subcutaneously are rather small (< 1.5 mL), therefore highly concentrated antibody formulations are needed which in turn increase the risk of protein aggregation and high viscosities ^{17,37-39}. Typical approaches nowadays are to exceed the formulation volume which makes infusion inevitable or to freeze dry the products to reach long term stability ^{37,40}. From an economical view, the latter strategy represents a

very cost and time intensive procedure. During drying, the product faces several stress factors including freezing and drying which can induce protein aggregation⁴¹⁻⁴³. An innovative idea to overcome the aforementioned obstacles is the development of protein drug suspensions, particularly crystalline suspensions⁴⁴.

Although macromolecular crystallization has already been presented in the 1920s and crystallization of monoclonal antibodies (mAb) has been subject of significant interest during the last 30 years, only one product - insulin crystals - has entered the market^{35,45,46}.

Nevertheless, crystal formulations potentially offer advantages already known from crystals of small therapeutic drug molecules:

- The crystalline state possesses a lower internal energy state and lower chemical reactivity. Consequently, the stability of protein crystals might be superior compared to amorphous or liquid formulations^{45,47-49}.
- Protein crystals might exhibit a superior protection against proteolytic enzymes compared to its amorphous or liquid counterparts⁴⁶.
- Protein crystals are per definition the most highly concentrated protein formulation possible. This enables the delivery of high doses without excessive increase in viscosity^{46,47}.
- As already shown for insulin formulations, protein crystals allow for a carrier free sustained release which might be dependent on the crystal morphology, the crystal size, the presence of excipient without creating new biological entities^{35,46,47,49}.
- Crystallization represents a common purification step in active pharmaceutical ingredient (API) manufacturing and therefore economization of the manufacturing procedure would be possible^{35,47}.

In case of antibody formulations, crystals could be administered by subcutaneous injection in form of a suspension. As mentioned before, antibodies often have to be administered in high concentrations which often leads to stability issues and high viscosity formulations^{17,37-39}. Here, a crystal suspension may provide a comfortable solution. Yang

et al. have shown a low viscosity over broad concentration range for crystalline infliximab formulations (Fig. 1-1)³⁵.

The Einstein equation explains this phenomenon by:

$$\frac{\eta}{\eta_0} = 1 + 2.5\phi$$

with (η) being the formulation viscosity, (η_0) the viscosity of the formulation vehicle and (ϕ) the volume fraction of the suspended matter⁴⁶. It illustrates that the viscosity of a suspension is mainly dependent on the viscosity of the formulation vehicle. However, Basu et al. already demonstrated that this low viscosity is not infinite. For crystalline amylase, an increase in viscosity could not be explained by the Einstein's equation beyond concentrations of 200 mg/mL⁴⁶.

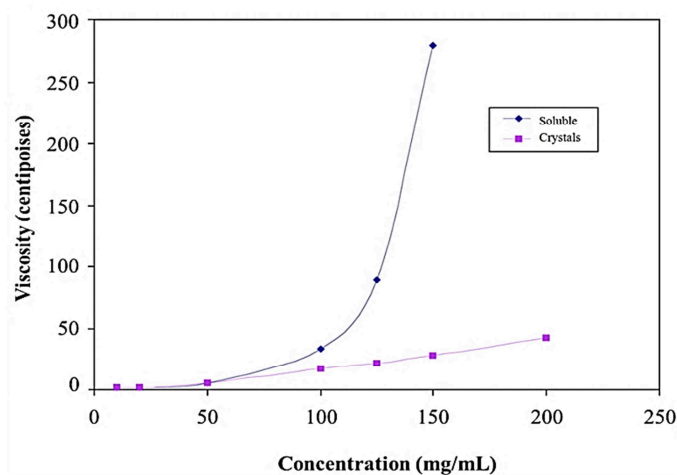


Figure 1-1 Comparison of viscosity for crystalline (pink boxes) and liquid (blue rhombuses) antibody formulations. Reproduced from Yang et al.⁴⁴.

Nevertheless, crystalline formulations possess certain drawbacks and requirements. For example, a sufficient resuspendability should be given, settling of the crystals needs to be controlled and particle size distribution is reported to be best when it is as small as possible⁴⁶. Notably, long term stability has to be considered case by case as it is not generally guaranteed for all protein crystal suspensions. Pikal et al. already stated a superior stability for an amorphous insulin formulation compared to its crystalline counterpart^{46,50}.

1.2 Macromolecular crystallization

The aforementioned fact that only one crystalline biopharmaceutical so far reached the market is quite surprising. Crystallographers possess a tremendous experience in protein crystallization for X-ray structure determination⁵¹. Until 2012, over 70.000 molecules were analyzed by this approach⁵². Adversely to therapeutic formulations, crystals needed for X-ray studies should be as large as possible (ideally > 500 µm) whereas the crystal yield, the crystallization time and the crystal size distribution remain rather unimportant (Tab. 1-1)^{53,54}. To obtain the desired large crystal sizes, crystallographers usually apply vapour diffusion techniques which provide only small amounts of crystals⁵⁵. Upscaling of such a technique can hardly be achieved and thus only few proteins have been crystallized successfully under large scale conditions^{35,46}. Furthermore, many crystallization conditions used for X-ray analysis are rarely applicable for therapeutic protein formulations since the employed excipients were not biocompatible⁴⁵. Consequently, the crystallization approaches in literature vary greatly and reproducibility of conditions is not always given^{35,46,53}. In summary, crystallization experiences gained from x-ray structure determination are not necessarily transferable to crystallization for therapeutic applications.

Table 1-1 Comparison of required crystals for x-ray diffraction and large scale crystallization. Reproduced after Shenoy et al.⁵³.

Parameter	X-ray crystallographic studies	Large scale crystallization
Crystal size	> 500 µm	0.1 - 100 µm
Crystal quality	Very important	Less important
Growth rate	Not important	Important
Yield	Not important	Very important
Precipitate	Usually present	Rarely present

Protein crystallization is a rather complicated approach compared to crystallization of small therapeutic drug molecules^{54,56,57}. In addition to the different molecular weight, the presence of surface oligosaccharides and a high degree of segmental flexibility often hinder the production of crystals from reproducible quality^{35,54}. Thus, with increasing homogeneity and purity of the proteinaceous material the probability of crystallization increases⁵⁴.

1.2.1 The mechanism of protein crystallization

1.2.1.1 Growth rate

Crystallization can be defined as “the transition of a solvated substance into the solid state which possesses a specific regular lattice structure”². This lattice is characterized by a three-dimensional long-range order whereas amorphous precipitates exhibit a short-range order over a few molecular dimensions^{48,53}.

The most substantial requirement in protein crystallization is the creation of a high level of supersaturation⁵⁴. Supersaturation is a non-equilibrium condition with some quantity of abundant protein which can be achieved by several approaches⁵⁴:

Table 1-2 Approaches for creating supersaturation. Reproduced after McPherson 2004⁵⁴.

Approaches for creating supersaturation
<ul style="list-style-type: none">• pH shift• Addition of ligands to change solubility• Removal of solvent (evaporation)• Addition of cross binding agents• Addition of salts to trigger “salting in” or “salting out”• Addition of polymers to trigger volume exclusion (polyethylene glycols)

The supersaturation is compensated energetically by amorphous or crystalline protein precipitation until reaching the equilibrium⁵⁴.

However, the creation of supersaturation will not cause crystallization compulsorily. An optimal level of supersaturation has rather to be reached (Fig. 1-2). In case of higher protein concentrations and/or higher precipitants concentrations the system is directed into the precipitation zone where amorphous particles are formed instead of crystals^{45,54}. Under optimal conditions, the labile zone (or crystallization zone) is reached. Nuclei start to form and the concentration of the protein in the solute drops⁵⁵. Following, the system crosses the metastable zone where crystal grow without any further formation of nuclei^{45,55}. By this, further reduction of the protein concentration in the solute, the solubility curve is reached and the system achieves again equilibrium⁵⁴.

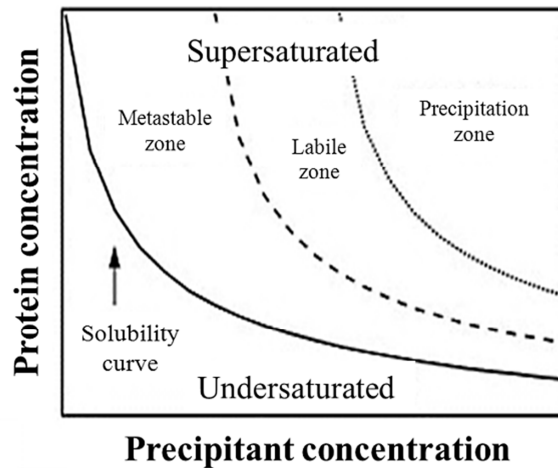


Figure 1-2 Quantitative phase diagram of sitting drop vapour diffusion crystallization of lysozyme (20 μ l scale). Black boxes represent clear drops, crosses stand for crystallization and black circles represent formation of precipitates. Reproduced from Hekmat et al ⁵⁸.

The crystallization process can kinetically be divided into two different steps: nucleation and growth. Herein, nucleation represents the most difficult step in theory and practice ⁵⁴. This phenomenon describes a first order phase transition over intermediates from an entirely disordered into an ordered state, called critical nuclei ^{54,55}. Formation of such nuclei occurs at high supersaturation whereas crystal growth is favored in the lower metastable region ⁵⁵. If the level of supersaturation is chosen too high, the crystal growth might be incomplete which results in formation of defects within the crystal structure ⁴⁵. Hence, the level of supersaturation alone is not responsible for the growth rate ^{56,59}.

One essential requirement for an appropriate protein incorporation into a well-ordered crystal is that the molecules show proper orientation and position to their neighbor molecules ⁵⁶. The molecules during their encounter collide with each other due to their rotationally and translationally diffusion ⁶⁰. By coincidence, one of these collisions results in an appropriate contact and thus incorporation of the molecules into the crystal lattice ⁵⁶. This process might be widely steered by electrostatic effects ^{56,61,62}. Surface studies beared the conclusion that protein crystal growth shows similarities to those of small molecules ^{45,56}. This concept was augmented by the observation of soluble protein aggregate formation which function as building units. The formation of such building

units represents the first step in the crystallization and crystal growth process ^{56,63}. However, the complete mechanism of crystallization is still not fully understood ^{54,58}.

1.2.1.2 Crystallization agents

1.2.1.2.1 Long chain polymers

The most prominent class of polymers used for macromolecular precipitation is represented by polyethylene glycols (PEG) which are part of a vast amount of screening kits ^{54,64-67}. PEG is a polymerization product of ethylene oxide units resulting in the following structure ⁶⁸:



The most useful PEGs for protein precipitation possess a molecular weight in the range of 2000 to 8000 ⁵⁴. PEG shows different properties dependent on its molecular weight ⁶⁹. Larger polymers are more effective in reducing protein solubility ⁷⁰.

Their feature to precipitate or crystallize proteins is ascribed to a preferential exclusion effect in that the polymer chains occupy certain space within the solvent ^{65,71}. Hence, the protein is sterically excluded from the solution and is concentrated until the solubility limit is reached and precipitation starts ⁵⁴. This mechanism explains why these polymers are not part of the crystal lattice in contrast to salt ions used also as precipitants ^{54,70}. One fundamental benefit of PEG is the preservation of the native conformation of the proteins during crystallization which was shown by structure determination of many proteins using PEG as precipitant ⁵⁴.

1.2.1.2.2 Salts

The two main mechanisms induced by the addition of salts are: “salting out” and “salting in” ⁵⁴.

“Salting in” describes the effect of increasing protein solubility in low ionic strength solutions by increasing the salt concentration. At higher salt concentrations a reverse effect occurs: the “salting out” effect. “Salting out” describes a competition of salt ions,

mainly anions, and protein molecules for hydrogen bonds with surrounding water molecules in solution. Such bonds are essential for maintenance of solubility^{54,72}. If an excess of salt ions hinders the formation of sufficient protein hydrogen bonds to saturate electrostatic requirements, the protein molecules will start to form hydrophobic intermolecular interaction resulting in crystalline or amorphous precipitates⁵⁴. The effectiveness of the anion is dependent on its ionic strength (I) which is defined as:

$$I/2 = \sum mv^2$$

with (m) being molarity and (v) being the valence. It appears that polyvalent ions are more effective than monovalent ions. This fact is displayed by the Hofmeister series which classically sorts anions to their ability to precipitate proteins⁷³⁻⁷⁶. Differences in the effectiveness of ions from the same valence are explained by their different ability to destroy or form hydrogen bonds. Herein, ions are divided into “kosmotropic” ions which are strongly hydrated but possess a strong ability for “salting out”, whereas weakly hydrated and thus inferior precipitants are classed as “chaotropic” ions^{77,78}.

Hofmeister series:

anions: Carbonate > Sulphate > Dihydrogen phosphate > Acetate > Chloride > Iodide

cations: Ammonium > Potassium > Sodium > Lithium > Magnesium > Calcium

The mechanism behind protein precipitation by ions of the Hofmeister series is not entirely understood. It appears that not changes in the general water structure were of importance but also specific interactions between ions and proteins which might result in protein destabilization. Especially salts with strong “salting in” effects (e.g. I⁻, SCN⁻) might foster protein denaturation by preferably interacting with the unfolded state⁷⁹.

However, the influence of ions on protein solubility can be much more complicated. Besides the aforementioned “salting out” and “salting in” mechanisms, specific non-

destructive protein-ion interactions may also play an important role. In this context, the crystalline insulin zinc complex represents an excellent example ⁵⁴.

1.2.1.2.3 Organic solvents

Crystallization of proteins by organic solvents is ascribed to multiple mechanisms. Organic solvents can function as “anti-solvent” similar to kosmotropic salts or can decrease the dielectric constant of an aqueous medium. The latter effect enhances intermolecular interactions and thus fosters protein precipitation. One representative of this class which is often used is ethyl alcohol. This compound tends to solubilize hydrophobic residues which can end in unfolding and denaturation, therefore usage at lower temperatures and low ionic strengths is recommended ^{54,70,80}.

1.2.2 Protein crystal properties

A transfer of the advantageous attributes of small molecule crystals to protein crystals would be desirable. However, crystals of proteins show differences in many aspects. They represent rather an ordered gel with extensive interstitial spaces than a solid state with highly ordered structures ⁵⁴. Furthermore, the crystals contain up to 90 % bound water which is needed to maintain the protein’s integrity and its native structure which commonly remains unchanged ^{54,81,82}.

For crystals of small molecules, a significant fraction of functional groups is involved in the crystal lattice interactions ⁵⁴. In contrast, the crystalline macromolecules show considerably less bonds and interactions to adjacent molecules in proportion to their molecular size ^{45,54}. Most of these interactions are of intra-molecular and notably not intermolecular nature which weakens the crystalline structure ⁵⁶. Consequently, the reduction in free order and molecule mobility is small within the crystal lattice ^{50,56}. With that in mind it is obvious that crystals of proteins show different attributes in e.g. stabilization of the molecules. They show only a minor stability advantage compared to amorphous counterparts which is confirmed by small internal energy differences ⁵⁴. Besides the quoted differences, a multitude of others exist as listed in Table 1-3:

Table 1-3 Comparison of crystalline small molecules (e.g. salt) and macromolecules (e.g. proteins). Reproduced from McPherson and Jen & Merkle ^{45,54}.

Small molecule crystals	Protein crystals
<ul style="list-style-type: none"> • Firm lattice forces • Relatively highly ordered structure • Physically hard and brittle • Easy to manipulate • Exposition to air is possible • Strong optical properties • Intense x-ray diffraction 	<ul style="list-style-type: none"> • More limited in size • Very soft and easily crushable • Dehydration can result in disintegration • Weak optical properties • Weak x-ray diffraction

Analysis of protein crystals is difficult as they show weak x-ray diffraction properties which is caused by their low internal order ⁵⁴. The resolution is limited by permeating liquid channels and solvent filled cavities. These characteristics and the isotropic globular character of the protein units also cause poor birefringence of protein crystals under polarized light in comparison to small molecule crystals ⁴⁵.

Another specific property of protein crystals is polymorphism which is the co-existence of different crystalline lattice structures with the same chemical composition ^{2,54}. These diverse habits and unit cells even may develop from conditions that do not differ considering most of the standard parameters ⁵⁴. Control of the crystal shape may be achieved by variation of the buffer or the precipitant ^{83,84}. For small molecules this phenomenon is well documented. Polymorphs can show different properties regarding e.g. solubility, stability, bioavailability, and melting points ⁸³.

1.3 Crystallization of mAb1 and mAb2: The achievements of a preliminary study on mAb crystallization and process up-scaling

As abovementioned, mAb crystal formulations potentially offer superior features compared to their liquid counterparts in terms of stability and reduced viscosity enabling subcutaneous injection ⁴⁴. However, antibody crystallization must not necessarily succeed under biocompatible conditions. In general, adverse conditions are required to actually achieve protein crystallization. A precise prediction of condition parameters necessary to induce crystallization is extremely complex and hardly achievable in the majority of cases. Identification of suitable crystallization formulations usually ends in extensive screening approaches ^{45,85}.

Nonetheless, the opportunity to generate stable mAb crystal formulations with superior properties would compensate the effort and the high risk of failure.

Therefore, a project (preliminary study - PhD thesis Stefan Gottschalk at LMU Munich) was conducted with the purpose to find suitable and biocompatible crystallization conditions for two full length IgG₁ antibodies (mAb1 and mAb2) and one antibody fragment. The aim of the project was to administer the crystal formulations subcutaneously or to use them as sustained release formulation platform. Large scale crystallization conditions could successfully be determined in the case of the antibodies and the antibody fragment, however, resulting in low protein crystal stability against ambient or higher temperatures. Furthermore, the effect of vacuum drying on the stability of mAb1 crystals and embedding the crystals in sustained release formulations was studied.

The study started with microscale crystallization in vapor diffusion experiments to identify suitable and biocompatible crystallization conditions. Therefore, only physiological acceptable crystallization conditions were examined. Subsequently, lead conditions were validated and optimized in grid screens by varying parameters against each other. Finally, the most promising crystallization formulations were transferred to the batch crystallization method. For each antibody, lead conditions were defined as described in this section ⁸⁶. The lead crystallization conditions only from mAb1 and mAb2 will be presented in the following as only these two molecules were subject of the present study.

1.3.1 mAb1 lead crystallization conditions (preliminary study)

mAb1 was found to crystallize in a 5 mg/mL protein solution in presence of 11 - 12% (w/v) PEG 4000. Therefore, a 10 mg/mL antibody solution in 0.1 M sodium acetate buffer at pH 5.5 was mixed in a 1:1 ratio with a 22 - 24% (w/v) PEG 4000 solution (0.1 M sodium acetate buffer at pH 5.5). This mixture was stored at ambient temperature for 1 - 2 months. Crystallization, using the 23% (w/v) PEG solution showed the best results in terms of crystallization potency and quality and was therefore defined as lead concentration. It combined a relatively fast crystallization with high yield and homogeneous particle size (plate like crystals, see Fig. 1-3). Using 24% (w/v) PEG for crystallization, time and yield were acceptable, but initially formed needle like clusters converted to plate like crystals after 180 days of crystallization. Higher PEG concentrations triggered amorphous precipitates. In contrast, usage of a 22% (w/v) PEG solution resulted in a lower maximum crystal yield (60% vs. 65 - 70%) and a longer crystallization period (80 days vs. 40 - 50 days). Lower PEG concentrations did not trigger any crystallization.

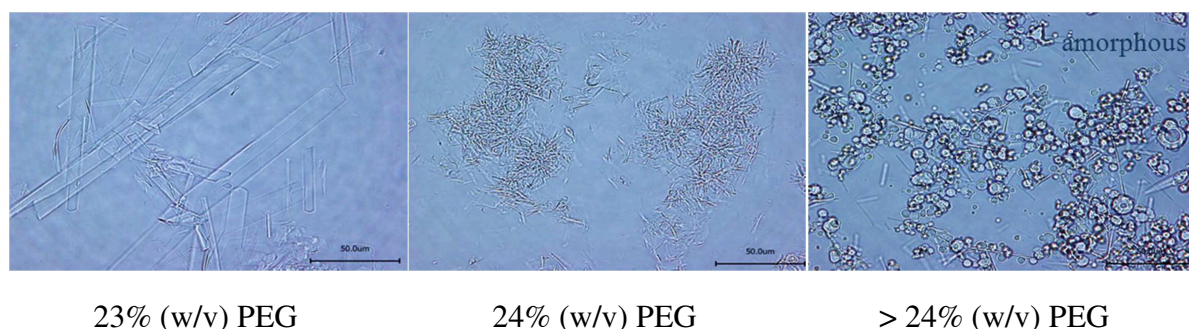
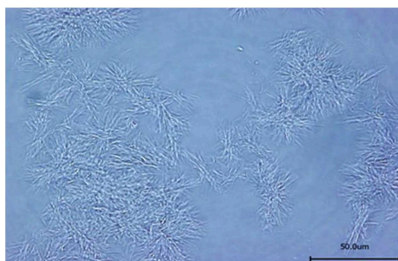


Figure 1-3 Light microscopic images from mAb1 crystallized with different amounts of PEG. Platelet shaped crystals were obtained with 23% (w/v) PEG 4000 (left). Small needle cluster occur using 24% (w/v) PEG 4000 (middle). Above 24% (w/v) PEG 4000 amorphous precipitates were obtained.

1.3.2 mAb2 lead crystallization conditions (preliminary study)

In contrast to mAb1, crystallization of mAb2 was only possible in a salt based crystallizing system. Similar to mAb1, crystallization was carried out from a 10 mg/mL protein solution. Therefore, the initial stock solution at pH 5.2 was diluted with highly purified water. Subsequently, the protein solution was admixed in a 1:1 ratio with a 4.2 M sodium dihydrogen phosphate solution in a 0.1 M sodium acetate buffer at pH 4.1. The mixture was stored for one week at ambient temperature. Notably, mAb2 initially pre-

precipitates amorously after mixing the two solutions. Transition into crystals starts immediately and is usually completed after 2 days and sea-urchin like crystal structures could be observed (Fig. 1-4) ⁸⁶.



mAb2 crystals

Figure 1-4 shows a light microscopic picture of mAb2 crystals obtained after crystallization with the lead conditions.

Table 1-4 summarizes the lead conditions used during the present study as defined by the preliminary study.

Table 1-4 shows the optimized crystallization lead conditions for the two full length IgG₁ antibodies ⁸⁶.

mAb1	mAb2
<ul style="list-style-type: none"> • 10 mg/mL protein solution • 22% - 24% (w/v) PEG 4000 solution • 0.1 M sodium acetate buffer pH 5.50 • Batch crystallization (admixing 1:1) • Ambient temperature 	<ul style="list-style-type: none"> • 10 mg/mL protein solution • 4.2 M sodium dihydrogen phosphate solution • 0.1 M sodium acetate buffer pH 4.10 • Batch crystallization (admixing 1:1) • Ambient temperature

1.3.3 Stability of antibody crystals (preliminary study)

During the preliminary study, aggregate formation was observed for mAb1 and mAb2 in their crystalline states (see section 1.3.3.1 and 1.3.3.2). To describe the stability of both antibodies, one needs to differentiate between stability during the crystallization process and under storage conditions after maximum crystal yield has been reached. Analysis of the secondary structure did not reveal any changes in the crystalline state compared to the dissolved state. Therefore, the aforementioned aggregate formation observed during the preliminary study was not linked to protein unfolding so that a different mechanism for protein instability was anticipated.

It was assumed that the aggregation occurs inside the crystal lattice due to residual flexibility of the antibodies supported by the short distances between the molecules ⁸⁶. These characteristics theoretically result in highly concentrated microsystems which in general foster aggregation due to macromolecular crowding. An additional influence of the formulation excipients, which are able to move through the solvent channels and thus permeate the crystals, was also considered. However, investigations on molecular level were not presented ⁸⁶.

1.3.3.1 mAb1 stability during crystallization and storage (preliminary study)

For mAb1, aggregate formation was observed immediately after mixing the antibody solution with the PEG 4000 solution. Samples stored at 2-8°C remained quite stable whereas storage at 25°C and especially at 40°C resulted in high levels of aggregates. After 3 months storage time at 25°C, the amount of soluble aggregates reached approximately 6.5% and continued up to 9% after 6 months. Interestingly, the aggregate formation can be associated to the PEG concentration; the higher the PEG concentration the higher the observed aggregate content. It was already assumed that initial aggregates might serve as primary nuclei for crystallization and thus were concentrated in the crystalline phase. However, this could not explain the further aggregation during storage. Stabilization of the antibody by association within a crystal lattice was obviously not naturally given as a comparison of the crystalline suspensions and their liquid counterparts revealed a higher stability for the liquid formulations ⁸⁶.

1.3.3.2 mAb2 stability during crystallization and storage (preliminary study)

mAb2 crystals showed a loss of total monomer content of about 0.4% immediately after crystallization. The aggregate content continuously increased to approximately 5% during storage at ambient temperature for 6 months and increased to 10% after one year. As the crystal yield was almost 100%, the aggregates were likely not formed during storage as primary nuclei. Extended stability studies for mAb2 were performed over 3 months at 2-8°C, 25°C and 40°C with similar results as for mAb1. All tested formulations remained stable at 2-8°C. After storage at 25°C and 40°C, significant aggregate and fragment levels could be observed. In conclusion, both model proteins did show a superiorly stability in their crystallized states compared to its liquid formulations ⁸⁶.

1.4 Objectives of the thesis

The feasibility of the concept to grow highly stable mAb crystals from biocompatible conditions was still arguable at the end of the preliminary study. Therefore, the present study was carried out in order to prove this concept and to stabilize the crystals from the two IgG₁ antibodies by, amongst others, drying and to use them as platform for sustained release formulations.

As proof of concept, a small initial study should be conducted as fundament for the main work. By means of a model protein a lead procedure from the crystallization itself towards a dry and stable product was to be developed. The investigated strategies and methods should subsequently be transferred to mAb1 and mAb2. Lysozyme was chosen as model protein as, in contrast to the two antibodies, several stable polymorphic forms were already known. Consequently, the whole concept of the present study could be demonstrated and pre-assessed without limitations arising from unstable and inappropriate protein crystal material (Chapter 2).

Dry crystalline products were anticipated to be beneficial for protein crystal stabilization and long term storage properties and thus an appropriate drying procedure was to be developed. Herein, the first step was to reproduce and to evaluate the vacuum drying procedure from the preliminary study. Additional innovative drying techniques such as hot-air drying were also to be assessed (Chapter 3).

The crystallization lead conditions resulted in needle-like structures which were considered thermodynamically very unfavorable⁵⁸. Therefore, a screening for different polymorphs was to be conducted in order to obtain polymorphic crystals of higher stability (Chapter 4).

Investigation of the underlying aggregation pathways was to be performed to set the stabilization of the two mAb crystals on a rational level (Chapter 5).

Multiple administrations are not well accepted for the patient. Applicable sustained release formulations are required which allow to reduce the frequency of administration. Protein crystals might possess beneficial attributes for long term protein drug release. Therefore, the crystals of the two antibodies were to be assessed for their ability to function as innovative platform for several sustained release formulations (Chapter 6).

Amorphous precipitates might occur as impurities during protein crystallization. Commonly used analytical techniques such as microscopy do not allow for a high throughput analysis with respect to differentiate between crystalline and amorphous structures as well as to quantify the amorphous impurity. Therefore, an alternative analytical technique (flow cytometry) was to be assessed for this purpose (Chapter 7).

1.5 References

1. Carter, P.J., *Introduction to current and future protein therapeutics: A protein engineering perspective*. Experimental Cell Research, 2011. **317**(9): p. 1261-1269.
2. Ammon, H.P., *Hunnius Pharmazeutisches Wörterbuch*. 2010: Walter de Gruyter.
3. Walsh, G., *Biopharmaceutical benchmarks 2010*. Nature Biotechnology, 2010. **28**(9): p. 917.
4. Leader, B., Baca, Q.J., Golan, D.E., *Protein therapeutics: a summary and pharmacological classification*. Nature Reviews Drug Discovery, 2008. **7**(1): p. 21-39.
5. Nicolaides, N.C., Sass, P.M., Grasso, L., *Advances in targeted therapeutic agents*. Expert Opinion on Drug Discovery, 2010. **5**(11): p. 1123-1140.
6. Elvin, J.G., Couston, R.G., van der Walle, C.F., *Therapeutic antibodies: Market considerations, disease targets and bioprocessing*. International Journal of Pharmaceutics, 2013. **440**(1): p. 83-98.
7. Reichert, J.M., *Antibodies to watch in 2013: Mid-year update*. MAbs, 2013. **5**: p. 0--1.
8. Hoekstra, W.P.M., Smeekens, S.C.M., *Molecular Biotechnology*, in *Pharmaceutical Biotechnology*, Crommelin, D.J.A., Sindelar, R.D., Editor. 2002, Taylor & Francis. p. 1-21.
9. Köhler, G., Milstein, C., *Continuous cultures of fused cells secreting antibody of predefined specificity*. Nature, 1975. **256**(5517): p. 495-497.
10. Winter, G., Milstein, C., *Man-made antibodies*. Nature, 1991. **349**(6307): p. 293-299.
11. Pechenov, S., Shenoy, B., Yang, M.X., Basu, S.K., Margolin, A.L., *Injectable controlled release formulations incorporating protein crystals*. Journal of Controlled Release, 2004. **96**(1): p. 149-158.
12. Strohl, W.R., *Therapeutic monoclonal antibodies: past, present, and future*, in *Therapeutic Monoclonal Antibodies: From Bench to Clinic*, An, Z., Editor. 2009: p. 1-50.
13. Chowdhury, P.S., Wu, H., *Tailor-made antibody therapeutics*. Methods, 2005. **36**(1): p. 11-24.
14. Wang, W., *Instability, stabilization, and formulation of liquid protein pharmaceuticals*. International Journal of Pharmaceutics, 1999. **185**(2): p. 129-188.

15. Crommelin, D.J., Storm, G., Verrijck, R., de Leede, L., Jiskoot, W., Hennink, W.E., *Shifting paradigms: biopharmaceuticals versus low molecular weight drugs*. International Journal of Pharmaceutics, 2003. **266**(1): p. 3-16.
16. Manning, M.C., Chou, D.K., Murphy, B.M., Payne, R.W., Katayama, D.S., *Stability of protein pharmaceuticals: an update*. Pharmaceutical Research, 2010. **27**(4): p. 544-575.
17. Wang, W., *Protein aggregation and its inhibition in biopharmaceuticals*. International Journal of Pharmaceutics, 2005. **289**(1): p. 1-30.
18. Chi, E.Y., Krishnan, S., Randolph, T.W., Carpenter, J.F., *Physical stability of proteins in aqueous solution: mechanism and driving forces in nonnative protein aggregation*. Pharmaceutical Research, 2003. **20**(9): p. 1325-1336.
19. Jiskoot, W., Randolph, T.W., Volkin, D.B., Middaugh, C.R., Schöneich, C., Winter, G., Friess, W., Crommelin, D.J., Carpenter, J.F., *Protein instability and immunogenicity: Roadblocks to clinical application of injectable protein delivery systems for sustained release*. Journal of Pharmaceutical Sciences, 2012. **101**(3): p. 946-954.
20. Rosenberg, A.S., *Effects of protein aggregates: an immunologic perspective*. The AAPS journal, 2006. **8**(3): p. E501-E507.
21. Carpenter, J.F., Randolph, T.W., Jiskoot, W., Crommelin, D.J.A., Middaugh, C.R., Winter, G., Fan, Y.-X., Kirshner, S., Verthelyi, D., Kozlowski, S., Clouse, K.A., Swann, P.G., Rosenberg, A., Cherney, B., *Overlooking subvisible particles in therapeutic protein products: Gaps that may compromise product quality*. Journal of Pharmaceutical Sciences, 2009. **98**(4): p. 1201-1205.
22. Johnson, R., Jiskoot, W., *Models for evaluation of relative immunogenic potential of protein particles in biopharmaceutical protein formulations*. Journal of Pharmaceutical Sciences, 2012. **101**(10): p. 3586-3592.
23. Daugherty, A.L., Mersny, R.J., *Formulation and delivery issues for monoclonal antibody therapeutics*. Advanced Drug Delivery Reviews, 2006. **58**(5): p. 686-706.
24. Strohl, W.R., Knight, D.M., *Discovery and development of biopharmaceuticals: current issues*. Current Opinion in Biotechnology, 2009. **20**(6): p. 668-672.
25. Johnson-Léger, C., Power, C.A., Shomade, G., Shaw, J.P., Proudfoot, A.E., *Protein therapeutics-lessons learned and a view of the future*. Expert Opinion on Biological Therapy, 2006. **6**(1): p. 1-7.
26. Fuh, K., *Modern-day challenges in therapeutic protein production*. Expert Review of Proteomics, 2011. **8**(5): p. 563-564.

27. Antosova, Z., Mackova, M., Kral, V., Macek, T., *Therapeutic application of peptides and proteins: parenteral forever?* Trends in Biotechnology, 2009. **27**(11): p. 628-635.
28. Mahmood, I., Green, M.D., *Pharmacokinetic and pharmacodynamic considerations in the development of therapeutic proteins.* Clinical Pharmacokinetics, 2005. **44**(4): p. 331-347.
29. Fahy, J.V., Cockcroft, D.W., Boulet, L.-P., Wong, H.H., Deschesnes, F., Davis, E.E., Ruppel, J., Su, J.Q., Adelman, D.C., *Effect of aerosolized anti-IgE (E25) on airway responses to inhaled allergen in asthmatic subjects.* American Journal of Respiratory and Critical Care Medicine, 1999. **160**(3): p. 1023-1027.
30. Orive, G., Hernandez, R.M., Gascón, A.R.g., Domínguez-Gil, A., Pedraz, J.L., *Drug delivery in biotechnology: present and future.* Current opinion in biotechnology, 2003. **14**(6): p. 659-664.
31. Mitragotri, S., Blankschtein, D., Langer, R., *Ultrasound-mediated transdermal protein delivery.* Science, 1995. **269**(5225): p. 850-853.
32. Kalluri, H., Banga, A.K., *Transdermal delivery of proteins.* AAPS PharmSciTech, 2011. **12**(1): p. 431-441.
33. Frokjaer, S., Otzen, D.E., *Protein drug stability: a formulation challenge.* Nature Reviews Drug Discovery, 2005. **4**(4): p. 298-306.
34. Bhambhani, A., Kissmann, J.M., Joshi, S.B., Volkin, D.B., Kashi, R.S., Middaugh, C.R., *Formulation design and high-throughput excipient selection based on structural integrity and conformational stability of dilute and highly concentrated IgG1 monoclonal antibody solutions.* Journal of Pharmaceutical Sciences, 2012. **101**(3): p. 1120-1135.
35. Yang, M.X., Shenoy, B., Disttler, M., Patel, R., McGrath, M., Pechenov, S., Margolin, A.L., *Crystalline monoclonal antibodies for subcutaneous delivery.* Proceedings of the National Academy of Sciences, 2003. **100**(12): p. 6934-6939.
36. Frokjaer, S., Otzen, D.E., *Protein drug stability: a formulation challenge.* Nature Reviews Drug Discovery, 2005. **4**(4): p. 298-306.
37. Shire, S.J., Shahrokh, Z., Liu, J., *Challenges in the development of high protein concentration formulations.* Journal of Pharmaceutical Sciences, 2004. **93**(6): p. 1390-1402.
38. Harris, R.J., Shire, S.J., Winter, C., *Commercial manufacturing scale formulation and analytical characterization of therapeutic recombinant antibodies.* Drug development research, 2004. **61**(3): p. 137-154.
39. Kanai, S., Liu, J., Patapoff, T.W., Shire, S.J., *Reversible self-association of a concentrated monoclonal antibody solution mediated by Fab–Fab interaction*

- that impacts solution viscosity*. Journal of Pharmaceutical Sciences, 2008. **97**(10): p. 4219-4227.
40. Brange, J., Andersen, L., Laursen, E.D., Meyn, G., Rasmussen, E., *Toward understanding insulin fibrillation*. Journal of Pharmaceutical Sciences, 1997. **86**(5): p. 517-525.
 41. Wang, W., *Lyophilization and development of solid protein pharmaceuticals*. International Journal of Pharmaceutics, 2000. **203**(1-2): p. 1-60.
 42. Bhatnagar, B.S., Bogner, R.H., Pikal, M.J., *Protein stability during freezing: separation of stresses and mechanisms of protein stabilization*. Pharmaceutical Development and Technology, 2007. **12**(5): p. 505-523.
 43. Carpenter, J.F., Pikal, M.J., Chang, B.S., Randolph, T.W., *Rational design of stable lyophilized protein formulations: some practical advice*. Pharmaceutical Research, 1997. **14**(8): p. 969-975.
 44. Yang, M.X., Shenoy, B., Distler, M., Patel, R., McGrath, M., Pechenov, S., Margolin, A.L., *Crystalline monoclonal antibodies for subcutaneous delivery*. Proceedings of the National Academy of Sciences of the United States of America, 2003. **100**(12): p. 6934-6939.
 45. Jen, A.Merkle, H.P., *Diamonds in the Rough: Protein Crystals from a Formulation Perspective*. Pharmaceutical Research, 2001. **18**(11): p. 1483-1488.
 46. Basu, S.K., Govardhan, C.P., Jung, C.W., Margolin, A.L., *Protein crystals for the delivery of biopharmaceuticals*. Expert Opinion on Biological Therapy, 2004. **4**(3): p. 301-317.
 47. Shenoy, B., Wang, Y., Shan, W., Margolin, A.L., *Stability of crystalline proteins*. Biotechnology and Bioengineering, 2001. **73**(5): p. 358-369.
 48. Hancock, B.C., Zografi, G., *Characteristics and significance of the amorphous state in pharmaceutical systems*. Journal of Pharmaceutical Sciences, 1997. **86**(1): p. 1-12.
 49. Margolin, A.L., Khalaf, N.K., Clair, N.L.S., Rakestraw, S.L., Shenoy, B.C., *Stabilized protein crystals formulations containing them and methods of making them*. 2003, US Patent 6,541,606 B2.
 50. Pikal, M.J., Rigsbee, D.R., *The stability of insulin in crystalline and amorphous solids: observation of greater stability for the amorphous form*. Pharmaceutical Research, 1997. **14**(10): p. 1379-1387.
 51. McRee, D.E., *Practical protein crystallography*. 1999: Access Online via Elsevier.
 52. <http://www.rcsb.org/pdb/statistics/holdings.do>, 2012.

53. Shenoy, B., *Crystals of whole antibodies and fragments thereof and methods for making and using them*. 2010, US Patent 7,833,525 B2.
54. McPherson, A., *Introduction to protein crystallization*. *Methods*, 2004. **34**(3): p. 254-265.
55. Chayen, N., *Comparative Studies of Protein Crystallization by Vapour-Diffusion and Microbatch Techniques*. *Acta Crystallographica Section D*, 1998. **54**(1): p. 8-15.
56. Durbin, S., Feher, G., *Protein crystallization*. *Annual review of physical chemistry*, 1996. **47**(1): p. 171-204.
57. Feigelson, R.S., *The relevance of small molecule crystal growth theories and techniques to the growth of biological macromolecules*. *Journal of Crystal Growth*, 1988. **90**(1): p. 1-13.
58. Hekmat, D., Hebel, D., Schmid, H., Weuster-Botz, D., *Crystallization of lysozyme: From vapor diffusion experiments to batch crystallization in agitated ml-scale vessels*. *Process Biochemistry*, 2007. **42**(12): p. 1649-1654.
59. Forsythe, E., Ewing, F., Pusey, M., *Studies on tetragonal lysozyme crystal growth rates*. *Acta Crystallographica Section D: Biological Crystallography*, 1994. **50**(4): p. 614-619.
60. von Hippel, P.H., Berg, O., *Facilitated target location in biological systems*. *Journal of Biological Chemistry*, 1989. **264**(2): p. 675-678.
61. Sharp, K., Fine, R., Honig, B., *Computer simulations of the diffusion of a substrate to an active site of an enzyme*. *Science*, 1987. **236**(4807): p. 1460-1463.
62. Karshikov, A., Bode, W., Tulinsky, A., Stone, S.R., *Electrostatic interactions in the association of proteins: An analysis of the thrombin-hirudin complex*. *Protein Science*, 1992. **1**(6): p. 727-735.
63. McPherson, A., *Crystallization of biological macromolecules*. Vol. 586. 1999: Cold Spring Harbor Laboratory Press New York.
64. Grimm, C., Chari, A., Reuter, K., Fischer, U., *A crystallization screen based on alternative polymeric precipitants*. *Acta Crystallographica Section D: Biological Crystallography*, 2010. **66**(6): p. 685-697.
65. Atha, D.H., Ingham, K.C., *Mechanism of precipitation of proteins by polyethylene glycols. Analysis in terms of excluded volume*. *Journal of Biological Chemistry*, 1981. **256**(23): p. 12108-12117.
66. Bhat, R., Timasheff, S.N., *Steric exclusion is the principal source of the preferential hydration of proteins in the presence of polyethylene glycols*. *Protein Science*, 1992. **1**(9): p. 1133-1143.

67. McPherson, A., *Use of polyethylene glycol in the crystallization of macromolecules*. *Methods in enzymology*, 1985. **114**: p. 120-125.
68. Kumar, V., Kalonia, D.S., *Removal of peroxides in polyethylene glycols by vacuum drying: Implications in the stability of biotech and pharmaceutical formulations*. *AAPS PharmSciTech*, 2006. **7**(3): p. 47-53.
69. Henning, T., *Polyethylene glycols (PEGs) and the pharmaceutical industry*. *SÖFW-Journal*, 2001. **127**(10): p. 28-32.
70. Wiencek, J., *New strategies for protein crystal growth*. *Annual review of biomedical engineering*, 1999. **1**(1): p. 505-534.
71. Arakawa, T., Timasheff, S.N., *Mechanism of polyethylene glycol interaction with proteins*. *Biochemistry*, 1985. **24**(24): p. 6756-6762.
72. Ryu, S., Lee, B., Hong, S., Jin, S., Park, S., Hong, S.H., Lee, H., *Salting-out as a scalable, in-series purification method of graphene oxides from microsheets to quantum dots*. *Carbon*, 2013. **63**(0): p. 45-53.
73. Zhang, Y., Furyk, S., Bergbreiter, D.E., Cremer, P.S., *Specific ion effects on the water solubility of macromolecules: PNIPAM and the Hofmeister series*. *Journal of the American Chemical Society*, 2005. **127**(41): p. 14505-14510.
74. Arakawa, T., Timasheff, S.N., *Preferential interactions of proteins with salts in concentrated solutions*. *Biochemistry*, 1982. **21**(25): p. 6545-6552.
75. Arakawa, T., Timasheff, S.N., *Mechanism of protein salting in and salting out by divalent cation salts: balance between hydration and salt binding*. *Biochemistry*, 1984. **23**(25): p. 5912-5923.
76. Schwierz, N., Netz, R.R., *Effective interaction between two ion-adsorbing plates: Hofmeister series and salting-in/salting-out phase diagrams from a global mean-field analysis*. *Langmuir*, 2012. **28**(8): p. 3881-3886.
77. Gurau, M.C., Lim, S.-M., Castellana, E.T., Albertorio, F., Kataoka, S., Cremer, P.S., *On the mechanism of the Hofmeister effect*. *Journal of the American Chemical Society*, 2004. **126**(34): p. 10522-10523.
78. Collins, K.D., *Ions from the Hofmeister series and osmolytes: effects on proteins in solution and in the crystallization process*. *Methods*, 2004. **34**(3): p. 300-311.
79. Baldwin, R.L., *How Hofmeister ion interactions affect protein stability*. *Biophysical Journal*, 1996. **71**(4): p. 2056-2063.
80. Kiese, S., Pappenberg, A., Friess, W., Mahler, H.C., *Shaken, not stirred: mechanical stress testing of an IgG1 antibody*. *Journal of Pharmaceutical Sciences*, 2008. **97**(10): p. 4347-4366.

81. Matthews, B.W., *Solvent content of protein crystals*. Journal of Molecular Biology, 1968. **33**: p. 491-497.
82. Frey, M., *Water structure associated with proteins and its role in crystallization*. Acta Crystallographica Section D: Biological Crystallography, 1994. **50**(4): p. 663-666.
83. Shekunov, B.Y., York, P., *Crystallization processes in pharmaceutical technology and drug delivery design*. Journal of Crystal Growth, 2000. **211**(1-4): p. 122-136.
84. Lee, T.S., Vaghjiani, J.D., Lye, G.J., Turner, M.K., *A systematic approach to the large-scale production of protein crystals*. Enzyme and microbial technology, 2000. **26**(8): p. 582-592.
85. Kantardjieff, K.A., Rupp, B., *Protein isoelectric point as a predictor for increased crystallization screening efficiency*. Bioinformatics, 2004. **20**(14): p. 2162-2168.
86. Gottschalk, S., *Crystalline Monoclonal Antibodies: Process Development for Large Scale Production, Stability and Pharmaceutical Applications*. Thesis Munich, 2008.

Chapter 2

2 Case study: From protein bulk crystallization towards dry protein products

2.1 Abstract

Drying of protein crystals is challenging. Specific levels of residual intra-crystalline water are required to preserve the protein's integrity within the crystal lattice. Utilization of standard drying techniques for biopharmaceuticals as freeze drying or vacuum drying easily can end in overdrying and protein denaturation. Consequently, alternative drying techniques are required to achieve dry protein crystals. During the present study, protein crystals were washed with a volatile organic solvent which was subsequently evaporated using a heated inert gas stream of nitrogen. An appropriate crystal had to be insoluble and stable within the organic washing liquid and during the drying procedure itself. It was assumed that only certain crystal polymorphs would possess such required attributes. Therefore, lysozyme was crystallized into different morphologies. Three polymorphs were characterized for processability, mechanical properties and solubility in organic solvents. During an extensive solvent screening isopropanol 95% was found to be the best washing liquid. Only one crystal polymorph was insoluble and stable in this solvent. A crystalline free flowing powder was obtained which showed very low residual isopropanol and water contents and fully retained specific activity of the protein. The crystal morphology was shown to be a key factor within the presented approach.

2.2 Introduction

Although protein crystallization has been performed for almost 150 years, only one biopharmaceutical is on the market comprising the protein drug in crystal form: insulin¹⁻⁵. In contrast, crystals made of small molecules have been utilized in therapeutic formulations for decades possessing well-known attractive attributes, e.g. stability and handling⁶. Hence, transferring these advantageous properties of small molecule crystals to proteins would be a desirable target. Furthermore, the crystalline state might prevent biological, chemical or physical degradation of the biopharmaceutical drug^{6,7}. Protein crystals may also enable sustained release of protein molecules eventually in combination with specific excipients^{2,5-7}. In addition, as there is a need for administration of highly concentrated protein formulations (e.g. antibodies), the solid state should also allow a reduction of the required dosage volume due to a comparatively low viscosity (Einstein equation) of crystal suspensions^{2,5,8}. Therefore, protein crystals were already referred to as “diamonds in the rough” by Jen and Merkle in 2001⁶.

However, development of crystalline protein formulations is complicated by the fact that many proteins only crystallize at inappropriate conditions, which means that the applied temperatures, pH, solvents and precipitation agents are not biocompatible or significantly affect protein stability⁶. In literature, only few parameters are described to have a positive impact on the crystallization process^{2,9}. Thus, screening for optimal crystallization conditions is quite complex and can end in extensive efforts although a number of screening kits and proved crystallization strategies are available⁹. Even if an acceptable crystallization condition is found, the observed crystal morphology may not fulfill the requirements for further processing like acceptable handling (e.g. mechanical stability), solubility, stability, and capability for drying. Especially in the case of antibody crystals, the occurrence of needle-shaped morphologies is often reported, representing a very unfavorable morphology³.

With regard to storage stability and shelf life, dry formulations are considered to be superior to liquid protein formulations. The need of a protein crystal to contain a specific amount of intra-crystalline water (up to 90%) to maintain protein stability is complicating this issue^{4,10}. It was even stated that protein crystals cannot be dried in general¹¹. On the contrary, studies showed that certain protein crystals remain stable after drying and at a water content of only 10% or 3%^{8,12}. However, overdrying of the crystals has

to be prevented. Crystalline suspensions usually contain crystals of different sizes and with different amounts of solvent. Theoretically, each crystal would have an optimal drying time that could not be adjusted in a bulk process like freeze drying and vacuum drying¹³. Furthermore, lyophilization requires freezing of the crystalline suspension which might be destructive to the crystal lattice as a result of ice crystal formation^{14,15}. In consequence, other drying strategies have to be applied for protein crystals. The mother liquor could be exchanged by an organic solvent which is subsequently evaporated^{13,14,16}. However, this process is only applicable when the protein crystal is insoluble in the employed liquid. Furthermore, the crystal must protect the protein from denaturation upon contact with the organic solvent. Different crystal morphologies of one protein can eventually show different attributes toward organic solvent exposition, but systematic studies on this matter have not been published, yet.

It was the aim to present a suitable new approach for drying protein crystals. In that context, protein crystals are washed with an organic liquid and subsequently the solvent is evaporated with an inert gas stream of nitrogen. Hence, such a protein crystal must be insoluble and stable during exposition to an organic washing liquid and during the drying procedure. These attributes were deemed to be polymorph dependent and a model protein was therefore crystallized in different morphologies. For that purpose, lysozyme was chosen since several crystal shapes have already been reported in literature¹⁷⁻²¹. Mechanical properties, processability, and solubility in diverse organic solvents were compared for the different polymorphs. Furthermore, the best washing liquid was identified which maintained the crystal and protein integrity. Finally, a free flowing powder of lysozyme crystals was obtained after inert gas drying. In summary, a model procedure to obtain protein crystals in a dry powder formulation is presented which can be applied for pharmaceutical proteins. This process includes, the crystallization itself, a morphology screening, the assessment of crystal properties, a solvent screening, assessment of protein and crystal stability, and finally the drying procedure.

2.3 Materials and Methods

2.3.1 Materials

Lysozyme from chicken egg white (lyophilized powder, protein > 90%, > 40,000 units/mg protein) was obtained from Sigma-Aldrich (Taufkirchen, Germany). Sodium chloride (AnalaR NORMAPUR) as crystallization agent was purchased from VWR Prolabo (Leuven, Belgium). Sodium acetate (USP standard) was of analytical quality from Merck (Darmstadt, Germany). All other used reagents or solvents were of analytical grade and purchased either from Sigma-Aldrich (Taufkirchen, Germany) or from VWR Prolabo (Leuven, Belgium).

2.3.2 Methods

2.3.2.1 Crystallization of lysozyme

The crystallization was carried out as batch crystallization in 50 mM sodium acetate buffer (pH 8) at room temperature without stirring in 60 mL PETG Nalgene vessels (Thermo Scientific, Langensfeld, Germany). Sodium chloride was used as crystallization agent in different concentrations from 0.5 M to 2 M. The concentration of lysozyme was set to 4% (m/V). 10 mL sodium chloride solution was poured carefully to 10 mL of lysozyme solution while the vessel was gently shaken to dissolve the initial precipitation. For each condition four identical batches were prepared.

2.3.3 Drying of lysozyme crystals

2.3.3.1 Inert gas drying

Inert gas drying of lysozyme crystals was performed in a Barkey® Hot-Air Dryer “Flowtherm” (Leopoldshöhe, Germany). The system consists of a heater that allows the tempering of a nitrogen gas stream (upper part) and a bottom heater for the sample (lower part) (Fig. 2-1). 300 µL of the crystal slurry were filled into 2R glass vials and placed into the sample holder. The nitrogen gas stream (10 L/min) was tempered to 30 °C and guided through a needle into 10 vials. The bottom heater was set to 20°C. After drying, the vials were closed and sealed.

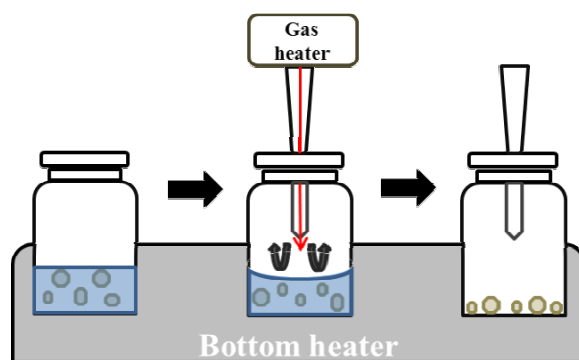


Figure 2-1 Schematic illustration of drying lysozyme crystals using the Barkey® Hot-Air Dryer “Flowtherm”. 2R vials containing the crystals suspended in an organic liquid are placed in the sample holder (left). Subsequently, the nozzle is inserted into the vials and drying with an inert gas stream of nitrogen is performed (red arrow) - (middle). After evaporation of the liquid, a free flowing powder of protein crystals powder remains in the vials (right).

2.3.3.2 Freeze Drying

Freeze drying of lysozyme crystal suspension was performed using a Christ Epsilon 2-6D pilot scale freeze dryer (Christ, Osterode am Harz, Germany). 1 mL of the suspensions were filled into 2R glass vials and semi stoppered. Subsequently, the temperature was decreased to -40°C at a rate of $1^{\circ}\text{C}/\text{min}$ and was held for 1h and 10min. In the last 10 min pressure was reduced to 0.08 mbar. In the next step, temperature was increased to -10°C at a rate of $1^{\circ}\text{C}/\text{min}$ and held for 16.66 h. Finally, temperature was increased to 25°C at a rate of $0.15^{\circ}\text{C}/\text{min}$ and held for 10 h. At the end of the drying cycle the chamber was aerated with nitrogen and the vials were stoppered automatically within the chamber. The samples were stored until analytical examination at $2-8^{\circ}\text{C}$.

2.3.3.3 Test for mechanical properties

Centrifugation was performed in a Sigma® 4K15 centrifuge for the assessment of mechanical properties. 500 μL of a crystal suspension were centrifuged for 10 min at 25,150 g. Subsequently, the precipitate was suspended and the procedure was repeated twice. The crystal integrity was verified microscopically. If the integrity had been affected, the procedure was repeated with a reduced spin speed.

2.3.3.4 Transferability and handling properties

To examine the handling properties of the crystal suspensions, pipetting through three different Eppendorf pipette tips with a volume of 10 μL , 200 μL , and 1000 μL was used as a simple surrogate method. The respective maximum tip volume of a homogenized

stock suspension of lysozyme crystals was withdrawn, subsequently ejected (90%) and sucked again for 1-, 5-, and 20 - times. After each step, the crystal integrity was verified microscopically.

2.3.3.5 Solvent screening

Solubility and stability of lysozyme crystals in different organic solvents were assessed by transferring the crystals into the respective organic solvent (three times centrifugation, replacement of supernatant with respective solvent). After each washing step, the crystal integrity was verified microscopically. A dissolution test in isotonic 10 mM phosphate buffer solution (PBS) at pH 7.4 was performed at the end of the washing procedure.

2.3.3.6 Protein yield determination

Protein concentration was assessed by UV-spectrometry at 280 nm using an Agilent® 8453 UV spectrometer (Böblingen, Germany).

The yield was determined after centrifugation (11,200 g, 15 min) of an aliquot from the crystal suspension and subsequent determination of residual protein concentration in the supernatant. The fraction of crystallized protein was calculated by subtraction of the concentration in supernatant from the initial protein concentration before crystallization. The amount of crystallized protein in percent of the initial protein concentration represented the yield.

2.3.3.7 Microscopic examination

The crystal integrity was determined microscopically using a Nikon Labophot equipped with a JVC TK-C1381 color video camera and the Screen Measurement / Comet – Software Version 3.52a. Glass cover slides were used for sample preparation. Octagonal shaped protein crystals were placed on sample holders with convexities to prevent crystal breakage. Examination was performed at 200 fold magnification.

2.3.3.8 Determination of residual moisture

A Karl Fischer coulometric titrator (652-KF Coulometer and 737-KF Coulometer, Metrohm, Filderstadt, Germany) was used for determination of residual moisture. 2 mL methanol (Hydranal®-Methanol dry, Fluka, Sigma-Aldrich Chemie GmbH) was added to the protein crystals (5 – 10 mg). The samples were placed in an ultrasonic water bath

and incubated for 15 min prior to injection of 1 mL aliquot into the reaction vessel. Measurement was performed until the drift dropped below the start value ($< 10 \mu\text{g}/\text{min}$).

2.3.3.9 Size exclusion high performance liquid chromatography (SE-HPLC)

Monomer content and total protein recovery were determined by SE-HPLC. The analysis was performed on a Thermo separation system using a Superose 12 10/300 GL column (GE Healthcare, Uppsala). The mobile phase consisted of 200 mM sodium phosphate at a pH of 6.8. The flow rate was 0.6 mL/min and the protein was detected at 215 nm and 280 nm, respectively.

2.3.3.10 Nephelometry

Turbidity was measured using a Nephla Dr. Lange turbidimeter (Dr. Lange GmbH, Düsseldorf, Germany) by 90° light scattering at a wavelength of $\lambda = 860 \text{ nm}$ (Ph. Eur. 2.2.1). Results are given in formazine normalized units. Crystals were dissolved in phosphate buffer solution (0.01M, pH 7.4, isotonic) (PBS) and concentration was set to 1 mg/mL. 2 mL of each sample were filled into round glass cuvettes and placed into the sample holder.

2.3.3.11 Gas Chromatography (GC)

Determination of residual isopropanol was performed according to Ph. Eur. 7.0/2.4.24. Gas chromatography was carried out using an Agilent GC 6890 system, a S/SL injector and a flame ionization detector. The system contained a MPS-2 auto sampler with headspace loading. An Agilent DB-624 capillary column (30 m x 0.32 mm x 3 μm) was used with nitrogen as carrier gas. The linear flow rate was 40 cm/sec and a splitless-loading was employed. During the static headspace-sample draw, the temperature was set to 80°C and equilibrated for 60 min. 1 mL of the samples was injected at a transition temperature of 80°C . The temperature of the injector was 140°C , for the detector 250°C . The temperature of the column was 40°C for 20 min and subsequently heated up to 240°C with a rate of $10^\circ\text{C}/\text{min}$ and held for 20 min.

Different from the Ph. Eur. protocol, the amount of sample was reduced by ten due to shortage in dry crystal material obtained from the drying procedure. In consequence, the isopropyl standards were also reduced and a splitless loading was performed. In order to reach the required amount for analysis, all samples from one drying process were mixed. Thus, the result represented the average of the samples.

2.3.3.12 Particle counting

Size and amount of particles between 1 and 200 μm were determined using a PAMAS SVSS-C40 (PAMAS GmbH, Rutesheim, Germany) light blockage system. Particles were counted classified into 16 different size ranges. Crystals were dissolved in PBS and concentration was set to 1 mg/mL. The number of measurements was set to three for each sample with a measuring volume of 0.3 ml. The rinsing volume was 0.5 ml.

2.3.3.13 Determination of lysozyme activity

The lysozyme activity was determined by the decrease in absorption of a *Micrococcus lysodeikticus* (ATCC No. 4698) suspension. The assay was performed in a 66 mM phosphate buffer, pH 6.2. The concentration of the substrate suspension was 0.5 mg/mL. Measurement was performed in 96 well-plates using a microplate reader. The decrease in absorption was determined at 450 nm for 5 min. For calculation, the linear slope of the first minute was calculated by linear regression.

2.4 Results

2.4.1 Polymorph-screening

Crystallization was performed employing only one buffer system and precipitation agent. Otherwise, ascription of crystal properties only on the basis of their morphologies would not be possible. Same shapes containing varying salts would differ at least in their solubility²². Merely the precipitant's concentration was altered. In literature, the crystallization agent concentration was reported to have strong impact on crystal morphology¹⁷.

Four distinct crystal shapes were obtained depending on the sodium chloride concentration (Fig. 2-2). More than 2 M sodium chloride led to amorphous lysozyme precipitates (data not shown). For each shape, the obtained yield was approximately 90%.

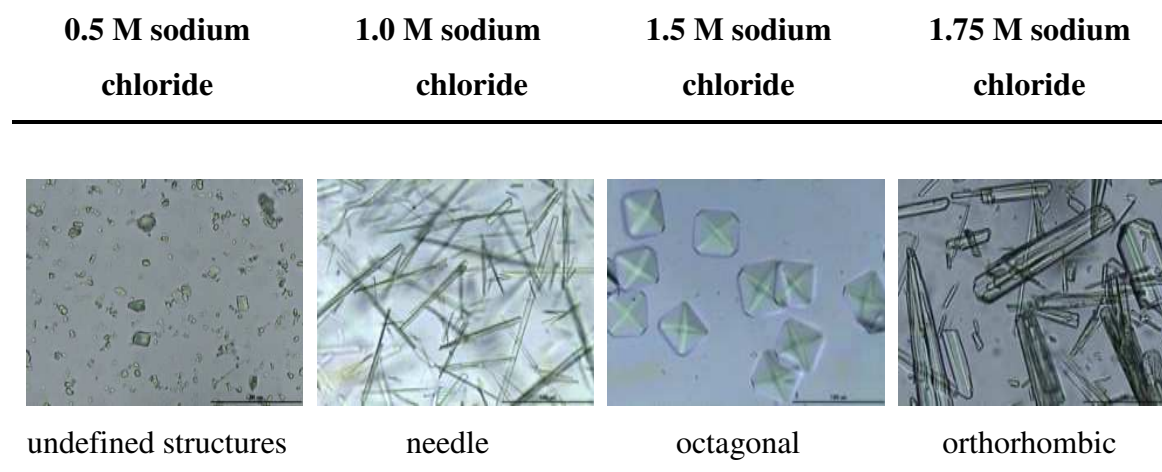


Figure 2-2 The microscopic pictures show four different crystal appearances after crystallization of lysozyme by varying the sodium chloride concentrations. The scale bar represents 100 μm .

In the following, studies on crystal properties were only performed for needle, octagonal, and orthorhombic crystals.

2.4.2 Crystal properties dependent on the polymorphic form

2.4.2.1 Handling and mechanical properties

Handling properties and mechanical stability of protein crystals are of fundamental importance for processing. Thus, the first step was to assess these properties in relation to the crystal's morphology.

Transfer by pipetting is the most often used stress during a bench scale study and is reported to be crucial for protein crystals⁶. For this reason, extensive pipetting was performed as surrogate for mechanical process stress to examine discrepancies between the three crystal morphologies.

Pipetting was performed 1 -, 5 -, and 20 times through three different pipette tips with volumes of 10 μ L, 200 μ L, and 1000 μ L. Interestingly, all three crystal morphologies withstood the stress and neither damages nor debris were observed. Consequently, in the further course of our studies no limitations in pipetting had to be taken into account.

In addition, centrifugation was chosen as surrogate to examine mechanical stability further. This method allows application of high gravitational forces and may give insight into assorted breaking points for each crystal morphology.

During this test the maximal force was 25,150 x g which represented the technical limit of our centrifuge. The spin speed was reduced if the respective crystal morphology broke during any of the three cycles, which each lasted for 10 min. Surprisingly, needle shaped crystals remained stable at the speed limit of the centrifuge. In contrast, octagonal and orthorhombic shaped crystals showed mechanical damage already at 700 xg and 450 xg, respectively (Fig. 2-3). The defined speed limits were applied during further experiments.

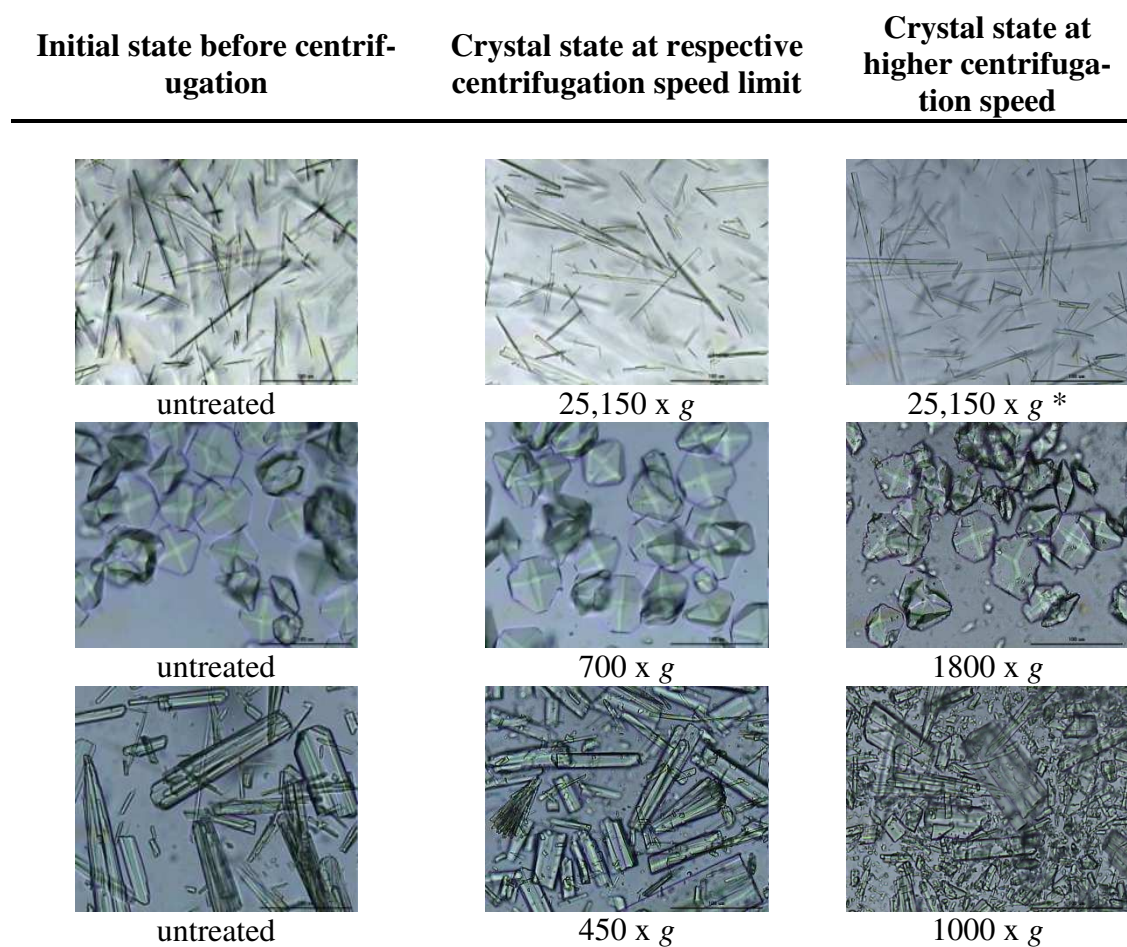


Figure 2-3 The microscopic pictures represent the crystal's condition after a third round of centrifugation at the respective spin speed. The scale bar represents 100 μm . (*The needle shaped crystals remained stable up to the technical limit of the Sigma® 4k15 centrifuge).

2.4.2.2 Solubility and stability during organic liquid exposure

Protein crystals in dry powder form should be reached by exchanging the mother liquid with a volatile organic solvent which would subsequently be evaporated by an inert gas stream of nitrogen¹³. Therefore, a solvent screen was performed to identify organic liquids where the crystals and the protein remained stable. Transfer into the respective washing liquid was performed by a defined procedure including several microscopical examinations (see methods). At the end, a dissolution test in PBS was performed to test if severe aggregation inside the crystal lattice or at the crystal surfaces took place which might be fostered by the reduced polarity of the organic liquids^{23,24}. Irreversible non-covalent aggregation had been previously reported as a factor which could prevent dissolution of protein crystals²⁴.

A high number of organic solvents were examined. Needle shaped crystals passed the whole washing procedure merely in ethyl acetate. They dissolved or were insoluble in PBS after washing with the other liquids. For orthorhombic crystals, four appropriate solvents were found: acetyl acetone, ethyl acetate, triacetine, and triethyl citrate. However, crystal aggregation was observed during extensive washing which might hinder sufficient drying. Octagonal lysozyme crystals passed the procedure in the same four solvents and in higher ethanol and isopropanol concentrations (Tab. 2-1). For the latter two liquids no crystal aggregation was observed during washing. Deusser et al. already described that phenomenon for insulin crystals. A complete removal of inter-crystalline water was required, otherwise, the crystals formed large aggregates¹³. This finding was confirmed during our solvent screening. Hence, it was decided to apply only ethanol and isopropanol as washing liquids as they are water miscible, volatile and show low toxicity. Only octagonal shaped crystals remained stable in both solvents, and thus, only this polymorph was applied for further studies.

Table 2-1 List of applicable washing liquids. In all cases, the crystals remained stable and dissolved in PBS after the washing procedure.

Needle	Octagonal	Orthorhombic
	Acetyl acetone	Acetyl acetone
	Ethanol 90 - 100%	
Ethyl acetate	Ethyl acetate	Ethyl acetate
	Isopropanol 90 - 100%	
	Triacetine	Triacetine
	Triethyl citrate	Triethyl citrate

2.4.3 Hot-Air drying

In a first test, crystals were washed with different liquids (ethanol 90 - 100% or isopropanol 90 - 100%) and subsequently dried in an inert gas stream of nitrogen. Therefore, 300 µL of each crystal suspension were placed into 2 R glass vials and placed in the sample holder of the Barkey® Hot-Air Dryer (Fig. 2-1). Drying time was set to 30 min. Interestingly, film like structures were obtained after drying crystal suspensions containing ethanol (90 - 100%) and isopropanol 90% (data not shown).

In contrast, a free flowing powder resulted from suspensions containing isopropanol 95% and 100% (Fig. 2-5 right). Subsequently, to assess the crystal integrity by light

microscopy, the protein powder was suspended in the respective washing liquid. No alterations of the crystal shape were observed (Fig. 2-4).

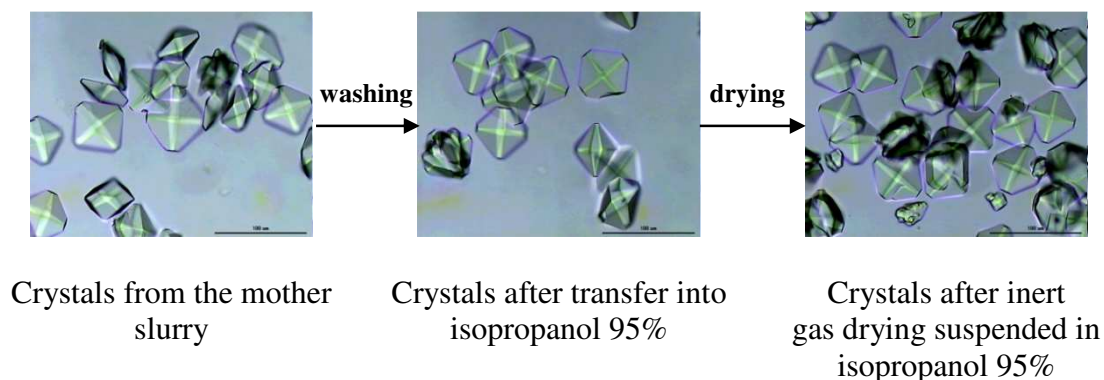


Figure 2-4 Light microscopy pictures of crystals after crystallization (left), washing with isopropanol 95% (middle), and inert gas drying (right). The scale bar presents 100 μ m.

Hence, only isopropanol 95% and 100% were applied as washing liquids for the additional studies.

After freeze drying



After hot-air drying



Figure 2-5 Light microscopy picture: Broken lysozyme crystals after freeze drying (left). Photo camera picture: Free flowing powder of lysozyme crystals after washing with isopropanol 95% and drying in an inert gas stream of nitrogen (right).

2.4.4 Comparative study assessing the suitability of freeze drying to obtain dry and stable protein crystal products

In a comparative experiment, freeze drying was applied on the same lysozyme crystal polymorph. This study should illustrate the challenge to freeze dry protein crystals. Since the crystals would dissolve in an aqueous solution of sugar, drying was performed employing four different approaches: Drying from the crystallization liquid or after washing the crystals with PEG 6,000, isopropanol 95% or 100%. For the latter two conditions, evaporation of the organic solvent was assumed immediately after reduction of

pressure (vacuum drying). As for freeze drying, cake formation was observed for samples containing the mother slurry and PEG 6,000. However, crystal suspensions washed with isopropanol 95% or 100% dried by film formation. After reconstitution of the dried material, an extensive crystal breakage was observed in all cases (Fig. 2-5 left).

2.4.5 Assessment of crystal and protein integrity during the hot-air drying procedure

Aggregate formation after crystallization and washing with an organic liquid was examined by SE-HPLC, turbidity, and light blockage. First, crystals were separated from the mother slurry by centrifugation and decanting (3 x) and subsequently dissolved in PBS for aggregate analytics. Then, other crystals were washed with isopropanol 95% and 100% incubated for 2 hours at room temperature in the respective liquid. The organic solvents were removed by centrifugation and decanting (3 x). Finally, the crystals were also dissolved in PBS to perform aggregate analysis.

SE-HPLC analysis was used to assess total protein recovery which was calculated against a lysozyme stock solution in PBS. No significant decrease was detected for fresh crystallized lysozyme and crystals washed and incubated with isopropanol 95% (Fig. 2-6). However, washing of crystals with isopropanol 100% led to a significant decrease in total protein recovery to 95.9% ($\pm 1.3\%$). Interestingly, soluble aggregates could not be detected for any sample.

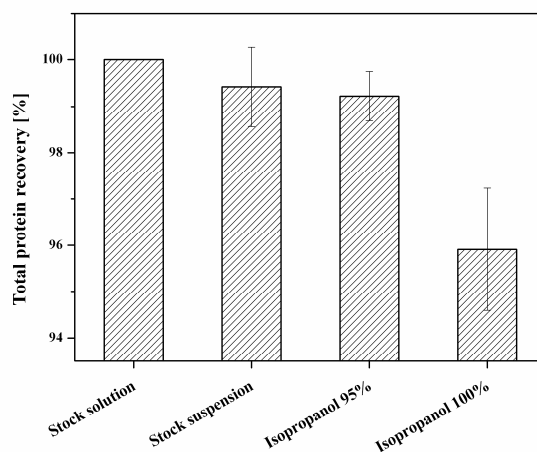


Figure 2-6 Total protein recovery after crystallization (stock suspension) and incubation of octagonal lysozyme crystals in the respective liquid. The displayed protein recovery is calculated against a lysozyme stock solution in PBS. The bars represent the mean of three samples and \pm standard deviation.

Further, the same samples were analyzed for turbidity and subvisible particle count. Whereas the lysozyme solution and freshly crystallized protein showed about the same turbidity and particle count, a remarkable increase in both parameters occurred after exposition to both isopropanol concentrations (Fig. 2-7). Washing with isopropanol 95% resulted in an increase in turbidity by 0.8 FNU and total particle count of approximately 30,000 particles per mL. Pure isopropanol as washing liquid led to an increase in turbidity of about 1.1 FNU and the subvisible particle count was further increased to 80,000 particles per mL. Consequently, isopropanol 95% was used for the final experiments.

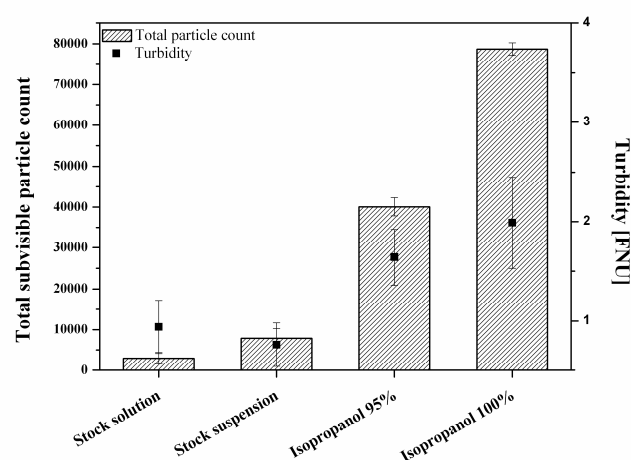


Figure 2-7 Total subvisible particle count (1 - 200 μm) (left) and the turbidity [FNU] (right) of a lysozyme stock solution and octagonal lysozyme crystals directly dissolved in PBS (stock suspension) or after impregnation with isopropanol 95% and isopropanol 100%.

Next, crystals were washed with isopropanol 95% and dried. Subsequently, they were examined for residual isopropanol and water contents in order to optimize the drying time. In accordance to the EMA guideline for class III solvents, organic residues of $\leq 0.5\%$ were aimed. Gas chromatography following Ph. Eur. 7.0/2.4.24 was used for analysis. Before analysis, the drying time was set to 30 min, 15 h and 24 h. As expected, residual isopropanol contents were dependent on the applied drying time. After 30 min of drying, organic residues of 2.5% ($\pm 0.2\%$) were detected while after 15 h and 24 h values of 0.85% ($\pm 0.08\%$) and 0.24% ($\pm 0.1\%$) were found, respectively. Hence, the drying time was set to 24 h for further studies.

To determine residual moisture contents, the Karl Fischer Methanol extraction technique was applied. Water residues of 1.15% ($\pm 0.7\%$) were detected after 24 h of inert gas drying which was considered to be acceptable.

After definition of an acceptable drying time, the effect of inert gas drying on the protein integrity was evaluated. For that purpose, SE-HPLC, turbidity, and subvisible particle count measurements were performed on crystals which were dried for 24 h and subsequently dissolved in PBS.

SE-HPLC revealed no formation of soluble aggregates and protein recovery was $\sim 100\%$. Interestingly, turbidity and subvisible particle counts were reduced for dried crystals in comparison to washed crystals without drying (Fig. 2-8). However, compared to the lysozyme stock solution, the values still showed a small increase.

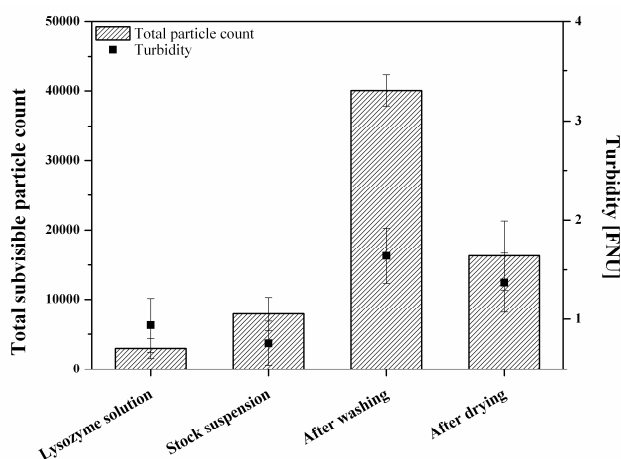


Figure 2-8 Total subvisible particle count (1 - 200 μm) (left) and turbidity [FNU] (right) of a lysozyme solution, immediately dissolved crystals (stock suspension) and crystals dissolved after washing into isopropanol 95% (after exposition) and after drying.

Finally, maintenance of the biological activity of lysozyme was assessed by applying a well-established activity assay. The specific activity was determined at 98% ($\pm 1\%$), and thus, no significant loss in the biological activity was found for the dry product.

2.5 Discussion

It is stated in literature that drying of protein crystals is difficult as certain amounts of intra-crystalline water are required to maintain the protein integrity⁴. Overdrying, destruction of the crystals and denaturation of protein is risked by application of standard drying techniques for biopharmaceuticals like freeze drying. Residual moistures are different for each crystal as they are related to the crystal size and surface which commonly show distribution for protein crystal suspensions¹³. Indeed, application of freeze drying resulted in crystal breakage even after exchanging the matrix with organic liquids due to ice crystal formation in inclusion bodies within the crystals (Fig. 2-5). Therefore, an alternative approach was tested. The crystallization liquid was removed by washing with a water miscible organic liquid which subsequently was evaporated by inert gas drying in stream of heated nitrogen. An appropriate protein crystal had to be insoluble and stable during washing with an organic liquid and would withstand the subsequent drying procedure. The crystal morphology was deemed to be the key factor determining crystal properties. However, only polymorphs grown in the same buffer with the same precipitant would allow ascribing differences in their attributes to varying morphologies. Even same shapes crystallized in other buffers or with different precipitants would vary at least in their solubility²². Hence, several lysozyme morphologies were made by changing only the concentration of the crystallization agent. Three shapes, needle, orthorhombic and octagonal were applied for property characterization as a clear optical definition as polymorph was not possible for the fourth precipitate (Fig. 2-2).

With regard to mechanical stability, the needle shape was the most stable polymorph (Fig. 2-3). This can be explained by a dense package of the crystals during centrifugation which prevents from breakage. Interestingly, the polymorphs showed a significant different solubility in organic liquids. Only octagonal crystals were insoluble and stable in ethanol (> 90%) and isopropanol (> 90%) (Tab. 2-1).

Furthermore, the solvent screen revealed that only water miscible liquids allow to obtain suitable crystal suspensions for drying by reduction of the inter-crystalline water. The other liquids fostered formation of large crystal aggregates during the washing procedure which prevents sufficient drying. This finding was in accordance to Deusser et. al which already described the need to remove the inter-crystalline water for proper drying

of insulin crystals¹³. Hence, only octagonal shaped lysozyme crystals and ethanol (> 90%) as well as isopropanol (> 90%) were applied for further studies.

In a first test, octagonal crystals were washed with the aforementioned liquids and subsequently dried in an inert gas stream of nitrogen at 30°C. A film like structure was obtained after 30 min of drying for samples which contained ethanol (90% - 100%) and 90% isopropanol. Likely, the tempered nitrogen gas stream fostered dissolution of the lysozyme crystals. The dissolved protein precipitated by film formation during drying. Reduction of the drying temperature might prevent dissolution, and even “cooling” for example to 15°C might be suitable to evaporate the volatile liquids. However, a free flowing powder was obtained for samples which contained isopropanol 95% or 100%. Maintenance of the crystal shape and integrity throughout the procedure led to application of these two liquids for further analysis (Fig. 2-4).

No significant loss in total protein recovery was detected after crystallization and after washing with isopropanol 95%, respectively. However, a loss of approximately 4% total protein was found after washing with isopropanol 100% which demonstrated that even little differences in the concentration of organic washing liquids can significantly affect protein stability (Fig. 2-6). This finding was supported by light blockage and turbidity measurements. Both analytics showed higher values for samples washed with isopropanol 100%. Total particle count was doubled (40,000 vs 80,000) and the turbidity increased by 0.3 FNU in comparison to washing into isopropanol 95% (Fig. 2-7). Hence, isopropanol 95% was chosen as washing liquid. Deusser et al already described that mixtures of water and organic solvents are superior washing liquids as lower organic residue levels were found after drying¹³. However, stability data were not presented.

To optimize the drying time with respect to residual isopropanol and water contents, different drying intervals from 30 min to 24 h were tested. Isopropanol residues could be reduced from 2.5% to 0.24% after prolonging the drying time from 30 min to 24 h. The latter value even meets EMA guideline requirements for class III solvents. Furthermore, residual moisture was found to be 1.15% after 24 h inert gas drying which also was considered to be acceptable.

Analysis of total subvisible particle count and turbidity revealed reduced values for crystals which were washed and subsequently dried in comparison to washed crystals

without any drying (Fig. 2-8). This finding can be ascribed to lower organic liquid residues after drying which might be higher for crystals without drying. These higher levels of organic residues might foster aggregate formation during dissolution prior to analysis.

Finally, the biological activity of the dry material was analyzed and found to be fully retained. Hence, it was shown that neither the crystallization, the washing with isopropanol 95% nor the inert gas drying affected the protein integrity with regard to its biological activity.

2.6 Conclusion

In conclusion, a model study is presented which describes a procedure to obtain a dry, stable and biologically active crystalline protein material. During the procedure the crystals were transferred into a volatile organic liquid and subsequently dried in an inert gas stream of nitrogen. Furthermore, the necessity was demonstrated to screen for polymorphs which exhibit different properties as only one crystal morphology was insoluble and stable in the suitable organic washing liquids. Furthermore, it was shown that only one solvent was applicable to maintain both the crystal and protein integrity. Besides a polymorph screening, a reasonable solvent screen must be performed. Nevertheless, it can be considered that creation of “tailor-made” therapeutic or diagnostic protein crystals with desired attributes for later use and storage forms or intermediates for novel formulations can be achieved. Furthermore, the feasible drying method using a heated gas stream of nitrogen opens new possibilities in storage and handling of protein crystals.

2.7 References

1. Walsh, G., *Biopharmaceutical benchmarks 2010*. Nature Biotechnology, 2010. **28**(9): p. 917.
2. Basu, S.K., Govardhan, C.P., Jung, C.W., Margolin, A.L., *Protein crystals for the delivery of biopharmaceuticals*. Expert Opinion on Biological Therapy, 2004. **4**(3): p. 301-317.
3. Hekmat, D., Hebel, D., Schmid, H., Weuster-Botz, D., *Crystallization of lysozyme: From vapor diffusion experiments to batch crystallization in agitated ml-scale vessels*. Process Biochemistry, 2007. **42**(12): p. 1649-1654.
4. McPherson, A., *Introduction to protein crystallization*. Methods, 2004. **34**(3): p. 254-265.
5. Yang, M.X., Shenoy, B., Disttler, M., Patel, R., McGrath, M., Pechenov, S., Margolin, A.L., *Crystalline monoclonal antibodies for subcutaneous delivery*. Proceedings of the National Academy of Sciences, 2003. **100**(12): p. 6934-6939.
6. Jen, A., Merkle, H.P., *Diamonds in the Rough: Protein Crystals from a Formulation Perspective*. Pharmaceutical Research, 2001. **18**(11): p. 1483-1488.
7. Pechenov, S., Shenoy, B., Yang, M.X., Basu, S.K., Margolin, A.L., *Injectable controlled release formulations incorporating protein crystals*. Journal of Controlled Release, 2004. **96**(1): p. 149-158.
8. Shenoy, B., Wang, Y., Shan, W., Margolin, A.L., *Stability of crystalline proteins*. Biotechnology and Bioengineering, 2001. **73**(5): p. 358-369.
9. Kantardjieff, K.A., Rupp, B., *Protein isoelectric point as a predictor for increased crystallization screening efficiency*. Bioinformatics, 2004. **20**(14): p. 2162-2168.
10. Matthews, B.W., *Solvent content of protein crystals*. Journal of Molecular Biology, 1968. **33**: p. 491-497.
11. McPherson, A., *Crystallization of biological macromolecules*. Vol. 586. 1999: Cold Spring Harbor Laboratory Press New York.
12. Nagendra, H., Sukumar, N., Vijayan, M., *Role of water in plasticity, stability, and action of proteins: the crystal structures of lysozyme at very low levels of hydration*. Proteins: Structure, Function, and Bioinformatics, 1998. **32**(2): p. 229-240.
13. Deusser, R., Kraemer, P., Thurow, H., *Process for drying protein crystals*. 2002, US Patent 6,408,536.
14. Shenoy, B., *Crystals of whole antibodies and fragments thereof and methods for making and using them*. 2010, US Patent 7,833,525 B2.

15. Garman, E.F., Schneider, T.R., *Macromolecular cryocrystallography*. Journal of Applied Crystallography, 1997. **30**(3): p. 211-237.
16. Margolin, A.L., Khalaf, N.K., Clair, N.L.S., Rakestraw, S.L., Shenoy, B.C., *Stabilized protein crystals formulations containing them and methods of making them*. 2003, US Patent 6,541,606 B2.
17. Müller, C.Ulrich, J., *A more clear insight of the lysozyme crystal composition*. Crystal Research and Technology, 2011. **46**(7): p. 646-650.
18. Yin, D.-C., Wakayama, N.I., Lu, H.-M., Ye, Y.-J., Li, H.-S., Luo, H.-M., Inatomi, Y., *Uncertainties in crystallization of hen-egg white lysozyme: reproducibility issue*. Crystal Research and Technology, 2008. **43**(4): p. 447-454.
19. Forsythe, E.L., Judge, R.A., Pusey, M.L., *Tetragonal Chicken Egg White Lysozyme Solubility in Sodium Chloride Solutions*. Journal of Chemical & Engineering Data, 1999. **44**(3): p. 637-640.
20. Steinrauf, L., *Preliminary X-ray data for some new crystalline forms of [beta]-lactoglobulin and hen-egg-white lysozyme*. Acta Crystallographica, 1959. **12**(1): p. 77-79.
21. Sukumar, N., Biswal, B.K., Vijayan, M., *Structures of orthorhombic lysozyme grown at basic pH and its low-humidity variant*. Acta Crystallographica Section D, 1999. **55**(4): p. 934-937.
22. Shekunov, B.Y., York, P., *Crystallization processes in pharmaceutical technology and drug delivery design*. Journal of Crystal Growth, 2000. **211**(1-4): p. 122-136.
23. Wang, W., *Instability, stabilization, and formulation of liquid protein pharmaceuticals*. International Journal of Pharmaceutics, 1999. **185**(2): p. 129-188.
24. Wang, W., *Protein aggregation and its inhibition in biopharmaceutics*. International Journal of Pharmaceutics, 2005. **289**(1): p. 1-30.

Chapter 3

3 Drying of mAb crystals

3.1 Introduction

Storage stability is a major issue during protein formulation development. Proteins are prone to chemical and physical degradation. To achieve long term stability during storage protein solutions are often stored at -80°C ¹⁻³. Despite the stabilizing feature to restrict molecular mobility low temperatures foster protein drug degradation by cold-denaturation⁴⁻⁶. Therefore, drying strategies are applied to avoid extensive protein exposure towards destructive temperatures. In addition to reduced protein mobility the water content is decreased in a dried product. Consequently, water mediated degradation processes such as hydrolysis, oxidation and aggregation are avoided or at least reduced^{7,8}. Commonly used drying techniques for biopharmaceuticals comprise freeze-drying, vacuum drying, spray drying and combined techniques such as spray-freeze drying⁸⁻¹².

The drying itself is a crucial procedure during development of stable solid biopharmaceuticals products. The loss of the hydration shell can cause protein unfolding and thus protein degradation⁶. Following, the drying technique and the drying regime have to be chosen carefully for each protein.

3.1.1 Freeze drying (lyophilization)

Freeze drying is the most often used drying technique for biopharmaceuticals⁸. During the drying step water is removed from a frozen solution by ice sublimation⁴. The features of lyophilization are a low primary drying temperature, the possibility for sterile process conditions and favorable rehydration properties due to a porous end-product¹³. However, a drying process which comprises additional freezing stresses can promote protein degradation by different pathways⁶:

- During the freezing step, protein and salt (e.g. buffer salt) concentrations can increase by ice crystal formation.
- Precipitation of a less water soluble buffering agent can provoke pH changes.
- The formation of ice / freeze concentrate interfaces represent another stress factor detrimental to protein stability¹⁴.

- Both, freezing stresses and drying stresses are known to alter protein secondary structure which finally can result in protein aggregation.

Finally, lyophilization represents a very unfavorable procedure from an economical point of view. It requires an elaborate process, an enormous amount of time and energy which lead to extensive production costs^{5,14,15}.

3.1.2 Vacuum drying

Vacuum drying represents a less time and energy consuming drying technique compared to freeze drying. Freezing steps are avoided and thus freezing associated protein degradation. However, the dry product does not show a porous matrix structure. It rather represents a rubber of high viscosity which finally reaches a glassy state and the end of the procedure. Protein concentrations are high in the rubber state and molecular motions are not hindered far enough to prevent physico-chemical protein drug degradation. Therefore, the process time should be as short as possible. Furthermore, the rubber state hinders convenient water evaporation and thus the total surface area is crucial for water evaporation and process times. Consequently, vacuum drying is usually carried out in low volume which is not suitable for large scale pharmaceutical production^{13,16}.

3.1.3 Spray drying

Spray drying can be performed continuously and thus is less time and cost consuming than freeze drying¹⁷. The final products are free flowing powders, granulates and agglomerates which are obtained from solutions, emulsions or pumpable suspensions¹⁸. However, powder yield is less compared to freeze drying¹⁹.

During spray drying, the liquid protein formulation is pumped to a nozzle. Rotary or nozzle atomizers generate small droplets which contact hot air in the drying chamber by formation of small solid particles. The inlet temperature usually exceeds 100°C which might be deemed detrimental to protein stability. Surprisingly, heat damage to proteins is reported negligible as the exposure to the high temperature is very short. The product duration in the drying chamber is longer and at lower temperatures (outlet temperature, often 50 – 70°C). Spray drying faces proteins to stresses such as shearing stresses in the nozzle, thermal stresses during drying and by formation of liquid/air interfaces during atomization. As for each drying technique, the drying itself might result in alteration of the protein secondary structure which can induce protein aggregation^{7,12,17,18}.

3.1.4 Spray-freeze drying

Spray-freeze drying combines the advantages of spray drying and freeze drying: a high yield of small drug particles which are formed at low temperatures.

During spray-freeze drying, the protein solution is atomized by a two-fluid or an ultrasonic nozzle and sprayed into a cryogenic medium such as liquid nitrogen where the droplets immediately freeze. Subsequently, the product is placed in a lyophilizer with pre-cooled shelves (usually -50 – -80°C) and undergoes a common freeze drying procedure. The protein drug faces varying stresses such as mechanical stresses during the spray drying step and freezing stress during the freeze drying step ^{7,12}.

3.1.5 Alternative drying methods suitable for protein crystals

Protein crystal suspensions open new possibilities for reaching dry biopharmaceutical products such as already described by Margolin et al ⁵. The crystals might be separated from the mother liquor by filtration and subsequent be air dried or by introduction of nitrogen. Alternatively, the supernatant can be exchanged with a volatile organic solvent such as ethanol or isopropanol followed by evaporation of this non-aqueous liquid ¹⁸. This procedure is already described for crystalline candida rugosa lipase suspended in cold isopropanol (4°C) and introduction of trehalose as additive ²⁰. However, this method is difficult to automatize. Loading and emptying remain hand-made which increases the risk for product contamination. Finally, this drying technique is foremost kinetically driven which results in a mixture of differently dried crystals (dry small crystals versus wet larger crystals). Therefore, Deusser et al. developed a machine that comprises centrifuge and dryer ²¹. This approach was shown to be applicable for insulin crystals. In brief, the insulin crystal suspension was filtrated and washed. The washing medium was replaced by a volatile organic solvent. The pellet was converted in fluid bed and introduced to nitrogen at 40°C. After one to four hours, the protein crystals were emptied into a container by nitrogen pressure. The best results were reported for mixtures of water and water miscible organic solvents such as methanol, ethanol, n-propanol and isopropanol as washing media. Applying of humid nitrogen allowed a thermodynamical control of the residual moisture which was following independent from the crystal size ²¹.

3.1.6 Stabilizing agents

Formulation scientists use cryoprotectants and lyoprotectants to stabilize proteins during freezing and drying procedures.

3.1.7 Cryoprotectants

Cryoprotectants such as sucrose, mannitol, trehalose, polyethylene glycol, Brij 30 and others are used to stabilize proteins during freezing processes. The stabilizing effect is ascribed to a preferential interaction. These interactions prevent the protein from conformational changes and denaturation upon freezing.^{6,22}

3.1.8 Lyoprotectants

Sucrose, trehalose, several amino acids and others are used as lyoprotectants. Upon lyophilization, the hydration shell of proteins is removed and thus the concept of preferential exclusion is no longer applicable. Two main hypotheses are still in discussion, the formation of an amorphous glass and the “water replacement hypothesis”. Formation of a glassy state hinders conformational protein motions which results in an increased protein stability. The “water replacement mechanism” involves the replacement of native protein-water hydrogen bonds by protein-excipient hydrogen bonds which prevents the protein from unfolding^{6,23}.

3.1.9 Chances of dry protein crystal material and challenges in producing it

A dry protein crystal material would potentially represent a pure, highly concentrated and convenient bulk storage form of superior stability¹⁶. The reduction of the water content and the formation of specific intermolecular interactions within a crystal lattice would reduce molecular motions and reactivity and thus would avoid or at least slow down protein drug degradation²⁴. This concept could be scrutinized by the need of protein crystals for a specific amount of intra-crystalline water to maintain protein stability. Consequently, crystals cannot be dried²⁵⁻²⁷. However, protein crystal drying even to low residual water contents by utilization of lyoprotectants is reported for crystalline glucose oxidase and *Candida rugosa* lipase^{20,28}.

Nevertheless, drying of protein crystals still remains challenging as crystal suspensions usually contain a mix of different crystal sizes with different amounts of solvent. In theory, an optimal drying time would have to be determined for each protein crystal to pre-

vent overdrying and protein degradation²¹. This can hardly be achieved by the common drying techniques for biopharmaceuticals. In addition, each of these drying techniques comprises specific challenges for protein crystal drying. Freeze drying would require crystal freezing during the drying procedure. Crystallographers already have shown that upon freezing the protein crystal lattice can easily be destroyed due to ice crystal formation. This destruction can result in the formation of a mix from amorphous and crystalline structures^{18,29}. Spray drying comprises high temperatures and harsh shear stresses which are detrimental for protein crystal stability. During the preliminary study, a low melting point between 60 and 80°C was shown for at least one mAb crystal¹⁶. Following, spray drying at inlet temperatures above 100°C and outlet temperatures between 50 and 70°C appears to be inappropriate for mAb crystal drying. Furthermore, the crystals would hardly maintain their shape during the shear stresses upon spray drying as they are known to be very soft and easy to crush^{26,30}. Spray-freeze drying would also not be an appropriate technique for mAb crystal drying. This technique comprises a combination of harmful conditions (e.g. shear stresses, freezing) for protein crystals from both techniques: spray- and freeze drying.

A vacuum drying procedure for mAb1 crystals has been presented by Stefan Gottschalk during the preliminary study. Within this study a small solvent screening was performed to identify suitable washing liquids in order to remove the mother liquor. The mAb1 crystals were found to remain stable in ethanol 85% which was subsequently applied as washing liquid. Sucrose was added as lyoprotectant. Only a low aggregate formation was reported for the vacuum-dried mAb1 crystals. However, compared to an amorphous mAb1 product the stability was less¹⁶.

In chapter 2, an alternative drying procedure for protein crystals is introduced. This method does not contain any freezing, heat or shear stresses and resulted in a free flowing powder. The most critical step is the identification of suitable (non-toxic, water miscible, volatile) washing liquids in which the crystal and the protein integrity would be maintained. Nevertheless, the introduced procedure is deemed promising for protein crystal drying.

Considering the aforementioned arguments, spray drying and spray-freeze drying were excluded from the present study. The introduced vacuum drying procedure for mAb1 was reproduced and protein stability was assessed. Freeze drying was investigated as

comparative drying procedure. Finally, it was the aim to transfer the presented hot-air drying technique from lysozyme to mAb1 and mAb2 crystals (see Chapter 2).

3.2 Materials and Methods

3.2.1 Materials

mAb1 and mAb2 were stored at - 80°C until required for use.

Sodium chloride (AnalaR NORMAPUR) as crystallization agent for lysozyme was purchased from VWR Prolabo (Leuven, Belgium). Sodium acetate (USP standard) was from Merck (Darmstadt, Germany). Sodium sulphate (99%) was from Grüssing GmbH (Filsum, Germany). Sodium dihydrogen phosphate-dihydrate (pure Ph. Eur., USP), disodium hydrogen phosphate-dihydrate (analytical grade), potassium dihydrogen phosphate and potassium chloride (both analytical grade) were obtained from Appli-chem GmbH (Darmstadt, Germany). PEG 4000S was from Clariant (Frankfurt a. M., Germany). Hydrochloric acid 32% (analytical grade), acetic acid 100 % and ortho-phosphoric acid 85% were all purchased from Merck KGaA (Darmstadt, Germany). Sodium azide (99%) was received from Acros Organics (New Jersey, USA). All other reagents or solvents used during the solvent screening were of at least analytical grade and purchased either from Sigma-Aldrich (Taufkirchen, Germany) or from VWR Prolabo (Leuven, Belgium).

3.2.2 Methods

3.2.2.1 Crystallization of mAb1

Crystallization of mAb1 was carried out in a 0.1 M sodium acetate buffer at a pH of 5.50. For crystallization, a 24% (w/v) PEG 4000 solution was added dropwise in a 1:1 ratio to a 10 mg/mL protein solution under gentle shaking. The final formulation was stored at 20°C for at least two weeks.

3.2.2.2 Crystallization of mAb2

Crystallization of mAb2 was performed in a 0.1 M sodium acetate buffer of 4.1. For crystallization, a 4.2 M sodium dihydrogen phosphate solution was added dropwise in a 1:1 ratio to a 10 mg/mL protein solution under gentle shaking. The final formulation was stored at 20°C for at least one week.

3.2.2.3 Solvent screening

Solubility and stability of mAb1 and mAb2 crystals in different organic solvents were assessed by transferring the crystals into the respective organic solvent (three times centrifugation, replacement of supernatant with respective solvent). After each washing step, the crystal integrity was verified microscopically. A dissolution test in isotonic 10 mM phosphate buffer solution (PBS) at pH 7.4 was performed at the end of the washing procedure.

3.2.2.4 Drying of protein crystals

3.2.2.4.1 Vacuum drying

Vacuum drying of mAb1 crystals was performed according to the procedure introduced by Stefan Gottschalk during the preliminary study¹⁶. The mAb1 crystals were washed with 22% PEG solution in 0.1 M sodium acetate buffer at a pH of 5.5 by three times of centrifugation (15 min) in a Sigma® 4K15 centrifuge at 4,000 rpm and subsequent replacement of the supernatant. After that, this procedure was repeated with EtOH 85% at 2°C. Finally, the pellet was suspended in 200 µl, 2°C cold EtOH 85% which contained 5% (w/v) sucrose. The protein concentration of the suspension was set to 100 mg/ml. Vacuum drying was carried out in a Martin Christ Epsilon 2-6 D pilot freeze dryer which was connected to a Vacuubrand CVC 2000 vacuum pump. The temperature was set to 2°C for 3 h at 20 mbar followed by 14 h at 0.1 mbar.

3.2.2.4.2 Inert gas drying

Inert gas drying was performed in a Barkey® Hot-Air Dryer “Flowtherm” (Leopoldshöhe, Germany). The system consists of a heater that allows the tempering of a nitrogen gas stream (upper part) and a bottom heater for the sample (lower part). 300 µL of the crystal slurry were filled into 2R glass vials and placed into the sample holder. The nitrogen gas stream (10 L/min) was tempered to 30°C and guided through a needle into 10 vials. The bottom heater was set to 20°C. After drying, the vials were closed and sealed.

3.2.2.4.3 Freeze Drying

Freeze drying of the mAb crystal suspensions was performed using a Christ Epsilon 2-6D pilot scale freeze dryer (Christ, Osterode am Harz, Germany). 1 mL of the crystal suspensions were filled into 2R glass vials and semi stoppered. Subsequently, the tem-

perature was decreased to - 40°C at a rate of 1°C/min and was held for 1h and 10min. In the last 10 min pressure was reduced to 0.08 mbar. In the next step, temperature was increased to - 10°C at a rate of 1°C/min and held for 16.66 h. Finally, temperature was increased to 25°C at a rate of 0.15°C/min and held for 10 h. At the end of the drying cycle the chamber was aerated with nitrogen and the vials were stoppered automatically within the chamber. The samples were stored until analytical examination at 2-8°C.

3.2.2.5 Assessment of crystal and protein integrity

3.2.2.5.1 Size exclusion high performance liquid chromatography (SE-HPLC)

Total protein release was determined by SE-HPLC. The analysis was performed on a Thermo separation system

3.2.2.5.1.1 mAb1

The mobile phase for mAb1 consisted of 0.092 M Na₂HPO₄ (anhydrous) and 0.211 M Na₂SO₄ (anhydrous) at a pH of 7. The flow rate was set to 0.25 mL/min. Analysis was performed at the wavelengths of 214 nm and 280 nm. A TSKgel G300SWXL coloum from Tosoh Bioscience GmbH (Stuttgart, Germany) was used for separation.

3.2.2.5.1.2 mAb2

The mobile phase for mAb2 consisted 0.02 M Na₂HPO₄ (dihydrate) und 0.15 M sodium chloride at a pH of 7.5. The flow rate was set to 0.50 mL/min. Analysis was performed at the wavelengths of 214 nm and 280 nm. For separation, a Suprose-6-HR-10/30-coloum from GE Healthcare (Uppsala, Sweden) was used.

3.2.2.5.2 Microscopic examination

The crystal integrity was determined microscopically using a Nikon Labophot equipped with a JVC TK-C1381 color video camera and the Screen Measurement / Comet – Software Version 3.52a. Glass cover slides were used for sample preparation. A polyrization filter was used to assess the crystalline state of the samples. Examination was performed at 200 fold magnification.

3.2.2.5.3 Nephelometry

Turbidity was measured using a Nephla Dr. Lange turbidimeter (Dr. Lange GmbH, Düsseldorf, Germany) by 90° light scattering at a wavelength of $\lambda = 860$ nm (Ph. Eur.

2.2.1). Results are given in formazine normalized units. Crystals were dissolved in phosphate buffer solution (0.01M, pH 7.4, isotonic) (PBS) and concentration was set to 1 mg/mL. 2 mL of each sample were filled into round glass cuvettes and placed into the sample holder.

3.2.2.5.4 Particle counting

Size and amount of particles between 1 and 200 μm were determined using a PAMAS SVSS-C40 (PAMAS GmbH, Rutesheim, Germany) light blockage system. Particles were counted classified into 16 different size ranges. Crystals were dissolved in PBS and concentration was set to 1 mg/mL. The number of measurements was set to three for each sample with a measuring volume of 0.3 ml. The rinsing volume was 0.5 ml.

3.3 Results

3.3.1 mAb1 and mAb2 crystal properties

In accordance to the presented concept in Chapter 2, handling properties and mechanical stability of mAb1 and mAb2 crystals were assessed to prevent crystal damage during the drying procedure. Therefore, pipetting was performed 1 -, 5 -, and 20 times by applying different pipette tips with the volumes of 10 μ L, 200 μ L, and 1000 μ L. Neither for mAb1 nor for mAb2 crystals were any debris or damages observed (not shown). Following, no limitations caused by pipetting had to be taken into account during the course of the present study.

Centrifugation was again chosen as surrogate to examine the mechanical properties of the crystals. In brief, the maximal force during the study was 25,150 x g which represented the technical limit of the Sigma® 4K15 centrifuge. This speed was chosen as starting point for the study. Three cycles of 10 min centrifugation were performed at a respective speed. The spin speed was reduced if the respective mAb crystal broke during any of the three cycles.

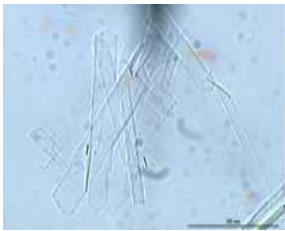
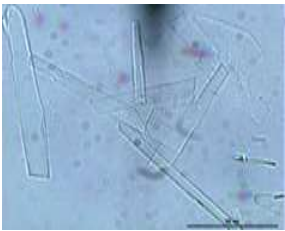
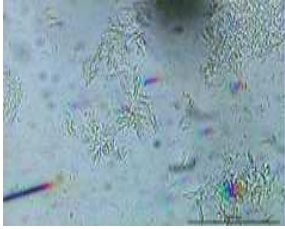
Initial state before centrifugation	Crystal state at respective centrifugation speed limit	Crystal state at higher centrifugation speed
 untreated mAb1	 1,789 x g	 7,155 x g *
 untreated mAb2	 1,789 x g	 4,025 x g

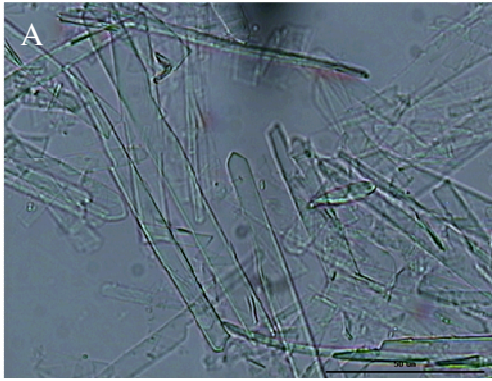
Figure 3-1 Light microscopic pictures which show the crystal's condition after three rounds of centrifugation at the respective spin speed. The scale bar represents 50 μ m.

Both mAb crystals remained stable up to 1,789 x g which was set as centrifugation speed limit during the course of the present study (Fig. 3-1). Above this spin speed, the mAb1 crystals broke while the mAb2 crystals started to disintegrate by losing their sea urchin like structure.

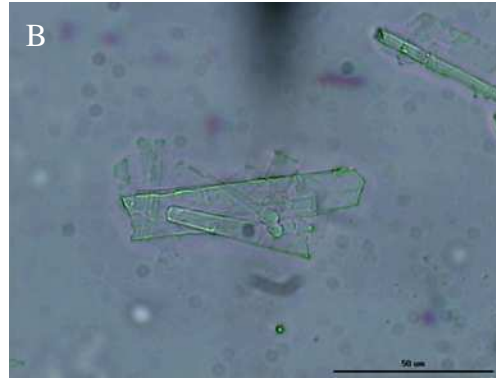
3.3.2 Reproducibility of the vacuum drying approach for mAb1 crystals

The vacuum drying procedure for mAb1 crystals introduced by Stefan Gottschalk was assessed for reproducibility and protein stability. The reported results suggested a promising starting point for further studies on mAb crystal drying¹⁶. In brief, mAb1 crystals were washed with a 22% (w/v) PEG 4000 solution and subsequent with ethanol 85% at 2°C. Finally, the pellet was suspended in 2°C cold EtOH 85% which contained 5% (w/v) sucrose.

SE-HPLC measurements revealed an aggregate formation of around 4% after drying and crystal dissolution in PBS. X-ray analysis of the crystal suspension prior to drying and after drying was performed externally. The results could not confirm the crystalline character neither for the suspension nor for dried crystals (not shown). The findings were in accordance to the results of the preliminary study¹⁶. However, light microscopic observations revealed a reduction in the count and the size of the crystals and the crystals appeared more transparent (Fig. 3-2 A & B). Total protein recovery detected by SE-HPLC analysis was reduced by approximately 25% and no free flowing powder was obtained by this procedure (Fig. 3-2 C). However, a free flowing powder could be generated by scratching the film with a spatula. By exert of pressure, the film burst into smaller pieces by forming a free flowing powder (Fig. 3-2 D). SE-HPLC analysis of the treated powder revealed a slight increase in aggregate formation of about 2%.



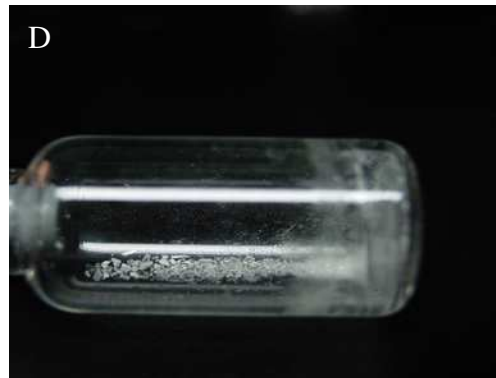
Before the vacuum drying procedure



After the vacuum drying procedure



Film after vacuum drying



Free flowing powder after film treatment

Figure 3-2 mAb1 crystals in their mother liquor before washing and drying and after washing with a sucrose-ethanol 85% mixture and subsequent vacuum drying (B, suspended in a 24 (w/v) PEG 4000 solution). Picture C shows the vacuum-dried product immediately after drying while picture D shows a free flowing powder after film treatment with a spatula. The scale bar represents 50 μm .

Table 3-1 shows the results regarding crystal size, crystal quality and achievement of a free flowing powder from the present study compared the preliminary study.

Table 3-1 Results from the reproduction experiment of the vacuum drying approach for mAb1 crystals compared to the results from the preliminary study ¹⁶.

	Present study	Preliminary study
Proof of crystallinity	No	No
Crystal size	Reduced	Not described
Aggregate fraction	3 - 4 %	2 - 3 %
Protein recovery	~ 75 %	Not described
Free flowing powder	No	Yes

3.3.3 Solvent screening for mAb1 and mAb2 crystals

To distinguish between the effect of the washing and the vacuum drying procedure on protein integrity, SE-HPLC measurements were performed to determine the aggregate fraction of total protein and the total protein recovery after washing with different concentrations of ethanol and isopropanol at 2°C. Both liquids were chosen as they were already stated to be applicable washing liquids for mAb1 crystals¹⁶. However, a stability based choice of the washing liquid had not been performed during the preliminary study. Ethanol has been preferred as it is already FDA approved for parenteral use¹⁶. Sucrose as additive was excluded from the study as it functions foremost as lyoprotectant and a stabilizing effect during the washing step was not anticipated. The same test was performed for a mAb1 solution (5 mg/mL) and amorphous mAb1 which was produced by freeze drying to highlight the effect of the crystalline state on protein integrity preservation. The formulation of the freeze-dried product was 5 mg/mL mAb1, 50 mg/mL sucrose in a 50 mM sodium acetate buffer pH 5.50. For the experiment, the total protein recovery was set to 100% for reference samples (mAb1 solution, crystals and lyophilisates) which were not treated with any organic solvent. Prior to analysis, the crystals and lyophilisates were dissolved in PBS.

The results showed significantly decreased total protein recoveries for all samples after washing with the organic solvent. The lowest total protein recovery was found for samples washed with ethanol. Interestingly, these samples showed only small aggregate levels (Tab. 3-2). After washing with isopropanol protein recovery was less reduced, but more aggregates could be detected (Tab. 3-2 & 3-3). Regarding total protein recovery and aggregate formation, mAb1 crystals showed the highest resistance against both liquids while freeze-dried mAb1 was prone to aggregation. Notably, protein recovery of the 85% ethanol washed crystals was reduced about 23% which confirmed the above-mentioned results (Tab. 3-1).

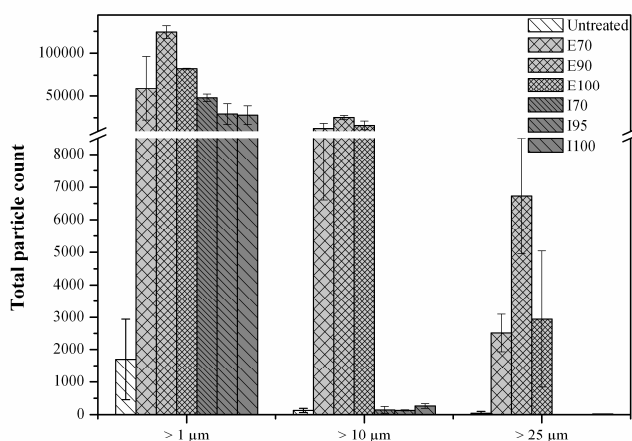
Table 3-2 Aggregate content and total protein recovery of mAb1 crystals, mAb1 in solution and freeze-dried mAb1 after incubation with different ethanol concentrations at 4°C.

Ethanol concentration [%]	mAb1 crystals		mAb1 solution		Freeze-dried mAb1	
	Aggreg. content [%]	Total protein recovery [%]	Aggreg. content [%]	Total protein recovery [%]	Aggreg. content [%]	Total protein recovery [%]
70	0.3	91.5	2.6	41.0	1.6	26.4
75	0.5	87.4	2.6	41.6	2.1	28.0
80	0.7	83.8	4.4	35.6	2.5	29.0
85	1.0	77.4	2.4	31.3	3.1	32.2
90	0.5	71.8	3.5	32.6	4.6	31.2
95	0.3	67.1	3.9	33.3	7.4	31.4
100	0.8	63.8	-	-	-	-

Table 3-3 Aggregate content and total protein recovery of mAb1 crystals, mAb1 in solution and freeze-dried mAb1 after incubation with different isopropanol concentrations at 4°C.

Isopropanol concentration [%]	mAb1 crystals		mAb1 solution		Freeze-dried mAb1	
	Aggreg. content [%]	Total protein recovery [%]	Aggreg. content [%]	Total protein recovery [%]	Aggreg. content [%]	Total protein recovery [%]
70	2.5	83.3	3.8	92.3	4.8	88.0
75	2.1	91.4	3.9	97.5	5.0	86.6
80	2.1	87.5	4.2	94.6	5.2	86.0
85	4.6	94.2	6.0	96.3	5.2	85.4
90	4.0	87.5	4.0	94.9	5.4	83.0
95	4.4	90.2	5.5	92.0	8.1	80.4
100	6.7	84.3	-	-	-	-

The SE-HPLC results were confirmed by light obscuration and turbidity measurements. Samples washed with ethanol showed significantly higher total particle counts as well as a significantly higher turbidity (Fig. 3-3).



Washing liquid	Turbidity [FNU]
Buffer	0.3
Untreated	0.6
E 70	4.5
E 90	9.2
E 100	6.6
I 70	1.2
I 95	1.8
I 100	1.2

Figure 3-3 Selective results for the total particle count obtained from light obscuration measurements and the turbidity after washing mAb1 crystals with different ethanol and isopropanol concentrations. The crystals were dissolved in PBS prior to analysis.

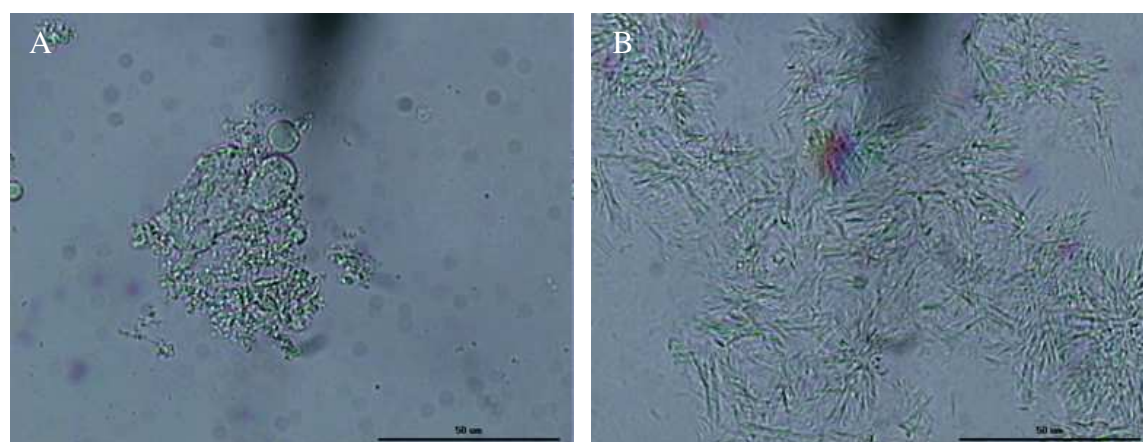
Consequently, the washing procedure was considered to be foremost responsible for the observed protein instability. Different washing liquids were to be found. Therefore, an extensive solvent screening was performed for mAb1 and mAb2 crystals.

During exposure to a suitable organic washing liquid the crystal and protein integrity has to remain unaffected. Therefore, the same solvent screening procedure as for lysozyme crystals was performed including microscopic observations during the washing procedure (see Chapter 2). A dissolution test in PBS was conducted at the end of the washing procedure to identify severe aggregation inside the crystals or at their surfaces. Such an aggregation is already reported to hinder protein crystal dissolution^{2,31}. Finally, aggregate analysis of the dissolved protein was performed after passing the solubility test by SE-HPLC, light obscuration and turbidity.

As for the lysozyme crystals, a high number of solvents were examined (see Chapter 2). However, only a small number of organic washing liquids passed the solubility test as well as a subsequent aggregate analysis.

Among other solvents, mAb2 crystals were insoluble after washing with different concentrations of ethanol or isopropanol. For these two liquids, a severe protein aggrega-

tion was already stated during the preliminary study and thus mAb2 crystals were excluded from the vacuum drying approach ¹⁶. After washing, the crystal integrity was affected and protein precipitation could be observed (Fig. 3-4 A). In contrast, the crystal shape was maintained during washing with ethyl acetate, acetyl acetone, triacetine and triethyl citrate (Fig. 3-4 B). Protein recovery, aggregate formation and total particle count gave no hint for protein degradation (not shown). Acetyl acetone, triacetine and triethyl citrate were considered to be inappropriate for drying processes due to their high boiling temperatures and their low water miscibility.



mAb2 crystal state after washing with ethanol 90 %

mAb2 crystal state after washing with ethyl acetate

Figure 3-4 Light microscopic pictures of mAb2 crystals after washing with ethanol 90% (A) and ethyl acetate (B). The scale bar represents 50 µm.

Except of ethyl acetate, different promising solvents were found for mAb1 crystals as for mAb2 crystals (Tab 3-4). Again, only ethyl acetate remained as promising washing liquid as a severe aggregate formation was observed after washing with isopropanol and ethanol (Tab. 3-2 & 3-3).

Table 3-4 Applicable washing liquids for mAb1 and mAb2 crystals. The crystals remained soluble in PBS after washing with the solvents listed.

mAb1	mAb2
Ethyl acetate	Acetyl acetone
Ethanol	Ethyl acetate
Isopropanol	-
	-
	Triacetine
	Triethyl citrate

During extensive washing with ethyl acetate, mAb1 and mAb2 crystal aggregation was observed. The same phenomenon was already described for lysozyme crystals (see Chapter 2). However, the mAb crystal agglomeration was irreversible (not shown). Drying after crystal washing with ethyl acetate was considered to be impossible.

3.3.4 Hot-Air drying of mAb1 crystals

Nevertheless, mAb1 crystals should be dried as straight-forward approach in accordance to the approach presented in Chapter 2. Therefore, mAb1 crystals were washed with different ethanol and isopropanol concentrations of up to 95% and placed in the Barkey® Hot-Air Dryer (see Chapter 2). The drying set-up was the same as for the lysozyme crystals, only the nitrogen gas stream was not heated.

For all samples, a glassy material of high viscosity was obtained. After prolonging the drying time up to one week, a thin powder like film was obtained which did not contain any crystals as assessed microscopically after sample reconstitution with a 24% (w/v) PEG 4000 solution.

3.3.5 Freeze drying

Finally, freeze drying was assessed as comparative drying technique for mAb crystals. Therefore, mAb1 and mAb2 crystals were either lyophilized in their mother liquor or after transfer into a 23% (w/v) PEG 4000 solution. As the freezing rate is described to affect the size and number of ice crystals which potentially can destruct the protein crystals upon freezing, the mAb suspensions were either slowly frozen during the lyophilization cycle or alternatively, quickly pre-frozen by dipping into liquid nitrogen⁶. The samples were visually inspected before and after drying for their crystalline character by

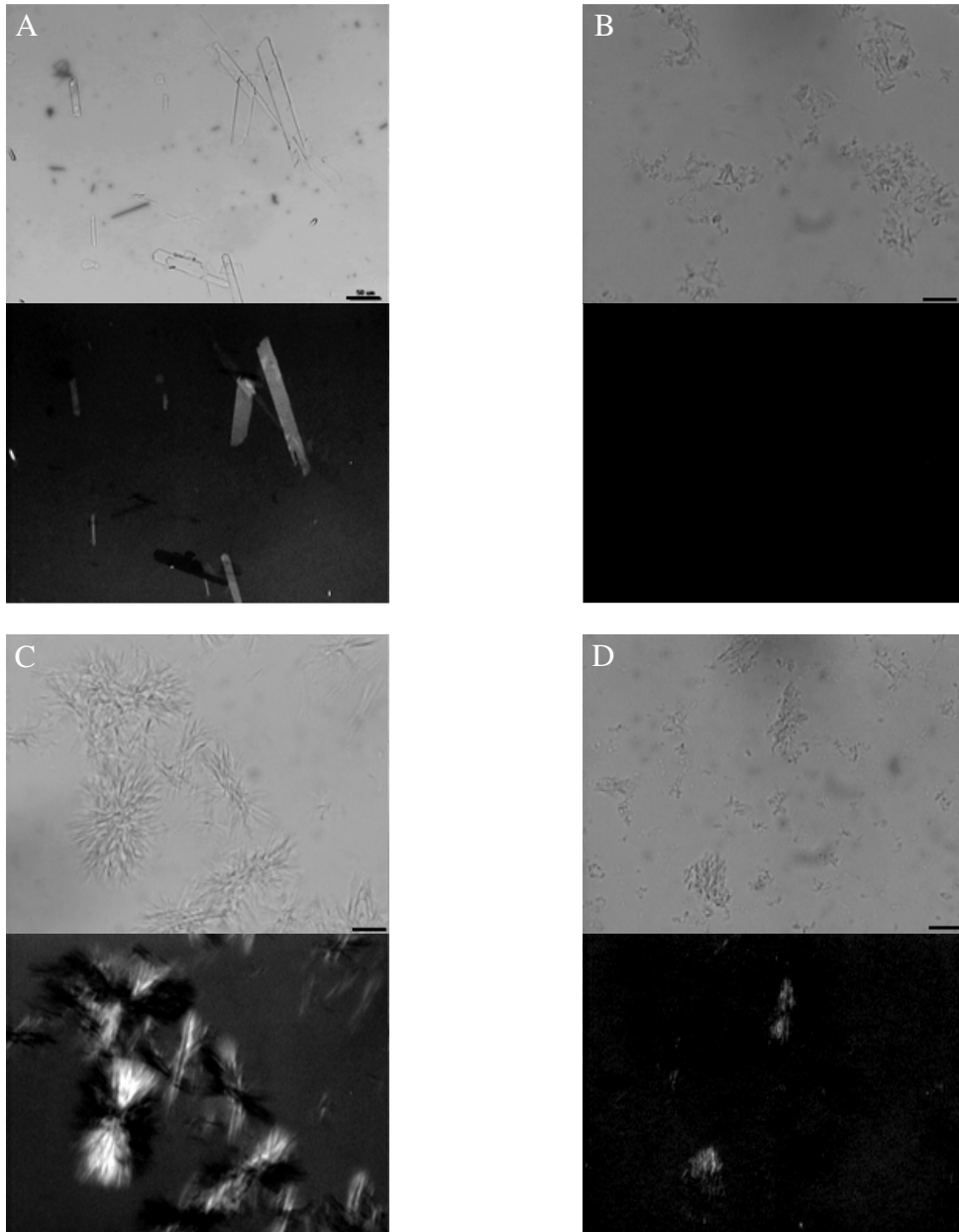
light microscopy with and without polarization filter (Fig. 3-5). Sample reconstitution was performed by replacing the calculated loss in weight after drying with the same amount of highly purified water.

The product cakes appeared pharmaceutically elegant after freeze drying of mAb1 and mAb2 crystals in PEG 4000 solutions. The product cake for the samples dried in the mother liquor was collapsed.



Figure 3-5 Photographic picture of the freeze-dried product after mAb crystal drying in a 23% (w/v) PEG 4000 solution (left) and in the mother liquor (right).

The crystalline state was confirmed before freeze drying by applying the polarization filter (Fig. 3-6 A & C). The mAb crystals appeared as bright structures and thus showed the birefringent behavior of a crystal state. After freeze drying, the crystals were optically destroyed and light polarization could no longer reveal crystallinity of the products (Fig. 3-6 B & D). Notably, the presented results were independent from the applied freezing rate.



Before freeze drying

After freeze drying

Figure 3-6 Light microscopic pictures of mAb1 and mAb2 crystals before freeze drying (A & C) and after freeze drying (B & D). To assess the crystalline character of the samples, light microscopy was performed with (upper pictures) and without (lower pictures) polarization filter.

3.4 Discussion

It is already emphasized in literature that drying of crystals from biopharmaceuticals is complicated^{25,26}. A certain amount of residual intra crystalline water is required to maintain the protein integrity even in its crystalline state^{25,26}. Standard drying techniques for biopharmaceuticals such as freeze drying are assumed to be inappropriate for protein crystals^{18,21,29}. This was confirmed during the present study already in Chapter 2 for lysozyme crystals, but also for both mAb crystals within this chapter. In all cases, crystal breakage was observed after freeze drying independent from the applied carrier matrix. Obviously, ice crystal formation within the protein crystals and thus volume expansion led to crystal destruction by formation of amorphous structures^{18,29}. Even smaller ice crystals obtained by fast sample freezing by dipping into liquid nitrogen can destroy the crystalline state.

The presented vacuum drying approach for mAb1 crystals was found to be inappropriate as it affects the protein integrity. The question whether the crystalline state was conserved or not still remains unanswered. X-ray analysis was not successful most probably due to the low internal order of the protein crystals²⁶. The reduced crystal sizes obtained after drying suggest crystal dissolution during the drying procedure. The reduction of birefringence, which also was already presented by the preliminary study, further confirms a loss in protein crystallinity. The significant loss in protein integrity might be caused by water replacement with organic liquid or crystal dissolution and thus protein denaturation within the organic solvent. Nevertheless, compared to mAb1 in solution and to its amorphous state, the crystals showed higher protection of the protein integrity upon contact to organic liquid.

Similar to the needle shaped lysozyme crystals (Chapter 2), only a small number of applicable organic washing solvents were found for both mAb crystals. Some liquids had to be excluded due to their high boiling temperatures (triacetone, triethyl citrate) or as they fostered crystal agglomeration during extensive washing procedures (ethyl acetate). This finding confirmed that a needle shaped protein crystal represents a very unfavorable polymorph which is unfortunately common for antibodies³². Only few intermolecular bindings are present within such a crystal and thus stabilization of the crystalline state itself as well as of the protein integrity is small³³. The concept study presented in Chapter 2 demonstrates the need to identify and characterize different crystal poly-

morphs. Unfortunately, further mAb1 and mAb2 morphologies were not found (see Chapter 4). This limited the possibilities for a convenient drying study.

3.5 Conclusion

No satisfying drying procedure for mAb crystals could be developed. Protein crystal drying remains a challenging approach which has to be assessed individually for each protein drug crystal. Common drying techniques for biopharmaceuticals such as vacuum drying or freeze drying comprise the risk for product overdrying and crystal destruction. As most suitable drying approach for protein crystals appears the replacement of the mother liquor with a volatile organic liquid which is subsequently evaporated. Ethanol and isopropanol are identified as the most suitable washing liquids. A stable crystal polymorph is required which is insoluble in the organic solvent and conserves the protein integrity. Generation of such a crystal might demand an extensive polymorph screening.

3.6 References

1. Wang, W., Nema, S., Teagarden, D., *Protein aggregation--Pathways and influencing factors*. International Journal of Pharmaceutics, 2010. **390**(2): p. 89-99.
2. Wang, W., *Instability, stabilization, and formulation of liquid protein pharmaceuticals*. International Journal of Pharmaceutics, 1999. **185**(2): p. 129-188.
3. Manning, M.C., Chou, D.K., Murphy, B.M., Payne, R.W., Katayama, D.S., *Stability of protein pharmaceuticals: an update*. Pharmaceutical Research, 2010. **27**(4): p. 544-575.
4. Frokjaer, S., Otzen, D.E., *Protein drug stability: a formulation challenge*. Nature Reviews Drug Discovery, 2005. **4**(4): p. 298-306.
5. Margolin, A.L., Khalaf, N.K., Clair, N.L.S., Rakestraw, S.L., Shenoy, B.C., *Stabilized protein crystals formulations containing them and methods of making them*. 2003, US Patent 6,541,606 B2.
6. Wang, W., *Lyophilization and development of solid protein pharmaceuticals*. International Journal of Pharmaceutics, 2000. **203**(1): p. 1-60.
7. Maa, Y.-F., Nguyen, P.-A., Andya, J.D., Dasovich, N., Sweeney, T.D., Shire, S.J., Hsu, C.C., *Effect of spray drying and subsequent processing conditions on residual moisture content and physical/biochemical stability of protein inhalation powders*. Pharmaceutical Research, 1998. **15**(5): p. 768-775.
8. Franks, F., *Freeze-drying of bioproducts: putting principles into practice*. European Journal of Pharmaceutics and Biopharmaceutics, 1998. **45**(3): p. 221-229.
9. Jameel, F., Pikal, M.J., *Design of a Formulation for Freeze Drying*. Formulation and Process Development Strategies for Manufacturing Biopharmaceuticals, 2010: p. 459.
10. Kumar, V., Sharma, V.K., Kalonia, D.S., *In situ precipitation and vacuum drying of interferon alpha-2a: Development of a single-step process for obtaining dry, stable protein formulation*. International Journal of Pharmaceutics, 2009. **366**(1): p. 88-98.
11. Searles, J., Mohan, G., *Spray drying of biopharmaceuticals and vaccines*. Formulation and Process Development Strategies for Manufacturing Biopharmaceuticals, 2010: p. 739-761.
12. Saluja, V., Amorij, J., Kapteyn, J., de Boer, A., Frijlink, H., Hinrichs, W., *A comparison between spray drying and spray freeze drying to produce an influenza subunit vaccine powder for inhalation*. Journal of Controlled Release, 2010. **144**(2): p. 127-133.

13. Willmann, M., *Stabilisierung von pharmazeutischen Proteinlösungen durch Vakuumtrocknung*. Thesis Munich, 2003.
14. Tang, X.C., Pikal, M.J., *Design of freeze-drying processes for pharmaceuticals: practical advice*. *Pharmaceutical Research*, 2004. **21**(2): p. 191-200.
15. Jovanović, N., Bouchard, A., Hofland, G.W., Witkamp, G.-J., Crommelin, D.J., Jiskoot, W., *Stabilization of proteins in dry powder formulations using supercritical fluid technology*. *Pharmaceutical Research*, 2004. **21**(11): p. 1955-1969.
16. Gottschalk, S., *Crystalline Monoclonal Antibodies: Process Development for Large Scale Production, Stability and Pharmaceutical Applications*. Thesis Munich, 2008.
17. Yoshii, H., Neoh, T.L., Furuta, T., Ohkawara, M., *Encapsulation of proteins by spray drying and crystal transformation method*. *Drying Technology*, 2008. **26**(11): p. 1308-1312.
18. Shenoy, B., Govardhan, C.P., Yang, M.X., Margolin, A.L., *Crystals of whole antibodies and fragments thereof and methods for making and using them*. 2010, US Patent 7,833,525 B2.
19. Maa, Y.F., Nguyen, P.A.T., Hsu, S.W., *Spray-drying of air-liquid interface sensitive recombinant human growth hormone*. *Journal of Pharmaceutical Sciences*, 1998. **87**(2): p. 152-159.
20. Shenoy, B., Wang, Y., Shan, W., Margolin, A.L., *Stability of crystalline proteins*. *Biotechnology and Bioengineering*, 2001. **73**(5): p. 358-369.
21. Deusser, R., Kraemer, P., Thurow, H., *Process for drying protein crystals*. 2002, US Patent 6,408,536.
22. Arakawa, T., Prestrelski, S.J., Kenney, W.C., Carpenter, J.F., *Factors affecting short-term and long-term stabilities of proteins*. *Advanced Drug Delivery Reviews*, 2001. **46**(1): p. 307-326.
23. Furlán, L.T.R., Lecot, J., Padilla, A.P., Campderrós, M.E., Zaritzky, N.E., *Calorimetric Study of Inulin as Cryo-and Lyoprotector of Bovine Plasma Proteins*. Elkordy, A.A., Editor. 2013, InTech. p. 197-218.
24. Margolin, A.L., Navia, M.A., *Protein crystals as novel catalytic materials*. *Angewandte Chemie International Edition*, 2001. **40**(12): p. 2204-2222.
25. Matthews, B.W., *Solvent content of protein crystals*. *Journal of Molecular Biology*, 1968. **33**(2): p. 491-497.
26. McPherson, A., *Introduction to protein crystallization*. *Methods*, 2004. **34**(3): p. 254-265.
27. McPherson, A., *Crystallization of biological macromolecules*. Vol. 586. 1999: Cold Spring Harbor Laboratory Press Cold Spring Harbor, NY.

28. Nagendra, H., Sukumar, N., Vijayan, M., *Role of water in plasticity, stability, and action of proteins: the crystal structures of lysozyme at very low levels of hydration*. *Proteins: Structure, Function, and Bioinformatics*, 1998. **32**(2): p. 229-240.
29. Garman, E.F., Schneider, T.R., *Macromolecular cryocrystallography*. *Journal of applied crystallography*, 1997. **30**(3): p. 211-237.
30. Jen, A., Merkle, H.P., *Diamonds in the Rough: Protein Crystals from a Formulation Perspective*. *Pharmaceutical Research*, 2001. **18**(11): p. 1483-1488.
31. Wang, W., *Protein aggregation and its inhibition in biopharmaceutics*. *International Journal of Pharmaceutics*, 2005. **289**(1): p. 1-30.
32. Hekmat, D., Hebel, D., Schmid, H., Weuster-Botz, D., *Crystallization of lysozyme: From vapor diffusion experiments to batch crystallization in agitated ml-scale vessels*. *Process Biochemistry*, 2007. **42**(12): p. 1649-1654.
33. Durbin, S., Feher, G., *Protein crystallization*. *Annual Review of Physical Chemistry*, 1996. **47**(1): p. 171-204.

Chapter 4

Statement: Within this chapter, the work related to section 4.3.3 includes results from the Master thesis “Impact of high hydrostatic pressure on the dissociation of protein aggregates and protein crystallization” by Benjamin Werner, LMU Munich, 2012. The results within section 4.3.3 are expressed in figures (4-7 – 4-18) and tables (4-3 – 4-11) which were reproduced in a modified form from the Master thesis.

The Master thesis has been planned, structured and carried out under my direct supervision. The results obtained and the conclusions drawn have been discussed under my supervision.

4 Different strategies to obtain mAb crystal polymorphs with higher stability

4.1 Introduction

Chapter 2 demonstrates a model approach from protein crystallization to a dry and stable crystalline product. The feasibility of this concept has been shown for the non-therapeutic lysozyme protein. An easy transfer to both antibodies was restricted already at the starting point. No crystal polymorphs and a constant aggregate formation for both proteins, mAb1 and mAb2, were reported by the preliminary study ¹. The protein instability was at least partially ascribed to the needle-like crystal morphology (see Chapter 1). Needle-like structures represent a very common shape for antibody crystals and were considered to be a very unfavorable polymorph ². Only few inter-molecular interactions are required to form such a crystal. The number of these interactions determines crystal attributes such as manufacturing, handling and pharmacokinetic properties. The latter are dependent on the solubility and dissolution kinetics which are reported to be very fast for mAb1 and mAb2 crystals ^{1,3-5}. This indicates low numbers of protein-protein interactions within the crystal lattice for both mAb crystals. The extent of protein stabilization in the crystalline state is probably also dependent on the number of inter-molecular interactions ⁶. For certain IgG crystals, free moving protein residues and unordered protein packages within the crystal lattice were reported in literature ⁷. These IgG crystal attributes might result in protein drug degradation even in the crystalline state. Consequently, higher protein stability was anticipated for different crystal polymorphs which exhibit higher numbers of inter-molecular interactions ^{1,6}.

Different approaches were already reported in literature to alter protein crystal morphologies. These approaches comprise foremost the modification of the crystallization temperature or the pH of the crystallization buffer. In addition, applying of additives or agitation during the crystallization process is also described as strong tool to create protein crystal polymorphism.

The crystallization temperature and the crystallization buffer pH directly influence protein interactions ^{3,8}. By alteration of these parameters, the number of protein-protein interactions might be influenced and thus the crystal shape. Especially the buffer pH is a strong tool as it affects the protein surface charges and the protein solubility ^{3,8}. Alteration of the crystallization temperatures, applying of temperature shifts or agitation dur-

ing the crystallization process result in altered crystal growth kinetics and thus potentially different crystal morphologies^{9,10}. The effects of additives are more complicated and dependent on the type of additive used. Dependent on the utilized class the protein interactions are either mediated directly by electrostatic interactions, covalent interactions, H-bondings or indirectly by modulating solvent properties¹¹⁻¹⁴.

Another approach to change the protein crystal morphology comprises the application of high hydrostatic pressure. Lorber et al. have already shown the transition from tetragonal lysozyme crystals to a needle form under increased pressure levels¹⁵. Despite the fact that protein crystallization under high hydrostatic pressure has been extensively investigated especially for lysozyme, it has not been described for antibodies, yet¹⁶⁻²³. Another specific attribute of high pressure is its feature to dissociate protein aggregates and oligomers by reducing hydrophobic and electrostatic protein interactions²⁴⁻²⁶. The protein agglomerates can be dissociated even at high protein concentrations with a high yield and without utilization of denaturing agents and any filtration or dilution steps. These features makes it potentially a superior approach²⁷⁻²⁹. Such a dissociation has already been demonstrated amongst others for human growth hormone, β -lactamase, nuclear receptors and enolase^{25,27,30,31}. However, pressure induced protein unfolding is also described at pressures above 400 MPa³¹⁻³⁵. So far, this technique has not been applied to antibodies or antibody crystals.

mAb1 and mAb2 were crystallized with the lead conditions of the preliminary study introduced by Stefan Gottschalk (see Chapter 1). A constant aggregate formation even in the crystalline state was followed over one year. This instability was ascribed to the unfavorable mAb1 and mAb2 crystal morphology. Therefore, several strategies to alter the crystallization conditions were investigated in order to find stable mAb1 and mAb2 crystal polymorphs. New polymorphs should be crystallized by alteration of the crystallization temperature and the pH of the crystallization buffer. Another approach was the addition of additives to the crystallization formulation or the application of agitation during crystallization. Finally, high hydrostatic pressure was introduced as new tool for mAb crystallization. This technique was investigated for its ability to allow for growing new mAb1 and mAb2 crystal polymorphs as well as to dissociate protein aggregates within the crystal suspensions.

4.2 Materials and Methods

4.2.1 Materials

mAb1 and mAb2 were two monoclonal antibodies from the IgG1 class. The samples were stored at - 80°C (antibodies) until required for use.

Sodium acetate (USP standard) was from Merck (Darmstadt, Germany). Ammonium sulphate (99%) was from Gruessing (Filsun, Germany). Sodium dihydrogen phosphate-dihydrate (pure Ph. Eur., USP), disodium hydrogen phosphate-dihydrate (analytical grade), potassium dihydrogen phosphate and potassium chloride (both analytical grade) were obtained from Applichem GmbH (Darmstadt, Germany). PEG 4000S, 6000P, 8000P, 10000P were from Clariant (Frankfurt a. M., Germany). Hydrochloric acid 32% (analytical grade), acetic acid 100% and ortho-phosphoric acid 85% were all purchased from Merck KGaA (Darmstadt, Germany). Sodium azide (99%) was received from Acros Organics (New Jersey, USA). All other reagents or solvents used during the solvent screening were of at least analytical grade and purchased either from Sigma-Aldrich (Taufkirchen, Germany) or from VWR Prolabo (Leuven, Belgium).

4.2.2 Methods

4.2.2.1 Crystallization of mAb1

Crystallization of mAb1 was carried out in a 0.1 M sodium acetate buffer at a pH of 5.50. For standard crystallization, a 23% or 24% (w/v) PEG 4000 solution was added dropwise in a 1:1 ratio to a 10 mg/mL protein solution under gentle shaking. The final formulation was stored at 20°C for at least two weeks.

4.2.2.2 Crystallization of mAb2

Standard crystallization of mAb2 was performed in a 0.1 M sodium acetate buffer at a pH of 4.1. For crystallization, a 4.2 M sodium dihydrogen phosphate solution was added dropwise in a 1:1 ratio to a 10 mg/mL protein solution under gentle shaking. The final formulation was stored at 20°C for at least one week.

4.2.2.3 Alteration of crystallization conditions

The mAb1 and mAb2 lead crystallization conditions were varied in order to obtain new mAb1 crystal polymorphs. The standard crystallization parameters remained unaltered if additives or different precipitants were used. Additives were mixed to the protein so-

lutions in the respective concentration prior to crystallization. The standard crystallization agents were replaced by the respective precipitant. Stirring was performed with stirring bars (2 x 2 mm). For sample rotating and teetering the Heidolph polymax 1040 (Heidolph Instruments, Schwabach, Germany) or the GFL Rocking Shaker 3013 (GFL GmbH, Burgwedel, Germany) was used, respectively. Colder crystallization temperatures were obtained by placing the samples in a lab refrigerator obtained from VWR Prolabo (Leuven, Belgium). Crystallization at elevated temperature was performed in lab incubator from Memmert GmbH & Co. KG (Schwabach, Germany).

4.2.2.4 High hydrostatic pressure

For sample pressurization a pressure intensifier from BOLENZ & SCHAEFER was used which was equipped with a hydraulically driven pressure generating unit and a 200 mL water jacketed chamber for temperature control. For each experiment, the temperature was set at 18.5 °C. The applied pressure medium consisted of 40% (v/v) Univis J13 (Esso Germany), 30% (v/v) diesel and 30% (v/v) petroleum. The experiments were performed as following:

- 3 min pressure increase to the preset pressure.
- 30 min hydraulic support to maintain the pressure.
- 23.5 h in which pressure is hold by the system without hydraulic support.
- Final depressurization for 3 min for the crystal morphology screening experiments. For all other experiments, the depressurization time was set to 20 min.

For all experiments, the samples were filled into 1 mL Nunc CryoTubes™ (Thermo Scientific, Waltham, MA, USA) with an external thread and a round bottom shape. The threads were wrapped with a layer of Teflon film. The tubes were sealed into three layers of polyethylene film (GROPACK Verpackung, Gräfelfing, Germany) which each were vacuumed.

4.2.2.4.1 mAb1

In order to grow new crystal mAb1 crystal morphologies under high hydrostatic pressure, 10 mg/mL protein solutions were mixed in a 1:1 ratio with 20%, 30%, 32%, 34%,

35%, 36%, 38%, 40% and 50% (w/v) PEG 4000 solutions. Subsequently, the samples were pressurized at different pressure levels for 24 h.

4.2.2.4.2 mAb2

To identify new mAb2 crystal morphologies under the impact of high hydrostatic pressure PEG 4000 and ammonium sulfate were used as crystallization agents. Therefore, 40%, 45% and 50% (w/v) PEG 4000, dissolved in sodium acetate buffer at pH 4.1 were mixed in a 1:1 ratio with a 10 mg/mL mAb2 solution. For crystallization with ammonium sulfate the 10 mg/mL protein solution was mixed in a 1:1 ratio with 2 M, 3 M, 3.62 M, 3.78 M and 3.88 M of ammonium sulfate solutions in sodium acetate buffer at pH 4.1.

4.2.2.4.3 Generation of stressed antibody solutions

It was the aim to investigate whether high hydrostatic pressure is able to dissociate antibody aggregates. Therefore, artificial aggregates were generated by four different kinds of stress: agitation, stirring, exposure to thermal stress at 30°C and 50°C and light with 60 watt/m². All experiments were conducted with 5 mg/mL protein solutions.

Shaking stress was induced to 1 mL of the protein solutions which were filled into 2 mL Eppendorf tubes. The caps were sealed with Parafilm and horizontally fixed on an Eppendorf Mixer 5432 for 8 h (Eppendorf AG, Hamburg, Germany). The samples were pooled to obtain a homogenous batch for the experiments.

Stirring stress was exerted on a Heidolph MR 3001 K (Heidolph Instruments, Schwabach, Germany) at a speed of 500 rpm for 8 h.

For temperature stresses, the protein solutions were placed in Greiner tubes and exposed to 50°C for 24 h.

For light stress was introduced for 24 h using the Suntest CPS from Heraeus Original (Hanau, Germany) equipped with a xenon lamp. The protein solutions were placed into high pressure liquid chromatography (HPLC) vials. Some vials were wrapped up with an aluminum film to assess the effect of light induced thermal stress which was set at 35°C. These samples were additionally used to assess temperature induced aggregate formation at 35°C. The light stressed samples were pooled to obtain a homogenous batch for the experiments.

4.2.2.5 Size exclusion high performance liquid chromatography (SE-HPLC)

Total protein recovery and soluble aggregate content were determined by SE-HPLC. The analysis was performed on a Thermo separation system

4.2.2.5.1 mAb1

The mobile phase for mAb1 consisted of 0.092 M Na₂HPO₄ (anhydrous) and 0.211 M Na₂SO₄ (anhydrous) at a pH of 7. The flow rate was set to 0.25 mL/min. Analysis was performed at the wavelengths of 214 nm and 280 nm. A TSKgel G300SWXL column from Tosoh Bioscience GmbH (Stuttgart, Germany) was used for separation. Crystals were dissolved in PBS prior to analysis.

4.2.2.5.2 mAb2

The mobile phase for mAb2 consisted 0.02 M Na₂HPO₄ (dihydrate) und 0.15 M sodium chloride at a pH of 7.5. The flow rate was set to 0.50 mL/min. Analysis was performed at the wavelengths of 214 nm and 280 nm. For separation, a Suprose-6-HR-10/30-coloum from GE Healthcare (Uppsala, Sweden) was used. Crystals were dissolved in PBS prior to analysis.

4.2.2.6 Microscopic examination

The crystal integrity was determined microscopically using either a Nikon Labophot equipped with a JVC TK-C1381 color video camera and the Screen Measurement / Comet – Software Version 3.52a or Biozero BZ-8000 (Keyence, Neu-Isenburg, Germany) microscope with the BZ Viewer application. Glass cover slides were used for sample preparation. A polarization filter was used to assess the crystalline state of the samples. Examination was performed at 400 fold magnification.

4.2.2.7 Nephelometry

Turbidity was measured using a Nephla Dr. Lange turbidimeter (Dr. Lange GmbH, Düsseldorf, Germany) by 90° light scattering at a wavelength of $\lambda = 860$ nm (Ph. Eur. 2.2.1). Results are given in formazine normalized units. Crystals were dissolved in phosphate buffer solution (0.01M, pH 7.4, isotonic) (PBS) and concentration was set to 1 mg/mL. 2 mL of each sample were filled into round glass cuvettes and placed into the sample holder.

4.2.2.8 Total subvisible particle count

Size and amount of subvisible particles between 1 and 200 μm were determined using a PAMAS SVSS-C40 (PAMAS GmbH, Rutesheim, Germany) light blockage system. Crystals were dissolved in PBS and concentration was set to 1 mg/mL. The number of measurements was set to three for each sample with a measuring volume of 0.3 ml. The rinsing volume was 0.5 ml.

4.3 Results

4.3.1 Reproducibility of mAb1 and mAb2 crystallization lead conditions

In a first experiment, the lead crystallization conditions for mAb1 and mAb2 were assessed for their reproducibility. In brief, a 10 mg/mL mAb solution was admixed in a 1:1 ratio either with a 23% or 24% (w/v) PEG 4000 solution in sodium acetate buffer at pH 5 or with a 4.2 M sodium dihydrogen phosphate dehydrate salt solution in a sodium acetate buffer at pH 4.1. The mixtures were stored at 20°C in a climate room. The samples were analyzed optically by light microscopy. Aggregate formation was followed by SE-HPLC. Analysis of the samples was performed over 1 year.

The same mAb1 and mAb2 crystals morphologies were found after one week of crystallization as described by the preliminary study (Fig. 4-1) ¹. Dependent on the PEG 4000 concentration, the mAb1 crystals appeared as platelet-like structures (23% (w/v) PEG) or needle-clusters (24% (w/v) PEG). Notably, crystallization of mAb by using 23% (w/v) PEG 4000 was not successful in each case. Therefore, it was decided to crystallize preferably with 24% (w/v) PEG during the present study. Sea-urchin like crystal structures were found for mAb2.

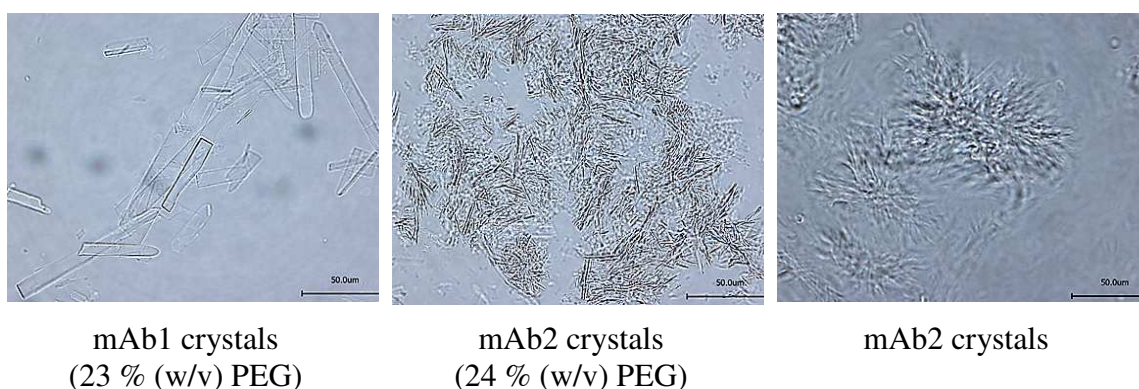


Figure 4-1 depicts light microscopy pictures of mAb1 (left, middle) and mAb2 (right) crystals after one week of crystallization. The mAb1 crystal shape was dependent on the PEG concentration used. The scale bar represents 50 µm.

SE-HPLC measurements confirmed a constant aggregate formation for both mAbs as described by the preliminary study (Fig. 4-2) ¹. Interestingly, aggregate formation for mAb1 crystallized with 24% (w/v) PEG was observed immediately after starting crystallization while mAb2 aggregation was first observed after 8 days. While total mono-

mer recovery was lower for mAb1 crystals compared to the supernatant, adverse results were found for mAb2 (Fig. 4-2). These observations had not been reported by Stefan Gottschalk during the preliminary study ¹. The extent of aggregate formation was less for the samples crystallized with 23% (w/v) PEG compared to the samples crystallized with 24% (w/v) PEG (not shown). Notably, aggregate formation was even detected for the non-crystallized samples which contained 23% (w/v) PEG. However, the aggregate levels strongly differed for these samples (not shown).

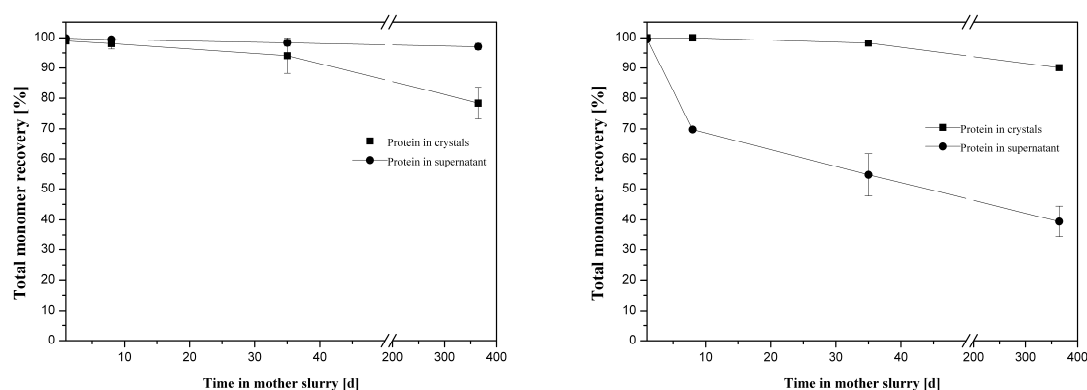


Figure 4-2 Total mAb1 (left) and mAb2 (right) protein monomer recovery in the crystals and the supernatant over 365 days. The results for mAb1 refer to crystallization using 24% (w/v) PEG. The x-axis displays a non-linear scaling. Nonetheless, the graph displays applicable values as the reduction in the total monomer recovery occurs in a nearly linear matter.

4.3.2 Alteration of mAb1 and mAb2 crystal morphology by variations in the crystallization lead conditions

The protein instability was ascribed to the unfavorable crystal polymorph with low numbers of protein-protein interactions within the crystal lattice. Protein stabilization should be reached by growing of other crystal polymorphs which possess a higher number of protein-protein bindings ⁶. Fundamental alterations of the crystallization lead conditions were avoided during the study in order to conserve biocompatibility.

4.3.2.1 Agitation and alternative crystallization temperatures

In a first experiment, only the crystallization temperature was changed and application of agitation was tested. mAb1 was crystallized with 23% (w/v) PEG while mAb2 crystals should be obtained with the lead formulation (4.2 M sodium dihydrogen phosphate). Table 4-1 shows the variations of the standard conditions used in order to obtain

new mAb1 and mAb2 crystal polymorphs. The crystallization samples were stored for 8 weeks at 20°C in a climate room. The optical crystal shape was assessed by light microscopy while total monomer recovery was analyzed by SE-HPLC.

Table 4-1 Alterations of the crystallization lead conditions in order to obtain new mAb crystal polymorphs.

Variations in the lead crystallization conditions
Crystallization at:
20°C + 200; 400 rpm stirring 20°C + 2; 20; 40 rpm teetering 20°C + 40 rpm rotating
2-8°C; 15°C, 30°C shift after two weeks : 2-8°C → 20°C shift after two weeks : 20°C → 2-8°C
2-8°C + 20 rpm teetering

Figure 4-3 shows the crystals shapes after 8 weeks of crystallization under modified conditions according to table 4-3. The crystal sizes were reduced after crystallization at altered temperatures. The platelet-shaped morphology was changed to small needle-like clusters. Beside the crystals amorphous aggregates could be observed for samples stored 2-8°C and 30°C. Notably, the smaller needle-shaped crystals obtained at lower temperatures grew to the platelet-shaped morphology after transfer to ambient temperature. However, the platelet-shape was conserved after the temperature shift from 20°C to 2-8°C.

The crystal morphology remained unaltered after crystallization under rotating. Interestingly, crystal breakage and small needles could only be observed after applying of teetering. Stirred samples showed only amorphous aggregates independent from the used speed.

Summarizing, no new mAb1 crystal polymorph was found under the tested conditions. The same trends were observed for mAb2 crystals (not shown).

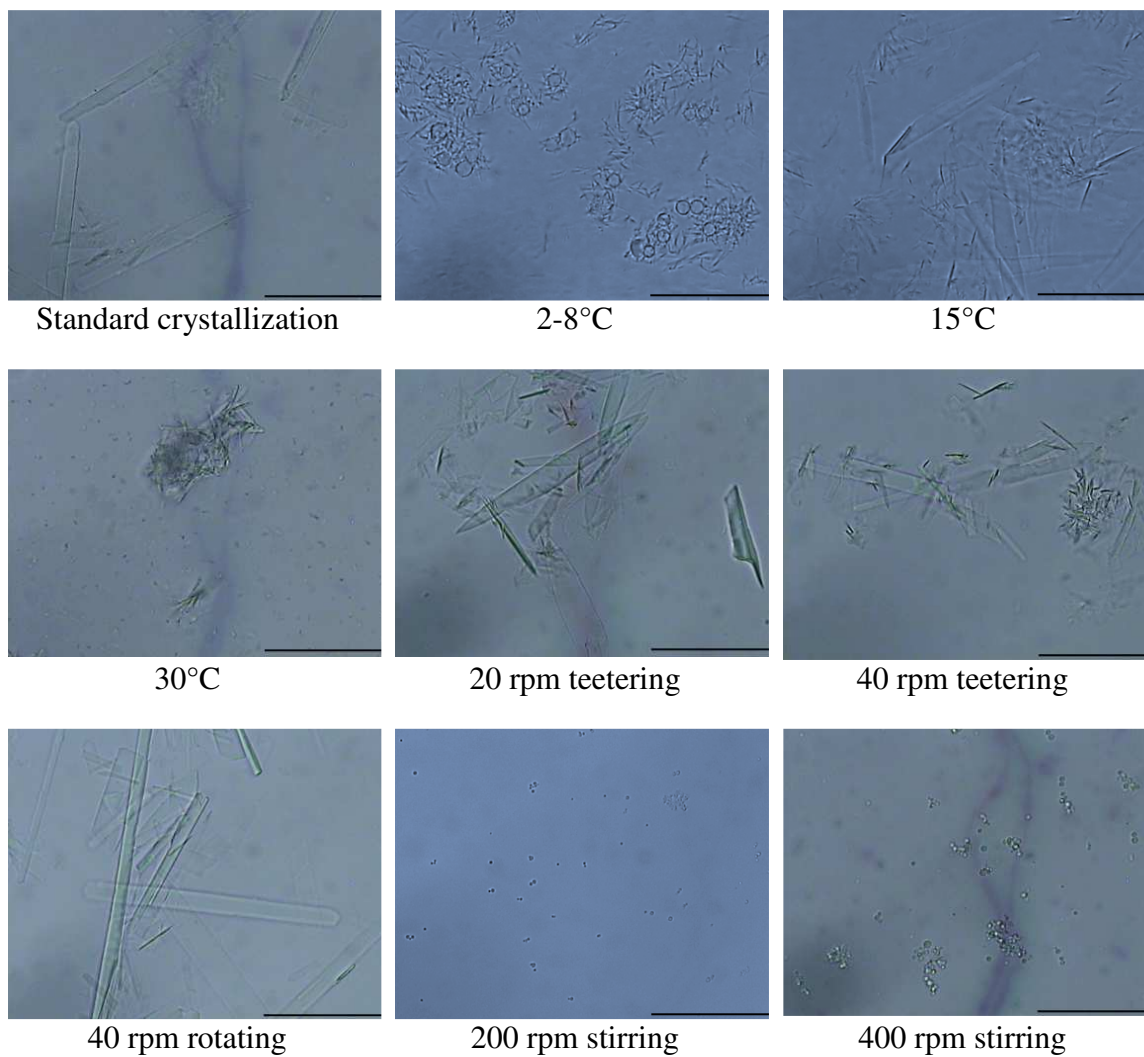


Figure 4-3 depicts light microscopic pictures of selected mAb1 samples. The figure captions refer to the alterations of the crystallization conditions compared to the lead conditions. The scale bar represents 50 μ m.

Analysis of the total monomer recovery revealed reduced values of about 1 – 2% for all mAb1 samples, except of the stirred samples, compared to samples crystallized under unaltered standard conditions (Fig. 4-4). The stirred samples showed a loss in total monomer recovery of about 5 – 6%. Only samples crystallized at 2-8°C showed increased protein stability which was indicated by a higher total monomer recovery.

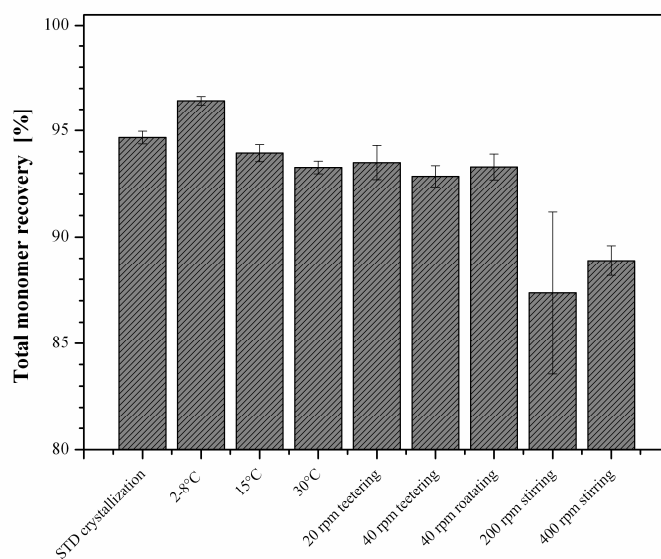


Figure 4-4 Total monomer recovery of selected mAb1 crystallization samples. The x-axis captions refer to alterations of the crystallization lead conditions. STD crystallization means mAb1 crystallization with 23% (w/v) PEG.

4.3.2.2 Additives, pH shifts and PEG of higher molecular weight

Since no satisfying effects could be obtained by modification of the crystallization temperature and applying of agitation, small pH shifts and additives were assessed in order to obtain new mAb1 and mAb2 crystal morphologies. In addition, PEGs of different chain lengths were investigated as alternative to PEG 4000 for crystallization of mAb1. The crystallization buffer pH is reported to be most important for protein crystallization. Macromolecular nucleation rate as well as protein-protein interactions are very sensitive towards the buffer pH. Even small changes of the pH value can result in crystalline products of different quality and quantity^{3,8,36}. Therefore, the pH of the crystallization buffers was only slightly changed.

Table 4-2 shows the pH shifts, additives and PEG molecular weights applied during the study. For the assessment of the pH shifts and additives, mAb1 was crystallized with both “standard” PEG concentrations (23% and 24% (w/v) PEG 4000). In contrast, the alternative PEG molecular weights were used in different concentrations (Tab. 4-2). All samples were prepared in accordance to the lead procedure introduced by Stefan Gottschalk (see 1.3.1) and subsequent stored at 20°C for 5 weeks. Light microscopy was performed to inspect the optical crystal morphology. SE-HPLC analysis was used to investigate aggregate formation.

Table 4-2 The pH shifts and additive concentrations examined to obtain new crystal morphologies. In addition, different PEG molecular weights were listed which were assessed as alternative to PEG 4000 for crystallization of mAb1. The percentages refer to values in w/v.

	mAb1	mAb2
pH Screen	pH 5.2, 5.5, 5.7, 5.9	pH 3.8, 4.1, 4.4, 4.6
Sucrose	0.1 %, 2.5 %, 5 %	0.1 %, 2.5 %, 5 %
Poloxamer	0.5 %, 2.5 %	0.5 %, 2.5 %
Hyaluronic acid	0.1 %	0.05 %
Ficoll 400	0.1 %, 1 %, 2.5 %	0.1 %, 0.5 %, 1 %
Cyclodextrin (Cavasol W7 HP)	0.1 %, 2.5 %, 5 %	0.1 %, 2.5 %, 5 %
Dextran 6,000	0.1 %, 2.5 %, 5 %	0.1 %, 2.5 %, 5 %
Fructose-6-phosphate	0.1 %, 1 %, 5 %	0.1 %, 1 %, 5 %
Carboxy methyl cellulose (low viscosity)	0.1 %, 2.5 %, 5 %	0.1 %, 2.5 %, 5 %
PEG 6000P	20 %	-
PEG 8000P	16 %, 20 %, 22 %, 24 %	-
PEG 10000P	12 %, 16 %	-

Light microscopic observations revealed only small changes in the optical mAb1 crystal morphology (Fig. 4-5).

For mAb1 crystallization with 23% (w/v) PEG 4000, smaller needle-like crystal structures were obtained after increasing the pH value of the buffer to 5.90. Addition or after cyclodextrin or ficoll to mAb1 crystallization systems with 24% (w/v) PEG 4000 resulted in small needle-like crystal structures and platelet-like mAb1 crystals (besides needle-like structures), respectively. However, Stefan Gottschalk has already considered that the smaller needle-like morphology does not represent a polymorphic crystal form towards the platelet-like crystal shapes ¹.

For mAb2, no changes in the crystal morphology could be obtained. Addition of cyclodextrine and Ficoll 400 resulted in different needle orientations which were associated to amorphous precipitates in the center of the needle-clusters (Fig. 4-5 bottom row).

Generally, application of higher additive concentrations resulted in the occurrence of amorphous structures.

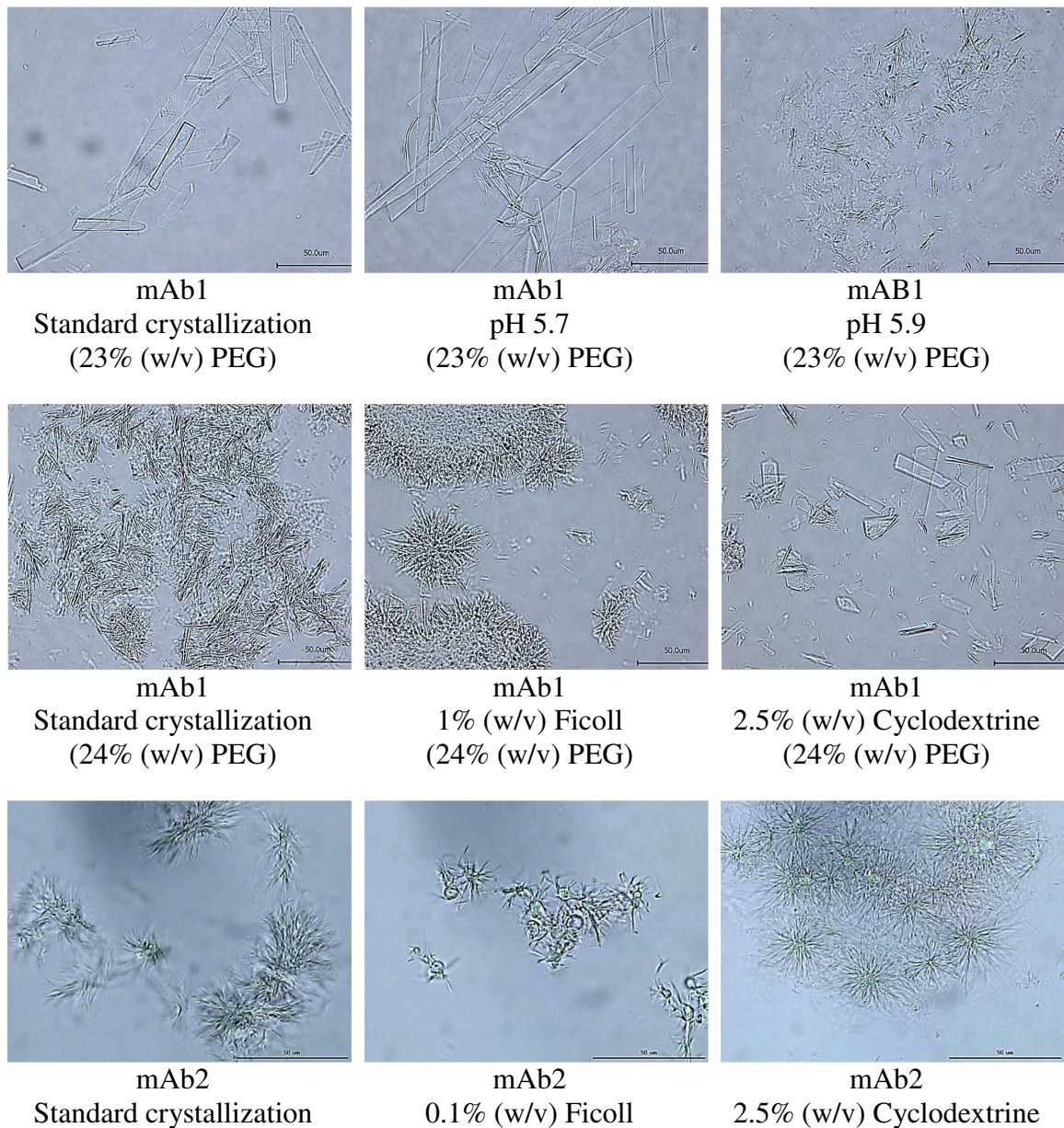


Figure 4-5 Light microscopic pictures of mAb1 and mAb2 crystals obtained after crystallization under the lead conditions (left column). The other pictures show crystal shapes obtained after application of pH shifts (first row, middle and right column) or additives (middle and bottom row, middle and right column). The scale bar represents 50 µm.

Amorphous mAb1 precipitates were also observed after crystallization with PEGs of higher molecular weight (not shown). Reduction of the PEG concentration again resulted in crystal formation, but again in needle-like morphologies (Fig. 4-6). However, amorphous structures could still be observed within these samples. Further reduction of

the PEG concentration did not foster mAb1 crystallization. Consequently, crystal formation without amorphous precipitates could not be reached with PEGs of higher molecular weight.

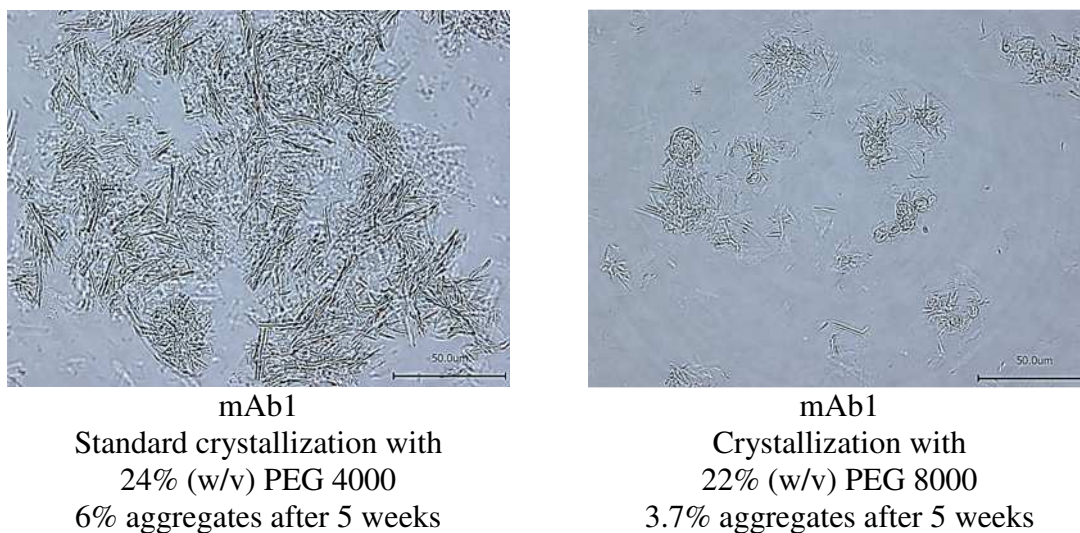


Figure 4-6 Light microscopic pictures of mAb1 crystals obtained after crystallization with 24% (w/v) PEG 4000 (left) or 22% (w/v) PEG 8000 (right). The scale bar represents 50 μ m.

Despite the occurrence of amorphous precipitates, SE-HPLC analysis revealed a reduction in aggregate formation after 5 weeks from 6% aggregates (lead conditions) to 3.7% aggregates (22% (w/v) PEG 8000) (Fig. 4-6). Application of the pH shifts and cyclodextrine resulted in increased aggregate levels of about 7 - 8%. All other additives did not affect the extent of aggregate formation (not shown).

Overall, no mAb1 or mAb2 crystal polymorph could be obtained by alteration of the crystallization buffer pH or with the tested additives. Small effects on the crystal shape were accompanied with increased aggregate formation. Only the application of higher molecular PEGs for mAb1 crystallization resulted in reduced aggregate formation after 5 weeks. However, usage of these PEGs led to amorphous precipitates besides the mAb1 crystals and thus to a reduced product quality of the crystal suspension.

4.3.3 High hydrostatic pressure

No alterations of mAb1 and mAb2 crystal morphology were reached by pH shifts, PEG of higher molecular weight and additives. Therefore, high hydrostatic pressure was tested. Beside the aim to grow new mAb1 and mAb2 crystal morphologies the reduction of

the aggregate content of stored crystal suspensions should be reached. However, it was not clear if mAb1 and mAb2 crystals would withstand exposure to elevated pressure levels.

4.3.3.1 mAb1 and mAb2 crystal stability at elevated pressure levels

First, crystallization was performed under lead conditions (24% (w/v) PEG for mAb1) for both antibodies. Then, the samples were pressured at 150 MPa to 500 MPa which represented the working span of the applied pressure intensifier from BOLZEN & SCHAEFER. Integrity of the crystalline state was assessed by light microscopy immediately after depressurization.

mAb1 crystals started to convert into an amorphous state already at 160 MPa. This transition was completed at 175 MPa. In contrast, mAb2 crystals withstood pressurization up to the technical limit of the pressure intensifier (Fig. 4-7).

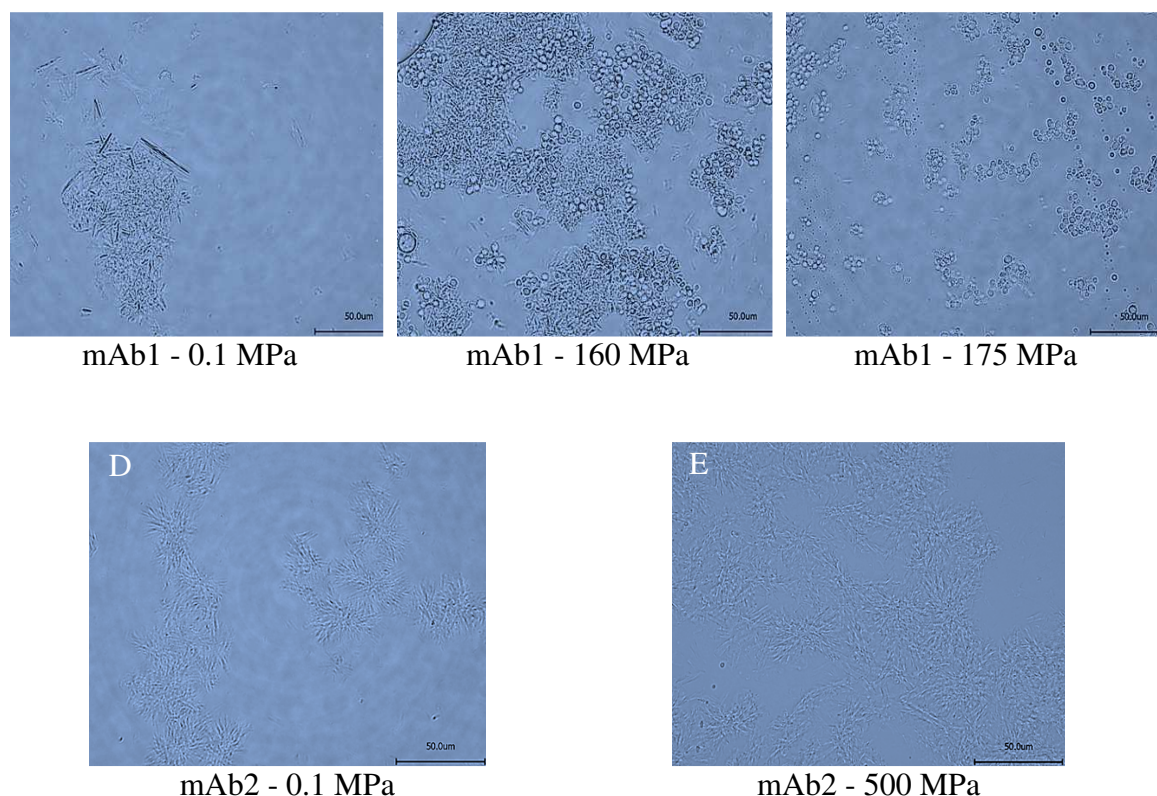


Figure 4-7 Light microscopic pictures of mAb1 and mAb2 crystals before pressurization (A, D) and after pressurization. Amorphous precipitate besides mAb1 crystals was observed already after pressurization at 160 MPa (B). Pressurization at 175 MPa resulted only in amorphous structures (C). mAb2 crystals maintained until the technical limit of the pressure intensifier (E).

4.3.3.2 The effect of high hydrostatic pressure on the mAb crystal morphology

In a further experiment, high hydrostatic pressure was used with the aim to obtain new mAb1 and mAb2 crystal morphologies. The opportunity to generate new crystal shapes was anticipated since the transition from one polymorph to a different one was already described for lysozyme crystals¹⁵. In a different study, recombinant human growth hormone was precipitated amorphously with high PEG concentrations at ambient pressure. This state was transitioned into crystals after application of elevated pressures¹⁹.

Therefore, 10 mg/mL mAb1 solutions were admixed with PEG solutions with concentrations from 20% to 50% (w/v). The mixtures were subsequently exposed to different pressure levels (Tab. 4-3). Experiments with pressures above 300 MPa were not conducted since mAb1 crystals did not withstand such conditions (see above). The samples were inspected visually by light microscopy immediately after pressurization. A polarization filter was used to distinguish between amorphous and crystalline states. The 20% (w/v) PEG 4000 concentration was chosen as for some proteins which were exposed to high hydrostatic pressures a reduction in solubility is reported^{16-18,23}.

For the higher PEG concentrations only amorphous precipitates could be observed after pressurization. In contrast, no precipitation was found for the samples mixed with 20% (w/v) PEG. These findings were independent from the applied pressure levels (Tab. 4-3). Protein agglomerates (melted sheets) of a different shape could be found already at ambient pressure for samples mixed with 30% (w/v) PEG. The shapes were observed after pressurization of samples from 30% to 35% (w/v) PEG. These structures were different to the typical amorphous mAb1 structures obtained so far (Fig. 4-8).

Table 4-3 mAb1 precipitate states after precipitation with different PEG 4000 concentrations and subsequent exposure to elevated pressure levels. 0.1 MPa refers to samples without pressure treatment.

PEG [%] (m/v)	0.1 MPa	160 MPa	200 MPa	250 MPa	300 MPa
20%	soluble		soluble		
30%	melted sheets		amorphous		
32%	amorphous		melted sheets		amorphous
34%	amorphous		melted sheets		amorphous
35%	amorphous	melted sheets		amorphous	
36%		amorphous			
38%		amorphous			
40%	amorphous		amorphous		
50%	amorphous		amorphous		

The new agglomeration shapes represented connected assemblies with round boundaries. This structure obtained with 30% (w/v) PEG could be disconnected at elevated pressure levels (Fig. 4-8 C). Application of the polarization filter could not confirm a crystalline state (Fig. 4-8 F). A new mAb1 crystal morphology could not be found under the tested conditions.

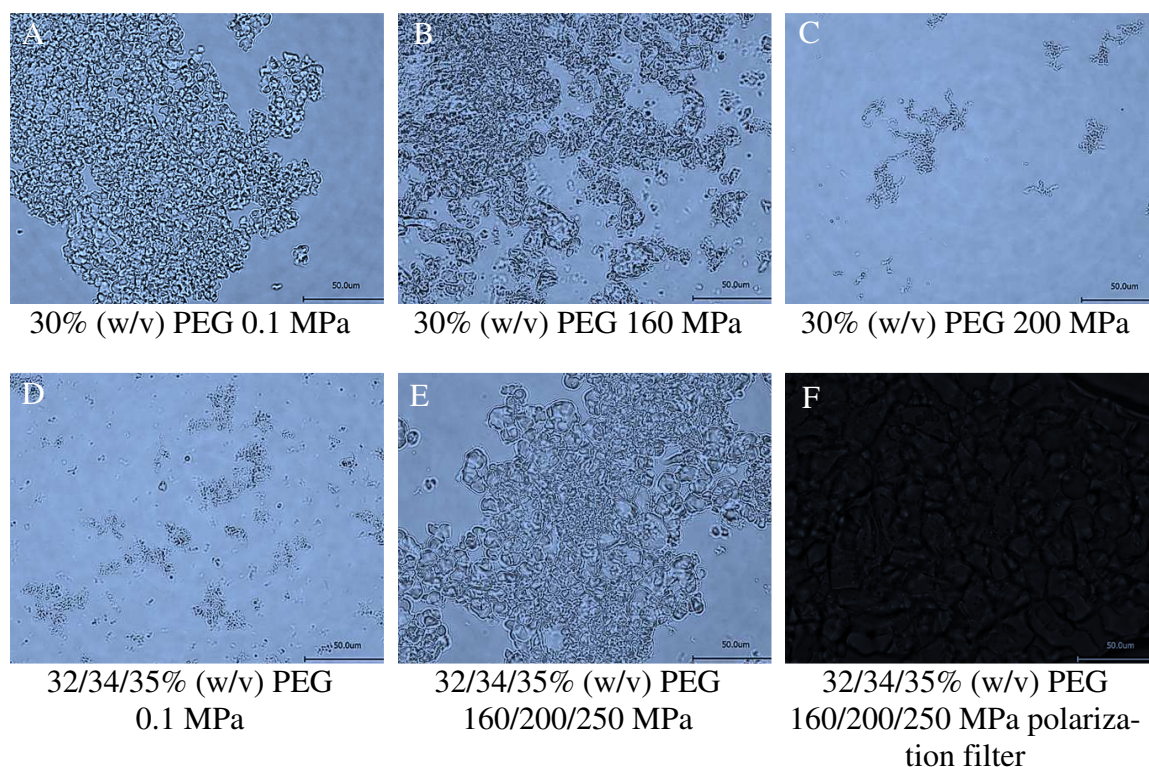


Figure 4-8 mAb1 precipitates obtained after crystallization with higher PEG concentrations (A, D) at atmospheric pressure and after exposure to higher pressure levels (B, C, E). The melted-sheet like structure obtained with 30% (w/v) PEG disappeared with increasing pressures (A, B, C). Samples precipitated with higher PEG concentration formed small amorphous structure (D). Pressurization of such samples resulted in formation of melted sheets (E). Application of a polarization filter revealed no crystalline state of the melted-sheet like structures (F). The scale bar represents 50 µm.

To grow new mAb2 crystal morphologies, a different test set-up was utilized. PEG 4000 was used as new crystallization agent for mAb2 under high hydrostatic pressure. A similar approach was already described in literature for recombinant human growth hormone¹⁹. PEG could not crystallize that protein under ambient pressure conditions but at elevated pressure levels. Therefore, a 10 mg/mL mAb2 solution was admixed with 20%, 22.5% and 25% (w/v) PEG solutions to obtain amorphous mAb2 precipitates at ambient pressure. These suspensions were exposed to high hydrostatic pressures. However, all samples retained its amorphous state (not shown).

A different strategy was followed by utilizing ammonium sulfate ((NH₄)₂SO₄) as crystallization agent for mAb2. In accordance to the Hofmeister series, ammonium sulfate should possess a stronger salting out feature³⁷. Consequently, lower concentrations would be required for mAb2 crystallization. Again, a 10 mg/mL mAb2 solution was admixed with different ammonium sulfate solutions with concentrations from 2 M to 3.88 M. The mixtures were subsequently pressurized. Light microscopy was used to assess the precipitant state.

Application of 3 M solutions resulted in mAb2 crystal formation. The crystals were similar to those obtained with ammonium phosphate but without the sea-urchin like crystal shape (Fig. 4-9 A).

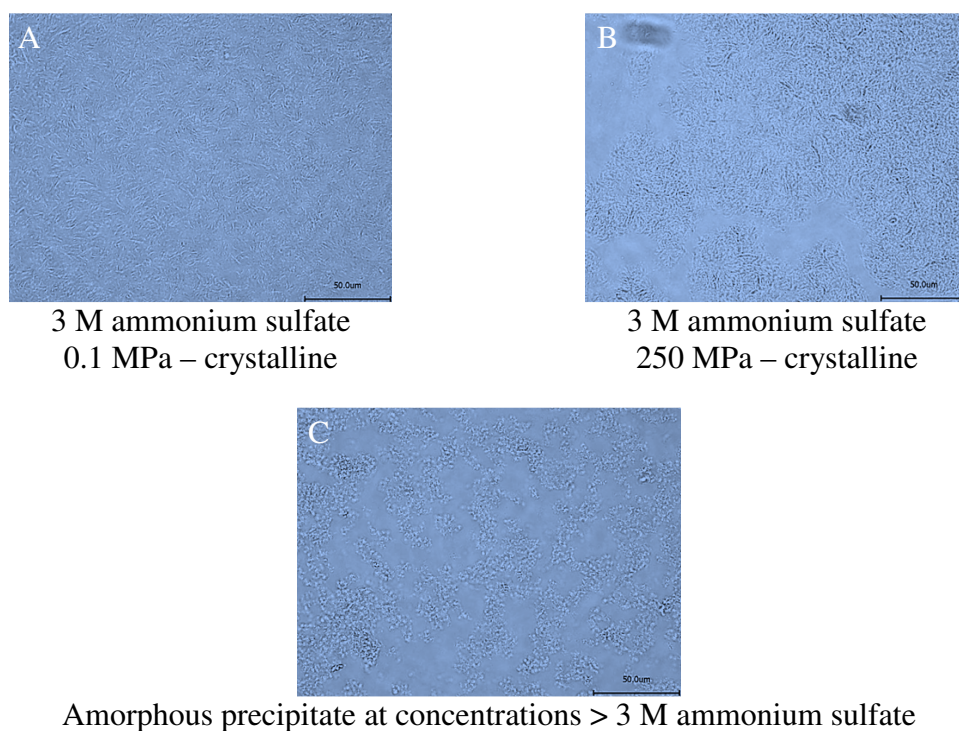


Figure 4-9 mAb2 crystals obtained after crystallization with 3 M ammonium sulfate (A). This state withstood increased pressure levels at 250 MPa (B). Application of higher ammonium sulfate concentrations (> 3 M) resulted in amorphous mAb2 precipitation (C). The scale bar represents 50 μ m.

The crystal morphology was maintained at elevated pressures (Fig. 4-9 B). Amorphous mAb2 precipitates were obtained at higher ammonium sulfate concentrations which also were retained at higher pressure levels (Fig. 4-9 C). Concentrations lower than about 3 M ammonium sulfate did not precipitate mAb2. As for mAb1, no new crystal morphology could be found under the tested conditions.

4.3.3.3 The effect of high hydrostatic pressure on mAb crystallization and the protein integrity

High hydrostatic pressure has the feature to dissociate aggregated protein in solution which is extensively described in literature^{25,27,30,31}. However, crystallization at high hydrostatic pressure was so far described for only three proteins. For glucose isomerase, accelerated protein crystallization but reduced crystal sizes were reported whereas decreased nucleation and growth rates were stated for lysozyme and subtilisin at elevated pressure levels. Hydrostatic pressure effects on mAb crystallization have not been reported, yet. Therefore, mAb1 and mAb2 solutions were admixed with the respective crystallization buffer and immediately pressurized. mAb1 samples were pressurized at 150 MPa while mAb2 samples were exposed to 150 MPa and 400 MPa as the crystals were found to withstand the higher pressure levels (see above). The crystal appearances were followed by light microscopy. Aggregate formation for the crystalline fraction was investigated by SE-HPLC, light obscuration and nephelometry after 1 day and 4 weeks. The results were compared to not-pressurized samples.

Pressurization at 150 MPa did not hinder mAb1 crystallization. However, the needle-like crystals were larger in number but smaller in their size. The morphology and crystal sizes did not change during the four weeks (not shown).

SE-HPLC analysis showed minor differences in the protein integrity between the pressurized and non-pressurized samples. About 1.5% soluble aggregates were detected after one day and around 3.3% after 4 weeks. However, total protein recovery was decreased about 3.8% for the pressurized samples after 4 weeks (Tab. 4-4).

Table 4-4 Soluble aggregate content and total protein recovery of mAb1 crystallization samples after 1 day and 4 weeks of storage obtained by SE-HPLC measurements. The values refer to samples pressurized at 150 MPa for 24 h immediately after mixing the protein solution with the precipitant solution and to samples without any treatment (0.1 MPa).

Pressure level	Storage time	Soluble aggregate content [%]	Total protein recovery [%]
0.1 MPa	1 day	1.6	100
150 MPa	1 day	1.3	100
0.1 MPa	4 weeks	3.4	100
150 MPa	4 weeks	3.1	96.2

This finding was confirmed by light obscuration and turbidity measurements. Both methods again revealed only small differences for the pressurized and non-pressurized samples with slightly increased values for the first ones (Fig. 4-10). Interestingly, turbidity and total subvisible particle count were reduced after 4 weeks for both samples.

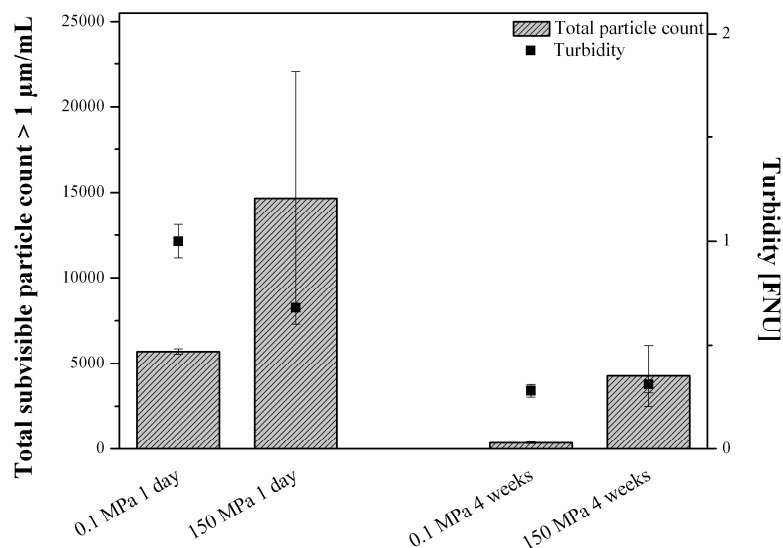


Figure 4-10 Light obscuration (left) and turbidity [FNU] (right) measurements for mAb1 samples without any treatment (0.1 MPa) and for samples pressurized at 150 MPa for 24 h immediately after starting the crystallization.

As for mAb1, pressurization at 150 MPa had no effect on mAb2 crystallization. However, pressurization at 400 MPa hindered mAb2 crystallization. Under standard conditions, the samples possess an amorphous state before the crystals start to form after approximately 2 days. Whereas samples pressurized at 150 MPa still become crystalline with the common morphology, the samples pressurized at 400 MPa remained amorphous over the 4 weeks (Fig. 4-11).

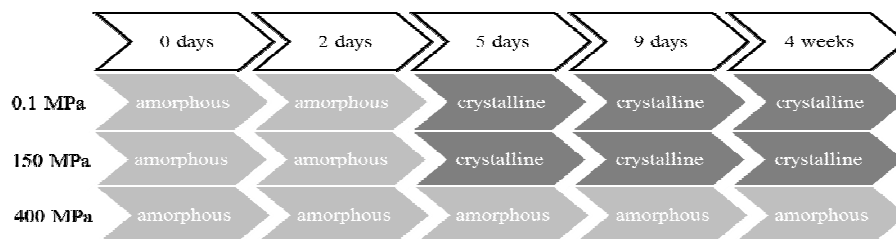


Figure 4-11 Precipitate state of mAb2 of differently treated crystallization samples. The states refer to samples without any treatment (0.1 MPa) and to samples pressurized at 150 MPa and 400 MPa for 24 h immediately after starting the crystallization.

With respect to aggregate formation, no differences between the samples pressurized at 150 MPa and the non-pressurized samples could be observed. No soluble aggregates were found after 1 day while about 2% soluble aggregates were detected after 4 weeks (Tab. 4-5). Total protein recovery was equal after 4 weeks for both samples. In contrast, samples pressurized at 400 MPa showed about 12.5% soluble aggregates after 1 day. After 4 weeks the soluble aggregate level was determined at 4.5%, but the total protein recovery dropped from 83% after 1 day to 65% after 4 weeks.

Table 4-5 Soluble aggregate content and total protein recovery of mAb2 crystallization samples after 1 day and 4 weeks of storage obtained by SE-HPLC measurements. The values refer to untreated samples (0.1 MPa) and samples pressurized at 150 MPa or 400 MPa for 24 h immediately after mixing the protein solution with the precipitant solution.

Pressure level	Storage time	Soluble aggregate content [%]	Total protein recovery [%]
0.1 MPa	1 day	0	100
150 MPa	1 day	0	100
400 MPa	1 day	12.5	95.8
0.1 MPa	4 weeks	1.9	100
150 MPa	4 weeks	2.2	100
400 MPa	4 weeks	4.5	69.2

Light obscuration and turbidity results were again higher after 1 day than after 4 weeks. Interestingly, the samples pressurized at 400 MPa showed lower subvisible particle counts and turbidities than samples pressurized at 150 MPa.

Overall, no positive effect of high hydrostatic pressure on mAb1 and mAb2 crystallization and aggregate formation could be observed (Fig. 4-12).

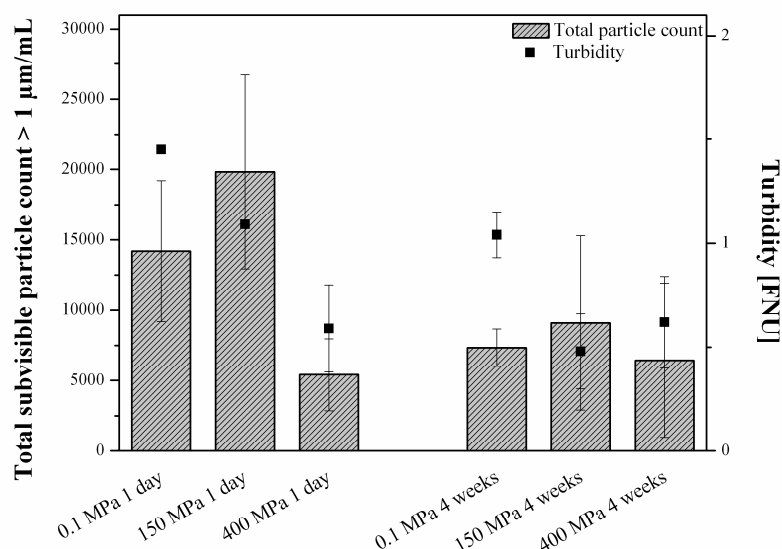


Figure 4-12 Light obscuration (left) and turbidity [FNU] (right) measurements for mAb2 samples without any treatment (0.1 MPa) and for samples pressurized at 150 MPa or 400 MPa for 24 h immediately after starting the crystallization.

4.3.3.4 Reduction of the aggregate contents of mAb crystal suspensions by application of elevated pressure levels

It was the aim of the following experiment to reduce the aggregate level of older mAb crystal suspensions by application of elevated pressure levels.

Therefore, matured mAb1 crystals which contained about 13.5% aggregates were pressurized at 160 MPa and 200 MPa. This pressure range was chosen as for it dissociation of protein aggregates in solution was already described^{24,25}. Furthermore, it has been shown that mAb1 crystals can withstand these pressure levels. Matured mAb2 crystals which possessed an aggregate content of about 4.3% were exposed to 175 MPa, 400 MPa and 500 MPa pressures. SE-HPLC, light obscuration and turbidity measure-

ments were used to assess the aggregate levels of the samples. The results were compared to untreated samples of the same age. For calculation of the total protein recovery after pressurization, the total protein recovery of the untreated comparison samples was taken as 100%.

For mAb1, SE-HPLC analysis revealed lower soluble aggregate levels which were accompanied with a significantly decreased total protein recovery for the pressurized samples. The reduction in total protein recovery was larger for samples pressurized at 160 MPa than for samples exposed to 200 MPa (Tab. 4-6). This reduction was ascribed to formation of insoluble aggregates which were not detectable by SE-HPLC.

Table 4-6 Soluble aggregate content and total protein recovery determined by SE-HPLC measurements of matured non-pressurized (0.1 MPa) and pressurized (160 MPa, 200 MPa) mAb1 crystal suspensions. Reduction in total protein recovery was ascribed to formation of insoluble aggregates which were not detectable by SE-HPLC.

Pressure level	Soluble aggregate content [%]	Total protein recovery [%]
0.1 MPa	13.5	100
160 MPa	10.5	88.1
200 MPa	9.7	95.4

This finding was supported by light obscuration and turbidity measurements which showed again the highest values for samples exposed to 160 MPa (Fig. 4-13).

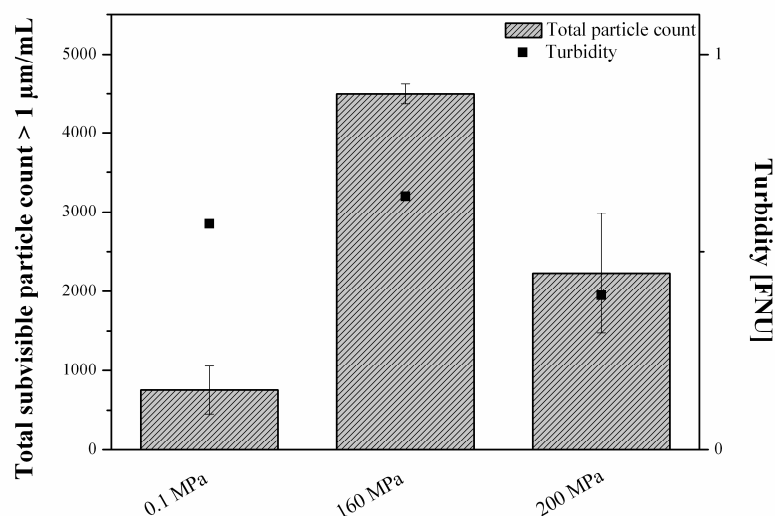


Figure 4-13 Total subvisible particle count > 1 μm per milliliter and turbidity [FNU] of matured mAb1 crystal suspensions without any pressurization (0.1 MPa) and after treatment at 160 MPa and 200 MPa.

The soluble aggregate content of mAb2 crystals was reduced about 2.5% after pressurization at 175 MPa (Tab. 4-7). Interestingly, the total protein recovery was increased compared to the untreated samples. In contrast, after exposure to 400 MPa and 500 MPa the soluble aggregate level remained unaltered, but the total protein recovery was decreased by 3.9% and 13.3%, respectively.

Table 4-7 Soluble aggregate content and total protein recovery determined by SE-HPLC measurements of matured mAb2 crystal suspensions which were either non-pressurized (0.1 MPa) or pressurized at 175 MPa, 400 MPa and 500 MPa.

Pressure level	Soluble aggregate content [%]	Total protein recovery [%]
0.1 MPa	4.3	100
175 MPa	1.9	105.8
400 MPa	4.0	96.1
500 MPa	4.7	86.7

Light obscuration and turbidity measurements showed increased values for the samples pressurized at 400 MPa and 500 MPa (Fig. 4-14). The lowest subvisible particle count but the highest turbidity was found for the samples pressurized at 400 MPa. The turbidity-

ty value of the samples pressurized at 175 MPa was slightly decreased compared to the untreated samples. However, the total subvisible particle count was not significantly altered. By that, it was concluded that for matured mAb2 the aggregate content can be decreased by application of high hydrostatic pressure at 175 MPa. For all other conditions, pressurization resulted in increased aggregate levels.

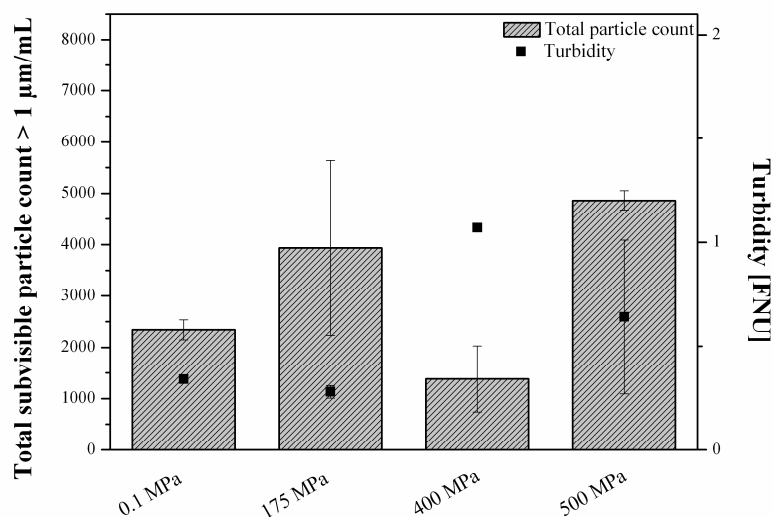


Figure 4-14 Total subvisible particle count > 1 µm per milliliter and turbidity [FNU] of matured mAb2 crystal suspensions without any pressurization (0.1 MPa) and after treatment at 175 MPa, 400 MPa and 500 MPa.

Overall, only for mAb2 crystals a reduction in the aggregate content was observed after pressurization at 175 MPa. All other conditions tested and for all mAb1 samples, the aggregate levels were increased after application of high hydrostatic pressure.

4.3.3.5 The impact of high hydrostatic pressure on the protein integrity of differently concentrated mAb solutions

To determine whether the crystalline state is responsible for increased aggregate levels after sample pressurization, mAb1 and mAb2 solutions of different concentrations were exposed to elevated pressure levels. Therefore, mAb1 solutions in concentrations of 5 mg/mL and 114 mg/mL respectively were pressurized at 160 MPa, 175 MPa, 300 MPa and 400 MPa. mAb2 solutions with concentrations of 5 mg/mL and 66 mg/mL were exposed to 400 MPa. The protein solutions used for the study were fresh and

without any aggregate contents. Aggregate analysis was performed immediately after pressure treatment by SE-HPLC, light obscuration and turbidity measurements.

The results reveal a significant reduction in the total protein recovery for all mAb1 samples. Higher concentrated protein solutions showed a higher loss in protein. The soluble aggregate contents remained nearly unaltered except for the 114 mg/mL protein solution which was pressurized at 400 MPa. For this sample the soluble aggregate level was significantly increased by 5.5% (Tab. 4-8).

Table 4-8 Soluble aggregate content and total protein recovery obtained by SE-HPLC for mAb1 solutions of 5 mg/mL or 114 mg/mL protein. The results refer to samples without any treatment (0.1 MPa) or pressurized samples (160 MPa, 175 MPa, 300 MPa, 400 MPa).

mAb1 concentration	Pressure level	Soluble aggregate content [%]	Total protein recovery [%]
5 mg/mL	0.1 MPa	0.4	100
	175 MPa	0.6	96.6
	300 MPa	0.7	93.9
114 mg/mL	0.1 MPa	0.4	100
	160 MPa	0.3	77.0
	400 MPa	6.0	62.2

Light obscuration and turbidity measurements revealed the same trend (Fig. 4-15). Higher subvisible particle counts and turbidity values were found for the pressurized samples with the highest count for the 114 mg/mL protein solution treated with 400 MPa. This sample showed also the highest turbidity value.

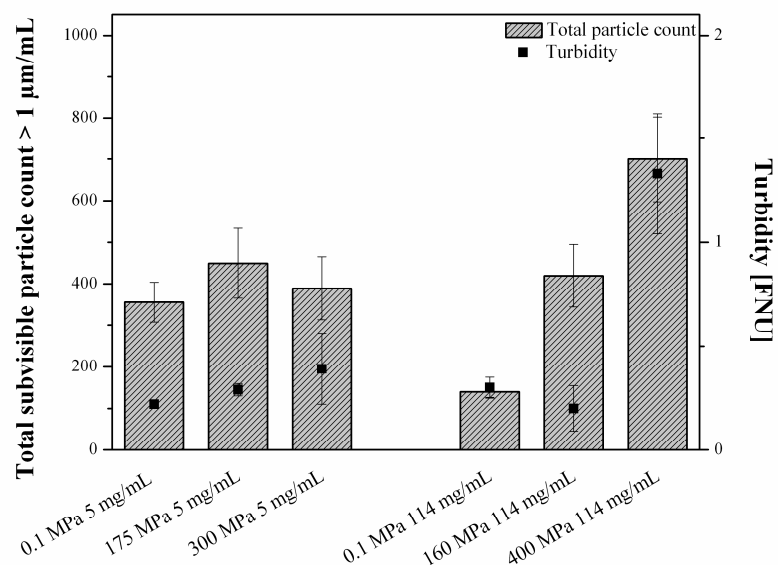


Figure 4-15 Total subvisible particle count (> 1 µm/mL) and the turbidity [FNU] for mAb1 solutions of 5 mg/mL and 114 mg/mL protein. The results refer to samples without any treatment (0.1 MPa) or to pressurized samples (160 MPa, 175 MPa, 300 MPa, 400 MPa).

Similar results could be obtained for the mAb2 protein solutions (Tab. 4-9). Pressurized samples showed a loss in total protein recovery, but with an adverse result compared to the mAb1 solutions. The reduction in total protein was higher for the lower concentrated mAb2 samples. However, the soluble aggregate content was again elevated for the higher concentrated protein solutions.

Table 4-9 Soluble aggregate content and total protein recovery obtained by SE-HPLC for mAb2 solutions of 5 mg/mL and 66 mg/mL protein. The results refer to samples without any treatment (0.1 MPa) or samples pressurized at 400 MPa.

mAb2 concentration	Pressure level	Soluble aggregate content [%]	Total protein recovery [%]
5 mg/mL	0.1 MPa	0.3	100
	400 MPa	0	75.9
66 mg/mL	0.1 MPa	0.3	100
	400 MPa	3.4	84.9

Light obscuration measurements revealed increased subvisible particle counts for the higher concentrated mAb2 solutions (Fig. 4-16). The pressurized samples showed fur-

ther increased values. The results of the turbidity analysis were nearly equal for the 5 mg/mL and 66 mg/mL protein solutions. Only the pressurized samples showed again slightly increased values.

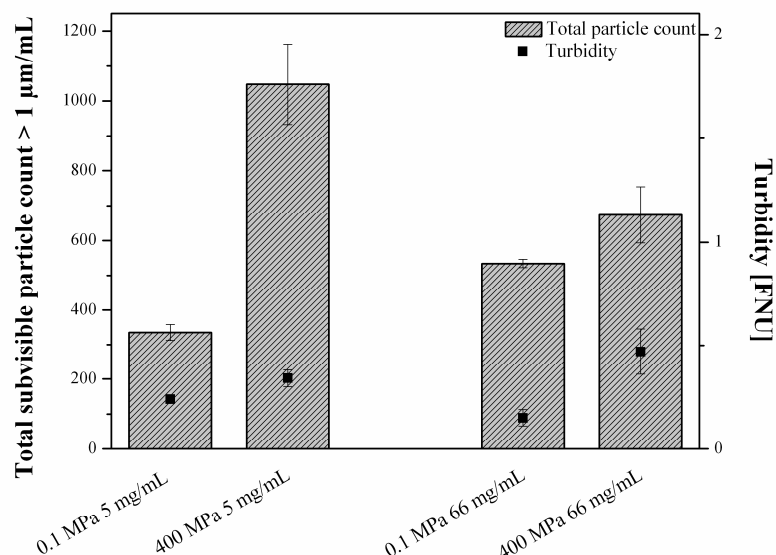


Figure 4-16 Total subvisible particle count (> 1 µm/mL) and the turbidity for mAb2 solutions (5 mg/mL and 66 mg/mL). The results refer to samples without any treatment (0.1 MPa) or samples pressurized at 400 MPa.

The results reveal a pressure induced aggregate formation for solutions of both antibodies which is dependent on the applied pressure level and protein concentration used.

4.3.3.6 Dissociation of mAb aggregates through high pressure

Despite the fact that adverse effects on protein stability in protein solutions were observed after exposure to high hydrostatic pressure, further studies on mAb aggregate dissociation should be performed. The protein solutions used so far did not contain any aggregates. Conclusions concerning potential antibody aggregate dissociation by high hydrostatic pressure could not be drawn. Therefore, mAb1 and mAb2 solutions were faced to different stresses in order to generate protein aggregates. The stresses utilized were light stress (60 watt/m³, 24 h), stirring stress (500 rpm with stirrer bar, 8 h), agitation stress (Eppendorf Mixer 5432, 8 h) and thermal stress at 35°C (24 h) and 50°C (24 h). After aggregate formation, the samples were exposed to 150 MPa or 400 MPa for 24 h and analyzed by SE-HPLC, light obscuration and turbidity.

For each stressed mAb1 sample aggregate formation could be observed (Tab. 4-10). The highest soluble aggregate level was determined for light stressed samples while the highest loss in total protein was detected for thermal stressed samples at 35°C. For the latter samples lower soluble aggregate contents as well as an increased total protein recovery could be observed after treatment at 150 MPa compared to the untreated counterparts. For all other samples, except the light stressed samples, smaller soluble aggregate contents, but also a decreased total protein recovery was found after exposure to 150 MPa. Treatment at 400 MPa resulted in increased soluble aggregate contents except for the light stressed samples. In all cases the total protein recovery was reduced by at least 58.5% at 400 MPa.

Table 4-10 Soluble aggregate content and the total protein recovery of differently stressed mAb1 solutions. The samples were either non-pressurized (0.1 MPa) or exposed to 150 MPa or 400 MPa prior to SE-HPLC analysis.

mAb1 sample	Pressure level	Soluble aggregate content [%]	Total protein recovery [%]
mAb1 in solution	0.1 MPa	0.4	100
Light stressed	0.1 MPa	18.5	91.1
	150 MPa	21.2	92.0
	400 MPa	8.9	30.4
Stirring stressed	0.1 MPa	2.5	100
	150 MPa	0.8	94.6
	400 MPa	6.9	35.2
Agitation stressed	0.1 MPa	2.1	100
	150 MPa	0.8	95.1
	400 MPa	8.0	37.2
Thermal stressed (35°C)	0.1 MPa	1.7	86.9
	150 MPa	1.0	95.3
	400 MPa	7.8	41.5
Thermal stressed (50°C)	0.1 MPa	2.1	100
	150 MPa	1.8	100
	400 MPa	6.3	34.3

Light obscuration and turbidity measurements revealed no clear trend for these samples (Fig. 4-17). Whereas the turbidity values increased with rising pressure treatment, except for the stirring stressed samples, the subvisible particle counts were increased for

the samples exposed to 150 MPa compared to samples pressured at 400 MPa. Only for the thermal stressed samples (50°C) the subvisible particle counts showed adverse results.

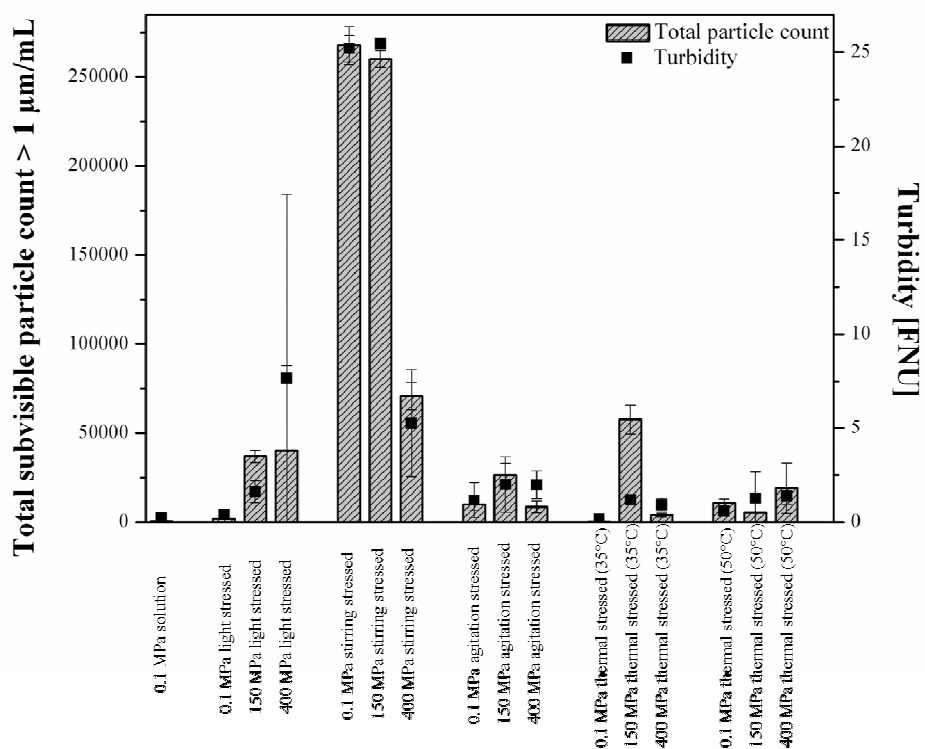


Figure 4-17 Total subvisible particle count (> 1 µm/mL) and the turbidity [FNU] of mAb1 solutions which remained either non-pressurized (0.1 MPa) or were exposed to 150 MPa or 400 MPa prior to light obscuration and turbidity measurements.

The results for the mAb2 samples followed similar trends (Tab. 4-11). Again, increased soluble aggregate levels and reduced total protein recovery were found for the stressed samples. Only for the stirred samples the results remained comparable towards the unstressed mAb2 solutions. Treatment at 150 MPa resulted in higher total protein recovery but increased soluble aggregate contents. For agitation stressed samples and thermal stresses samples (35°C) only slightly increased soluble aggregate contents of about 0.2 - 0.3% were found. As for mAb1, pressurization at 400 MPa led to increased soluble aggregate levels as well as to significantly reduced total protein recoveries. The light stressed samples again showed adverse results with smaller soluble aggregate contents.

Table 4-11 Soluble aggregate content and the total protein recovery of differently stressed mAb2 solutions. The samples were either non-pressurized (0.1 MPa) or exposed to 150 MPa or 400 MPa prior to SE-HPLC analysis.

mAb2 sample	Pressure level	Aggregate content [%]	Total protein recovery [%]
mAb2 in solution	0.1 MPa	0.3	100
Light stressed	0.1 MPa	9.0	68.8
	150 MPa	18.6	100
	400 MPa	7.1	55.5
Stirring stressed	0.1 MPa	0.2	100
	150 MPa	0.2	97.0
	400 MPa	31.3	69.1
Agitation stressed	0.1 MPa	0.1	93.8
	150 MPa	0.3	98.5
	400 MPa	23.0	51.1
Thermal stressed (35°C)	0.1 MPa	0.5	95.9
	150 MPa	0.8	99.3
	400 MPa	3.0	43.1
Thermal stressed (50°C)	0.1 MPa	6.2	60.8
	150 MPa	13.5	100
	400 MPa	40.5	79.5

Light obscuration and turbidity measurements again could not reveal a clear trend (Fig. 4-18). The light stressed, agitation stressed and thermal stressed (50°C) samples treated with 150 MPa showed the highest subvisible particle counts. In contrast, the thermal stressed samples (30°C) showed the highest subvisible particle counts after treatment at 400 MPa. Interestingly, untreated samples exposed to stirring stresses showed the highest subvisible particle counts. Except of the thermal stressed samples (50°C), the turbidity values were higher for samples exposed to 400 MPa as for those pressurized at 150 MPa. The untreated but thermal stressed (35°C) samples showed an exceptional high turbidity value.

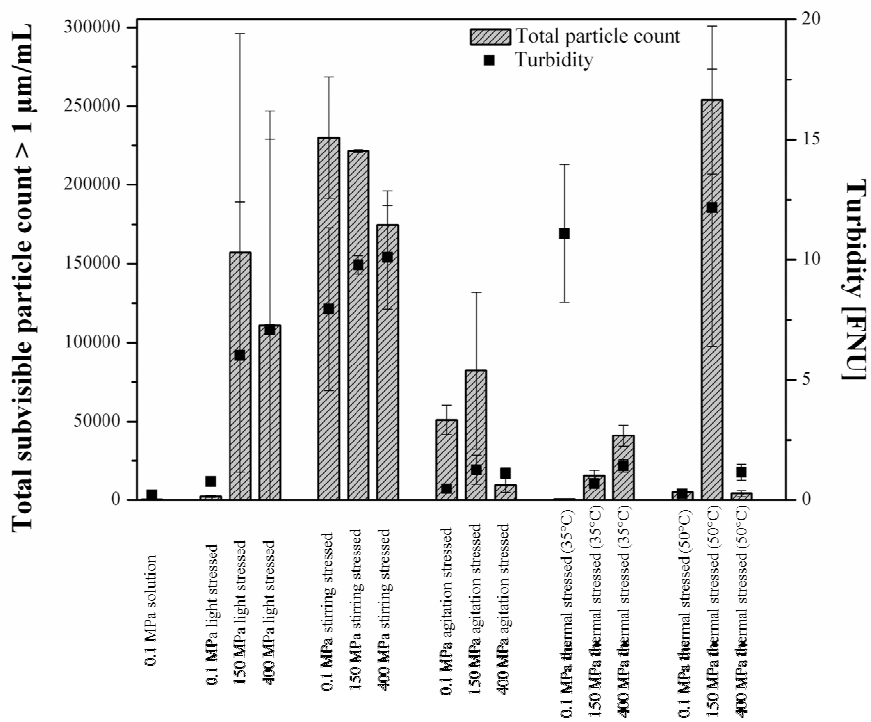


Figure 4-18 Total subvisible particle count (> 1 µm/mL) and the turbidity [FNU] of mAb2 solutions which remained either non-pressurized (0.1 MPa) or were exposed to 150 MPa or 400 MPa prior to light obscuration and turbidity measurements.

Summarizing, a reduction of artificial aggregate levels by application of high hydrostatic pressure could be found for thermal stressed (35°C) mAb1 solutions as well as for agitation and thermal stressed (35°C, 50°C) stressed mAb2 solutions.

4.4 Discussion

mAb1 and mAb2 crystallization with the lead condition presented by Stefan Gottschalk was reproducible. The crystal morphologies as well as the aggregate formation during crystallization and storage were the same as described during the preliminary study ¹. The unfavorable mAb1 and mAb2 crystal morphologies were deemed to be responsible for the instability ^{1,2}. Therefore, it was tried to obtain crystal polymorphs of higher stability in a first set of experiments by crystallization at higher or lower temperatures than under standard crystallization conditions or by applying of agitation during the crystallization. However, no crystal polymorphs of higher stability were obtained with these strategies, but amorphous precipitates, smaller needle-shaped crystals, crystal breakage under agitation and, except at crystallization at 2-8°C, a reduction in the total monomer recovery of 1-2% in average. The amorphous precipitates were obtained after application of extensive stirring. Incorporation into a crystal lattice is time consuming for proteins until the required contacts are formed ³. This process was hindered by an accelerated protein transport by stirring. The smaller needle-shaped crystals were obtained at crystallization at 2-8°C and after crystallization at 40 rpm teetering. At 2-8°C, the protein solubility is reduced which resulted in a higher nucleation rate and thus in a high number of smaller crystals ^{3,8}. Application of 40 rpm teetering changed the nucleation rates and crystal growth kinetics. Furthermore, it triggered the formation of a higher number of nuclei by increasing the mixing of protein in the samples ^{9,10}. However, after transfer of the small needle-like crystals to higher temperatures, the protein solubility increased and the crystals transited towards larger platelet-shaped crystals by Ostwald ripening. The formation of crystal debris resulted from mechanical abrasion at the container wall. The loss in total monomer recovery observed resulted from the mechanical agitation stress or the thermal stress at elevated temperature. The latter assumption was confirmed by an increased total monomer recovery at lower crystallization temperatures.

In a second experiment pH shifts, additives and PEGs of higher molecular weight were tested to change the mAb1 crystal morphology. However, the effects of these approaches remain neglectable. The occurrence of smaller crystals after the small pH shift from 5.5 to 5.9 highlights the strong effect of protein surface charges on protein-protein interactions under crystallization conditions ^{3,8}. Addition of additives resulted in the formation of amorphous aggregates which was ascribed to the additive feature to mediate

inter-molecular interactions¹¹⁻¹⁴. Application of PEG with higher molecular weight resulted in no new crystal morphology, but reduced aggregate formation. This effect resulted from lower PEG concentrations required to trigger crystallization and thus lower impurity levels.

Finally, application of high hydrostatic pressure was assessed for its effect on mAb crystallization and stability. In a first experiment, mAb1 and mAb2 resistance against elevated pressure levels was assessed to define suitable pressure ranges which could be used during following experiments. mAb1 crystals remained optically stable until a pressure level of 160 MPa. However, some amorphous structures could already be observed at this pressure level which was an effect of increased mAb1 solubility as it is described for other proteins at elevated pressure levels^{15,18,33}. Upon depressurization the protein precipitates fast by formation of amorphous structures. On contrast, mAb2 crystals withstood pressure levels until the technical limit of the pressure intensifier. A decreased crystal solubility, as known for other proteins under pressure, could not be proven^{16,17}. However, the absence of amorphous structures confirmed the hypothesis that mAb2 crystal did not dissolve at elevated pressure levels.

Hydrostatic pressure was also tested with the aim to find new mAb1 and mAb2 crystal polymorphs. For mAb1, melted-sheet like structures were obtained at 160-250 MPa which represented a different shape. However, application of polarized light revealed the morphology to be an amorphous state. The microstructure of the melted-sheet like structures was dependent on the PEG concentration and the applied pressure. This indicated protein reorganization during pressurization which resulted from elevated mAb1 solubility at higher pressure levels. However, a new crystallization window could not be found. For mAb2, PEG and ammonium sulfate were used as alternative crystallization agents against phosphate salt. Application of ammonium sulfate as crystallization agent under ambient pressures results in small needle-like crystals. Again, no new crystal morphology was found for this protein. Upon depressurization, the protein-protein contacts formed by mAb1 and mAb2 were not appropriate to form crystals. However, an extensive screening for a suitable crystallization buffer which allowed for suitable protein-protein interactions was not in scope of the present study.

In a further experiment, pressurization at 150 MPa immediately after starting mAb1 crystallization and pressurization at 150 MPa and 400 MPa immediately after starting

mAb2 crystallization was performed to test the effects of high hydrostatic pressure on the crystallization process and aggregate formation. While no effects on the crystallization process could be observed after pressurization at 150 MPa, mAb2 remained amorphous after pressurization at 400 MPa. All pressurized samples showed increased aggregate contents already after 1 day of crystallization. After 4 weeks, the aggregate contents of all pressurized samples were significantly higher compared to non-pressurized samples which indicated pressure induced protein unfolding. Undesired pressure-induced protein unfolding is already described for several proteins above 400 MPa^{31-33,35}. However, a small number of protein molecules can be denatured at lower pressure levels which results in small aggregate formation over the time. This effect was observed for the samples pressurized at 150 MPa.

In addition, high hydrostatic pressure was used to reduce aggregate contents of matured mAb1 and mAb2 crystal suspensions. While for mAb1 adverse effects were observed, mAb2 crystal pressurization at 175 MPa tend to reduced soluble aggregate levels and increased total protein recovery. Higher pressure equal or higher than 400 MPa resulted again in pressure-induced protein denaturation^{31-33,35}. Aggregate dissociated at 175 MPa was in accordance to literature which describes a range from 100 MPa to 300 MPa as to be applicable for that approach^{24,25}.

Finally, the effect of high hydrostatic pressure on the protein integrity of differently concentrated mAb1 and mAb2 solutions and different mAb1 and mAb2 aggregates was assessed as the effect of high hydrostatic pressure on mAb solutions or dissociation of mAb aggregates have not been reported so far. mAb1 and mAb2 aggregate formation was induced by different stresses: thermal stress, light stress and agitation stress. For both proteins, a significant aggregate formation could be observed after pressurization of fresh mAb solutions which was dependent on the pressure level and protein concentration. The aggregate formation could be detected under the reported limits for pressure-induced protein denaturation. In literature, the limit is set to 400 MPa or 500 MPa^{25,32,33}. These results contradict the reports about the feature of high hydrostatic pressure to reduce aggregate contents at lower pressure levels^{25,27,30,31}. In contrast, increased total protein recovery was detected after pressurization for light stressed and thermal stressed (35°C) mAb1 as well as agitation and thermal stressed (35°C, 50°C) mAb2 samples. For other samples, stressed by light exposure or stirring, no positive effects were observed. Thermal stress is described to result only partly in covalent mAb

aggregates ³⁸. In contrast, light exposure can induce disulfide bond formation and thus lead to covalently linked protein aggregates ³⁹. Consequently, the ability of high hydrostatic pressure to dissociate protein aggregates cannot be ascribed to the type of aggregation. The feature of high hydrostatic pressure to dissociate insoluble mAb aggregates in matured or stressed mAb was demonstrated.

4.5 Conclusion

mAb1 and mAb2 crystallization which was performed in accordance to the lead conditions introduced by Stefan Gottschalk led to a constant aggregate formation over the time. This instability resulted from the unfavorable needle-like crystal morphology which provides small numbers of protein-protein interactions and thus small protein stabilization.

No new mAb1 and mAb2 crystal morphologies were obtained under the tested crystallization conditions. Neither small variation of the buffer pH, the crystallization temperature nor the application of agitation had any effect on the mAb crystal morphology. However, the possibilities to alter the crystallization conditions, especially the buffer as strongest tool, were restricted to only small changes as it was required to maintain biocompatibility of the crystallization systems.

Application of high hydrostatic pressure as new tool for mAb crystallization did also not provide any mAb1 or mAb2 crystal polymorphs. This concept also suffered from the restriction to keep the crystallization buffer unchanged. However, it was demonstrated that mAb aggregates can be dissociated at low pressure levels around 150 MPa. Further research is required to improve complete understanding of this approach towards mAb crystallization and stability.

4.6 References

1. Gottschalk, S., *Crystalline Monoclonal Antibodies: Process Development for Large Scale Production, Stability and Pharmaceutical Applications*. Thesis Munich, 2008.
2. Hekmat, D., Hebel, D., Schmid, H., Weuster-Botz, D., *Crystallization of lysozyme: From vapor diffusion experiments to batch crystallization in agitated ml-scale vessels*. *Process Biochemistry*, 2007. **42**(12): p. 1649-1654.
3. Durbin, S., Feher, G., *Protein crystallization*. *Annual Review of Physical Chemistry*, 1996. **47**(1): p. 171-204.
4. Jarmer, D.J., Lengsfeld, C.S., Anseth, K.S., Randolph, T.W., *Supercritical fluid crystallization of griseofulvin: Crystal habit modification with a selective growth inhibitor*. *Journal of Pharmaceutical Sciences*, 2005. **94**(12): p. 2688-2702.
5. Pechenov, S., Shenoy, B., Yang, M.X., Basu, S.K., Margolin, A.L., *Injectable controlled release formulations incorporating protein crystals*. *Journal of Controlled Release*, 2004. **96**(1): p. 149-158.
6. Mozhaev, V.V., *Mechanism-based strategies for protein thermostabilization*. *Trends in Biotechnology*, 1993. **11**(3): p. 88-95.
7. Ramsland, P.A., Farrugia, W., *Crystal structures of human antibodies: a detailed and unfinished tapestry of immunoglobulin gene products*. *Journal of Molecular Recognition*, 2002. **15**(5): p. 248-259.
8. McPherson, A., *Introduction to protein crystallization*. *Methods*, 2004. **34**(3): p. 254-265.
9. Heng, M.H., *Method for rapidly obtaining crystals with desirable morphologies*. 2003, US Patent 6,593,118 B2.
10. Matthews, T., Bean, B. *Development of a scaleable protein purification process using crystallization*. in *232nd American Chemical Society National Meeting*. 2006.
11. McPherson, A., Koszelak, S., Axelrod, H., Day, J., Williams, R., Robinson, L., McGrath, M., Cascio, D., *An experiment regarding crystallization of soluble proteins in the presence of beta-octyl glucoside*. *Journal of Biological Chemistry*, 1986. **261**(4): p. 1969-1975.
12. Derewenda, U., Derewenda, Z., Dodson, E., Dodson, G., Reynolds, C., Smith, G., Sparks, C., Swenson, D., *Phenol stabilizes more helix in a new symmetrical zinc insulin hexamer*. *Nature*, 1989. **338**(1): p. 594-596.
13. Bolen, D., *Effects of naturally occurring osmolytes on protein stability and solubility: issues important in protein crystallization*. *Methods*, 2004. **34**(3): p. 312-322.

14. Collins, K.D., *Ions from the Hofmeister series and osmolytes: effects on proteins in solution and in the crystallization process*. *Methods*, 2004. **34**(3): p. 300-311.
15. Lorber, B., Jenner, G., Giege, R., *Effect of high hydrostatic pressure on nucleation and growth of protein crystals*. *Journal of Crystal Growth*, 1996. **158**(1): p. 103-117.
16. Visuri, K., Kaipainen, E., Kivimäki, J., Niemi, H., Leisola, M., Palosaari, S., *A new method for protein crystallization using high pressure*. *Nature Biotechnology*, 1990. **8**(6): p. 547-549.
17. Suzuki, Y., Sazaki, G., Visuri, K., Tamura, K., Nakajima, K., Yanagiya, S.-i., *Significant decrease in the solubility of glucose isomerase crystals under high pressure*. *Crystal Growth & Design*, 2002. **2**(5): p. 321-324.
18. Kadri, A., Damak, M., Jenner, G., Lorber, B., Giegé, R., *Investigating the nucleation of protein crystals with hydrostatic pressure*. *Journal of Physics: Condensed Matter*, 2003. **15**(49): p. 8253.
19. Crisman, R.L., Randolph, T.W., *Crystallization of recombinant human growth hormone at elevated pressures: Pressure effects on PEG-induced volume exclusion interactions*. *Biotechnology and Bioengineering*, 2010. **107**(4): p. 663-672.
20. Saikumar, M., Glatz, C., Larson, M., *Crystallization of lysozyme at high pressures*. *Journal of Crystal Growth*, 1995. **151**(1): p. 173-179.
21. Suzuki, Y., Sazaki, G., Miyashita, S., Sawada, T., Tamura, K., Komatsu, H., *Protein crystallization under high pressure*. *Biochimica et Biophysica Acta (BBA)-Protein Structure and Molecular Enzymology*, 2002. **1595**(1): p. 345-356.
22. Fourme, R., Kahn, R., Mezouar, M., Girard, E., Hoerentrup, C., Prangé, T., Ascone, I., *High-pressure protein crystallography (HPPX): instrumentation, methodology and results on lysozyme crystals*. *Journal of Synchrotron Radiation*, 2001. **8**(5): p. 1149-1156.
23. Kadri, A., Lorber, B., Charron, C., Robert, M.-C., Capelle, B., Damak, M., Jenner, G., Giegé, R., *Crystal quality and differential crystal-growth behaviour of three proteins crystallized in gel at high hydrostatic pressure*. *Acta Crystallographica Section D: Biological Crystallography*, 2005. **61**(6): p. 784-788.
24. Cioni, P., Strambini, G.B., *Pressure effects on the structure of oligomeric proteins prior to subunit dissociation*. *Journal of Molecular Biology*, 1996. **263**(5): p. 789-799.
25. Paladini Jr, A.A., Weber, G., *Pressure-induced reversible dissociation of enolase*. *Biochemistry*, 1981. **20**(9): p. 2587-2593.
26. Randolph, T.W., Seefeldt, M., Carpenter, J.F., *High hydrostatic pressure as a tool to study protein aggregation and amyloidosis*. *Biochimica et Biophysica*

- Acta (BBA)-Protein Structure and Molecular Enzymology, 2002. **1595**(1): p. 224-234.
27. Schoner, B.E., Bramlett, K.S., Guo, H., Burris, T.P., *Reconstitution of functional nuclear receptor proteins using high pressure refolding*. Molecular Genetics and Metabolism, 2005. **85**(4): p. 318-322.
 28. Aertsen, A., Meersman, F., Hendrickx, M.E., Vogel, R.F., Michiels, C.W., *Biotechnology under high pressure: applications and implications*. Trends in Biotechnology, 2009. **27**(7): p. 434-441.
 29. Seefeldt, M.B., Ouyang, J., Froland, W.A., Carpenter, J.F., Randolph, T.W., *High-pressure refolding of bikunin: Efficacy and thermodynamics*. Protein Science, 2004. **13**(10): p. 2639-2650.
 30. Fradkin, A.H., Carpenter, J.F., Randolph, T.W., *Immunogenicity of aggregates of recombinant human growth hormone in mouse models*. Journal of Pharmaceutical Sciences, 2009. **98**(9): p. 3247-3264.
 31. John, R.J.S., Carpenter, J.F., Randolph, T.W., *High pressure fosters protein refolding from aggregates at high concentrations*. Proceedings of the National Academy of Sciences, 1999. **96**(23): p. 13029-13033.
 32. Balduino, K.N., Spencer, P.J., Malavasi, N.V., Chura-Chambi, R.M., Lemke, L.S., Morganti, L., *Refolding by high pressure of a toxin containing seven disulfide bonds: bothropstoxin-1 from Bothrops jararacussu*. Molecular Biotechnology, 2011. **48**(3): p. 228-234.
 33. Gross, M.Jaenicke, R., *Proteins under pressure*. European Journal of Biochemistry, 1994. **221**(2): p. 617-630.
 34. Webb, J.N., Carpenter, J.F., Randolph, T.W., *Stability of subtilisin and lysozyme under high hydrostatic pressure*. Biotechnology progress, 2000. **16**(4): p. 630-636.
 35. Hayakawa, I., Linko, Y.-Y., Linko, P., *Mechanism of high pressure denaturation of proteins*. LWT-Food Science and Technology, 1996. **29**(8): p. 756-762.
 36. Judge, R.A., Jacobs, R.S., Frazier, T., Snell, E.H., Pusey, M.L., *The effect of temperature and solution pH on the nucleation of tetragonal lysozyme crystals*. Biophysical Journal, 1999. **77**(3): p. 1585-1593.
 37. Schwierz, N., Netz, R.R., *Effective interaction between two ion-adsorbing plates: Hofmeister series and salting-in/salting-out phase diagrams from a global mean-field analysis*. Langmuir, 2012. **28**(8): p. 3881-3886.
 38. Hawe, A., Kasper, J.C., Friess, W., Jiskoot, W., *Structural properties of monoclonal antibody aggregates induced by freeze-thawing and thermal stress*. European Journal of Pharmaceutical Sciences, 2009. **38**(2): p. 79-87.

39. Mahler, H.-C., Friess, W., Grauschopf, U., Kiese, S., *Protein aggregation: Pathways, induction factors and analysis*. Journal of Pharmaceutical Sciences, 2009. **98**(9): p. 2909-2934.

Chapter 5

Statement: Within this chapter, the work related to section 5.3.3.1.2 “Investigation of the origin of mAb1 aggregate formation during crystallization and storage” was performed together with Roman Mathaes and is planned to be submitted as publication in the *Journal of Pharmaceutical Sciences*.

The work related to section 5.3.3.1.2 would not have been possible without his remarkable effort and sound understanding of particle analytics. All analytical work related to protein aggregate detection and quantification by flow cytometry and confocal laser scanning microscopy was instructed by him. All work in context of sample preparation as well as size exclusion chromatography was guided by me. Antibody labelling and thesis writing was performed in equal parts.

5 The mechanisms behind the aggregate formation in mAb1 and mAb2 crystal suspensions

5.1 Introduction

Therapeutic antibodies represent a class of large protein molecules of high complexity. Scientists try to conserve antibody formulation's stability for long shelf lives up to 24 months. Degradation pathways can vary depending on the formulation and storage conditions which the proteins face. Different degradation pathways may happen simultaneously on chemical or physical level ¹⁻³.

5.1.1 Chemical instability

Chemical instabilities comprise protein modifications such as cross-linking, deamidation, oxidation, proteolysis, hydrolysis, beta elimination, isomerization and other processes which result in bond formation or cleavage ^{2,4,5}. The most common will be discussed in detail:

5.1.1.1 Deamidation

The term deamidation describes the conversion from an amide group of an amino side chain to a carboxylate or carboxylic acid group ⁶. Particularly asparagine and glutamine are reported to be prone to deamidation. This instability pathway is regarded as major cause for protein charge heterogeneity which results in a more acidic isoelectric point of the molecules ⁷. However, deamidation does not necessarily result in loss of bioactivity when the reaction does not take place in the binding region. The extent of deamidation is dependent on many factors such as the buffer pH and its ionic strength, the storage temperature and vicinal amino acids ^{1,2,7}.

5.1.1.2 Oxidation

More functional groups are susceptible to oxidation than to deamidation. However, oxidation is a less common instability pathway. The class of oxidizable amino acids comprises methionine, tyrosine, tryptophan, histidine, cysteine and phenylalanine ^{1,2,7}. Methionine and cysteine can easily be oxidized due to their thiol-groups. Tryptophan, histidine and phenylalanine stabilize radicals originated from oxidation by their aromatic residues ^{2,8}. Oxidation is induced by light exposure, elevated temperatures, metal catalysis and reactive oxygen species ^{7,8}.

Besides direct protein oxidation, formulation scientists have to consider auto-oxidation of ingredients. For example polysorbates are prone to auto-oxidation which results in formation of peroxides and thus protein oxidation⁹. The term auto-oxidation describes the uncatalyzed oxidation of a substrate by molecular oxygen, which induces a chain reaction in most of the cases¹⁰⁻¹².

5.1.1.3 Cross-linking

Cross-linking means the formation of inter- or intra-molecular connections. The most common cross-linking pathway results in the creation or exchange of disulfide-bonds initiated by reactive thiol groups of cysteinyl residues. This instability mechanism is pH dependent and occurs foremost at high formulation pH values. Even proteins without free cysteine groups are prone to cross-linking since existing bonds are able to scramble^{1,2}.

5.1.1.4 Fragmentation

Fragmentation is a common phenomenon for antibody formulations. This term comprises the molecule cleavage at the hinge region of one heavy chain resulting in a Fab and a Fab' + Fc fragment. This instability pathway is usually caused by non-enzymatic hydrolytic processes rather than by residual proteases. Fragmentation might be induced by for example low pH values, thermal treatment or freeze-thaw stresses. Fragmented proteins usually show a loss in bioactivity, different bio-distribution and increased toxicity^{1,7,13}.

5.1.2 Physical instability

Physical instability basically means protein degradation by denaturation or aggregation without covalent modifications.

5.1.2.1 Denaturation

During protein denaturation, the protein molecules lose their secondary, tertiary and quaternary structures. However, the native amino acid sequence is not affected. Denaturation can cause a loss in the biological specificity of the molecules. This instability is usually caused by temperature changes, shear stresses and other common manufacturing processes^{1,4,14,15}.

5.1.2.2 Aggregation

Protein aggregation represents the more common physical instability caused by stresses such as high protein concentrations, elevated viscosity, high ionic strength, inappropriate pH values, temperature changes, shaking, extensive storage and freeze-thaw stresses. Aggregation is characterized by protein-protein interactions which are affected by diffusion rates and geometric constraints and is therefore protein concentration dependent. Aggregates possess the risk for increased immunogenic potentials and reduced activities. By that, the WHO limited the aggregate levels for intravenous immunoglobulin therapeutics to less than 5%^{1,7,16}.

5.1.2.2.1 Mechanism behind aggregation

The underlying protein aggregation mechanisms will briefly be described: a native protein, thermodynamically most stable under physiological conditions, holds its hydrophobic residues in its interior to prevent their contacts to water molecules^{16,17}. However, the physical stability in this native state is only marginal and mostly driven by hydrophobic interactions such as repulsive interactions between the non-polar protein residues and water molecules^{2,16,18,19}. During unfolding, caused by inappropriate conditions, the hydrophobic residues become exposed to the protein surface which results in an increased energetic state for the molecule^{2,4,7}. Inter-molecular hydrophobic pairings result in protein-protein contacts in order to reduce the thermodynamic potential. Surface adsorption represents another mechanism for thermodynamically stabilization of unfolded protein states^{1,2,4}.

5.1.2.2.2 Aggregate classifications

Usually the term “aggregate” is used for all kinds of oligomeric or multimeric protein agglomerates. However, a protein can undergo several aggregation pathways which are dependent on the environmental conditions. Even the initial protein state can differ and thus result in different aggregation products. Such potential initial states comprise native structures, degraded structures, modified structures and partially or fully unfolded protein states^{5,20,21}. Mahler et al. recently suggested to classify protein aggregates into the following classes⁵:

5.1.2.2.2.1 Non-covalent and covalent aggregates

While non-covalently aggregate proteins are held together by weak forces such as Van der Waals interactions, hydrogen bonding or electrostatic forces, the covalent aggregates formed disulfide bridges or are linked by a non-disulfide reaction by dityrosine formation²².

5.1.2.2.2.2 Reversible and irreversible aggregates

Reversible aggregates are considered to represent protein self-assemblies which might quickly disassemble for example when diluted²³. In contrast, irreversible aggregates maintain even under denaturing or reducing conditions².

5.1.2.2.2.3 Soluble and insoluble aggregates

The term “soluble aggregates” described oligomeric protein aggregates of sizes up to 1 μm. Insoluble aggregates possess sizes larger 1 μm up to particle sizes even being visible for the eye. The form of such insoluble particles may be amorphous or fibrillar. Soluble and non-soluble aggregates can be separated from each other by centrifugation as soluble aggregates do not exhibit sedimentation²⁴.

5.1.2.2.2.4 Native and non-native aggregates

Aggregates which possess predominantly protein in its native structure were referred as native aggregates. In contrast, non-native aggregates result from proteins which had been undergone either conformational instability or chemical modifications².

5.1.3 Strategies to maintain protein stability

Nowadays, formulation scientists have several formulation strategies on hand to maintain protein instability²⁵:

5.1.3.1 Formulation pH

Proteins represent a class of large macromolecules characterized by many intra- and intermolecular electrostatic attributes. In consequence, the formulation pH value strongly influences the overall protein stability. Protein unfolding usually starts at pH values far from the isoelectric point as the charge density dramatically increases. This state fosters repulsion of accordant charges which is satisfied by molecular unfolding. However, at pH values close to the isoelectric point, the negative and positive charges can-

cel. At this state aggregation might occur as repulsive electrostatic forces are reduced and the attraction forces predominate. Therefore, protein stability is linked to a narrow pH range in the most cases. For most antibodies a weakly acidic conditions were deemed to be optimal ^{1,2,26}.

5.1.3.2 Surfactants

Surfactants stabilize proteins by interacting with their hydrophobic moieties. By that, the tendency for the proteins to form non-covalent aggregate or to adsorb to surfaces is reduced. The class of surfactants comprises among others polysorbate 20/80 and poloxamer 188 ²⁷⁻²⁹.

5.1.3.3 Antioxidants

Antioxidants should be used in stoichiometric quantities for optimal protein stabilization. The class of antioxidants can be divided into chelators such as EDTA, citric acid and polyols which chelate oxidation catalyzing metal ions and oxygen scavengers such as methionine and thiosulfate which deplete oxygen from the solution ^{30,31}.

5.1.3.4 Amino acids and Polyols

Amino acids and polyols such as polyethylene glycol (PEG) stabilize proteins by the excluded volume effect. The polymers occupy space in the solute which results in protein crowding. The macromolecules start to interact by formation of a state of minimal surface area which is thermodynamically favored.

However, PEGs possess destabilizing effects under certain conditions. Beside their tendency for auto-oxidation, PEGs interact with hydrophobic residues which are exposed in the unfolded state. Furthermore, a weak denaturation action in solution is described for PEGs ^{2,9,18,30,32,33}.

5.1.3.5 Salts

The effect of salts on protein stability is hardly predictable as the salt properties were strongly dependent on the type of salt used, the salt concentration and the buffer pH. Consequently, the search for suitable buffer compositions often results in an extensive screening in a trial and error fashion. The property of salts to stabilize proteins is referred to non-specific electrostatic shielding, specific ion binding and effects on the buffer properties ^{2,26,34}.

5.1.4 Protein stability in the crystalline state

In theory, protein crystals represent a state of lower inner energy and thus lower reactivity compared to the amorphous unordered state³⁵⁻³⁷. However, there is an ongoing discussion whether protein crystals really represent a state of superior stability.

Already in 1997, Pikal et al. compared the storage stability of crystalline and amorphous insulin at 40°C over 2 months. The results suggested a superior stability of the amorphous form³⁸. On the contrary, studies from Shenoy et al. demonstrated higher stability for crystalline suspensions than for their corresponding amorphous formulations and even compared to liquid formulations^{35,39}. These studies suggested that a superior protein crystal stability has to be proven in each single case and might be formulation dependent^{35,40-42}.

However, a deep insight study regarding protein aggregate formation in crystalline suspensions has not yet been presented. Studies should be performed which investigate the cause for aggregation, the type of aggregates formed and the origin of aggregates (crystals, supernatant). Therefore, several analytical tools such as SDS-PAGE, isoelectric focusing (IEF) and LC-MS were used for mAb1 and mAb2 aggregate characterization.

For both antibodies, the crystallization conditions itself were deemed to cause the aggregate formation during crystallization and storage. For mAb1, the high PEG concentration was suspicious. PEG is prone to auto-oxidation which results in formation of peroxides and formaldehyde which can cause aggregation by oxidation and protein-protein linkage⁹. Therefore, studies were conducted to investigate the influence of two PEG degradation products, peroxides and formaldehydes, on protein crystallization and stability. PEG was purified applying vacuum drying and freeze drying in order to evaluate the effectiveness of both techniques to reduce each impurity. Furthermore, the effectiveness of double purification (vacuum drying followed by freeze drying) was investigated and compared to single purification. Impurity effects such as aggregate formation during crystallization of mAb1 were followed by utilizing differently purified PEG. Addition of methionine prior to precipitation was applied to study the “neutralizing” effect of anti-oxidants on PEG impurities and thus aggregate formation. Addition of peroxides and formaldehydes in different concentrations to extensively purified PEG was studied to highlight their effects on mAb1 crystallization and aggregate formation.

Finally, protein stability during and after crystallization was followed after applying different PEG qualities purchased from varying vendors.

It was hypothesized for the present study that the crystalline state stabilizes the protein. Consequently, the origin of the aggregate formation would be the supernatant. A protein exchange between the crystals and supernatant would mandatory be required for aggregate incorporation into the crystals. This protein exchange should be investigated and visualized during a first experiment. Therefore, the supernatant was exchanged with an identical, but fluorescence labeled protein solution after the maximum crystal yield was achieved (about two weeks). Monitoring of this phenomenon was performed by confocal laser scanning microscopy (CLSM). Aggregate formation was followed by size exclusion high pressure chromatography (SE-HPLC) and flow cytometry (FACS). Furthermore, if the aggregates found in the crystalline state would show fluorescence signals, the origin of the protein would be in the supernatant.

To investigate the cause for mAb2 aggregate formation, the concentration of the crystallization agent and the buffer pH value were changed. Furthermore, methionine was added to investigate the effect of potential mAb2 oxidation the on aggregate formation. In addition, mAb2 was exposed to PEG in order to confirm findings for mAb1. The same analytical tools as for mAb1 were used for mAb2 aggregate characterization.

5.2 Materials and Methods

5.2.1 Materials

mAb1 and mAb2 were two monoclonal antibodies from the IgG1 class. The samples were stored at - 80°C (antibodies) until required for use.

Sodium chloride (AnalaR NORMAPUR) as crystallization agent for lysozyme was purchased from VWR Prolabo (Leuven, Belgium). Sodium acetate (USP standard) was from Merck (Darmstadt, Germany). Sodium sulphate (99%) was from Grüssing GmbH (Filsum, Germany). Sodium dihydrogen phosphate-dihydrate (pure Ph. Eur., USP), disodium hydrogen phosphate-dihydrate (analytical grade), potassium dihydrogen phosphate and potassium chloride (both analytical grade) were obtained from Appli-chem GmbH (Darmstadt, Germany). Polyethylene glycol 4000 was purchased from Clariant (Frankfurt, Germany), Alfa Aesar (Karlsruhe, Germany), BioUltra (Sigma-Aldrich, Taufkirchen, Germany), AppliChem (Darmstadt, Germany) and Croda (Nettetal Kaltkirchen, Germany) each in a quality according to the European Pharmacopeia. Hydrochloric acid 32% (analytical grade), acetic acid 100% and ortho-phosphoric acid 85% were all purchased from Merck KGaA (Darmstadt, Germany). Sodium azide (99%) was received from Acros Organics (New Jersey, USA). The fluorescence dye ATTO 633 (NHS-Ester) was from ATTO-TEC (Siegen, Germany). Slide-A-Lyzer dialysis cassettes 10,000 MWCO were purchased from Thermo Scientific (Rockford, USA). All other reagents or solvents used during the solvent screening were of at least analytical grade and purchased either from Sigma-Aldrich (Taufkirchen, Germany) or from VWR Prolabo (Leuven, Belgium).

5.2.2 Methods

5.2.2.1 Crystallization of mAb1

Crystallization of mAb1 was carried out in a 0.1 M sodium acetate buffer at a pH of 5.50. For crystallization, a 24% (w/v) PEG 4000 solution was added dropwise in a 1:1 ratio to a 10 mg/mL protein solution under gentle shaking. The final formulation was stored at 20°C for at least two weeks.

5.2.2.2 Crystallization of mAb2

Crystallization of mAb2 was performed in a 0.1 M sodium acetate buffer of 4.1. For crystallization, a 4.2 M sodium dihydrogen phosphate solution was added dropwise in a

1:1 ratio to a 10 mg/mL protein solution under gentle shaking. The final formulation was stored at 20°C for at least one week.

5.2.2.3 mAb1 labelling

mAb1 was labelled with ATTO 633 NHS ester functionalized staining kits (ATTO-TEC GmbH, Siegen, Germany) according to the manufacture protocol. In brief, a 1:1 molar ratio of Atto633 NHS ester and antibody solution was incubated for 1 hour. The unbound dyes were removed by dialyzing with Slide-A-Lyzer dialysis cassettes against a 0.1 M sodium acetate buffer at pH 5.50.

5.2.2.4 Supernatant exchange (mAb1)

mAb1 crystallization efficacy was monitored by quantifying un-crystallized protein in the supernatant. The yield is represented by the amount of crystallized protein in percent of the initial protein concentration, which reaches a maximum at week two. Then supernatants were exchanged by an identical but fluorescence labeled mAb1 solution.

5.2.2.5 Assessment of crystal and protein integrity

5.2.2.5.1 Size exclusion high performance liquid chromatography (SE-HPLC)

Formation of soluble aggregates was followed by SE-HPLC. The analysis was performed on a Thermo separation system.

5.2.2.5.1.1 mAb1

The mobile phase for mAb1 consisted of 0.092 M Na₂HPO₄ (anhydrous) and 0.211 M Na₂SO₄ (anhydrous) at a pH of 7. The flow rate was set to 0.25 mL/min. Analysis was performed at the wavelengths of 214 nm and 280 nm. A TSKgel G300SWXL coloum from Tosoh Bioscience GmbH (Stuttgart, Germany) was used for separation.

5.2.2.5.1.2 mAb2

The mobile phase for mAb2 consisted 0.02 M Na₂HPO₄ (dihydrate) und 0.15 M sodium chloride at a pH of 7.5. The flow rate was set to 0.50 mL/min. Analysis was performed at the wavelengths of 214 nm and 280 nm. For separation, a Suprose-6-HR-10/30-coloum from GE Healthcare (Uppsala, Sweden) was used.

5.2.2.6 Ion exchange chromatography (IEC)

Ion exchange chromatography was carried out at a Merck Hitachi separation system. The mobile phase consisted of 5.4 g (20 mM) Na₂HPO₄ (Heptahydrat) and 2.7 g (20 mM) CH₃COONa (Trihydrat) in 900 mL MilliQ-Water. The pH was set to 7.0. Mobile phase B was equal to mobile phase A, but with additional 23.4 g (400 mM) NaCl. The pH of the mobile phase B was set to 5.0. For separation, a ProPac® WCX-10 Analytical 4 x 250mm was used (Thermo Fisher scientific, Rockford, USA).

5.2.2.7 Confocal laser scanning microscopy (CLSM)

Protein crystals suspensions were examined using a Zeiss 510 LSMNLO confocal microscope (Carl Zeiss Microscope systems, Jena, Germany) with a consistent setting for all groups. A Carl- Zeiss 63x oil immersion objective was utilized for acquisition. Images were averaged 4 x and scan speed was set to 6. All experiments were performed in triplicates.

5.2.2.8 Flow cytometry (FACS)

A BD FACSCanto II flow cytometer (Becton, Dickinson and Company, San Jose, CA) equipped with a 488 nm and a 633 nm laser was utilized to analyze protein subvisible particles. 60 µL of each sample was analyzed in FACS tubes (Becton, Dickinson and Company, San Jose, CA). Detector gain was adjusted for optimal particle analysis. The forward scatter detector (FSC) was set to 231 volts and the side scatter detector (SSC) was set to 191 volts. All samples (1 mg/mL) were analyzed in the low flow rate mode of 10 µL/min for 1 min.

5.2.2.8.1 Sodium dodecyl sulphate-Polyacrylamide gel electrophoresis (SDS-Page)

SDS-PAGE was used to separate different protein fractions.

Non-reducing conditions:

For denaturation, the protein samples were mixed with a Laemmli buffer (250 mM Tris(hydroxymethyl)-aminomethane, 1% of a 0.1% Bromphenol blue solution (Merck, Darmstadt, Germany), 4% SDS (Sigma-Aldrich, Taufkirchen, Germany), 23% of glycerol (AppliChem, Darmstadt, Germany) in a 1:1 ratio and incubated at 95°C for 20 min. Sample separation was performed on a Novex NuPAGE 3 - 8% Bis-Tris gel (life technologies, Carlsbad, USA) which was placed in an electrophoresis module (Bio-Rad,

Munich, Germany) filled with a Novex NuPAGE MES SDS-Running buffer 20x (Life Technologies, Carlsbad, USA). Electrophoresis was carried out at 100 V for 15 min followed by 160 V for 45 min. The gel was transferred into a bath of Imperial Protein stain (Coomassie blue staining) (Thermo Fisher Scientific, Rockford, USA) for detection. Staining was carried out for 60 min. The Mark12 protein standard ladder (Invitrogen, Carlsbad, USA) and the Spectra Multicolor High Range Protein Ladder (Thermo Fisher Scientific, Rockford, USA) were used for estimation of the molecular weights.

Reducing conditions:

SDS-PAGE can also be performed under reducing conditions. For this purpose dithiothreitol (DTT) is used which fosters breaking-up of covalent disulfide bonds. Therefore, 250 mg of DTT (Sigma-Aldrich, Taufkirchen, Germany) were added to 5 mL Laemmli buffer.

Isoelectric focusing (IEF) was used to investigate changes in the isoelectric point (IEP) of the two antibodies. Therefore, 10 μ L of 0.5 mg/mL of desalted protein solutions were placed on a Prectos[®] gel (SERVA, Heidelberg, Germany).

5.2.2.8.2 Isoelectric focusing (IEF)

Isoelectric focusing (IEF) was used to investigate changes in the isoelectric point (IEP) of the two antibodies. Analysis was performed on a Multiphor II[™] electrophoresis system combined with an EPS 3501 XL power supply and a MultiTemp III thermostatic circulator (GE Healthcare Europe GmbH, Freiburg, Germany). 10 μ L of a 0.5 mg/mL desalted protein solutions were placed on precast Servalyt[®] Prectos[®] Wide Range pH 3 - 10 gel (SERVA Electrophoreses GmbH, Heidelberg, Germany). For detection a Serva Liquid Mix IEF Marker 3 - 10 was used. Final gel staining was accomplished using a mix of 2.5 mL 20 % (w/v) trichloroacetic acid and 125 mL staining solution which consisted of 50 mg SERVA Blue W powder in aqua demineralized.

5.3 Results

5.3.1 The initial state of mAb1 and mAb2 crystal stability

During the preliminary study, an aggregate formation was observed for mAb1 and mAb2 crystals when crystallization and storage had been performed in the lead crystallization buffer²⁵. Therefore, mAb1 and mAb2 were crystallized in accordance to the lead conditions in order to reassure the reported findings. mAb1 was crystallized with 24% (w/v) PEG 4000. The soluble aggregate formation was followed by SE-HPLC for 12 weeks (Fig. 5-1). Prior to analysis, the crystals were separated from the supernatant and dissolved in PBS.

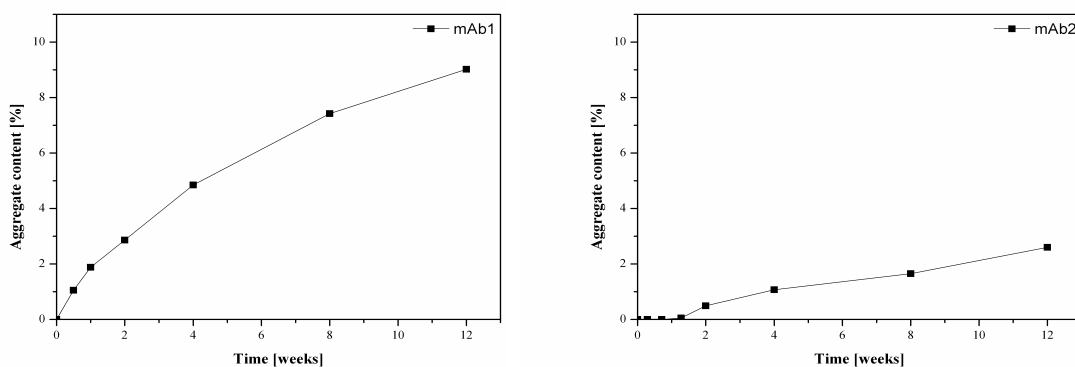


Figure 5-1 SE-HPLC data which illustrate the aggregate formation for crystalline mAb1 and mAb2 over 12 weeks.

The results revealed differences in the extent and rate of the aggregate levels for both antibody crystals. An initial aggregation, which occurred immediately after starting the crystallization, and high rates of aggregate formation were found for mAb1. In contrast, aggregates were first observed after 8 days for mAb2 and the increase of the aggregate level was distinctly smaller. This indicated two different underlying instability mechanisms for both proteins. Therefore, the “nature” of the aggregates was to be investigated.

5.3.2 Aggregate characterization

5.3.2.1 SDS-PAGE

In a first experiment, the mAb1 and mAb2 aggregates were characterized by SDS-PAGE. Covalently linked protein aggregates would indicate a chemical modification of the proteins. Therefore SDS-PAGE was performed under reducing and non-reducing conditions (Fig. 5-2 & 5-3). For both mAbs, dissolved crystals and the supernatant of freshly prepared and 9 months old crystal suspensions were analyzed to highlight the effect of long term storage. As mAb2 showed nearly 100% crystal yield, analysis of the supernatant was complicated and could only be successfully carried out for the reducing conditions (Fig. 5-3 II). In addition, freshly prepared solutions from both mAbs in their crystallization buffer without any crystallization agent were analyzed.

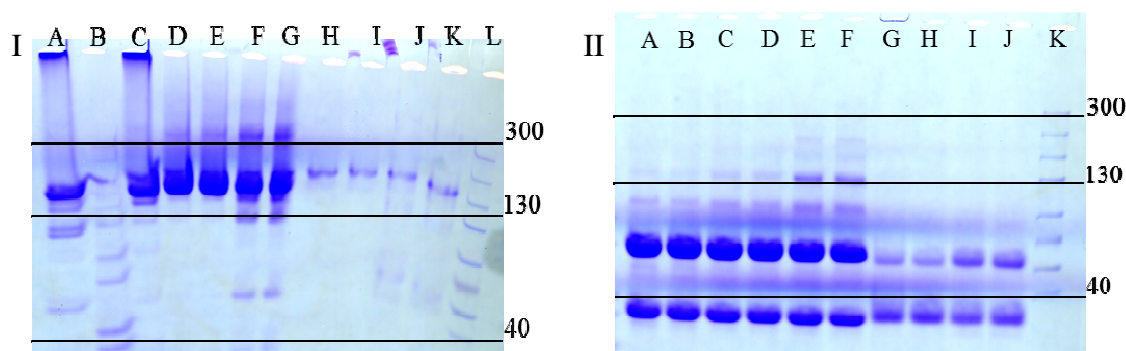


Figure 5-2 SDS-PAGEs performed for mAb1 under **I** non-reducing and **II** reducing conditions. The captions refer to **I**: A, C mAb1 crystals (9 month old); B, small range ladder; D, E mAb1 in buffer without PEG; F, G mAb1 crystals (fresh); H, I supernatant (9 month old); J, K supernatant (fresh); L high range protein ladder; **II**: A, B mAb1 in buffer without PEG; C, D mAb1 crystals (fresh); E, F mAb1 crystals (9 month old); G, H supernatant (fresh); I, J supernatant (9 month old); K high range protein ladder.

Non-reducing SDS-PAGE analysis revealed aggregates already for the freshly prepared mAb1 solutions (Fig. 5-2 I D, E). Higher aggregate contents as well as fragments were found for freshly prepared mAb1 crystals (Fig. 5-2 I F, G). The highest contents of both protein degradation products were found for the 9 months old crystals. Furthermore, the mAb1 aggregates of the 9 month old samples showed higher molecular weights (Fig. 5-2 I A, C). In contrast, only small aggregate and fragment contents were found in the supernatants independent from the sample age (Fig. 5-2 I H-K). Reducing SDS-PAGE analysis revealed covalently linked aggregate species for the freshly prepared mAb1 solution (Fig. 5-2 II C-F). Higher contents were detected for the dissolved mAb1 crystals with the highest levels for the 9 months old crystals (Fig. 5-2 II C-F). In contrast,

for the supernatants no covalently linked aggregates could be detected (Fig. 5-2 II G-J). These findings suggested a chemical modification of the protein during crystallization and storage.

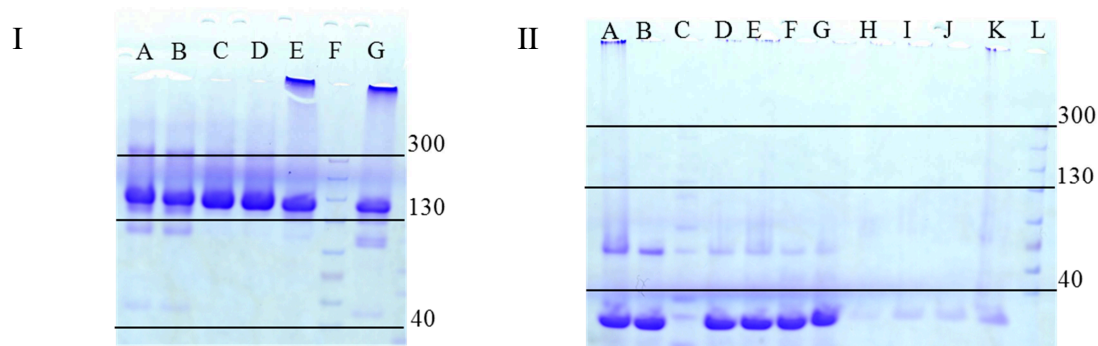


Figure 5-3 SDS-PAGEs performed for mAb2 under **I** non-reducing and **II** reducing conditions. The captions refer to **I**: A, B mAb2 crystals (fresh); C, D mAb2 in buffer without phosphate salt; E, G mAb2 crystals (9 months old); F high range protein ladder; **II**: A, B mAb2 in buffer without phosphate salt; C, small range ladder; D, E mAb2 crystals (9 months old); F, G mAb2 crystals (fresh); H, I supernatant (fresh); J, K supernatant (9 months old); L high range protein ladder.

For mAb2, the non-reducing SDS-PAGE analysis also revealed aggregates already for the freshly prepared mAb2 solution (Fig. 5-3 I C, D). Again, a higher aggregate content as well as fragments were found for freshly prepared mAb2 crystals (Fig. 5-3 A, B). Significantly increased aggregate levels of higher molecular weight were found for the 9 months old crystals (Fig. 5-3 E, G). SDS-PAGE analysis under reducing conditions did not show any covalently linked aggregate species for all samples. These findings indicated that the aggregate formation during crystallization of mAb1 and mAb2 were caused by two different instability pathways.

5.3.2.2 Isoelectric focusing (IEF)

In a next experiment, isoelectric focusing was performed for further investigation of the underlying instability mechanism of mAb1 and mAb2 crystals as SDS-PAGE analysis alone could not clarify the mechanism behind aggregate formation. Stored (mAb1: 9 months; mAb2: 12 months) crystal suspensions were analyzed and compared to mAb1 and mAb2 solutions without any crystallization agent. Furthermore, mAb2 was stored in the crystallization buffer at pH 3.9 without any phosphate salt to highlight the effect of the pH value on the protein. For cross-checking the effect of PEG on protein stability, mAb2 was precipitated amorphously using a 50% (w/v) PEG 4000 solution (Fig. 5-4 J & K).

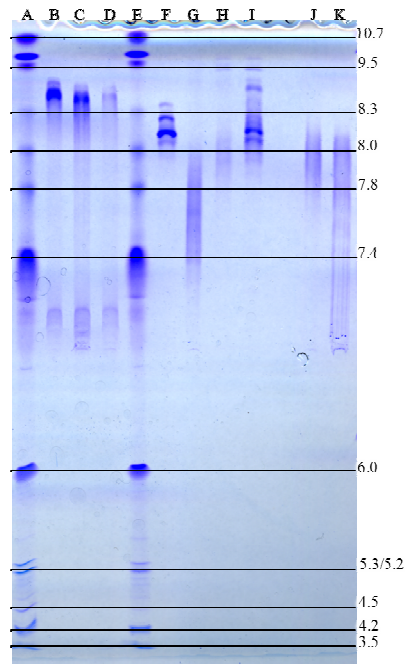


Figure 5-4 Results from an isoelectric focusing measurement: The captions refer to A SERVA marker mix; B mAb1 in buffer without PEG; C mAb1 crystals (12 months old); D mAb1 supernatant (12 months old); E SERVA marker mix; F mAb2 in buffer without phosphate salt (12 months old); G mAb2 crystals (9 months old); H mAb2 supernatant (9 months old); I mAb2 in buffer at pH 3.9 without phosphate salt (12 months old); J mAb2 supernatant with PEG; K mAb2 amorphyously precipitated with PEG.

The results did not show any alterations of the isoelectric point (IEP) for mAb1 (Fig. 5-4 B-D). In contrast, mAb2 protein from the crystals and the supernatant showed a significant drop in the IEP (Fig. 5-4 G & H). However, no changes could be observed for mAb2 stored in the crystallization buffer at pH 3.9 without precipitant (Fig. 5-4 I). This indicated that the high phosphate salt concentration was responsible for the shift in the IEP and thus the aggregate formation. Interestingly, mAb2 precipitated with PEG showed also a small decrease in the IEP (Fig. 5-4 J & K). These results demonstrated that the crystallization conditions cause the aggregate formation by two different pathways. For mAb2, deamidation was assumed to be responsible for the shift in the IEP and thus the aggregate formation. Consequently, PEG and phosphate salt of varying concentrations were to be tested to highlight the effects of the crystallization agents on the aggregate formation.

5.3.3 Investigation of critical crystallization formulation parameters

It was the aim to investigate critical crystallization formulation parameters of the lead conditions which potentially foster antibody aggregation. Therefore, the proteins were exposed to different precipitant concentrations, to conditions without precipitant and to different buffer pH values. Table 5-1 lists all conditions tested. Methionine was used as antioxidant for both antibodies to prove potential oxidative degradation processes causing the aggregate formation.

Table 5-1 lists all variations in the lead crystallization conditions tested to identify the responsible parameter for the aggregation observed during crystallization and storage of both mAbs.

mAb1	mAb2
24% PEG + 40 mM methionine 24% PEG	4.2 M phosphate salt
24% PEG freeze-dried	4.2 M phosphate salt + 40 mM methionine
24% PEG vacuum-dried	3 M phosphate salt
24% PEG freeze + vacuum-dried	50% PEG
26% PEG freeze + vacuum-dried	50% PEG freeze + vacuum-dried
storage in NaAc buffer at pH 5.50 without precipitant	storage in NaAc buffer at pH 3.90 without precipitant

PEG is prone to auto-oxidation which results in the formation of impurities such as peroxides and formaldehyde¹². These impurities are known to foster protein degradation by oxidation and protein-protein linkage. Kumar et al. developed a purification technique for PEG solutions which allowed to reduce protein degradation⁹. Therefore, mAb1 was exposed to unpurified and purified PEG to highlight the effect of the PEG degradation products on mAb1 aggregate formation. mAb2 was also exposed to PEG in order to cross-check the effect of this excipient on protein stability. mAb2 was introduced to varying phosphate salt concentrations and a very low pH without precipitant. Both parameters were suspicious to promote the mAb2 aggregation by deamidation.

5.3.3.1 mAb1: Investigation of the instability pathway

5.3.3.1.1 Investigation of polyethylene glycol (PEG) as destabilizing factor for mAb1

To study the effects of impurities, namely peroxides and formaldehyde, on mAb1 crystallization, first, purification of PEG was carried out. Removal of water by applying vacuum and freeze drying is already reported to reduce dissolved oxygen quantities ⁹. Therefore, the drying approach was exploited for reduction of formaldehyde in PEG solutions.

The decrease of both impurity contents was examined after vacuum and freeze drying, respectively. For freshly supplied PEG and aged PEG (21 days, ambient temperature or 50°C), residual degradation products as well as residual moisture were investigated (Tab. 5-2). Vacuum drying was found to be superior in reduction of peroxides compared to freeze drying and was dependent on former peroxide contents which was in accordance to Kumar et al. ⁹. At the highest peroxide content obtained during storage at ambient temperature (RT) removal of up to 85% was possible by vacuum drying whereas lyophilization maximally reached a reduction of approximately 60%. For freshly prepared PEG samples, extraction of peroxides was about 10% for both drying techniques. Residual moistures were 1% for vacuum-dried samples and 0.05% for lyophilized ones.

Table 5-2 The peroxide content [mM] of freshly prepared PEG (fPEG) solutions and solutions stored at 50°C (50°C) and ambient temperature (RT) before drying, after freeze drying and after vacuum drying are displayed.

	Before drying	After freeze drying	After vacuum drying
fPEG	0.032	0.029	0.029
50°C	0.109	0.035	0.028
RT	0.810	0.336	0.105

In contrast, freeze drying was found to be superior in extraction of formaldehyde residues for all samples (Tab. 5-3). Interestingly, at very high peroxide concentrations (RT) the formaldehyde content after vacuum drying was higher than before drying.

Table 5-3 The formaldehyde content [mM] of freshly prepared PEG (fPEG) solutions and solutions stored at 50°C (50°C) and ambient temperature (RT) before drying, after freeze drying and after vacuum drying are displayed.

	Before drying	After freeze drying	After vacuum drying
fPEG	0.318	0.184	0.243
50°C	3.824	0.313	1.576
RT	0.341	0.310	0.735

Both methods were found to be suitable to purify PEG solutions. Single purification might allow emphasizing effects of either peroxide or formaldehyde on mAb1 crystallization. Double purification by vacuum drying and subsequent freeze drying after sample reconstitution would lead to the highest PEG purity. This assumption was confirmed by pH measurements of differently purified PEG solutions. Removal of the acidic impurities results in more alkaline pH values. Therefore, purified (vacuum- or freeze-dried), double purified (vacuum-dried followed by freeze-dried) and unpurified PEG (12% (w/v) each) were dissolved in highly purified water. Subsequently, the pH values of the solvent (7.22) and the PEG solutions were determined (Fig. 5-5). In all cases, the dissolution of PEG led to an acidification. Notably, PEG solutions of double purified PEG showed the highest pH value of 6.93. In contrast, the dissolution of unpurified PEG resulted in the lowest pH value of 5.12 due to the highest amount of acidic residues. Vacuum drying of PEG resulted in a lower pH value (5.46) compared to solutions of freeze-dried PEG (5.88). Hence, double purification was found to be a suitable approach for extensive reduction of PEG impurities.

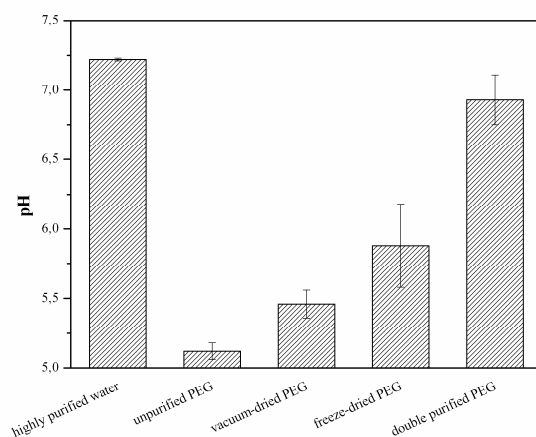


Figure 5-5 pH values of highly purified water and 12% (w/v) PEG solutions containing unpurified PEG and PEG which were purified by applying of vacuum drying, freeze drying or double purification prior to dissolution.

The role of the impurities was now studied on mAb1 crystallization. Therefore, a 10 mg/mL mAb1 solution was mixed with 24% (w/v) purified, double purified and unpurified PEG solutions and stored at 20°C in a climate room for 12 weeks in the dark. For a further batch, 40 mM methionine was added to unpurified PEG prior to crystallization. Aggregate formation was followed by SE-HPLC measurements over the whole period. Therefore, the crystal fraction was separated by three times centrifugation and decanting from the mother liquor, dissolved in a phosphate buffer solution (PBS) with a pH of 7.4 and analysed. Protein crystallization was obtained in all cases except for samples with a) 40 mM methionine and unpurified PEG and b) double purified PEG. However, at the very end of the test minor protein precipitation (mix of amorphous and crystalline precipitates) occurred also for the samples with double purified PEG. By increasing the concentration of double purified PEG from 12% (w/v) (initially 24% (w/v)) to 13% (m/v) (initially 26% (w/v)) mAb1 crystallization was again obtained. Interestingly, using unpurified PEG in the same concentration (13% (w/v)) leads to amorphous protein precipitates (data not shown).

Aggregate formation was observed for all samples but in a very different extend (Fig. 5-6). For crystallized samples, analysis was performed for the crystallized fraction (Fig 5-6 A-D) by dissolving the crystals in PBS as the aggregate counts remained negligible in the supernatant (see section 4.3.1). For non-crystallizing samples (Fig. 5-6 E,

F), the aggregate formation was measured directly in the protein solution. The highest aggregate levels were found for the mAb1 crystals. Notably, purification of PEG prior to crystallization halved the values independent from the applied drying technique (Fig 5-6 B-D).

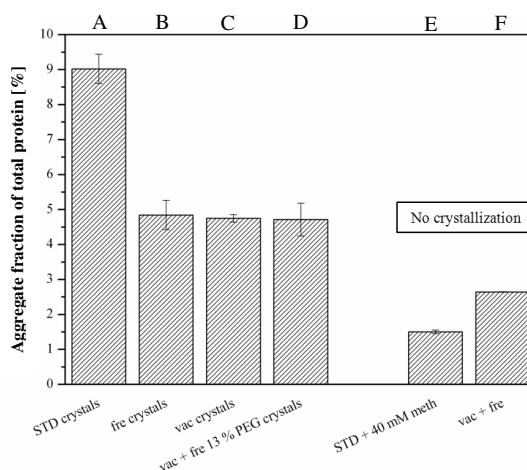


Figure 5-6 Aggregate fraction of total protein of crystallized protein (A - D) and not crystallized protein (E -F). STD: crystallization with unpurified PEG. Fre: refers to freeze-dried PEG and vac to vacuum-dried PEG. STD + 40 mM meth: samples containing unpurified PEG and 40 mM methionine. Vac + fre: double purified PEG.

Comparison of aggregate formation over time revealed a parallel and constant increase for purified and unpurified PEG (Fig. 5-7). Hence, and notably, both impurities appeared to be vital for mAb1 crystallization and responsible for aggregate formation. Furthermore, a certain level of aggregates appeared to be necessary for crystal formation as well.

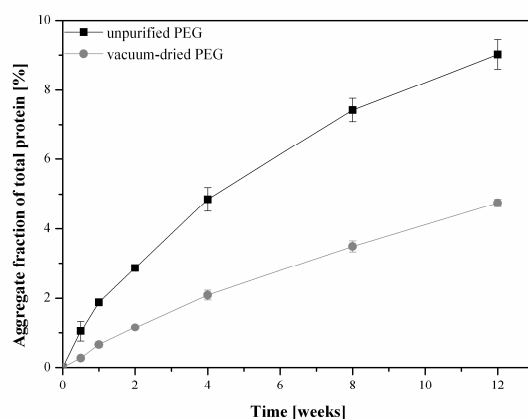
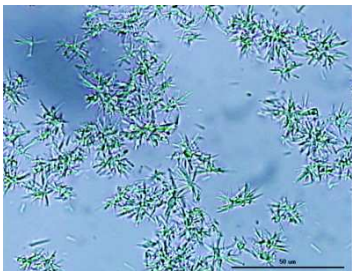
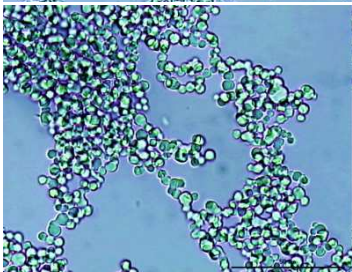


Figure 5-7 Increase of aggregate fraction in the crystalline precipitate over time in percentage of total protein. The values refer to samples crystallized with unpurified PEG (squares) and vacuum-dried PEG (circles).

For further confirmation of this assumption, peroxides or formaldehydes were assessed individually for their potential to induce crystallization and aggregate formation of our model protein. Therefore, double purified PEG at a concentration of 23% (w/v) was spiked with varying amounts of the impurities and mixed with a 10 mg/mL mAb1 solution. The samples were stored for 24 h at 20°C in a climate room. Subsequently, light microscopy and SE-HPLC measurements were performed. In case of crystal formation, the precipitate was separated from the mother liquor and dissolved in PBS. Both fractions were analyzed separately. For non-crystallizing samples, aggregate formation was analyzed in the solution.

Interestingly, addition of only peroxides did not provoke any precipitation while addition of only formaldehyde resulted in an amorphous mAb1 precipitate (Tab. 5-4). However, a certain mix of peroxides and formaldehydes led to a crystalline precipitation. By further increasing the peroxide content (> 0.05% (v/v)) again precipitation was prevented.

Table 5-4 The precipitate state after spiking of double purified PEG (23%) with different amounts of peroxides and formaldehydes. Light microscopic pictures are presented right. The scale bar represents 50 μm .

Double purified PEG 23% (w/v)	Precipitate state	Light microscopic picture
no addition of peroxides or formaldehyde	no precipitation	-----
+ peroxides	no precipitation	-----
+ 0.015% (v/v) formalde- hyde and 0.015% (v/v) peroxides	crystalline	
+ 0.015% (v/v) formalde- hyde	amorphous	

Regarding aggregate formation, the use of double purified PEG showed a minor increase compared to mAb1 solutions without any PEG (Fig. 5-8). Addition of peroxides led to very slight increases in aggregation. In contrast, after addition of formaldehydes, the amount of aggregates in the solution was significantly higher. The amorphous precipitate was insoluble, and thus, could not be dissolved for measurement. Notably, the crystalline fraction, obtained by a certain mixture of peroxides and formaldehydes, showed the highest aggregate level. Interestingly, after increasing the peroxide concentration for this mixture the aggregate formation was significantly reduced and the protein precipitation was prevented.

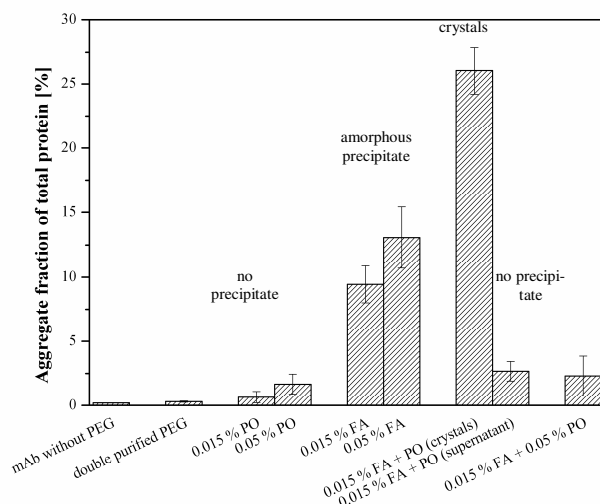


Figure 5-8 Aggregate fraction of total protein after spiking double purified 23% (m/v) PEG with different amounts of peroxides and formaldehydes. Incubation was performed for 24 h at 20°C. STD = Protein in NaAc buffer, double purified PEG = 23% (m/v) PEG solution, PO = percentage (v/v) of peroxide added to double purified PEG, FA = percentage (v/v) of formaldehyde added to double purified PEG.

Consequently, it was assumed that the extent of aggregate formation in protein crystal suspension was dependent on the PEG quality (impurity content) used. This could be confirmed by the study about the effect of PEG degradation products on mAb1 crystallization. It is known that residual peroxide contents can differ for each PEG manufacturer and thus would eventually lead to crystalline products varying in their extent of aggregate formation^{11,43-45}. Therefore, mAb1 was crystallized with 23% (m/v) PEG solutions from different vendors. Aggregate formation was followed by SE-HPLC measurements over a period of 105 days. Formation of acidic mAb1 species as a result of oxidation by peroxide impurities was assessed by IEC chromatography. The results revealed that the applied PEG had a significant effect on mAb1 stability (Tab. 5-5). PEG from Applichem, BioUltra, Clariant and Fluka showed similar results in aggregate formation. In contrast, aggregate levels were significantly elevated for samples crystallized with PEG from Croda and Alfa Aesar. Furthermore, the observed trends were correlated to a significant shift to acidic species in the IEC chromatography of up to 31.7% total acidic protein (TAP). TAP refers to the fraction of total protein which showed acidification most probably due to oxidation. The results demonstrated that the aggregate formation was linked to an acidic protein oxidation. This could be confirmed by LC-MS measurements which were performed externally (not shown).

Overall, the results indicated a superior quality for PEG from Applichem. In contrast, the highest aggregate level was found for PEG from AlfaAesar which indicated the lowest PEG quality (highest content of impurities). Consequently, a proper choice of the PEG used for protein crystallization is crucial with respect to the quality of the final crystalline suspension.

Table 5-5 SE-HPLC data and IEC data representing aggregate fraction (AF) and total acidic protein (TAP) in percentage of samples that were crystallized with PEG 4000 from different manufacturers. Aggregate and total acidic protein formation was followed over 105 days.

	Applichem	BioUltra	Clariant	Fluka	Croda	AlfaAesar
AF [%]	6.7	7.6	7.8	7.9	12.8	15.2
TAP [%]	11.5	13.3	13.6	13.9	26.9	31.7

5.3.3.1.2 Investigation of the origin of mAb1 aggregate formation during crystallization and storage

It was hypothesized that the crystalline state stabilizes the protein. Consequently, the origin of protein involved in the aggregate formation would be the supernatant. As increased aggregate contents were found in the crystalline state (see section 5.3.1), a protein exchange between the crystals and supernatant would be required to explain the situation. This protein exchange should be investigated and visualized during a first experiment. Therefore, mAb1 was crystallized for 2 weeks until the maximum mAb1 crystal yield was reached. The supernatant of the crystal suspension was replaced with an identical but red fluorescence labelled mAb1 solution to investigate the protein exchange between the crystalline state and the supernatant. If the anticipated protein exchange would take place at the equilibrium state, the crystals would start to show fluorescence signals. CLSM was utilized to follow the incorporation of the red fluorescence labelled antibodies into the crystals.

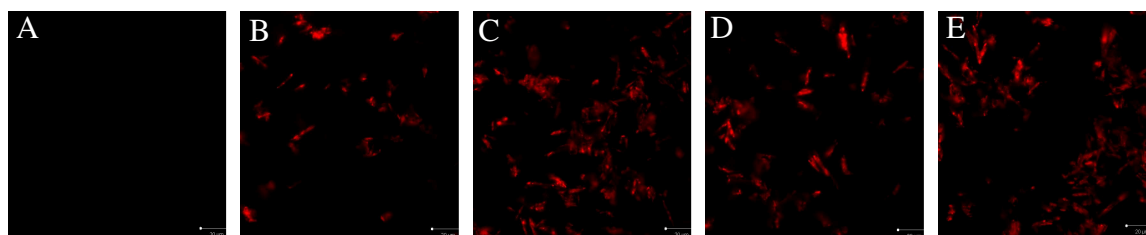


Figure 5-9 CLSM images of crystal suspensions after supernatant exchange. **A:** instantly after supernatant exchange; **B:** 2 weeks after exchange; **C:** 4 weeks after exchange; **D:** 8 weeks after exchange; **E:** 12 weeks after exchange. The scale bar represents 20 μm .

No labelled protein was detected in the crystalline state instantly after supernatant exchange (Fig. 5-9 A). A steady increase in labelled antibodies, obviously incorporated into the crystals, was detected by CLSM measurements until week four (Fig. 5-9 B). After that, the fluorescence intensity of the crystalline state remained on a constant level until week 12 which indicated the formation of equilibrium between labelled protein leaving the crystals and labelled protein being incorporated into the crystals (Fig. 5-9 C-E).

Following, the aggregate formation within in the crystalline state and its origin during storage (after reaching the maximum yield) was to be followed. The exchange of the supernatant with a fluorescent labeled mAb1 solution after reaching the equilibrium state together with the label free antibody crystals would allow a precise localization of the aggregate origin in the crystallization system. For all fluorescent aggregates, the origin of the involved protein would be in the solution and not in crystalline state itself. On the other hand, unlabeled protein aggregates were formed solely in the crystals. All experiments were also conducted by exchanging the supernatant with label free antibodies to investigate the effect of the fluorescence dye on protein aggregation. Non-crystallized samples without PEG were used as controls to highlight the effect of the crystallizing agent on the aggregate formation (compare to section 5.3.3.1.1). SE-HPLC and FACS analysis were performed for assessment of aggregate formation over 12 weeks. Therefore, the crystals were separated from the supernatant and dissolved in PBS. The FACS device was applied as new analytical tool for protein aggregate analysis as it allowed for easy detection of labeled protein aggregates even in the submicron range. In contrast, standard tools such as light obscuration and micro flow imaging sys-

tems were usually not equipped with a fluorescence detector and have lower detection limits in the submicron range.

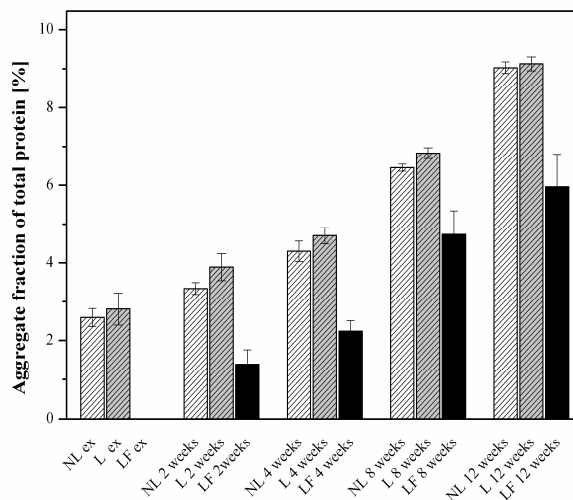


Figure 5-10 Aggregate fractions of total protein in percentage after supernatant exchange. NL = not labeled protein exchanged as control analyzed by UV detection (light grey); L = Labeled protein analyzed by UV detection (dark grey); LF = Labeled protein and analysis by fluorescence detection (black); EX = Measurements after exchange of supernatant; 2 weeks = Analysis 2 weeks after exchange of supernatant; 4 weeks = Analysis 4 weeks after exchange of supernatant; 8 weeks = Analysis 8 weeks after exchange of supernatant; 12 weeks = Analysis 12 weeks after exchange of supernatant.

The SE-HPLC results revealed no significant differences in the extent of aggregate formation in the crystalline state 12 weeks after supernatant exchange for labeled and non-labelled protein (Fig. 5-10: not labeled: $9.0\% \pm 0.2\%$ - light grey bars; labeled: $9.1\% \pm 0.2\%$ - dark grey bars). The same trend was found for the total particle count examined by flow cytometry (FACS) (data not shown).

A constant increase in the total aggregate content in the mAb1 crystals was detected for the labelled and non-labelled samples from around 2.6% (after supernatant exchange) to about 9.0 – 9.1% 12 weeks after supernatant exchange (Fig- 5-10, light grey bars). The share of aggregates detected in the crystalline state which contained the fluorescence dye and thus protein originated in the supernatant increased with similar kinetic from 0% (after supernatant exchange) to 6.0% 12 weeks after supernatant (Fig. 5-10, black bars). Consequently, rather all aggregates formed after the exchange of the supernatant contained a fluorescence dye and thus the protein within the aggregates had with in-

creasing value its root in the supernatant. Notably, non-crystallized samples did not show any aggregate formation after 12 weeks which indicated the crystallizing condition to be harmful for the protein which remains in solution (not shown).

For further analysis of the aggregates, their origin and the fluorescence intensity of the particles, additional analysis was performed by using flow cytometry. Therefore, the supernatant was again exchanged with an identical but fluorescence labeled mAb1 solution after reaching the crystallization equilibrium. Subvisible particle formation was followed for both, the supernatant and the crystals. Prior to analysis the crystals were separated from the supernatant and dissolved in PBS. Total subvisible particle count and fluorescence intensity were followed for 12 weeks after the exchange of supernatant.

A)

B)

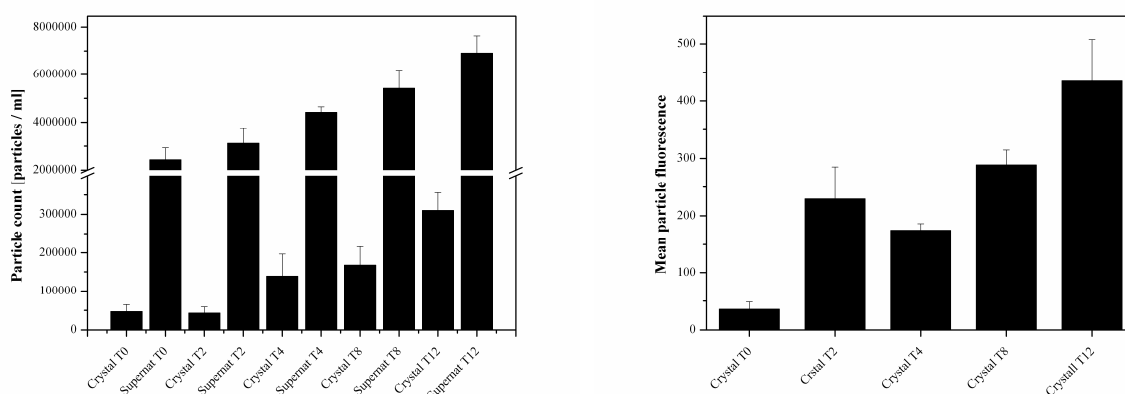


Figure 5-11 Flow cytometry measurements of subvisible protein aggregates. **A** Total particle counts of protein crystals and supernatant. **B** Mean fluorescence of crystal aggregates.

All samples displayed an increased particle count over time (Fig. 5-11 A). The crystals start out at $46,433 \pm 13,838$ particles / ml to $309,600 \pm 45,911$ particles / ml and the supernatant at a significantly higher count from $2,425,200 \pm 501,056$ particles / ml to $6,905,800 \pm 725,211$ particles / ml. The mean fluorescence / particle increased from 35.66 ± 12.71 to 434.66 ± 73.67 (Fig. 5-11 B and Fig. 5-12). These findings confirmed the SEC measurements: Most of the subvisible particles in crystals have their origin in the supernatant. The crystallizing conditions were harmful to the solved protein while the protein incorporated into a crystal lattice was protected against aggregate formation.

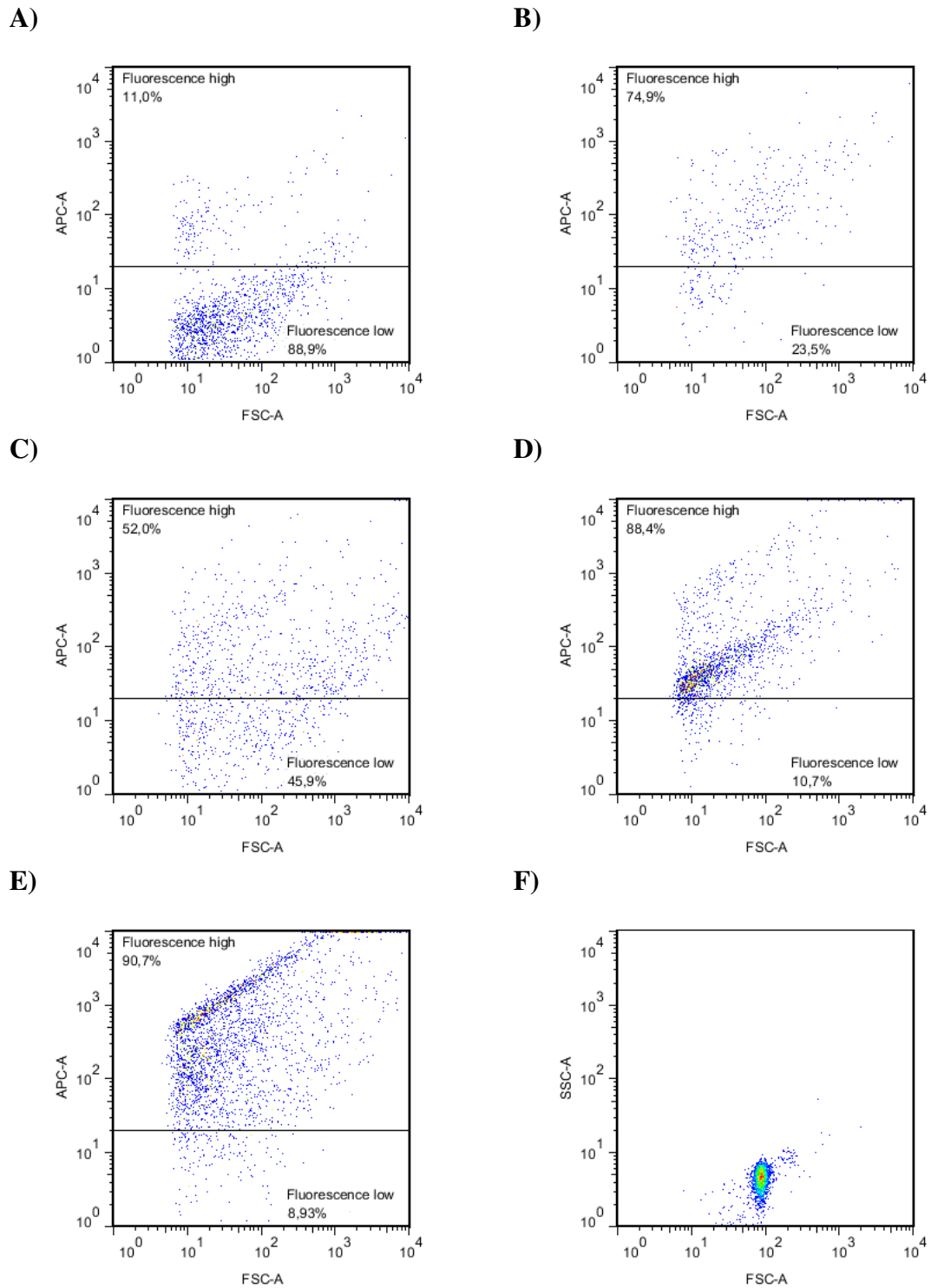


Figure 5-12 Flow cytometry dot plot measurements of subvisible protein aggregates at different time points after exchange of supernatant. The figures illustrate the particle sizes (x-axis) and the fluorescence intensity (y-axis) at the **A** starting point, after **B** two weeks, **C** 4 weeks, **D** 8 weeks, **E** 12 weeks. **F** shows 1 μ m silica beads.

The flow cytometry can be calibrated with 1.5 μ m silica calibration beads (Fig. 5-12 F) to roughly classify the mAb1 aggregate sizes in the FACS dot plots (Fig. 5-12 A - E).

The comparison suggests that the majority of subvisible antibody particles were in the submicron range. Non-crystallized samples showed with 1849 ± 617 the lowest aggregate count (not shown).

5.3.3.2 mAb2: Investigation of the aggregate formation

The IEF measurements suggested that mAb2 deamidation causes the aggregate formation. In general, deamidation reactions are induced by low buffer pH values, high ionic strengths and elevated storage temperatures ^{1,2,7}.

During the present study, only the buffer salt concentration and the buffer pH were evaluated to cause mAb2 aggregate formation. The crystallization temperature was held constant at a moderate level (20°C) for all experiments. Therefore, beside the lead conditions, mAb2 was exposed to a 3 M phosphate salt solution and an acetate buffer with a pH value of 3.9. Both conditions did not induce mAb2 crystallization. This was desired in order to highlight the effect of the protein crystallization itself on aggregate formation. Furthermore, 40 mM methionine was added to the lead condition to test the effect of potential oxidation (similar to mAb1) on mAb2 crystallization. mAb2 was additionally exposed to an unpurified and a double purified 50% (w/v) PEG (see section 5.3.3.1.1) solution which induced amorphous precipitation. SE-HPLC measurements were performed to determine the soluble aggregate levels of the respective precipitates (crystalline, amorphous) and the supernatant for each sample.

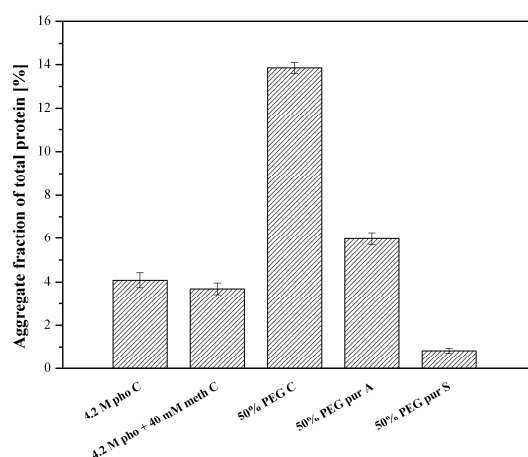


Figure 5-13 Total soluble aggregate fraction [%] from SE-HPLC measurements for mAb2 samples. A refers to aggregates from the amorphous precipitate; C refers to aggregates from the crystals; S refers to aggregates detected in the supernatant; **pur** refers to double purified PEG.

SE-HPLC analysis revealed no soluble aggregate formation in the supernatants (not shown) except for the samples which used double purified PEG as precipitant (Fig 5-13). However, only a small aggregate level of about 0.8% was detected. Aggregates could be found in all precipitated states with the highest counts for the samples containing PEG. No differences could be found for samples crystallized with phosphate salt containing methionine and samples without additional methionine ($\pm 4\%$ aggregates). The highest aggregate fraction of about 14% was observed for the samples with unpurified PEG. Double purification of the PEG resulted in a decreased aggregate level of 6%. Notably, the non-crystallizing mAb2 samples exposed to 3 M phosphate salt or with a pH of 3.9 did not show any aggregate formation (not shown).

Soluble aggregates might represent only a small amount of the total aggregated protein mass in protein samples. Therefore, FACS measurements were performed which allowed for particle analysis in the submicron as well as in the micron-range. To localize the aggregate formation, a similar approach as for mAb1 should be performed. However, no suitable fluorescence dye could be found for mAb2 as in all cases crystallization was prevented by addition of a dye. Consequently, FACS measurements were carried out for unlabeled and freshly as well as 3 months stored mAb2 crystal suspensions.

The FACS analysis revealed similar results as for mAb1 in terms of particle counts in the redissolved crystals and the supernatant. (Tab. 5-6). The results showed increased values for the stored samples compared to the freshly prepared crystal suspensions. As for mAb1, SE-HPLC measurements revealed higher aggregate levels for the crystals while FACS measurements revealed higher particle counts for the supernatants.

Table 5-6 Flow cytometry measurements of subvisible protein aggregates for freshly prepared or 9 months old mAb2 crystals and their supernatants. Buffer refers to sodium PBS buffer without protein.

	mAb2 crystals (fresh)	mAb2 crystals (old)	mAb2 su- pernatant (fresh)	mAb2 su- pernatant (old)	Buffer
Aggregate count	838 \pm 91	1871 \pm 420	36,313 \pm 3557	46,569 \pm 3648	318 \pm 20

In summary, the results for mAb2 indicated that the deamidation was predominately caused by the high phosphate salt concentration (4.2 M) necessary to induce crystalliza-

tion. This assumption was confirmed by LC-MS measurements performed externally (not shown).

5.4 Discussion

A steady increase in the aggregate levels could be detected over the time for mAb1 and mAb2 crystals. A higher growth rate of the aggregate content was observed for mAb1 as for mAb2. SDS-PAGE and IEF analysis of different mAb1 and mAb2 samples suggested different pathways of aggregate formation for both antibodies. The two different crystallization formulations were deemed to cause the mAb instability and thus were investigated for their role in mAb1 and mAb2 aggregate formation.

SDS-PAGE analysis revealed covalently linked aggregates in **mAb1** samples. High aggregate levels were detected for dissolved crystals while analysis of the supernatant showed small aggregate contents. Following, in a first evaluation the crystallization process itself was deemed to cause the aggregate formation. The results from the IEF measurements did not show any alteration of the IEP and thus protein degradation by deamidation was excluded. The PEG containing crystallization buffer was suspicious to foster mAb1 aggregation as PEG is prone to auto-oxidation which results in degradation products such as peroxides and formaldehyde. These PEG degradation products were known to cause protein degradation by protein oxidation and protein-protein linkage⁹⁻¹². Consequently, it was the aim to highlight the effects of these PEG impurities on mAb1 crystallization and aggregate formation. Therefore, differently purified PEG was to be utilized for crystallization. Removal of water by applying vacuum and freeze drying is known to reduce peroxide levels⁹. Therefore, both drying techniques were used for reducing peroxides and formaldehyde impurities.

During the present study, vacuum drying was found to be superior in reduction of peroxide levels in PEG solutions compared to freeze drying which was in accordance to Kumar et al.⁹. Kumar et al. had also been shown that the relative reduction of peroxide residues was dependent on the initial contents of the PEG solutions which was confirmed by the present study⁹. Following, freshly prepared PEG solutions which contained the lowest amounts of peroxides showed the lowest relative peroxide reduction after drying. Storage of PEG solutions at 50°C fostered peroxides degradation into aldehydes like formaldehyde. Since residual moisture of vacuum-dried samples was higher than that of lyophilized samples, these observations cannot be ascribed to water effects.

Regarding the reduction of formaldehyde impurities, freeze drying was found to be superior. Interestingly, samples stored at ambient temperature even showed increased

formaldehyde contents after vacuum drying. This indicated a degradation of peroxides to formaldehyde during vacuum drying and is the reason for its superiority in the reduction of peroxides.

As PEG degradation products mostly represent acidic species, pH measurements of PEG solutions were deemed to give a hint on the impurity levels⁴⁶. Solutions from vacuum-dried PEG showed lower pH values as samples from freeze-dried PEG. This was ascribed to higher formaldehydes levels due to a lower effectiveness in reduction of this impurity for vacuum drying. Almost a complete removal of both compounds and thus extensive purification was demonstrated for double purified PEG. Only a minor reduction of the pH value was observed for the double purified samples.

The role of PEG impurities during mAb1 crystallization and aggregate formation was highlighted by crystallization using purified PEG, double purified PEG and addition of 40 mM methionine prior to crystallization. The reduction in aggregate formation after purification of PEG clearly showed that mAb1 aggregation is correlated to PEG degradation products. A general strong effect on protein crystallization was demonstrated as extensive reduction of the impurities by double purification as well as addition of methionine, and thus, inactivation of **peroxides totally prevented protein crystallization** when the same PEG concentration was used. Yet, **even for these samples aggregate formation was observed**. Methionine only disables peroxides. Hence, the aggregates were ascribed to formaldehyde⁴⁷. However, extensive purification by drying might not allow a complete removal of peroxides and formaldehydes and thus allowed for small mAb1 aggregation. As double purified PEG at a higher concentration (26% vs 24% (w/v)) induced crystallization, a minimum content of PEG impurities was shown to be vital to mAb1 crystallization. This was confirmed by samples which contained double purified PEG at a concentration of 24% (w/v) without initial mAb1 crystallization. During storage, these samples started to show mAb1 crystallization. Obviously, PEG degraded to peroxides and further to formaldehyde which triggered the crystallization.

The dependency of mAb1 crystallization and aggregate formation on peroxide and formaldehyde was ultimately confirmed by addition of both compounds to extensively purified PEG. Obviously, both impurities were required to initiate crystallization. A complex interaction of both compounds can be assumed. Probably, formaldehyde induces small aggregates which represent a seeding to initiate protein precipitation. Perox-

ides function as modulator which oxidize the protein itself at thiol and primary amino groups which are required for formaldehyde linkage and thus aggregate formation ⁴⁷. This assumption is confirmed as higher peroxide levels prevented any precipitation and reduced significantly the extent in aggregate formation. Furthermore, externally performed LC-MS measurements confirmed the presence of significantly oxidized mAb1 species in PEG containing samples. Consequently, the applied PEG quality defined by the content of impurities would have a strong effect on the final crystal suspension quality. This was demonstrated by applying PEGs from varying manufactures for mAb1 crystallization ⁴³⁻⁴⁵. Different aggregate levels as well as different acidic species levels were found for dissolved mAb1 crystals and were depended on the applied PEG. A connection between PEG impurities and aggregate formation was clearly demonstrated.

However, these findings could not completely explain an ongoing aggregate formation in the crystalline state after reaching the state of maximum yield. The crystalline state should suppress further aggregate formation by fixation of the proteins within the crystal lattice. Therefore, an aggregate formation in the supernatant followed by an incorporation of the aggregates into the crystals was considered. Consequently, it was the aim to further investigate the protein aggregation and its origin within mAb1 crystal suspensions. Therefore, the supernatant was exchanged with an identical, but fluorescence labeled protein solution at equilibrium (maximum yield). If the anticipated protein exchange would take place at the equilibrium state, the crystals would start to show fluorescence signals. In addition, if aggregates found in the crystalline state show fluorescence signals, the origin of the involved protein would be in the supernatant. All experiments were also conducted by exchanging the supernatant with label free antibodies to investigate the effect of the fluorescence dye on protein aggregation.

In the experimental setup the fluorescence label had no significant effect on protein aggregation. Therefore, a significant change of the results due to labelled protein could be excluded.

Labeled protein in the supernatant proved the existence of a dynamic equilibrium by increasing fluorescence signals of the crystalline state over the time. This observation was made at the state of maximum yield, which did not change during the study. Consequently, a pure attachment of labelled protein without protein leaving the crystals was

excluded. A dynamic equilibrium was already mentioned in literature but demonstrated and visualized by CLSM during the presented study ^{40,48}.

SE-HPLC and FACS measurements showed significant aggregate formation for the crystallized samples whereas almost no aggregates were found for the non-crystallized samples. This finding was in the first view in contrast to the assumption that the crystalline state stabilizes protein formulations ³⁷. However, this aggregate formation was not necessarily linked to the crystallization itself as aggregate formation was also observed for non-crystallizing mAb1 samples which contained double purified PEG (see section 5.3.3.1.1) or lower PEG concentrations (see section 4.3.1). Furthermore, the labeled protein in the supernatant revealed the origin of the protein involved in the aggregate formation. The aggregates of the crystalline fraction formed after the supernatant exchange mostly contained labelled protein. FACS results showed significantly higher aggregate levels for the supernatant of crystallized samples. Consequently, an incorporation of the aggregates from the supernatant was assumed. The protein in the supernatant is faced to PEG degradation products such as peroxides and formaldehyde and aggregates (see section 5.3.3.1.1). Following, the mAb1 aggregation is not necessarily an intrinsic phenomenon solely of the crystallization or crystalline state, but occurs predominantly in the supernatant of crystallization systems. Incorporation of aggregated proteins as “crystal building blocks” is already stated in literature but could not be proven in the course of the present study. However, this incorporation of aggregates was discussed in context of crystal forming building blocks and not related to protein crystal impurities ⁴⁹.

For **mAb2**, a different pathway of aggregate formation was demonstrated as for mAb1 (see above). SDS-PAGE did not show any covalently linked aggregates for mAb2 and IEF measurements showed significantly decreased IEPs. This indicated mAb2 deamidation as cause for aggregate formation which could be confirmed by LC-MS measurements performed externally (not shown) ⁷. Oxidative protein degradation as for mAb1 could be excluded as for example no effects on aggregate formation were observed after addition of methionine to mAb2 crystallization systems.

Deamidation is caused by low pH values and high ionic strength solutions ^{1,2,7}. Both were present in the mAb2 crystallization formulation. However, exposure to only a low buffer pH value or a smaller phosphate salt concentration unable to induce crystalliza-

tion did not result in aggregate formation. Consequently, the deamidation of mAb2 is not associated to one single parameter of the crystallization formulation, but to the final crystallization composition itself. This was confirmed by FACS measurements which revealed increased aggregate counts for the supernatant compared to dissolved mAb2 crystals. Similar to mAb1, the protein in solution is exposed to the harsh crystallization conditions (high phosphate salt concentration associated with a low pH value) and started to aggregate. The aggregates were finally attached to the crystals or incorporated into the crystal lattice.

In addition, mAb2 was exposed to PEG in order to confirm the findings for mAb1. The results obtained by these experiments confirmed the concept of oxidative protein degradation at higher PEG concentrations. The protein instability could be ascribed to the PEG impurities as double purification of PEG resulted in decreased aggregate levels.

5.5 Conclusion

Two different pathways for aggregate formation within mAb1 and mAb2 crystallization systems were found. “Harsh” crystallization conditions caused the aggregate formation in both cases. Expansion of the analytical tools for aggregate quantification from SE-HPLC to the more sensitive (in the sub-micron range) FACS revealed higher aggregate levels in the supernatants where the protein is exposed to the destructive components of the crystallization formulations.

It was clearly demonstrated that the protein involved in the aggregate formation had its origin in the supernatant. Aggregate formation in the supernatant followed by aggregate incorporation into the crystals or aggregate formation during attachment of the protein to the crystals might explain these findings. Nevertheless, the results confirmed stabilizing properties of the crystalline state even within the crystallization formulations. Consequently, an intrinsic protein instability in the crystalline state cannot be stated.

For mAb1, oxidative protein degradation caused by impurities (peroxides, formaldehyde) from PEG auto-oxidation were responsible for the aggregate formation. A clear dependency of the level of aggregate formation on peroxides and formaldehyde was shown. Furthermore, it was demonstrated that a minimum level of both compounds was vital to start crystallization. The crystallization is accompanied by aggregate formation since both, precipitation and aggregate formation, are dependent on formaldehyde induced protein linkage. An uncritical use of PEG for crystallization of therapeutic biopharmaceuticals has to be scrutinized.

Deamidation was found for mAb2 as cause for the instability induced by the low crystallization buffer pH and the high phosphate salt concentration of the final crystallization formulation.

Overall, successful mAb crystallization was impossible as either oxidation and protein linkage or deamination was vital to trigger the mAb crystallization. Suitable crystals from therapeutic protein can only be obtained from crystallization conditions which provide both, the feature to grow stable protein crystals and uncritical conditions for the protein which remains in the supernatant.

5.6 References

1. Wang, W., Singh, S., Zeng, D.L., King, K., Nema, S., *Antibody structure, instability, and formulation*. Journal of Pharmaceutical Sciences, 2007. **96**(1): p. 1-26.
2. Wang, W., *Instability, stabilization, and formulation of liquid protein pharmaceuticals*. International Journal of Pharmaceutics, 1999. **185**(2): p. 129-188.
3. Crommelin, D.J., Storm, G., Verrijck, R., de Leede, L., Jiskoot, W., Hennink, W.E., *Shifting paradigms: biopharmaceuticals versus low molecular weight drugs*. International Journal of Pharmaceutics, 2003. **266**(1): p. 3-16.
4. Manning, M.C., Patel, K., Borchardt, R.T., *Stability of protein pharmaceuticals*. Pharmaceutical Research, 1989. **6**(11): p. 903-918.
5. Mahler, H.-C., Friess, W., Grauschopf, U., Kiese, S., *Protein aggregation: Pathways, induction factors and analysis*. Journal of Pharmaceutical Sciences, 2009. **98**(9): p. 2909-2934.
6. Catak, S., Monard, G., Aviyente, V., Ruiz-Lopez, M.F., *Reaction mechanism of deamidation of asparaginyl residues in peptides: effect of solvent molecules*. The Journal of Physical Chemistry A, 2006. **110**(27): p. 8354-8365.
7. Daugherty, A.L., Mersny, R.J., *Formulation and delivery issues for monoclonal antibody therapeutics*. Advanced Drug Delivery Reviews, 2006. **58**(5-6): p. 686-706.
8. Hovorka, S.W., Schöneich, C., *Oxidative degradation of pharmaceuticals: Theory, mechanisms and inhibition*. Journal of Pharmaceutical Sciences, 2001. **90**(3): p. 253-269.
9. Kumar, V., Kalonia, D.S., *Removal of peroxides in polyethylene glycols by vacuum drying: implications in the stability of biotech and pharmaceutical formulations*. AAPS PharmSciTech, 2006. **7**(3): p. E47-E53.
10. Hamburger, R., Azaz, E., Donbrow, M., *Autoxidation of polyoxyethylenic non-ionic surfactants and of polyethylene glycols*. Pharmaceutica Acta Helvetiae, 1975. **50**(1-2): p. 10.
11. Ha, E., Wang, W., Wang, Y.J., *Peroxide formation in polysorbate 80 and protein stability*. Journal of Pharmaceutical Sciences, 2002. **91**(10): p. 2252-2264.
12. Johnson, D.M., Taylor, W.F., *Degradation of fenprostalene in polyethylene glycol 400 solution*. Journal of Pharmaceutical Sciences, 1984. **73**(10): p. 1414-1417.
13. Cordoba, A.J., Shyong, B.-J., Breen, D., Harris, R.J., *Non-enzymatic hinge region fragmentation of antibodies in solution*. Journal of Chromatography B, 2005. **818**(2): p. 115-121.

14. Tanford, C., *Protein denaturation*. Advances in Protein Chemistry, 1968. **23**: p. 121.
15. Arat, F., *Immunological Characteristics of Denatured Proteins*. Nature, 1966. **212**: p. 848.
16. Frokjaer, S., Otzen, D.E., *Protein drug stability: a formulation challenge*. Nature Reviews Drug Discovery, 2005. **4**(4): p. 298-306.
17. Dobson, C.M., *Protein folding and misfolding*. Nature, 2003. **426**(6968): p. 884-890.
18. Arakawa, T., Kita, Y., Carpenter, J.F., *Protein-solvent interactions in pharmaceutical formulations*. Pharmaceutical Research, 1991. **8**(3): p. 285-291.
19. Chiti, F., Taddei, N., Baroni, F., Capanni, C., Stefani, M., Ramponi, G., Dobson, C.M., *Kinetic partitioning of protein folding and aggregation*. Nature Structural & Molecular Biology, 2002. **9**(2): p. 137-143.
20. Philo, J.S., *Characterizing the aggregation and conformation of protein therapeutics*. American Biotechnology Laboratory, 2003. **21**(11): p. 22-29.
21. Cromwell M.E., Jacobson F., *Protein Aggregation and Bioprocessing*. AAPS Journal., 2006. **8**(3): p. E572-E579.
22. Malencik, D., Anderson, S., *Dityrosine as a product of oxidative stress and fluorescent probe*. Amino Acids, 2003. **25**(3-4): p. 233-247.
23. Wang, W., *Protein aggregation and its inhibition in biopharmaceutics*. International Journal of Pharmaceutics, 2005. **289**(1): p. 1-30.
24. Gabrielson, J.P., Brader, M.L., Pekar, A.H., Mathis, K.B., Winter, G., Carpenter, J.F., Randolph, T.W., *Quantitation of aggregate levels in a recombinant humanized monoclonal antibody formulation by size-exclusion chromatography, asymmetrical flow field flow fractionation, and sedimentation velocity*. Journal of Pharmaceutical Sciences, 2007. **96**(2): p. 268-279.
25. Gottschalk, S., *Crystalline Monoclonal Antibodies: Process Development for Large Scale Production, Stability and Pharmaceutical Applications*. Thesis Munich, 2008.
26. Chi, E.Y., Krishnan, S., Randolph, T.W., Carpenter, J.F., *Physical stability of proteins in aqueous solution: mechanism and driving forces in nonnative protein aggregation*. Pharmaceutical Research, 2003. **20**(9): p. 1325-1336.
27. Katakam, M., Banga, A.K., *Use of poloxamer polymers to stabilize recombinant human growth hormone against various processing stresses*. Pharmaceutical Development and Technology, 1997. **2**(2): p. 143-149.
28. Bam, N.B., Cleland, J.L., Yang, J., Manning, M.C., Carpenter, J.F., Kelley, R.F., Randolph, T.W., *Tween protects recombinant human growth hormone against*

- agitation-induced damage via hydrophobic interactions.* Journal of Pharmaceutical Sciences, 1998. **87**(12): p. 1554-1559.
29. Chou, D.K., Krishnamurthy, R., Randolph, T.W., Carpenter, J.F., Manning, M.C., *Effects of Tween 20® and Tween 80® on the stability of Albutropin during agitation.* Journal of Pharmaceutical Sciences, 2005. **94**(6): p. 1368-1381.
 30. Li, S., Schöneich, C., Borchardt, R.T., *Chemical instability of protein pharmaceuticals: mechanisms of oxidation and strategies for stabilization.* Biotechnology and Bioengineering, 1995. **48**(5): p. 490-500.
 31. Lam, X.M., Yang, J.Y., Cleland, J.L., *Antioxidants for prevention of methionine oxidation in recombinant monoclonal antibody HER2.* Journal of Pharmaceutical Sciences, 1997. **86**(11): p. 1250-1255.
 32. Arakawa, T., Timasheff, S.N., *Mechanism of polyethylene glycol interaction with proteins.* Biochemistry, 1985. **24**(24): p. 6756-6762.
 33. Farruggia, B., Garcia, G., D'Angelo, C., Picó, G., *Destabilization of human serum albumin by polyethylene glycols studied by thermodynamical equilibrium and kinetic approaches.* International Journal of Biological Macromolecules, 1997. **20**(1): p. 43-51.
 34. Moelbert, S., Normand, B., De Los Rios, P., *Kosmotropes and chaotropes: modelling preferential exclusion, binding and aggregate stability.* Biophysical Chemistry, 2004. **112**(1): p. 45-57.
 35. Shenoy, B., Wang, Y., Shan, W., Margolin, A.L., *Stability of crystalline proteins.* Biotechnology and Bioengineering, 2001. **73**(5): p. 358-369.
 36. Hancock, B.C., Zografi, G., *Characteristics and significance of the amorphous state in pharmaceutical systems.* Journal of Pharmaceutical Sciences, 1997. **86**(1): p. 1-12.
 37. Jen, A., Merkle, H.P., *Diamonds in the Rough: Protein Crystals from a Formulation Perspective.* Pharmaceutical Research, 2001. **18**(11): p. 1483-1488.
 38. Pikal, M.J., Rigsbee, D.R., *The Stability of Insulin in Crystalline and Amorphous Solids: Observation of Greater Stability for the Amorphous Form.* Pharmaceutical Research, 1997. **14**(10): p. 1379-1387.
 39. Yang, M.X., Shenoy, B., Disttler, M., Patel, R., McGrath, M., Pechenov, S., Margolin, A.L., *Crystalline monoclonal antibodies for subcutaneous delivery.* Proceedings of the National Academy of Sciences of the United States of America, 2003. **100**(12): p. 6934-6939.
 40. McPherson, A., *Introduction to protein crystallization.* Methods, 2004. **34**(3): p. 254-265.
 41. Schmit, J.D., Dill, K.A., *The Stabilities of Protein Crystals.* The Journal of Physical Chemistry B, 2010. **114**(11): p. 4020-4027.

42. Thrash, S.L., Otto, J.C., Deits, T.L., *Effect of divalent ions on protein precipitation with polyethylene glycol: mechanism of action and applications*. Protein Expression and Purification, 1991. **2**(1): p. 83-89.
43. Wasylaschuk, W.R., Harmon, P.A., Wagner, G., Harman, A.B., Templeton, A.C., Xu, H., Reed, R.A., *Evaluation of hydroperoxides in common pharmaceutical excipients*. Journal of Pharmaceutical Sciences, 2007. **96**(1): p. 106-116.
44. Jaeger, J., Sorensen, K., Wolff, S., *Peroxide accumulation in detergents*. Journal of Biochemical and Biophysical Methods, 1994. **29**(1): p. 77-81.
45. McGinity, J.W., Patel, T.R., Naqvi, A.H., Hill, J.A., *Implications of peroxide formation in lotion and ointment dosage forms containing polyethylene glycols*. Drug Development and Industrial Pharmacy, 1976. **2**(6): p. 505-519.
46. Bindra, D.S., Williams, T.D., Stella, V.J., *Degradation of O6-benzylguanine in aqueous polyethylene glycol 400 (PEG 400) solutions: concerns with formaldehyde in PEG 400*. Pharmaceutical Research, 1994. **11**(7): p. 1060-1064.
47. Metz, B., Kersten, G.F., Hoogerhout, P., Brugghe, H.F., Timmermans, H.A., De Jong, A., Meiring, H., ten Hove, J., Hennink, W.E., Crommelin, D.J., *Identification of formaldehyde-induced modifications in proteins reactions with model peptides*. Journal of Biological Chemistry, 2004. **279**(8): p. 6235-6243.
48. Durbin, S., Feher, G., *Protein crystallization*. Annual Review of Physical Chemistry, 1996. **47**(1): p. 171-204.
49. Nadarajah, A., Pusey, M.L., *Growth mechanism and morphology of tetragonal lysozyme crystals*. Acta Crystallographica Section D: Biological Crystallography, 1996. **52**(5): p. 983-996.

Chapter 6

Statement: Chapter 6 includes results from the Master thesis “Development and optimization of *in situ* precipitating depot systems for *in vitro* monoclonal antibody release” by Bistra Nikolaeva Rainova, LMU Munich, 2013. The results within this chapter related to the Master thesis were expressed in figures and graphs which were either copied or reproduced in a modified form.

The Master thesis has been planned, structured and carried out under my direct supervision. The results obtained and the conclusions drawn have been discussed under my supervision.

The work related and the results presented in sections 6.3.2 and 6.3.3 (Fig. 6-11 – 6-13) were not subject to the Master thesis.

6 Case study: Sustained release formulations containing mAb crystals

6.1 Introduction

Protein therapeutics represents a class with approximately 200 market products¹. However, a major drawback of protein formulations is their low oral bioavailability as well as degradation processes *in vivo*²⁻⁴. Thus they have to be administered by multiple administrations by injection or infusion which represent very inconvenient procedures for the patients^{4,5}. Hence, development of biodegradable depot formulations would minimize clinical stays and enhance the patient's acceptance for the therapeutic settings^{4,6}. Besides conventional methods to achieve protein sustained release formulations including implants, liposomes and oily depots, two more recent approaches are available: a) microencapsulation within biodegradable poly (D, L- lactide-co-glycolide) (PLGA) or other polymers and b) *in situ* precipitating systems which form an implant upon injection^{7,8}. ATRIGEL[®] represents an example for the latter approach where the drug is mixed with a biocompatible organic solvent that contains the water immiscible, biodegradable PLGA polymer⁹⁻¹¹. After intramuscular (i.m.) or subcutaneous (s.c.) injection, the polymer hardens under entrapment of the drug. This solidification is driven by a solvent exchange between the organic carrier solvent and the physiological fluid which penetrates into the forming depot^{10,12,13}. Besides the well-established polyesters such as PLGA, new materials including the non-polymeric sucrose acetate isobutyrate (SAIB) aroused attention¹⁴⁻¹⁶. This water insoluble sugar derivate was introduced as part of the innovative SABER technology from Southern Biosystems (now DURECT, Cupertino, USA)^{12,17}. The depots are fabricated under the same precipitation conditions used for PLGA^{18,19}. However, following injection this material forms a semi-solid viscous depot rather than a solid implant. SAIB is characterized as a low molecular weight, high viscosity liquid with a viscosity of > 5.000 cP at 37°C²⁰. Another feature is its low viscosity (50 - 200 cP) in organic solvents even at very high SAIB concentrations of about 90% (w/v)^{19,21}. SAIB provides similar attributes as PLGA with respect to sustained release matters and allows reduction of the dose frequency, the total dose and the side effects^{19,22}.

Proteins show physical and chemical instability, properties which impart the development and evaluation of protein sustained release formulations in general but especially

the development of *in situ* precipitating depot systems¹². During manufacturing, the protein is susceptible to different potential damaging conditions including the exposure to organic solvents, water/organic solvent interfaces, hydrophobic surfaces, detergents, agitation and elevated temperatures^{7,23}. In addition, polymer degradation, as it was shown for PLGA, causes acidic microenvironments which would be destructive to the majority protein drugs²⁴. By that, protein crystals were deemed to allow circumventing the aforementioned obstacles^{12,25,26}. The crystalline state may offer a better protection against organic solvents or water/organic solvent interfaces as well as destructive interactions between the protein and the matrix polymer^{25,27}. Furthermore, the crystals enable for higher loadings due to their compact structure²⁸. To date, incorporation of protein crystals into sustained release formulations appears to be a very useful and attractive approach. Margolin et al. assumed that crystallized proteins might *per se* offer protracted action even without additional entrapment within a polymer formulation due to a prolonged redissolution *in vivo*²⁵. In contrast, Stefan Gottschalk demonstrated a fast dissolution of mAb1 and mAb2 crystals upon contact with an aqueous media²⁹. This finding was supported by other researchers who showed fast dissolving mAb crystals of different molecules^{25,26,28}.

Feasibility of protein crystals as platform for sustained release formulations has already been demonstrated by Pechenov et al. where a PLGA/acetonitrile and a SAIB/ethanol based *in situ* forming depot formulation for crystalline α -amylase was introduced¹². Stability of the crystalline protein against organic solvents was shown¹². Furthermore, the crystal morphology as well as drying of the crystals prior to their formulation are reported to be strong tools to alter the release profiles¹².

Besides the abovementioned PLGA and SAIB materials, lipids have attracted researcher's interest during the last two decades. Lipids exhibit excellent attributes such as biocompatibility and biodegradability by lipases or body fluids³⁰⁻³³. Especially triglyceride based, compressed implants are reported to allow a long term release and are easily prepared³⁴⁻³⁶. Recently, novel lipid-based solid implants prepared by twin-screwed extrusion were introduced by the group of Prof. G. Winter. This new manufacturing strategy represents an advancement of the commonly used direct compression technique and allows for production of rod-shaped implants of varying diameters³⁷. The implants are easily administered and show a more sustained protein drug release^{37,38}. So far, feasibility of such implants as depot formulation for protein crystals has yet to be investigated.

As shown in Chapter 3, mAb1 and mAb2 crystals do not offer an increased protein stability and protection against organic solvents. Consequently, the experiments presented within this chapter were conducted with awareness of the insufficient mAb1 and mAb2 crystal stability. It was decided to perform this study despite the lack in suitable antibody crystal material to obtain further insight into *in situ* forming depot formulations containing mAb crystals. Therefore, the present experiments represent a first “proof of concept” study.

As part of the present study, mAb1 and mAb2 crystals were incorporated into *in situ* precipitating formulations which consisted of PLGA (502H and 755S) or SAIB, respectively. A solvent screen was performed to identify applicable liquids. Suited carrier solvents for *in situ* precipitating depot formulations have to fulfill several requirements such as biocompatibility, polymer dissolution and miscibility with the aqueous release medium⁹. Another important factor is a good processability characterized by a suitable viscosity of the polymer solution which allows a convenient injection into the release media by a syringe. As the surface area of the depots would have a significant effect on the protein drug release, a standard manufacturing procedure was developed to obtain uniform *in situ* precipitating implants. The mAb crystals comprising sustained release formulations were compared to identical formulations which contained freeze-dried, amorphous mAb1 or mAb2. As drying of mAb1 and mAb2 crystals could not be successfully carried out (see Chapter 3), a comparison to its dry amorphous counterparts was exceptionally challenging. In order to enhance protein stability, certain additives like sucrose and in case of PLGA pH modifiers such as magnesium hydroxide and sodium carbonate were added to the standard formulations. These compounds would also enhance protein release by their function as pore formers. This study was completed by depot degradation studies, investigation of the phase inversion dynamics of the PLGA formulations and assessment of the syringeability of different PLGA and SAIB depot formulations.

Additionally, twin-screw extruded lipid implants were formulated together with vacuum-dried mAb1 crystals. The dry material was obtained by the vacuum drying procedure introduced by the preliminary study²⁹. Despite the fact that stability and crystallinity of the dry material remained questionable, studies were performed to get a first insight into the release kinetics of crystalline mAb from lipid implants. A formulation

introduced by Gerhard L. Sax was adopted for mAb1 crystals as it allowed for a very long and steady antibody release³⁷.

Finally, as drying of lysozyme crystals could be successfully carried out; a straightforward study to highlight the effects of protein crystal drying on the release kinetics for lysozyme is also presented within this chapter.

6.2 Materials and Methods

6.2.1 Materials

Lysozyme from chicken egg white as lyophilized powder (protein > 90%, > 40,000 units/mg protein) was purchased from Sigma-Aldrich (Taufkirchen, Germany). mAb1 and mAb2 were two monoclonal antibodies from the IgG1 class. The samples were stored at - 80°C (antibodies) or at - 20°C (lysozyme) until required for use.

RESOMER[®] RG 502H (PLGA 502H) and RESOMER[®] RG 755S (PLGA 755S) were purchased from Evonik Industries (Darmstadt, Germany). Sucrose acetate isobutyrate (SAIB) (kosher food grade) was obtained from Sigma-Aldrich.

The triglycerides D118 (100% stearic acid, melting range 70 – 72°C) and H12 (71% palmitic acid, 27% myristic acid, 2% lauric acid, melting range 37 – 40°C) were a gift from Sasol (Witten, Germany)³⁷.

Sodium chloride (AnalaR NORMAPUR) as crystallization agent for lysozyme was purchased from VWR Prolabo (Leuven, Belgium). Sodium acetate (USP standard) was from Merck (Darmstadt, Germany). Sodium sulphate (99%) was from Grüssing GmbH (Filsum, Germany). Sodium dihydrogen phosphate-dihydrate (pure Ph. Eur., USP), disodium hydrogen phosphate-dihydrate (analytical grade), potassium dihydrogen phosphate and potassium chloride (both analytical grade) were obtained from Appli-chem GmbH (Darmstadt, Germany). PEG 4000S was from Clariant (Frankfurt a. M., Germany). Hydrochloric acid 32% (analytical grade), acetic acid 100% and ortho-phosphoric acid 85% were all purchased from Merck KGaA (Darmstadt, Germany). Sodium azide (99%) was received from Acros Organics (New Jersey, USA). L-histidine was from Sigma-Aldrich (St. Louis, MO, USA). All other reagents or solvents were of at least analytical grade and purchased either from Sigma-Aldrich (Taufkirchen, Germany) or VWR Prolabo (Leuven, Belgium).

6.2.2 Methods

6.2.2.1 Crystallization of mAb1

Crystallization of mAb1 was carried out in 0.1 M sodium acetate buffer at pH 5.50. For crystallization, a 24% (w/v) PEG 4000 solution in the same buffer was added dropwise

to a 10 mg/mL protein solution under gentle shaking to obtain a 1:1 ratio. The final formulation was stored at 20°C for at least two weeks.

6.2.2.2 Crystallization of mAb2

Crystallization of mAb2 was performed in a 0.1 M sodium acetate buffer of 4.1. For crystallization, a 4.2 M sodium dihydrogen phosphate solution was added dropwise to a 10 mg/mL protein solution under gentle shaking to obtain a final ratio of 1:1. The final formulation was stored at 20°C for at least one week.

6.2.2.3 Crystallization of lysozyme

The crystallization was carried out as batch crystallization in 50 mM sodium acetate buffer (pH 8) at room temperature without stirring in 60 mL PETG Nalgene vessels (Thermo Scientific, Langenselbold, Germany). Sodium chloride was used as crystallization agent in different concentrations from 0.5 M to 2 M. The concentration of lysozyme was set to 4% (m/V). 10 mL sodium chloride solution was poured carefully to 10 mL of lysozyme solution while the vessel was gently shaken to dissolve the initial precipitation. For each condition four identical batches were prepared.

6.2.2.4 Drying of protein crystals

6.2.2.4.1 Inert gas drying (lysozyme)

Inert gas drying of lysozyme crystals was performed in a Barkey® Hot-Air Dryer Flowtherm (Leopoldshöhe, Germany). The system consisted of a heater which allowed the tempering of a nitrogen gas stream (upper part) and a bottom heater for the sample (lower part). 300 µL of the crystal slurry were filled into 2R glass vials and placed into the sample holder. The nitrogen gas stream (10 L/min) was tempered to 30°C and guided through a needle into 10 vials. The bottom heater was set to 20°C. After drying, the vials were closed and sealed.

6.2.2.4.2 Vacuum drying (mAb1)

Vacuum drying of mAb1 crystals was performed in accordance to a procedure described by the preliminary study²⁹. The mAb1 crystals were washed with 22% PEG solution in 0.1 M sodium acetate buffer (pH 5.5) by three times of centrifugation (15 min) in a Sigma® 4K15 centrifuge at 4,000 rpm and subsequent replacement of the supernatant. After that, this procedure was repeated with EtOH 85 % at 2°C. Finally, the pellet was suspended in 200 µl EtOH 85% which contained 5% (w/v) sucrose. The concentration of the protein solution was set to 100 mg/ml. Vacuum drying was carried out in a Martin Christ Epsilon 2-6 D pilot freeze-dryer which was connected to a Vacuubrand CVC 2000 vacuum pump. The temperature was set to 2°C for 3 h at 20 mbar followed by 14 h at 0.1 mbar.

6.2.2.4.3 Freeze-Drying (lysozyme, mAb1, mAb2)

Freeze-drying of the protein crystal suspensions was performed using a Christ Epsilon 2-6D pilot scale freeze-dryer (Christ, Osterode am Harz, Gemany). A volume of 1 mL of the suspensions was filled into 2 R glass vials and semi stoppered. Subsequently, the temperature was decreased to - 40°C at a rate of 1°C/min and was maintained at this temperature for 1 h and 10 min. In the last 10 min the pressure was reduced to 0.08 mbar. In the next step, temperature was increased to - 10°C at a rate of 1°C/min and held for 16.66 h. Finally, temperature was increased to 25°C at a rate of 0.15°C/min and held for 10 h. At the end of the drying cycle the chamber was aerated with nitrogen and the vials were stoppered automatically within the chamber. The samples were stored at 2-8°C until analytical examination.

6.2.2.5 Preliminary screening approaches

6.2.2.5.1 Solvent screening

In order to investigate the solubilizing properties of different organic solvents with PLGA and SAIB, a solvent screening was performed. Therefore, PLGA solutions in concentrations of 25%, 30%, 40%, 45% and 50% (w/w) and SAIB solutions in concentrations of 40%, 45%, 50%, 80%, 85% and 90% (w/w) were prepared with PEG 200, PEG 300, PEG 400, isopropanol 100% and ethyl acetate as solvents. To support dissolution, the samples were stored at 60°C for at least 2-3 h until complete dissolution. The produced formulations were inspected visually to appraise solubilizing capacity of the

different solvents.

6.2.2.5.2 Sieve screening

The depot should be placed in the middle of the release container to allow an unhindered solvent exchange upon depot solidification. This should be reached by placing the aqueous depot formulations on a mesh. The mesh should be subsequently placed above the bottom of the release container to allow protein diffusion to all sides from the implants during and after complete depot hardening. Therefore, a sieve screening was performed in order to identify suitable mesh diameters which restrain the liquid PLGA and SAIB formulations prior to hardening. Mesh diameters of 10 μm , 20 μm , 40 μm , 80 μm and 100 μm were investigated which were all made of stainless steel. In addition, a 10 μm sieve, which was made of polyester (VWR, Leuven, Belgium), was applied during the study. 20% and 30% (w/w) PLGA formulations in PEG 400 were tested as well as 40%, 45%, 50%, 60%, 70%, 75%, 80%, 85% and 90% (w/w) solutions in ethyl acetate. Each formulation was ejected on the corresponding sieve and evaluated for leakage occurring during 5 min of waiting.

6.2.2.6 Preparation of *in situ* forming depot devices (mAb1, mAb2)

A volume of 0.5 mL of each formulation was injected with a 1 mL NORM-JECT[®] Luer syringe (Henke Sass Wolf, Tuttlingen, Germany) onto a BD Falcon[™] nylon cell strainer with a mesh diameter of 70 μm (BD Bioscience, Durham, NC, USA) which was placed in a MULTIWELL[™] 6-well plate (Becton, Dickinson Labware, Franklin Lakes, NJ, USA). Subsequently, 10 mL of phosphate buffer saline (PBS) were added. For SAIB based formulations, the cell strainer was covered with a 10 μm (mesh diameter) polyester nylon foil. The plate was covered and sealed with a parafilm and stored in an incubator at 37°C under 10 rpm rotating.

The aforementioned basket approach was compared against an approach in that the same depot formulations were directly administered onto the bottom of the 6-well plate.

6.2.2.6.1 Drug release studies

Drug release studies were performed at least in triplets. The implants were formed in a disc like shape. Samples (5 mL) were taken after 2 h, 24 h, 48 h, 7 d, 14 d, 21 d and 28 d and replaced with fresh PBS (37°C).

6.2.2.6.2 Size exclusion high performance liquid chromatography (SE-HPLC)

Total protein release was determined by SE-HPLC. The analysis was performed on a Thermo separation system

6.2.2.6.2.1 mAb1

The mobile phase for mAb1 consisted of 0.092 M Na₂HPO₄ (anhydrous) and 0.211 M Na₂SO₄ (anhydrous) at a pH of 7. The flow rate was set to 0.25 mL/min. Analysis was performed at the wavelengths of 214 nm and 280 nm. A TSKgel G300SWXL column from Tosoh Bioscience GmbH (Stuttgart, Germany) was used for separation.

6.2.2.6.2.2 mAb2

The mobile phase for mAb2 consisted 0.02 M Na₂HPO₄ (dihydrate) und 0.15 M sodium chloride at a pH of 7.5. The flow rate was set to 0.50 mL/min. Analysis was performed at the wavelengths of 214 nm and 280 nm. For separation, a Suprose-6-HR-10/30-coloum from GE Healthcare (Uppsala, Sweden) was used.

6.2.2.6.2.3 Lysozyme

The mobile phase for lysozyme consisted of 0.2 M sodium phosphate at a pH of 6.8. The flow rate was 0.6 mL/min and the protein was detected at 215 nm and 280 nm, respectively. A Superose 12 10/300 GL column (GE Healthcare, Uppsala) was utilized for separation.

6.2.2.7 Depot characterization

6.2.2.7.1 Phase inversion dynamics (PEG staining)

In order to evaluate the time for complete solvent exchange a blue stained PEG 400 was utilized to dissolve PLGA 502H and PLGA 755S each at concentrations 20%, 25%, 30% (w/v). The dye was composed of 0.2041 g potassium thiocyanate and 0.2023 g cobalt nitrate dissolved in 10 mL of dichloromethane. The dye was diluted at a 1:9 ratio with the respective polymer solution. For analysis, the formulation was ejected directly onto a 6-well plate and the solvent exchange which could be identified by dye decolorization, was recorded with a photo camera.

6.2.2.7.2 Optical depot degradation

Optical depot degradation was monitored using a Keyence VHX-500f digital microscope (Keyence, Neu-Isenburg, Germany) equipped with a VH-Z100R objective (magnification 100x - 1000x) enhanced with a Real Zoom Lens. Following incubation for four weeks at 37°C, the depot degradation was investigated by complete buffer removal and subsequent vacuum drying.

6.2.2.7.3 Syringeability

Syringeability was tested by applying a TA.XT.plus Texture Analyser (Stable Micro Systems, Godalming, UK) with the integrated software Exponent 32-bit. The experiments were carried out with 20 G, 25 G, 27 G needles and 1 mL and 5 mL syringes. All formulations were investigated by ejection 0.5 mL of a polymer formulation within 10 s depending on the syringe size and needle diameter. The formulations were considered to be injectable if the required ejection force did not exceed 10 N.

6.2.2.8 Preparation of lipid implants (mAb1)

Preparation of lipid implants was performed by using a Twin-screw extruder MiniLab[®] Micro Rheology Compounder (Thermo Haake GmbH, Karlsruhe, Germany). The temperature was set to 41°C. The melt was directed through a 1.9 mm outlet. The rotation speed was set to 40 rpm and the bypass channel was closed for all manufactures. The basic formulation for all samples was characterized by a 1 to 2.3 ratio of the low melting (H12) and the high melting (D118) compound. Crystalline and amorphous mAb1 counted for 5% (w/w) and PEG, if used, for 10% (w/w). The composition was chosen in accordance to Gerhard Ludwig Sax³⁷.

6.2.2.9 Release study for SAIB based *in situ* precipitating lysozyme depots

For depot preparation, 100 mg formulation was placed on the bottom of a 2 mL LoBind Eppendorf tube (Eppendorf AG, Hamburg, Germany). Subsequently, 1 mL PBS was added as release buffer. The Eppendorf tube was stored in an incubator at 37°C under gentle teetering at 10 rpm. The standard formulation consisted of 5% (w/w) lysozyme (amorphous or crystalline), 85% (w/w) SAIB and 10% (w/w) isopropanol 95%.

6.3 Results

6.3.1 *In situ* precipitating depot formulations for mAb1 and mAb2 crystals

6.3.1.1 Preliminary screening approaches

6.3.1.1.1 Solvent screening

Suited solvents for *in situ* precipitating depot systems must be biocompatible and of low toxicity to minimize irritation at the injection site⁹. They should easily dissolve the polymer and should be miscible with the aqueous media (e.g. body fluids) in which the polymer should precipitate by formation of an implant. The latter attribute is of vital importance as it determines the phase inversion dynamics during solidification of the depot system (see section 3.1.4)³⁹.

mAb1 and mAb2 crystals show low stability during contact with the most organic solvents (see Chapter 3) but remain stable in PEG solutions. Therefore, a solvent screening with PEG of different molecular weight was performed in order to assess the solubility of PLGA 502H, PLGA 755S and SAIB in these liquids. Ethyl acetate and isopropanol 100% were included into the study as they have been demonstrated to be acceptable washing liquids for mAb1 and mAb2 crystals (see Chapter 3). PLGA solutions in concentrations of 25%, 30%, 40%, 45% and 50% (w/w) and SAIB solutions in concentrations of 40%, 45%, 50%, 80%, 85% and 90% (w/w) were prepared with PEG 200, PEG 300, PEG 400, isopropanol 100% and ethyl acetate as solvents. To support PLGA and SAIB dissolution, the mixtures were stored at 60°C until complete (optically tested) dissolution.

Whereas PLGA 502H and 755S were insoluble in isopropanol 100%, solubility in ethyl acetate was satisfying (Tab. 6-1). However, due to markedly high viscosities, these polymer solutions could not be handled and thus were declared to be inappropriate for implant preparation. PLGA solubility in PEG 200 and PEG 300 was poor. The dissolution was a very slow process and even after long time periods (overnight) undissolved polymer was visible. Again, these preparations showed high viscosity which was deemed to hinder a convenient implant manufacture. In contrast, PLGA 502H and 755S were excellently soluble in PEG 400. Regarding the viscosity, merely the solutions of up to 30% (w/w) PLGA were considered suitable for the further studies.

SAIB was not soluble in any PEG (Tab. 6-1). Even a phase separation was observed upon cooling to ambient temperature. In contrast, solubility in isopropanol 100% and ethyl acetate was excellent. Interestingly, even at the highest SAIB concentrations tested, the viscosity was considered to allow for a convenient handling and depot preparation.

By that, it was concluded to use PEG 400 as solvent for both PLGA copolymers whereas isopropanol 100% and ethyl acetate were chosen as solvents for SAIB.

Table 6-1 Solubility of PLGA and SAIB in different solvents. S: soluble, IS: insoluble.

	PLGA 502H	PLGA 755S	SAIB
PEG 200	S	S	IS
PEG 300	S	S	IS
PEG 400	S	S	IS
Ethyl acetate	S	S	S
Isopropanol 100%	IS	IS	S

6.3.1.1.2 Sieve screening

Drug release from implant based systems is dependent on many factors such as texture, size, shape and surface area of the depot which might result in a variable and unpredictable release in many cases⁴⁰. Generation of uniform implant surfaces appears to be vital for consistent drug release studies. Therefore, production of *in situ* precipitating depots in similar flat discs was considered. To enable liquid diffusion from the entire depot surface, they were placed on a mesh above the bottom of the release container (six-well plate) (Fig. 6-1).

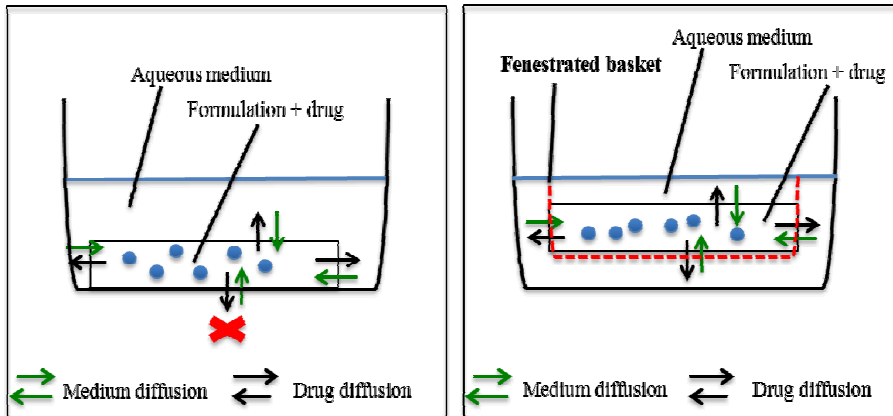


Figure 6-1 Depicts the limitations in drug diffusion out of implants placed on the bottom of the release container (left). If the depot is placed on a fenestrated mesh which is placed in the middle of the container, hindering in drug diffusion is reduced (right).

The fenestration of such a mesh can be variable in size. Hence, a set of different mesh sizes (steel sieves) were assessed for their ability to restrain different PLGA and SAIB formulations during hardening. Permeability of the meshes was tested optically for 5 min by placing the sieve on a white paper. If a polymer solution dropped through the mesh, a stain on the paper was visible (Fig. 6-2).

For SAIB, only concentrations above 70% (w/w) in isopropanol 100% and concentrations above 40% (w/w) in ethyl acetate were restrained by a 10 μM mesh. None of the SAIB formulations was held back by a 20 μM sieve. No PLGA 502H and 755S solution leaked through an 80 μM sieve.

In general, higher polymer concentrations resulted in solutions of higher viscosity which reduced the amount of formulation that passed through the sieve. This was confirmed by smaller stains on the paper below the sieves.

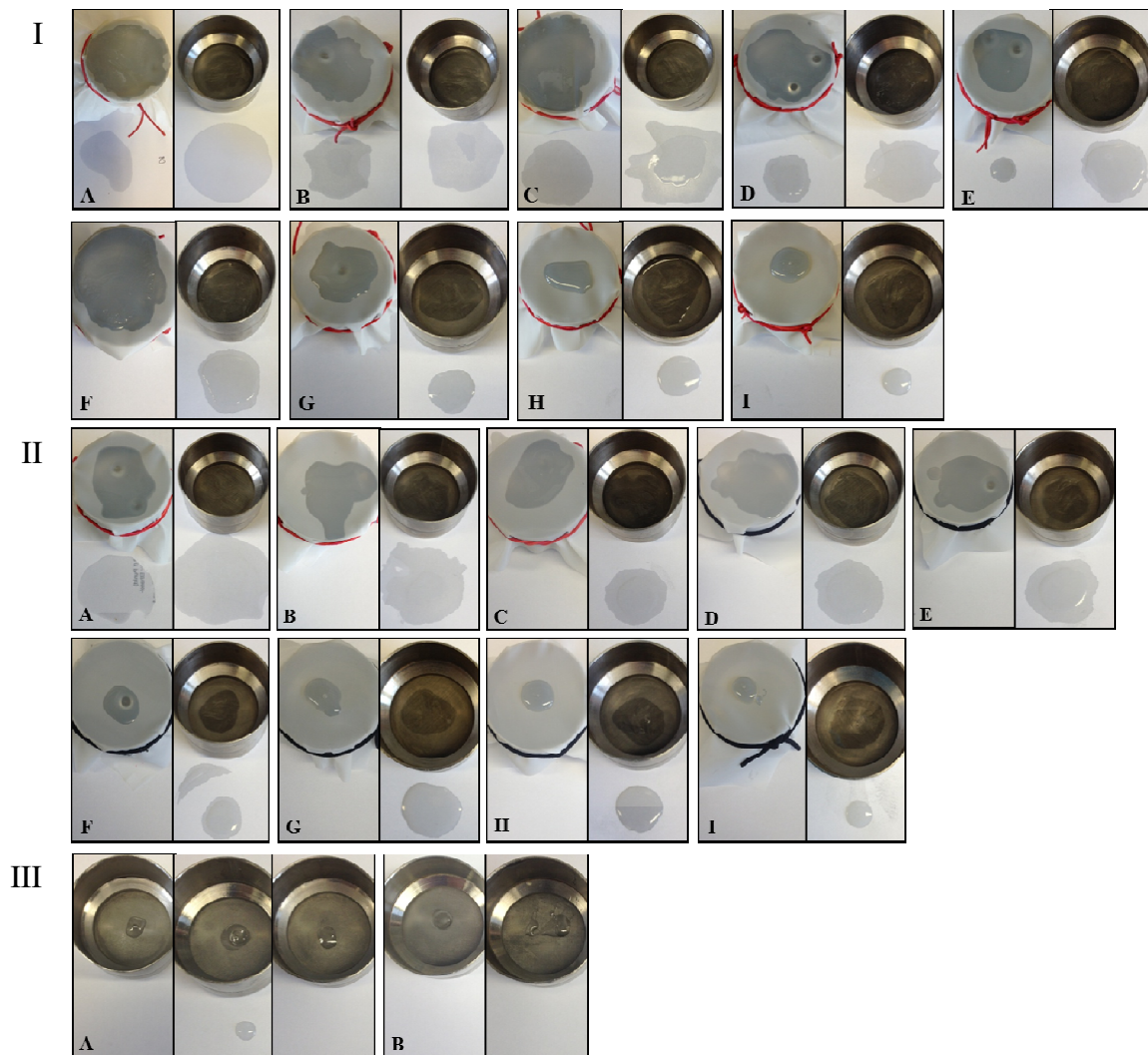


Figure 6-2 Photographic pictures from the sieve screening. For I (SAIB in isopropanol 100%) and II (SAIB in ethyl acetate), a polyester tissue with a mesh diameter of 10 μM (left) and stainless steel sieves of 20 μM mesh diameters (right) were tested. The tested polymer concentrations were [w/w]: A: 40%; B: 45%; C: 50 %; D: 60%; E: 70%; F: 75%; G: 80%; H: 85%; I: 90%. For III (PLGA in PEG 400), A: stainless steel sieves with mesh diameters of 80 μM (left) were tested for 25% (w/v) PLGA formulations. For 30% (w/w) PLGA 755S formulations sieve mesh diameter of 100 μM (middle) and 80 μM (right) were used. B: For 25% (w/w) PLGA 502H formulations stainless steel sieves with mesh diameters of 100 μM (left) were tested as well as for 30% (w/v) PLGA 502H formulations (right). The sieves were placed on a white paper for 5 min to follow permeation of the formulations through the sieves.

For implant manufacture, a 90% (w/w) SAIB concentration was considered for both solvents (isopropanol 100%, ethyl acetate) whereas concentrations of 25% and 30% (w/w) for PLGA 502H / 755S were chosen. Falcon strainers (baskets) with a mean mesh diameter of 70 μM , which in the case of SAIB were lined with 10 μM (mesh diameter) nylon tissues, were used.

6.3.1.1.3 Assessment of the basket approach

To assess the suitability of the falcon strainers to generate uniform implants and thus reproducible release kinetics, this approach was assessed in comparison to a classical set up in which the depots were injected at the bottom of the release container.

Therefore, mAb2 crystals were incorporated in a 90% (w/w) SAIB solution in ethyl acetate. The depots were prepared by injection of the formulations either on a 70 μm falcon strainer sealed with a 10 μm (mesh diameter) nylon mesh placed in a six-well plate or by injection directly at the bottom of the well plate, respectively. The release was followed for 14 days and measured by HP-HPLC.

After 14 days, more protein was released from the depots placed in the basket compared to implants formed directly on the well plate bottom (Fig. 6-3). The latter one showed a small initial burst release followed by an almost steady state with merely low protein release. In contrast, the release curve was much steeper for the implants placed in the baskets.

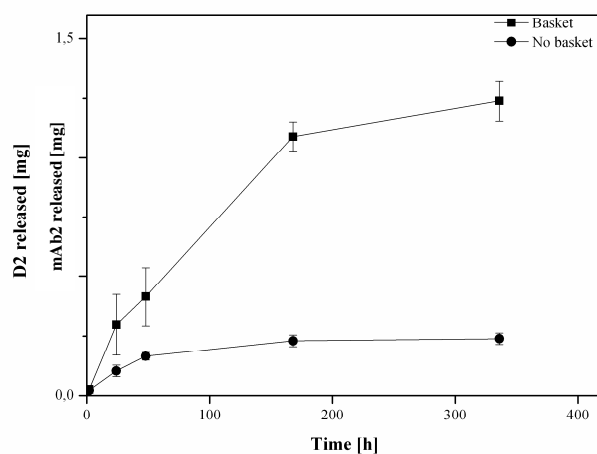


Figure 6-3 *In vitro* release of SAIB 90% in EtAc containing crystallized mAb2 with or without basket over a period of 2 weeks. Data shown is expressed as mean \pm SD.

Therefore, the basket approach was considered to be reasonable for consistent drug release studies.

6.3.1.2 *In vitro* drug release

The impact of the polymer type, polymer concentration, presence of additives and the protein state (crystalline or amorphous) on the *in vitro* release was assessed.

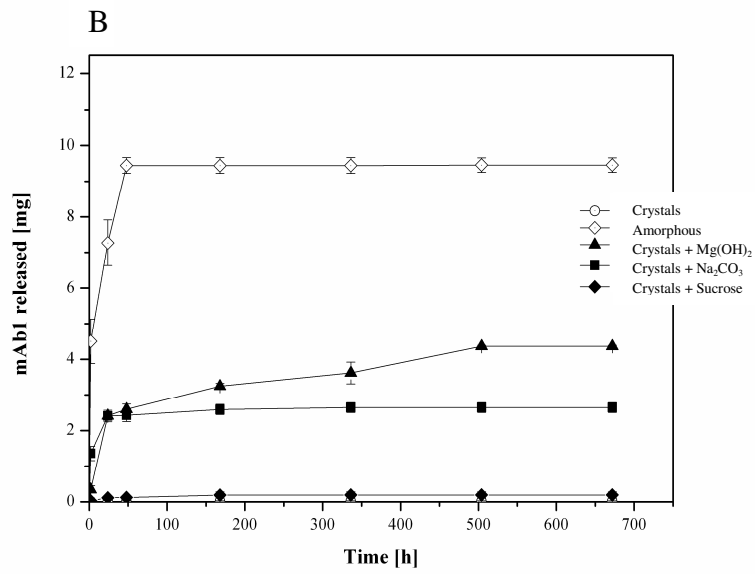
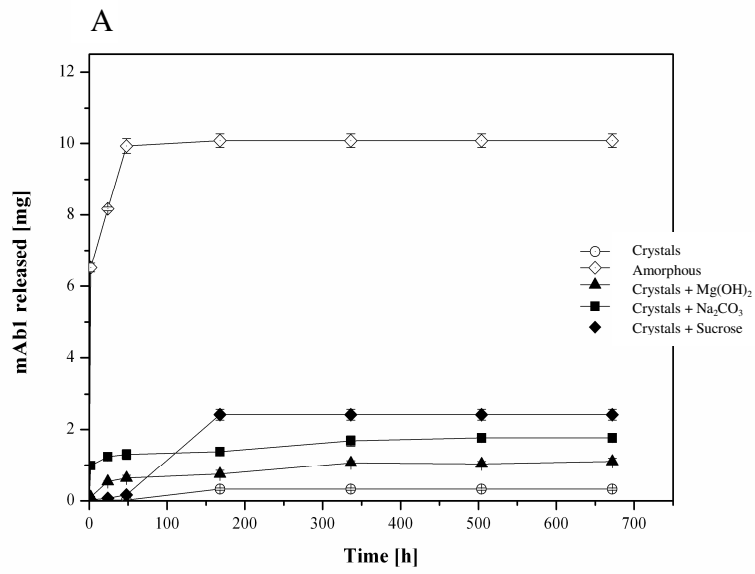
Therefore, *in situ* precipitating depot formulations based on PLGA 502H, PLGA 755S and SAIB containing either crystalline or amorphous (freeze-dried) mAb1 or mAb2 were prepared in the standard formulations as shown in Table 6-2. Pore formers and pH modifiers were only added to formulations which contained mAb1 or mAb2 in its crystalline state as the freeze-dried material already contained 5% (w/v) sucrose.

Table 6-2 depicts the standard formulations for PLGA 502H, PLGA 755S and SAIB based implant formulations. If pore formers and/or pH modifiers were added to the formulation, the amount of solvents was reduced.

PLGA 502H / 755S 20-30% (w/w)	SAIB 90% (w/w)
mAb1 / mAb2 crystalline or amorphous 5% (w/w)	mAb1 / mAb2 crystalline or amorphous 5% (w/w)
Pore former Sucrose 3% (w/w)	Pore former Sucrose 3% (w/w)
pH modifier Mg(OH) ₂ / Na ₂ CO ₃ 3% (w/w)	-
PEG 400 62 - 80% (w/w)	Isopropanol 100% / Ethyl acetate 2 - 10% (w/w)

6.3.1.2.1 mAb1 and mAb2 release studies from PLGA 502 and PLGA 755S implants

Depots which contained amorphous mAb1 and mAb2 showed a large initial drug burst release followed by a steady state phase (Fig. 6-4 & 6-5 A-D). In contrast, for depots formulated with crystalline mAb (not dried), the initial drug burst release was lower as well as the total protein amount released. For all formulations, both parameters were dependent on the type and concentration of the polymer used. Higher polymer concentrations hindered protein release and slowed down the initial burst release.



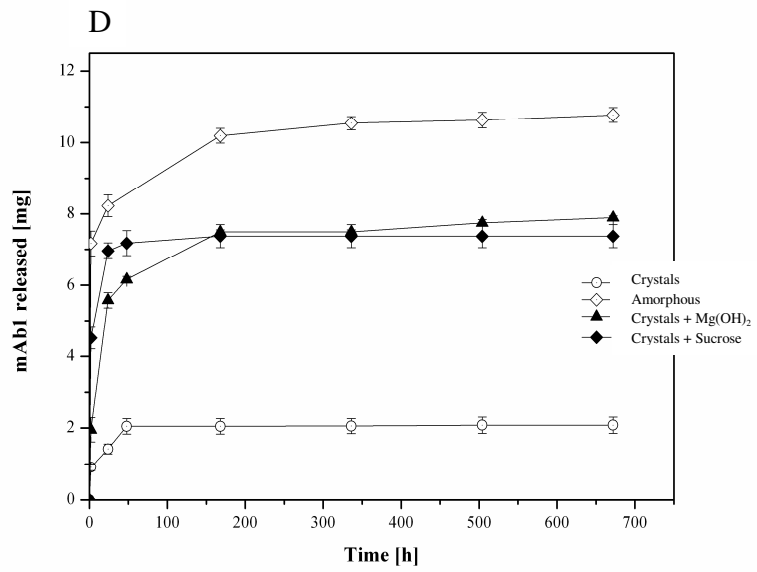
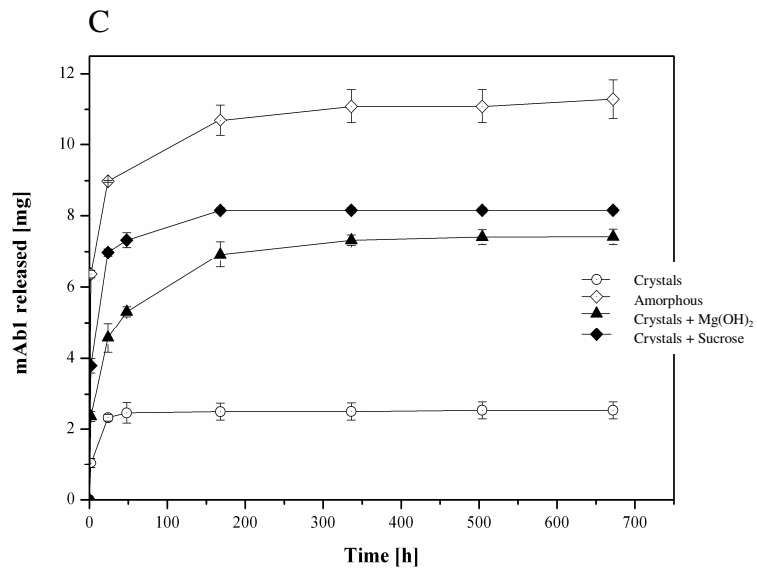
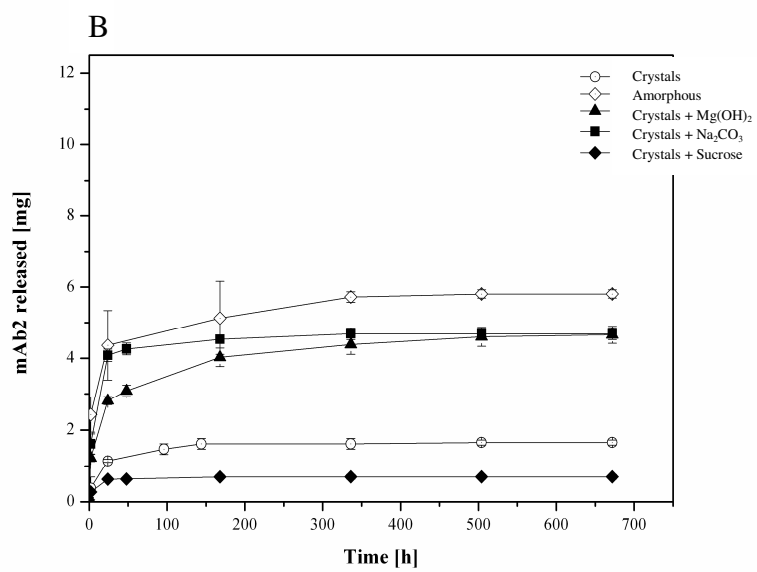
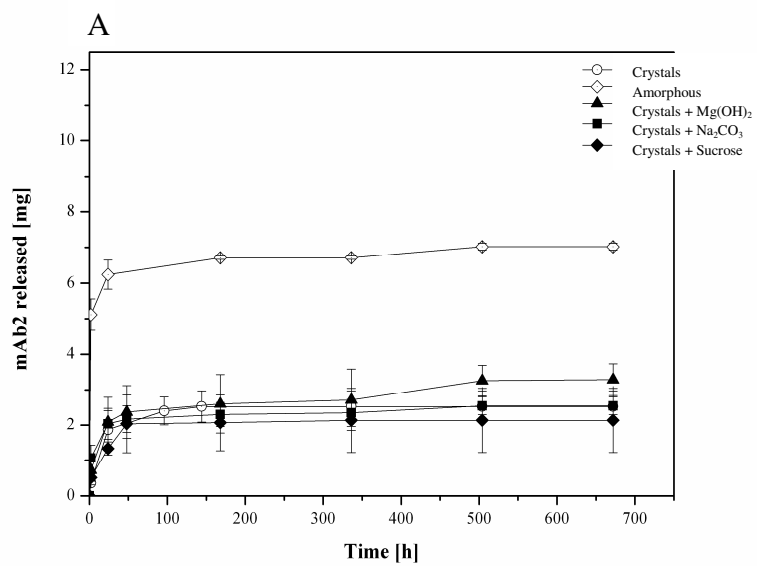


Figure 6-4 mAb1 *in vivo* release profiles from depots which contained A 20% (w/w) PLGA 502H; B 30% (w/w) PLGA 502H; C 20% PLGA 755S; D 30% PLGA 755S. Amorphous refers to freeze-dried mAb1. Additives were only formulated together with crystallized mAb1.



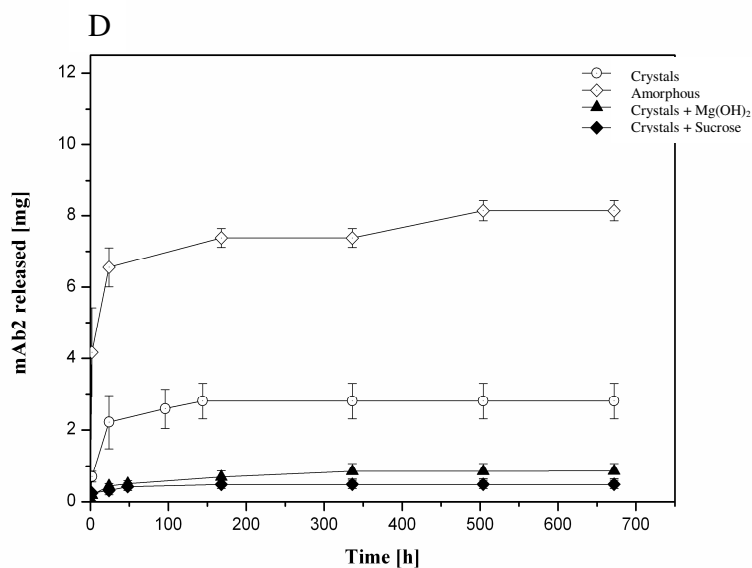
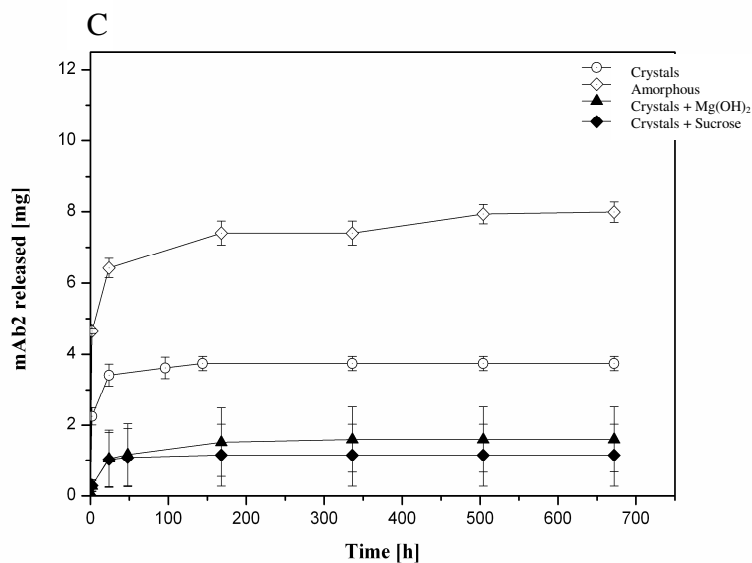


Figure 6-5 mAb2 *in vivo* release profiles from depots which contained A 20% (w/w) PLGA 502H; B 30% (w/w) PLGA 502H; C 20% PLGA 755S; D 30% PLGA 755S. Amorphous refers to freeze-dried mAb2. Additives were only formulated together with crystallized mAb2.

Stabilizing approaches to persevere the protein integrity by addition of excipients were also assessed. PLGA is known to degrade into acidic species which can potentially trigger physical and chemical protein instability⁴¹. By this, magnesium hydroxide (Mg(OH)₂) and sodium carbonate (Na₂CO₃) were exploited as pH modifiers in order to

prevent a pH drop within the depot which might be harmful to the proteins. Such basic salts are already reported to reduce acidic catalyzed degradation of the incorporated drug or the polymer itself⁴².

Protein release was increased for formulations which contained one of these two basic excipients (Fig. 6-4 & 6-5 A – D). Only the PLGA 755S formulations showed a reduction in protein release after addition of magnesium hydroxide.

To enhance the protein drug release sucrose was added as pore forming agent. However, a controversial effect was observed for all mAb2 depot formulations which showed a significantly reduced protein release. Interestingly, for mAb1 depot formulations, the opposite effect was observed except for the PLGA 502H 30% (w/w) formulations without additives.

Overall, formulations which contained $Mg(OH)_2$ showed the best and most sustained mAb release.

6.3.1.2.2 mAb1 and mAb2 release studies from SAIB depot formulations

For SAIB, no degradation into acidic species is known and thus no pH modifiers were applied. Only sucrose was utilized as pore forming agent in order to enhance protein drug release. Only one SAIB polymer was available and thus the focus of the present study was on the effect of the carrier solvent on amorphous and crystalline mAb1 and mAb2 release.

Again, the highest initial protein burst was observed for formulations which contained amorphous mAb1 or mAb2 except for depot formulations which contained crystalline mAb1 and ethyl acetate as carrier solvent (Fig 6-6). In all cases, utilization of isopropanol 100% as carrier solvent led to a decreased protein release compared to formulations with ethyl acetate. The lowest protein amounts were released from formulations with sucrose as pore forming agent. Notably, almost no protein was released from the formulations which contained crystalline mAb2. This was explained by the low compatibility of mAb2 to both solvents (see section 3.3.3).

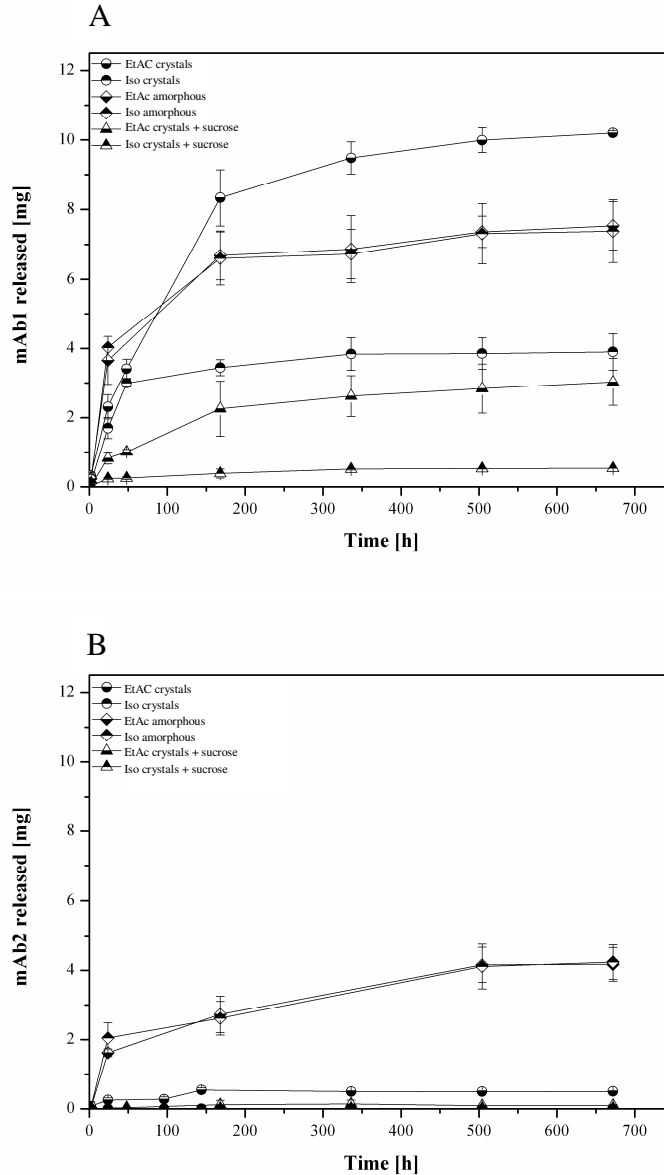


Figure 6-6 mAb1 (A) and mAb2 (B) *in vitro* release from SAIB 90% (w/w) depot formulations with isopropanol 100% (Iso) or ethyl acetate (EtAc) as solvent. Furthermore, sucrose was added as pore forming agent only to formulations which contained mAb crystals.

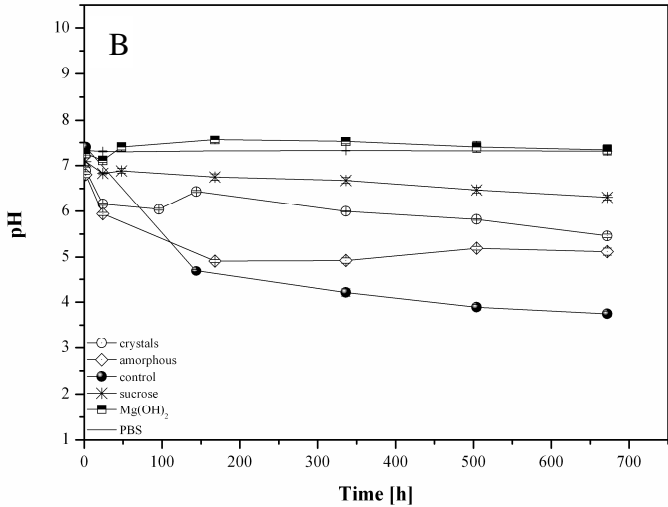
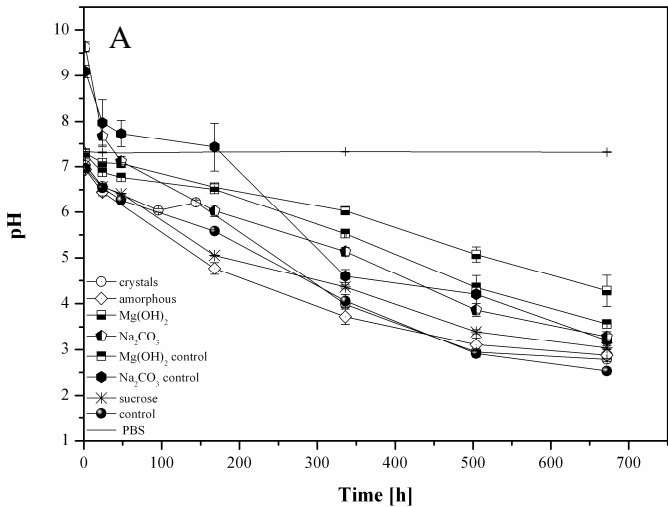
Compared to the PLGA based mAb1 depot formulations, the release from SAIB depots was much higher and in a more sustained manner.

6.3.1.3 Influence of degradation on pH

PLGA is reported to degrade into acidic species which can affect the stability of proteins entrapped within the depot^{23,24}. Therefore, the pH value of the different formulations was monitored over 4 weeks (Tab. 6-2). To highlight the effect of buffer replace-

ment, as performed during the release studies, control samples (control) without any buffer replacement were also tested. To investigate the depot degradation associated with the pH drop, the depots were investigated visually by digital microscopy at each sample draw.

Figure 6-7 shows the pH values measured for 30% (w/w) PLGA 502H, PLGA 755S and SAIB formulations containing mAb1 in its amorphous or crystalline state over 4 weeks. The results for the other formulations did not differ (not shown).



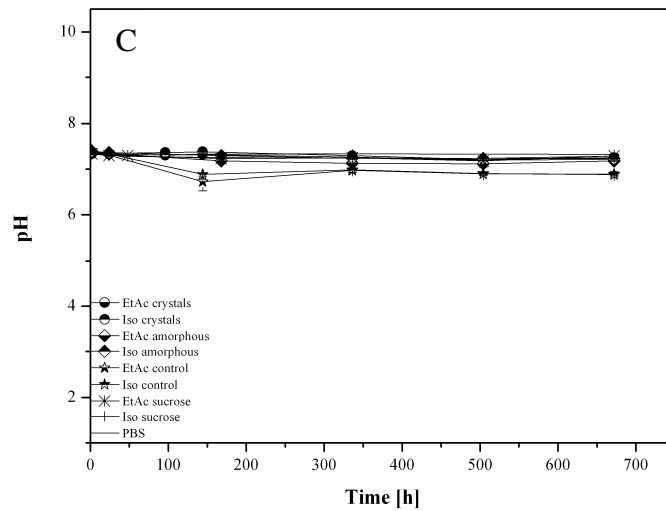


Figure 6-7 pH values of different formulations containing: A. 30% (w/w) PLGA 502H; B. 30% (w/w) PLGA 755S; C. 90% (w/w) SAIB as polymer. For PLGA 502H and PLGA 755S, all samples with additives contained crystallized mAb. For SAIB, either isopronaol 100% (Iso) or ethyl acetate (EtAc) was used as carrier solvent. Control refers to samples with direct pH measurements without buffer exchange.

Generally, the pH values of PLGA 502H formulations dropped to lower levels as for PLGA 755S formulations. For both polymers, the controls showed the largest pH drops after the 4 weeks. Addition of magnesium hydroxide was able to maintain the pH values at around 7.4 for PLGA 755S formulations while for PLGA 502H formulations pH values of approximately 4.5 were measured. Sodium carbonate showed initially the highest pH values (> 9.5) whereas a significant pH drop could be observed after 4 weeks (> 4.0). Interestingly, the addition of sucrose also allowed a reduction of the pH drop. For SAIB, only the controls showed a light pH drop below a value of 7.0. All other SAIB formulations remained unaltered.

Figure 6-8 displays the optical depot degradation for PLGA 502H and SAIB formulations over 4 weeks. A significant decrease in PLGA implant density and diameter could be seen for all samples. The same trend was also found for all other PLGA formulations (data not shown). However, SAIB degradation could not be observed visually in any case.

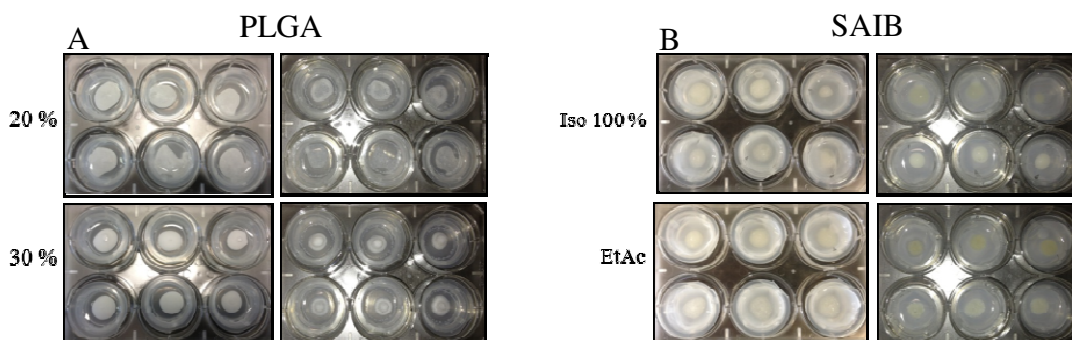


Figure 6-8 Optical degradation from A 20% and 30% (w/w) PLGA 502H formulations which contained amorphous mAb1 (top rows) and mAb2 (bottom rows); B SAIB formulations with amorphous mAb1 (top rows) or mAb2 (bottom rows) and either isopropanol 100% (Iso 100%) or ethyl acetate (EtAc) as carrier solvent. The left boxes show the depots immediately after injection and the right boxes after 4 weeks of incubation at 37°C

The results did not allow to draw conclusions with respect to SAIB degradation. Neither the pH value nor the optical integrity of the SAIB depots changed during the study. However, this study confirmed an even optically visible PLGA into acidic species which was associated to a pH drop. Basic additives such as magnesium hydroxide were able to reduce the pH drop (PLGA 502H) or even to maintain the pH value at the around 7.4 (PLGA 755S). The increased pH values hindered acidic catalyzed degradation of the polymer which resulted in a more sustained mAb release (PLGA 755S; Fig. 6-4 & 6-5). Furthermore, the acidic catalyzed protein degradation was also minimized which allowed an increased protein release from PLGA 502H depots (see section 6.3.1.2.1)⁴².

6.3.1.4 Depot characteristics

6.3.1.4.1 Phase inversion for PLGA depot systems

The phase inversion is deemed to be an important factor which determines the extent of the initial drug burst release. This process of dynamic polymer solidification can be regulated by different factors such as the overall polymer concentration, the polymer molecular weight, the applied carrier solvent and additives⁴⁰. Slow inverting systems are reported to show small primary burst release⁴³. Higher polymer concentrations show a slower water influx and thus the time of the phase inversion itself is prolonged^{9,44,45}. Therefore, it was the aim to confirm the previously reported correlations to the PLGA formulations used and to their degrees of initial drug burst release. To evaluate the phase inversion dynamics, 20%, 25% and 30% (w/w) of PLGA 502H

and 755S were dissolved in PEG 400 which was stained with a blue colored “PEG-dye”. Phase separation was completed when PEG had completely diffused out from the polymer depot. This state was indicated by “PEG-dye” discoloration upon contact to the surrounding aqueous phase (Fig. 6-9).

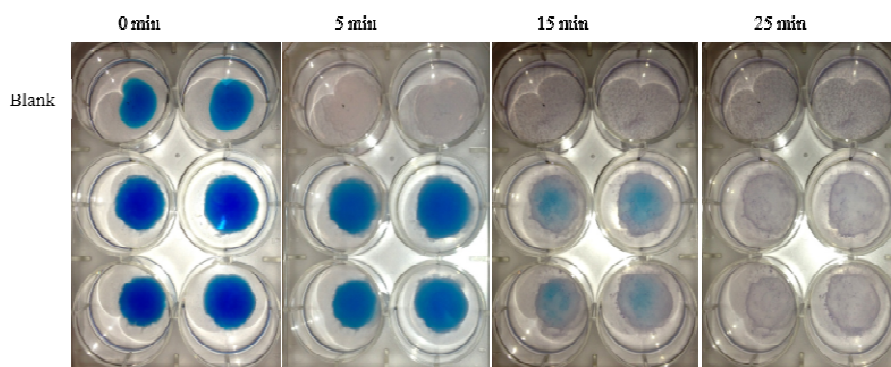


Figure 6-9 Example for a phase inversion study for a 20% (w/w) PLGA 502H depot formulation. Blank refers to colored PEG 400 without any PLGA 502H.

For both PLGA polymers, time until complete discoloration was elevated with increased polymer concentrations (Tab. 6-3).

Table 6-3 Time of complete discoloration and thus duration of dynamic phase inversion for different PLGA 502H and PLGA 755S solutions in PEG 400.

Polymer % [w/w]	Time until complete discoloration
20% PLGA 755S	25
25% PLGA 755S	60
30% PLGA 755S	140
20% PLGA 502H	100
25% PLGA 502H	160
30% PLGA 502H	220

Notably, formulations which contained PLGA 502H showed longer phase inversion periods as systems consisted of PLGA 755S. A slower phase inversion indicates a slower solvent exchange of the depot and thus smaller primary burst releases⁴³. However, detrimental observations were made during the release studies.

6.3.1.4.2 Syringeability

Regarding patient compliance, syringeability is an important factor. It indicates the ability of a formulation to be administered by a thin needle with moderate pressure forces.

The PLGA 502H/755S and SAIB formulations were assessed for their syringeability by variation of the needle diameter (20 G, 25 G, 27 G) and the syringe size (1 mL, 5 mL). Depletion time (10 s) and injection volume (0.5 mL) were kept constant during all tests. Syringeability was considered to be acceptable if the required force to eject a polymer solution within 10 s did not exceed 10 N⁴⁶. It could be observed that the syringeability was dependent on a series of factors (Fig. 6-10 A – C).

An increased syringe volume resulted in a smaller outlet gap compared to the overall diameter of the syringe plunger and thus led to a dramatically increased force required for ejection (Fig. 6-10 A). Even the system check performed with highly purified water and an empty syringe showed larger values. A second important factor was the inner diameter of the injection needle. Smaller inner diameters resulted in increased ejection forces required (not shown). Notably, the values were distinctly elevated within a small polymer concentration range between 25% (w/w) and 30% (w/w) for PLGA 502H and PLGA 755S (Fig. 6-10 B). Syringeability for PLGA formulations was only achieved by applying a 20 G needle and polymer concentrations of 25% (w/w) and below.

Generally, SAIB formulations were found to be superior compared to PLGA formulations with respect to their required injection forces (Fig. 6-10 C). However, higher concentrated polymer solutions required large needle diameters to fulfill the predefined requirements for syringeability.

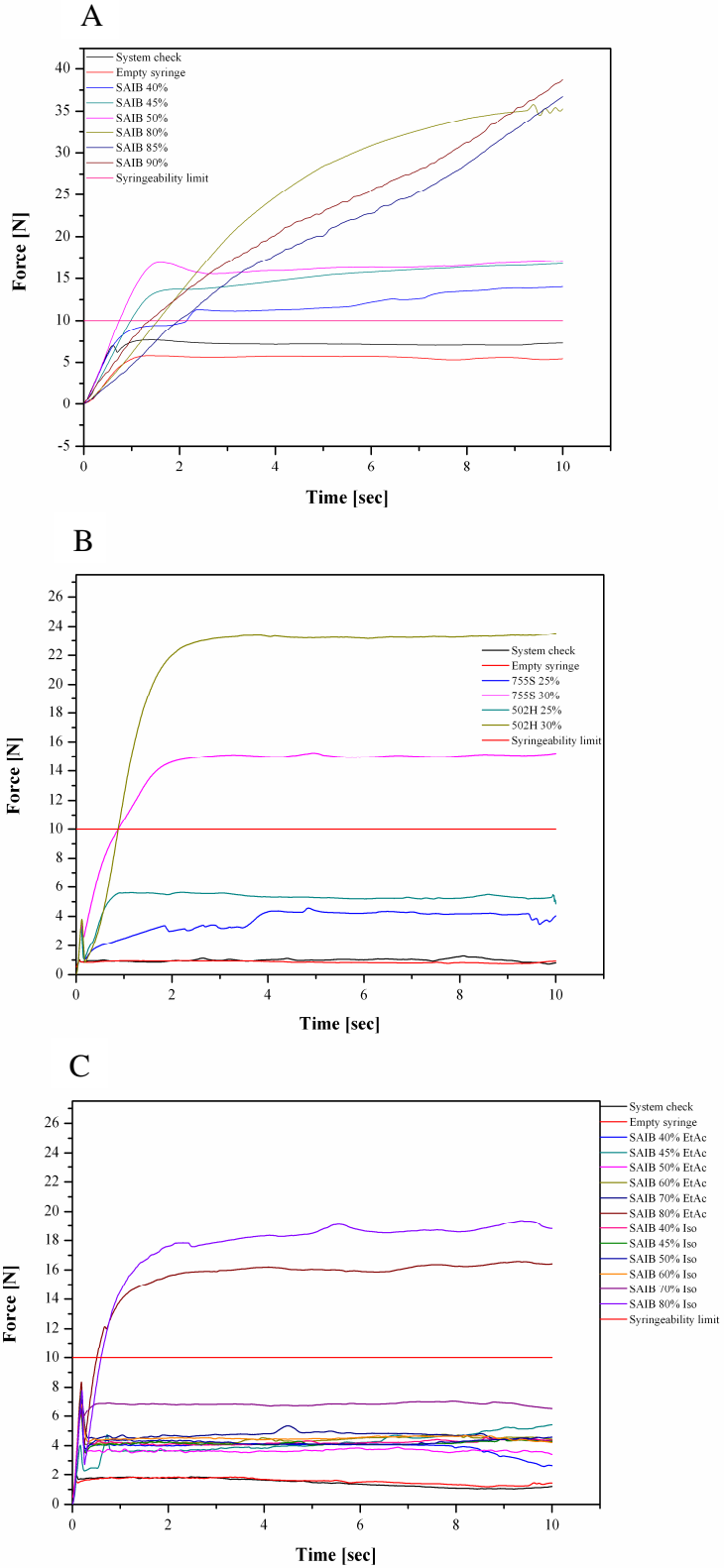


Figure 6-10 Forces [N] required for ejection of 0.5 mL depot formulation within 10 s by using a 1 mL syringe. **A** shows the results for 40 - 90% (w/w) SAIB in ethyl acetate and 80 - 90% (w/w) SAIB in isopropanol 100% through a 20 G needle. **B** depicts the required ejection forces for 25% and 30% (w/w) PLGA solution in PEG 400 through a 20 G needle. **C** shows the results for 40 - 90% (w/w) SAIB formulations with ethyl acetate as carrier solvent ejected through a 27 G needle and a 5 mL syringe.

As summarized in Table 6-4 a dependency between polymer concentration and in case of SAIB, the carrier solvent and the required force for ejection was clearly demonstrated.

Table 6-4 Syringeability of different SAIB and PLGA formulations in dependency to the needle diameter. Syringeability was considered acceptable if the polymer solution could be ejected within 10 s with a force not exceeding 10 N. NS means that no tested formulations met the defined requirements for syringeability. The percentage refers to (w/w).

Needle diameter	SAIB		PLGA	
	Ethyl acetate	Isopropanol 100%	502H	755S
27 G	40 - 50%	NS	NS	NS
25 G	60 - 75%	40 - 75%	NS	NS
20 G	80 - 90%	80 - 90%	< 25%	< 25%

6.3.2 Lipid implants

Lipid implants represent a novel and promising drug sustained release platform for biopharmaceutics. Recently, Gerhard L. Sax presented a lipid formulation consisting of a low melting (H12) and a high melting (D118) lipid compound which allowed for a long acting and constant antibody release. Here the applicability of this formulation was tested for mAb1 crystals³⁷. However, this approach required a protein in a dry state and thus mAb2 had to be excluded as no successful drying approach could be developed (see Chapter 3). mAb1 was vacuum-dried in accordance to a procedure introduced by Stefan Gottschalk during the preliminary study²⁹. Freeze-dried mAb1 was utilized as comparison to highlight the effect of the crystalline state on the protein drug release. PEG was used as pore forming agent as beneficial release modifying effects have already been introduced in literature^{35,47}. Furthermore, additional impact towards a constant and prolonged release was anticipated as PEG also functions as crystallizing agent for mAb1.

All lipid implants were produced applying the twin-screw extrusion procedure³⁷. Crystals and amorphous mAb1 were each formulated with and without PEG as release modulator (Fig. 6-11).

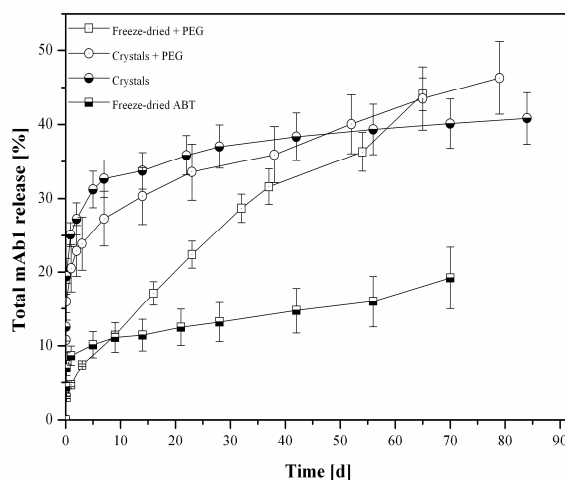


Figure 6-11 Total mAb1 releases from various lipid implants. The implants contained either amorphous or crystalline mAb1 \pm PEG 4000 as release modifier.

In comparison, formulations containing PEG showed a lower concentration of mAb1 released initially (burst). However, the slope of the release curves was steeper compared to their PEG free counterparts. A higher total protein release could be observed for these formulations until the end of the study. The highest bursts were observed for formulations containing crystalline mAb1. With respect to a constant, prolonged protein drug release without initial drug burst, the implants containing amorphous mAb1 and PEG were found to be superior towards all other implant formulations.

In a following experiment, SEM measurements were performed to investigate a potential attachment of the mAb1 crystals on the implant surface. Due to the crystal sizes ($> 50 \mu\text{m}$) a complete or partial exposure was deemed to be responsible for the initial drug burst release. Furthermore, it was aimed to investigate possible differences in the implant morphology after release. Therefore, the same lipid implant formulations were prepared by twin-screw extrusion and subsequently incubated for 10 weeks at 37°C . SEM microscopy was performed before (Fig. 13 D – E) and after incubation (Fig. 13 A – C).

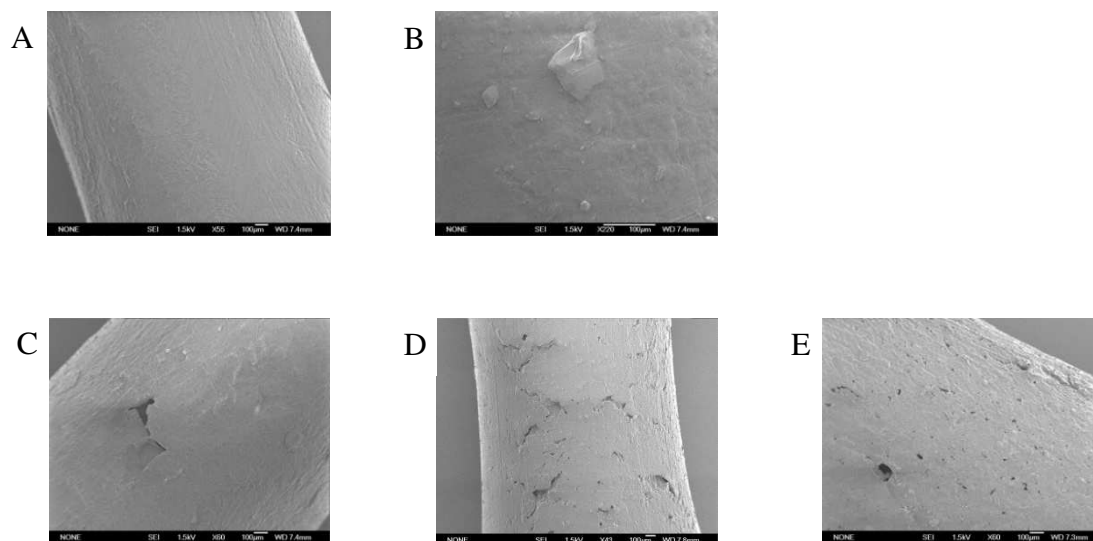


Figure 6-12 SEM micrographs of lipid implants which were incubated and contained A freeze-dried mAb1 before implant incubation; B crystalline mAb1 before incubation; C crystalline mAb1 (after incubation); D freeze-dried mAb1 (after incubation); E PEG 4000, but no protein (after incubation).

Dependent on the protein state and presence of PEG, different surface appearances could be observed. After incubation, implants with crystalline mAb1 showed large cavities at the implant surface (Fig. 6-12 A). More and also larger cavities were observed throughout the whole surface of implants which contained freeze-dried PEG (Fig. 6-12 B). Implants without any protein but PEG showed very small holes on their surfaces (Fig. 6-12 C). Before incubation, a smooth surface could be seen for implants which contained amorphous mAb1 whereas visible attachments were observed for implants with mAb1 crystals (Fig. 6-12 D - E).

6.3.3 SAIB depots containing dried lysozyme crystals

The effect of protein crystal drying prior to incorporation into a depot formulation was already highlighted by Pechenov et al.¹². Dried crystals showed a slower drug release compared to undried crystals. To confirm the presented considerations, a similar approach was researched for hot air dried lysozyme crystals (see Chapter 2). The crystals (5% (w/w)) were formulated with 85% (w/w) SAIB and 10% (w/w) isopropanol 95%. The protein release was compared to formulations from freeze-dried lysozyme and non-dried lysozyme crystals (Fig. 6-13).

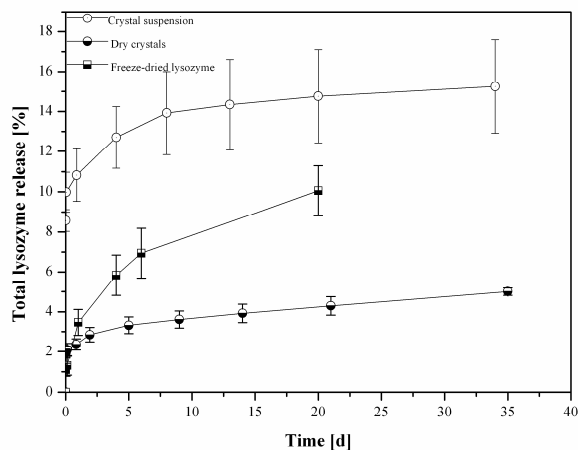


Figure 6-13 Total lysozyme release from a 85% (w/w) SAIB formulation. The formulations contained either freeze-dried lysozyme, hot air dried or non-dried lysozyme crystals.

The results showed a discrepancy between the hot air dried and the non-dried lysozyme crystals. While a large initial drug burst release was observed for the non-dried crystals, a little initial burst with a subsequently slow and constant lysozyme release was detected for the dried crystals. The freeze-dried lysozyme also showed a rather small initial burst release, but the following constant release was faster than for the dried and non-dried lysozyme crystals. The results presented by Pechenov et al. could be confirmed by the present study for lysozyme crystals. Notably, no superior release kinetics could be confirmed for mAb crystals compared to freeze-dried mAb.

6.4 Discussion

For mAb1 and mAb2, *in situ* forming depot formulations based on PLGA 502H, 755S and SAIB should be developed. Suitable polymer concentrations and solvents were defined with respect to convenient preparation process (e.g. fast polymer dissolution) and viscosity of the final formulation. A low viscosity was deemed mandatory for a convenient injectability of the final depot formulation. However, it was clear that by decreasing the polymer concentration the sustained release properties of the depot formulation would be reduced. Therefore, a compromise, especially for the PLGA depots was inevitable. PLGA dissolution in PEG 200 and PEG 300 resulted in solutions of high viscosity not suitable for injection, and thus, these solvents were excluded from the following studies. PEG 400 was identified as suitable solvent with acceptable viscosity of the final solution for PLGA 502H and 755S concentrations up to 30% (w/w). Consequently, PLGA concentrations of 20% and 30% (w/w) were applied for the following studies. SAIB was insoluble in all PEGs tested. Therefore, Isopropanol 100% and ethyl acetate were defined as solvents. SAIB showed a low viscosity in both solvents even at a concentration of 90% (w/w) which was chosen for the following studies.

In vitro studies investigating *in situ* precipitating depot formulations are complicated by sophisticated implant preparation methods. The drug release is dependent on depot size, shape, thickness and contact points to the release container which hinder drug diffusion¹⁰. To reduce the hindrance of drug diffusion, a new testing method was assessed in that the depot was injected on a mesh to form discs of similar shapes. This mesh was placed in the middle of the release container. For each depot formulation, suitable mesh diameters were identified which allowed depot hardening without depot formulation leakage through the mesh. The validity of this set-up was confirmed by a higher protein release rate compared to disc shaped depots placed on the bottom of the release container. The latter one mimics a sustained release which is however caused by reduced depot surfaces with contact to the release media. The location on a mesh above the bottom allowed the protein drug to diffuse in all directions. It was clear that the mesh side would not allow a complete unimpeded release, but limitations by contact to container walls were diminished.

Subsequently, mAb release studies from different PLGA and SAIB depot formulations were carried out. mAb1 and mAb2 concentrations of 5% (w/w) were used for all formu-

lations. $\text{Mg}(\text{OH})_2$ and Na_2CO_3 were tested as pH modifier for the PLGA depots while sucrose was applied as pore former for SAIB depots as well. All additives were used in a concentration of 3% (w/w). These additives were assessed for their effect on the protein drug release. The drug release from any device is influenced besides others by the type of drug, its water solubility, the drug load, the water content of the depot, the type of polymer used, the presence of additives and the properties of the carrier solvent¹². Eliaz et al. stated that for low protein depot loadings the release would be determined by the rate of polymer degradation whereas for higher protein loadings additional diffusion processes enhance the drug release¹³. By this, mAb release from PLGA and SAIB *in situ* precipitating depot systems should be determined by a combination of osmotic mediated events and polymer erosion and by drug diffusion^{10,48}.

The results for PLGA implants without any additives showed that by trend higher polymer concentrations were linked to reduced initial drug burst which was in accordance to literature¹³. This is usually caused by higher viscosities, decreased phase separation and water influx and thus lower protein diffusion into the surrounding medium during hardening¹³. Generally, formulations with freeze-dried mAb showed a higher initial burst release and a higher total amount of released protein compared to formulations with mAb crystals. This was caused by sucrose which functioned as pore forming agent and thus release enhancer for the amorphous mAb. Sucrose was an unavoidable ingredient (5% (w/v)) for the freeze-dried product as it was required for mAb stabilization during the freeze drying procedure. Sucrose functions as pore former due to its water absorptive properties and thus increased water contents within the depot without changing the polymer degradation by affecting the acid-base chemistry⁴⁹. Furthermore, sucrose was used to stabilize proteins due to its preferential hydration effects⁵⁰. However, additional sucrose used as pore forming agent even led to a reduced release of crystalline mAb2. On the contrary, the release of crystalline mAb1 was increased in a sustained fashion in presence of sucrose. The results show that protein release is not solely influenced by the pore forming agent. Stability issues were also considered to reduce the protein release from formulations which contained crystalline mAb as it was shown that PEG induces mAb degradation (see Chapter 5). Furthermore, PLGA is known to degrade into acidic species which also can trigger protein instability⁴¹. To overcome potential protein instability and to improve the protein release, the antacid $\text{Mg}(\text{OH})_2$ and Na_2CO_3 were used as pH modifiers²³. Addition of such pH modifiers can enhance the

protein drug stability by inhibiting the formation of insoluble protein aggregates and hydrolytic effects⁵¹. In addition, this class of additives can promote protein release by volume expansion. It triggers the formation of a pore network by increased water uptake⁴⁹. Notably, positive effects on the mAb release could be observed. The overall amount of released protein was increased in a sustained manner for both additives. Overall, these findings demonstrated that the protein drug release was enhanced by both, the pore forming effect of sucrose and the stabilizing properties by Mg(OH)₂ and Na₂CO₃.

SAIB was used as polymer for depot formulations with superior preservation of protein stability compared to PLGA depots as no degradation into acidic species is known for SAIB. Isopropanol 100% and ethyl acetate were chosen as carrier solvents for SAIB depot formulations even though their negative effect on mAb1 and mAb2 stability was known (see Chapter 3). No suitable alternative to these two solvents was available which was able to dissolve SAIB and to preserve the mAb1 and mAb2 stability. The present study was supposed to provide a first insight into SAIB depot formulations containing mAb crystals. Furthermore, it was anticipated that the low organic solvent content of 10% (w/w) required for depot formulation would not trigger protein degradation. However, especially mAb2 crystal stability was obviously affected by the solvents as almost no protein was released from the depot formulations. This indicated severe protein degradation. Notably, a sustained release was obtained for the freeze-dried mAb2 which indicated superior protection of the protein integrity in the dry, amorphous protein state compared to the crystalline state. The higher mAb1 release rates were also ascribed to higher protein stability during organic solvent contact (see Chapter 3). Here, the release from SAIB formulations with ethyl acetate was superior to the release from implants with isopropanol 100%. This was caused by an effect of the organic solvent on the protein integrity. Ethyl acetate was shown to preserve the crystal integrity best (see Chapter 3). The inferior mAb1 and mAb2 release from implants which contained sucrose as pore forming agent remained unclear and needs further investigation. One explanation is based on a faster crystal dissolution accompanied with enhanced contact to the organic carrier liquids during hardening caused by an increased water uptake of the depots triggered by sucrose⁴⁹.

The degradation of the PLGA and SAIB depots was assessed by visual inspection and measuring of the pH. Depot degradation connected to the pH value was assumed as

PLGA degrades by formation of acidic species. For SAIB such a dependency is not described and thus was assessed. Furthermore, the effect of the additives used during the release study on the pH values was tested. The study confirmed PLGA degradation into acidic species. pH values of 3 for PLGA 502H and 4 for PLGA 755S could be measured. The PLGA degradation was also optically visible. A protein degradation at such low pH values is plausible. Addition of magnesium hydroxide was able to reduce the pH drop (PLGA 502H) or even to maintain the pH value at around 7.4 (PLGA 755S). Consequently, both additives protected the mAb against acidic mediated drug degradation which resulted in enhanced release profiles⁴². The effect of sucrose on the pH value is caused by its pore forming effect. The acidic degradation products were washed out by an increased water influx into the depot.

For SAIB, polymer degradation could not be assured by alteration of the pH value or by visible inspection. Consequently, the mAb release was predominately determined by drug diffusion.

In a further experiment, phase inversion dynamics for PLGA depots was studied to assess a dependency between the required time for phase inversion for different polymer concentrations and the primary burst release. Formulations from PLGA 502H showed longer phase inversion periods than depots consisting of PLGA 755S. A slower phase inversion should indicate a slower solvent exchange of the depot and thus smaller primary burst releases⁴³. Detrimental observations were made during the release studies which were explained by high protein diffusion rates during the solidification phase of the depot. The semi-solid state did not hinder the protein release which compensated the slow phase inversion. Furthermore, the effect of the additives on the phase inversion has to be studied in further experiments.

Syringeability of the PLGA and SAIB depot formulations has also been studied. It is an important feature for patient compliance. For the injection study, 10 N was chosen as force limit as it was reported to allow for a easy and convenient injection⁴⁶. In accordance with literature, all factors tested such as formulation viscosity, plunger size and needle diameter had an effect on the required injection force⁴⁶. SAIB formulations showed superior syringeability which raised attention with respect to further clinical application. In contrast, the PLGA formulations showed an acceptable syringeability only through a 20 G needle and at concentrations below 25% (w/w). Notably, the PLGA

polymer concentrations used for depot preparation during the present study were lower compared to approaches presented in literature. Pechenov et al. showed an excellent protein release from a 50% (w/w) PLGA/acetonitrile formulation which contained amylase crystals¹². This formulation would hardly be injectable with the aforementioned results regarding syringeability of 30% (w/w) PLGA formulations in mind. As significant lower polymer concentrations result in faster protein releases, formulation scientists would have to find a compromise between an acceptable syringeability and desired release properties.

Lipid implants were tested as novel sustained release formulations for mAb crystals. However, no beneficial release kinetic was observed for mAb1 crystals. The initial high drug burst release was ascribed to the fact that protein crystals represent the highest concentrated protein formulation possible^{28,52}. Furthermore, the mAb1 crystals (platelet shape) could reach sizes of more than 100 μm . Considering a lipid implant diameter of approximately 2 mm, it would be obvious to expect certain crystal contacts to the implant surface. This might result in a high initial drug burst release due to a fast unloading of the crystalline protein depot. This assumption was confirmed by SEM micrographs which showed crystalline structure on the implant surface while an even and uniform surface structure was observed for formulations which contained amorphous mAb1. As washing of mAb1 crystals with EtOH (see Chapter 3) reduces protein recovery of SE-HPLC measurements, certain inaccuracy of the presented release profiles was considered. By that, steeper release curves and thus faster protein dumping into the release media can be anticipated for stable protein crystals.

Dried protein crystals were shown to slow down protein release which could be confirmed for dry lysozyme crystals during the present study¹². A SAIB based depot formulation was tested for hot air dried lysozyme crystals, undried lysozyme crystals and freeze-dried lysozyme. The crystals in the wet state were surrounded of dissolved protein and thus the protein was washed out faster of the depot with a large initial burst release. Drying of protein crystals reduced the water content of the crystals and thus resulted in prolonged rehydration times which slowed down the protein release^{53,54}. Compared to amorphous protein, protein crystals have a reduced surface in contact with the solvent and thus dissolved much slower. Consequently, the small initial burst release from the freeze-dried protein was followed by a faster protein release compared to the dried and non-dried lysozyme crystals.

6.5 Conclusion

In conclusion, the vision of applicable depot formulations for mAb crystals could not be realized. No clear trend towards a superior drug release was found for the formulations tested. In all cases, amorphous mAb material showed favorable properties such as higher stability (SAIB depot with isopropanol 100%) and higher total protein release. Utilization of additives enhanced protein release from crystalline mAb for only one mAb2 formulation (30% (w/w) PLGA 502H and magnesium hydroxide). Regarding syringeability, a compromise between an applicable polymer concentration enabling a desired protein drug release and the required injection force which allows for a convenient application has to be found.

SAIB still appears as promising polymer for depot formulations. Release kinetics as well as syringeability properties were superior compared to PLGA formulations. However, the choice of a suitable carrier solvent which preserves the protein drug integrity remains crucial.

Vacuum dried mAb1 crystals did not show enhanced sustained release profiles compared to freeze dried and thus amorphous mAb1. As the amorphous mAb1 showed an optimal, constant release profile without any burst it remains questionable if the crystalline mAb material would be able to provide distinct improvement during further studies.

Studies with SAIB based depot formulations which contained hot-air dried lysozyme crystals, undried lysozyme crystals and freeze-dried lysozyme revealed enhanced release profiles for the dried crystals. This experiment proved the feasibility of protein crystals to offer superior features for depot formulations. However, the studies with mAb1 and mAb2 showed that a transfer of these findings to other protein crystals remains challenging and has to be assessed for each single molecule.

6.6 References

1. Walsh, G., *Biopharmaceutical benchmarks 2010*. Nature Biotechnology, 2010. **28**(9): p. 917.
2. Frokjaer, S., Otzen, D.E., *Protein drug stability: a formulation challenge*. Nature Reviews Drug Discovery, 2005. **4**(4): p. 298-306.
3. Antosova, Z., Mackova, M., Kral, V., Macek, T., *Therapeutic application of peptides and proteins: parenteral forever?* Trends in Biotechnology, 2009. **27**(11): p. 628-635.
4. Yewey, G., Duysen, E.G., Cox, S.M., Dunn, R.L., *Delivery of proteins from a controlled release injectable implant*, in *Protein Delivery*. 2002, Springer. p. 93-117.
5. Mahmood, I., Green, M.D., *Pharmacokinetic and pharmacodynamic considerations in the development of therapeutic proteins*. Clinical Pharmacokinetics, 2005. **44**(4): p. 331-347.
6. Yang, M.X., Shenoy, B., Disttler, M., Patel, R., McGrath, M., Pechenov, S., Margolin, A.L., *Crystalline monoclonal antibodies for subcutaneous delivery*. Proceedings of the National Academy of Sciences, 2003. **100**(12): p. 6934-6939.
7. Johnson, O.L., Cleland, J.L., Lee, H.J., Charnis, M., Duenas, E., Jaworowicz, W., Shepard, D., Shahzamani, A., Jones, A.J., Putney, S.D., *A month-long effect from a single injection of microencapsulated human growth hormone*. Nature Medicine, 1996. **2**(7): p. 795-799.
8. Vandorpe, J., Schacht, E., Dunn, S., Hawley, A., Stolnik, S., Davis, S., Garnett, M., Davies, M., Illum, L., *Long circulating biodegradable poly (phosphazene) nanoparticles surface modified with poly (phosphazene)-poly (ethylene oxide) copolymer*. Biomaterials, 1997. **18**(17): p. 1147-1152.
9. Dunn, R.L., English, J.P., Cowsar, D.R., Vanderbilt, D.P., *Biodegradable in-situ forming implants and methods of producing the same*. 1994, US Patent 4,938,763 A.
10. Astaneh, R., Erfan, M., Moghimi, H., Mobedi, H., *Changes in morphology of in situ forming PLGA implant prepared by different polymer molecular weight and its effect on release behavior*. Journal of Pharmaceutical Sciences, 2009. **98**(1): p. 135-145.
11. Dunn, R., *Application of the ATRIGEL® implant drug delivery technology for patient-friendly, cost-effective product development*. Drug Delivery Technology, 2003. **3**(6).
12. Pechenov, S., Shenoy, B., Yang, M.X., Basu, S.K., Margolin, A.L., *Injectable controlled release formulations incorporating protein crystals*. Journal of Controlled Release, 2004. **96**(1): p. 149-158.

13. Eliaz, R.E., Kost, J., *Characterization of a polymeric PLGA-injectable implant delivery system for the controlled release of proteins*. Journal of Biomedical Materials Research, 2000. **50**(3): p. 388-396.
14. Smith, D.A., Tipton, A., *A novel parenteral delivery system*. Pharmaceutical Research, 1996. **13**(9): p. 300.
15. Pisal, D.S., Kosloski, M.P., Balu-Iyer, S.V., *Delivery of therapeutic proteins*. Journal of Pharmaceutical Sciences, 2010. **99**(6): p. 2557-2575.
16. Okumu, F.W., Dao, L.N., Fielder, P.J., Dybdal, N., Brooks, D., Sane, S., Cleland, J.L., *Sustained delivery of human growth hormone from a novel gel system: SABER TM*. Biomaterials, 2002. **23**(22): p. 4353-4358.
17. Packhaeuser, C.B., Schnieders, J., Oster, C.G., Kissel, T., *In situ forming parenteral drug delivery systems: an overview*. European Journal of Pharmaceutics and Biopharmaceutics, 2004. **58**(2): p. 445-455.
18. Hatefi, A., Amsden, B., *Biodegradable injectable in situ forming drug delivery systems*. Journal of Controlled Release, 2002. **80**(1): p. 9-28.
19. Lu, Y., Tang, X., Cui, Y., Zhang, Y., Qin, F., Lu, X., *In vivo evaluation of risperidone-SAIB in situ system as a sustained release delivery system in rats*. European Journal of Pharmaceutics and Biopharmaceutics, 2008. **68**(2): p. 422-429.
20. Gibson, J.W., Sullivan, S.A., Middleton, J.C., Tipton, A.J., *High viscosity liquid controlled delivery system and medical or surgical device*. 2002, US Patent 6,413,536 B1
21. Lu, Y., Yu, Y., Tang, X., *Sucrose acetate isobutyrate as an in situ forming system for sustained risperidone release*. Journal of Pharmaceutical Sciences, 2007. **96**(12): p. 3252-3262.
22. Dong, W., Körber, M., López Esguerra, V., Bodmeier, R., *Stability of poly (D, L-lactide-co-glycolide) and leuprolide acetate in in-situ forming drug delivery systems*. Journal of Controlled Release, 2006. **115**(2): p. 158-167.
23. Fu, K., Klibanov, A.M., Langer, R., *Protein stability in controlled-release systems*. Nature Biotechnology, 2000. **18**(1): p. 24-25.
24. Fu, K., Pack, D., Klibanov, A., Langer, R., *Visual evidence of acidic environment within degrading poly (lactic-co-glycolic acid)(PLGA) microspheres*. Pharmaceutical Research, 2000. **17**(1): p. 100-106.
25. Margolin, A.L., Navia, M.A., *Protein Crystals as Novel Catalytic Materials*. Angewandte Chemie International Edition, 2001. **40**(12): p. 2204-2222.
26. Shenoy, B., Govardhan, C.P., Yang, M.X., Margolin, A.L., *Crystals of whole antibodies and fragments thereof and methods for making and using them*. 2010, US Patent 7,833,525 B2.

27. van de Weert, M., Hennink, W.E., Jiskoot, W., *Protein Instability in Poly(Lactic-co-Glycolic Acid) Microparticles*. *Pharmaceutical Research*, 2000. **17**(10): p. 1159-1167.
28. Basu, S.K., Govardhan, C.P., Jung, C.W., Margolin, A.L., *Protein crystals for the delivery of biopharmaceuticals*. *Expert Opinion on Biological Therapy*, 2004. **4**(3): p. 301-317.
29. Gottschalk, S., *Crystalline Monoclonal Antibodies: Process Development for Large Scale Production, Stability and Pharmaceutical Applications*. Thesis Munich, 2008.
30. Kreye, F., Siepmann, F., Siepmann, J., *Lipid implants as drug delivery systems*. *Expert Opinion on Drug Delivery*, 2008. **5**(3): p. 291-307.
31. Maschke, A., Lucke, A., Vogelhuber, W., Fischbach, C., Appel, B., Blunk, T., Göpferich, A. *Lipids: an alternative material for protein and peptide release*. in *ACS Symposium series*. 2004: ACS Publications.
32. Wang, P.Y., *Lipids as excipient in sustained release insulin implants*. *International Journal of Pharmaceutics*, 1989. **54**(3): p. 223-230.
33. Walduck, A., Opdebeeck, J., Benson, H., Prankerd, R., *Biodegradable implants for the delivery of veterinary vaccines: design, manufacture and antibody responses in sheep*. *Journal of Controlled Release*, 1998. **51**(2): p. 269-280.
34. Guse, C., Koennings, S., Maschke, A., Hacker, M., Becker, C., Schreiner, S., Blunk, T., Spruss, T., Göpferich, A., *Biocompatibility and erosion behavior of implants made of triglycerides and blends with cholesterol and phospholipids*. *International Journal of Pharmaceutics*, 2006. **314**(2): p. 153-160.
35. Herrmann, S., Mohl, S., Siepmann, F., Siepmann, J., Winter, G., *New insight into the role of polyethylene glycol acting as protein release modifier in lipidic implants*. *Pharmaceutical Research*, 2007. **24**(8): p. 1527-1537.
36. Koennings, S., Tessmar, J., Blunk, T., Göpferich, A., *Confocal microscopy for the elucidation of mass transport mechanisms involved in protein release from lipid-based matrices*. *Pharmaceutical Research*, 2007. **24**(7): p. 1325-1335.
37. Sax, G.L., *Twin-screw extruded lipid implants for controlled drug delivery*. Thesis Munich, 2012.
38. Schulze, S., Winter, G., *Lipid extrudates as novel sustained release systems for pharmaceutical proteins*. *Journal of Controlled Release*, 2009. **134**(3): p. 177-185.
39. Brodbeck, K., DesNoyer, J., McHugh, A., *Phase inversion dynamics of PLGA solutions related to drug delivery: Part II. The role of solution thermodynamics and bath-side mass transfer*. *Journal of Controlled Release*, 1999. **62**(3): p. 333-344.

40. Bakhshi, R., Vasheghani-Farahani, E., Mobedi, H., Jamshidi, A., Khakpour, M., *The effect of additives on naltrexone hydrochloride release and solvent removal rate from an injectable in situ forming PLGA implant*. *Polymers for Advanced Technologies*, 2006. **17**(5): p. 354-359.
41. Ji, W., Yang, F., Seyednejad, H., Chen, Z., Hennink, W.E., Anderson, J.M., van den Beucken, J.J.J.P., Jansen, J.A., *Biocompatibility and degradation characteristics of PLGA-based electrospun nanofibrous scaffolds with nanoapatite incorporation*. *Biomaterials*, 2012. **33**(28): p. 6604-6614.
42. Houchin, M.L., Neuenswander, S.A., Topp, E.M., *Effect of excipients on PLGA film degradation and the stability of an incorporated peptide*. *Journal of Controlled Release*, 2007. **117**(3): p. 413-420.
43. Graham, P., Brodbeck, K., McHugh, A., *Phase inversion dynamics of PLGA solutions related to drug delivery*. *Journal of Controlled Release*, 1999. **58**(2): p. 233-245.
44. Pompe, C., *Development of New In-situ Hardening and Bioactivated Composite Materials for Orthopedic Indications*. 2008: Cuvillier Verlag.
45. Wang, L., Venkatraman, S., Kleiner, L., *Drug release from injectable depots: two different in vitro mechanisms*. *Journal of Controlled Release*, 2004. **99**(2): p. 207-216.
46. Rungseevijitprapa, W., Bodmeier, R., *Injectability of biodegradable in situ forming microparticle systems (ISM)*. *European Journal of Pharmaceutical Sciences*, 2009. **36**(4-5): p. 524-531.
47. Siepman, F., Herrmann, S., Winter, G., Siepman, J., *A novel mathematical model quantifying drug release from lipid implants*. *Journal of Controlled Release*, 2008. **128**(3): p. 233-240.
48. Lambert, W.J., Peck, K.D., *Development of an in situ forming biodegradable poly-lactide-coglycolide system for the controlled release of proteins*. *Journal of Controlled Release*, 1995. **33**(1): p. 189-195.
49. Kang, J., Schwendeman, S.P., *Comparison of the effects of Mg(OH)₂ and sucrose on the stability of bovine serum albumin encapsulated in injectable poly (d, l-lactide-co-glycolide) implants*. *Biomaterials*, 2002. **23**(1): p. 239-245.
50. Liu, F.-F., Ji, L., Zhang, L., Dong, X.-Y., Sun, Y., *Molecular basis for polyol-induced protein stability revealed by molecular dynamics simulations*. *The Journal of Chemical Physics*, 2010. **132**: p. 225103.
51. Frokjaer, S., Otzen, D.E., *Protein drug stability: a formulation challenge*. *Nature Reviews Drug Discovery*, 2005. **4**(4): p. 298-306.
52. Shenoy, B., Wang, Y., Shan, W., Margolin, A.L., *Stability of crystalline proteins*. *Biotechnology and Bioengineering*, 2001. **73**(5): p. 358-369.

53. McPherson, A., *Introduction to protein crystallization*. *Methods*, 2004. **34**(3): p. 254-265.
54. Matthews, B.W., *Solvent content of protein crystals*. *Journal of Molecular Biology*, 1968. **33**(2): p. 491-497.

Chapter 7

This chapter is already published in the *Journal of pharmaceutical science*:

Mathaes R*, Hildebrandt C*, Winter G, Engert J, Besheer A 2013. Quality Control of Protein Crystal Suspensions Using Microflow Imaging and Flow Cytometry. *Journal of Pharmaceutical Sciences* 102(10):3860-3866.

*both authors contributed equally

Roman Mathaes has to be thanked for the excellent collaboration and his outstanding knowledge in the field of particle analysis by light obscuration, flow cytometry and micro flow imaging. All work was conducted together. Roman Mathaes guided the analytical methods while all work related to the crystallization was instructed by me. The publication has been written in equal parts.

Acknowledgements

The authors would like to thank Sanofi-Aventis (Frankfurt a. Main, Germany) for the kind gift of Insuman[®] basal.

7 Quality control of protein crystal suspensions using micro flow imaging and flow cytometry

7.1 Abstract

Protein crystallization is an attractive method for protein processing and formulation. However, minor changes in the crystallization set up can lead to changes in the crystal structure or the formation of amorphous protein aggregates, which affect product quality. Only few analytical tools for qualitative and quantitative differentiation between protein crystals and amorphous protein exist. Electron microscopy requires expensive instrumentation, demanding sample preparation and challenging image analysis. Therefore, there is a need to establish other analytical techniques. It was the aim of this study to investigate the capability of light obscuration (LO), micro flow imaging (MFI) and flow cytometry (FC) in differentiating the amorphous and crystalline states of insulin as a relevant model. Qualitative discrimination of the two populations based on particle size was possible using LO. Quantitative determination of amorphous protein and crystals by MFI was challenging due to overlapping size distributions. This problem was overcome by particle analysis based on mean light intensity. Additionally, flow cytometry was applied as a new method for the determination of the quality and quantity of amorphous protein by differences in light scattering. Our results show the potential of MFI and FC for rapid high through-put screening of crystallization conditions and product quality.

Keywords: Insulin, crystallization, analysis, proteins, high-throughput technologies, flow cytometry, micro flow imaging, light obscuration, microscopy

7.2 Introduction

Crystallization is an important protein processing, formulation and delivery tool, which is actively investigated at both the academic and industrial levels. This is because crystallization offers a wide field of application, including controlling/prolonging drug release reducing the viscosity of highly concentrated solutions by using crystal suspension increasing protein stability¹⁻⁴. However, it also offers a number of challenges, including the need to identify protein friendly crystallization processing conditions. Among the problems in protein crystal development is the fact that minor changes in crystallization conditions (changes in temperature, pH, concentration of additives or mechanical treatment) can lead to changes in product quality, such as changes in crystal morphology, size, stability or even precipitation of the protein in an amorphous form^{3,5}. Rapid evaluation of product quality is difficult, as there are still very few analytical methods for the quantitative characterization of protein crystals. The methods are traditionally divided into those that characterize morphology, and those that prove crystallinity. For the assessment of particle morphology and size distribution, microscopy, particularly electron microscopy is the most common method to analyze protein crystals⁶. Despite the strength electron microscopy, it is a time consuming, low-throughput method that requires expensive instrumentation and non-trivial image analysis⁷. On the other hand, X-ray diffraction is commonly utilized to assess crystallinity, but needs perfectly grown crystals larger than 50 μm ⁸. Therapeutic protein crystals should be much smaller due to syringeability issues⁸. Thus, it would be beneficial to establish different analytical methods, which can overcome these drawbacks and allow a simultaneous determination of amorphous impurities and proof crystallinity.

In the current study, we investigated the ability of microflow imaging and flow cytometry to rapidly characterize the quality of protein crystals. For this purpose, we used insulin as a model protein. Crystalline insulin products from different manufacturers have huge market sales and have regulatory approval since decades^{8,9}. Minor changes in insulin's crystallization process are known to change the crystal morphology, and foster amorphous precipitation¹⁰. Accordingly, microflow imaging (MFI) and flow cytometry (FC) were benchmarked against standard methods, namely light obscuration (LO), light microscopy (LM) and scanning electron microscopy (SEM).

7.3 Materials and Methods

7.3.1 Materials

Insulin in crystal form (Insuman[®] basal) was a kind gift from Sanofi-Aventis (Frankfurt a. Main, Germany). Human insulin (Humulin) (100 I.E. injection solution) from Lilly (Gießen, Germany) was purchased from the market. Lysozyme from chicken egg white as lyophilized powder (protein > 90 %, > 40,000 units/mg protein) was purchased from Sigma-Aldrich (Taufkirchen, Germany). Sodium acetate (USP standard, analytical quality) was obtained from Merck (Darmstadt, Germany). Sodium chloride (AnalaR NORMAPUR) was obtained from VWR Prolabo (Leuven, Belgium). Zinc chloride was purchased from Ceasar & Lorenz (Hilden, Germany).

7.3.2 Methods

7.3.2.1 Amorphous precipitation of insulin

Amorphous insulin precipitates were obtained by mixing human insulin with a saturated zinc chloride solution in highly purified water at a 1:2 ratio.

7.3.2.2 Light microscopy

For microscopy a Biozero BZ-8000 microscope from Keyence (Neu-Isenburg, Germany) was used. The application BZ viewer was employed for analysis purposes. The samples were covered with glass cover slides. Examinations were carried out at 400 fold magnification.

7.3.2.3 Scanning electron microscopy (SEM)

A JEOL JSM 6500F scanning electron microscope (Jeol Ltd, Tokyo, Japan) with Inca Software (Oxford instruments, Oxfordshire, UK) was utilized for particle morphology confirmation. Samples were sputtered with carbon after sample fixing with self-adhesive tape on aluminum stubs. Samples were viewed at a magnification of 2000 – 11000 fold.

7.3.2.4 Particle counting (LO)

A PAMAS SVSS-C40 (PAMAS GmbH, Rutesheim, Germany) light blockage system was utilized to size (1 - 200 µm) and count particles. Particle count was classified into 16 different size ranges. The rinsing volume was set to 0.5 mL and the measurement volume to 0.3 mL.

7.3.2.5 Micro flow Imaging (MFI)

Particle size and mean intensity was measured using a micro flow imaging system from Brightwell Inc. (Ottawa, Canada). A constant particle stream was confirmed by utilizing a peristaltic pump. The sample volume was set to 1 mL. Calibration was performed with 5 μm polystyrene particle standards (Thermo Scientific, USA).

7.3.2.6 Flow cytometry (FACS)

A Bioscience flow cytometer FACS Canto II (Bioscience, Franklin Lakes NJ, USA) equipped with forward- and side scattering laser was utilized to analyze protein crystals and amorphous precipitates. Detectors gain and sensitivity were optimized to maximize particle detection. The forward scatter detector (FSC) was set to 231 volts and the side scatter (SSC) detector was set to 191 volts.

7.4 Results

Insuman[®] basal is an approved crystalline insulin product, therefore chosen as a model crystalline protein. Samples containing crystals and amorphous precipitate were produced by mixing suspended insuman basal samples (1 mL) with 2 μ L of precipitated human insulin to simulate product impurities. This set up was employed for all analytical assessments.

Light microscopy and electron microscopy were utilized to characterize particle size and shape. Both methods displayed an oblong shape for the crystals with a Ferret diameter of 8 μ m and 1 μ m in width (Fig. 7-1). Amorphous precipitates appeared as spherical particles sized up to 2 μ m that tend to form clusters. After mixing of crystals and amorphous precipitates, both structures remained unaltered and were easily detectable. However, only qualitative information could be obtained from the images. Quantification was not possible due to clustering of the particles and the transparency of some particles.

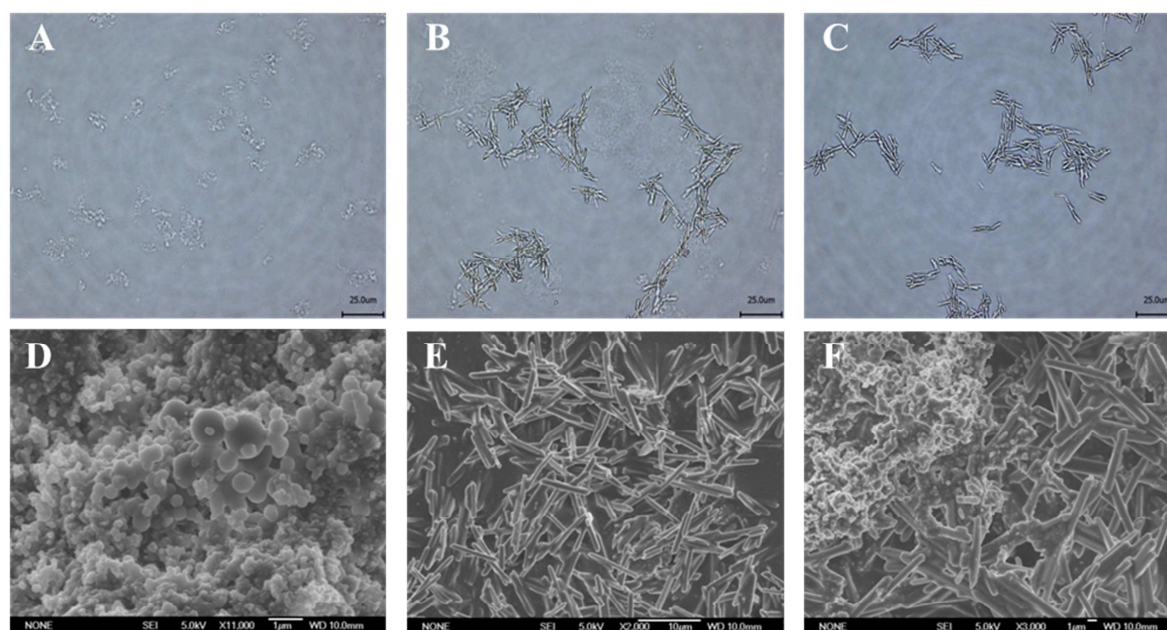


Figure 7-1 Light microscopy images of a) amorphous human insulin b) insuman basal crystals c) mixture of insuman basal crystals and human insulin amorphous precipitates. The scale bar represents 25 μ m. SEM micrographs of d) human insulin amorphous precipitates e) insuman basal crystals f) mixture of insuman basal crystals and human insulin amorphous precipitates

The different samples were analyzed by light obscuration (LO), a standard method for particle characterization. LO measurements of the different protein samples showed that they differ in the mean size (1.64 vs. 10.24) and PDI (2.13 vs 11.66) (Tab. 7-1) for the amorphous and crystalline particles, respectively (Fig. 7-2 a, b). Over 99% of the amorphous aggregates were smaller than 4.1 μm (Fig. 7-2 a) while over 93% of the crystalline insulin were larger than 4.1 μm . Thus, two distinct particle fractions can be discriminated, even in the mixture of both materials (Fig. 7-2 c).

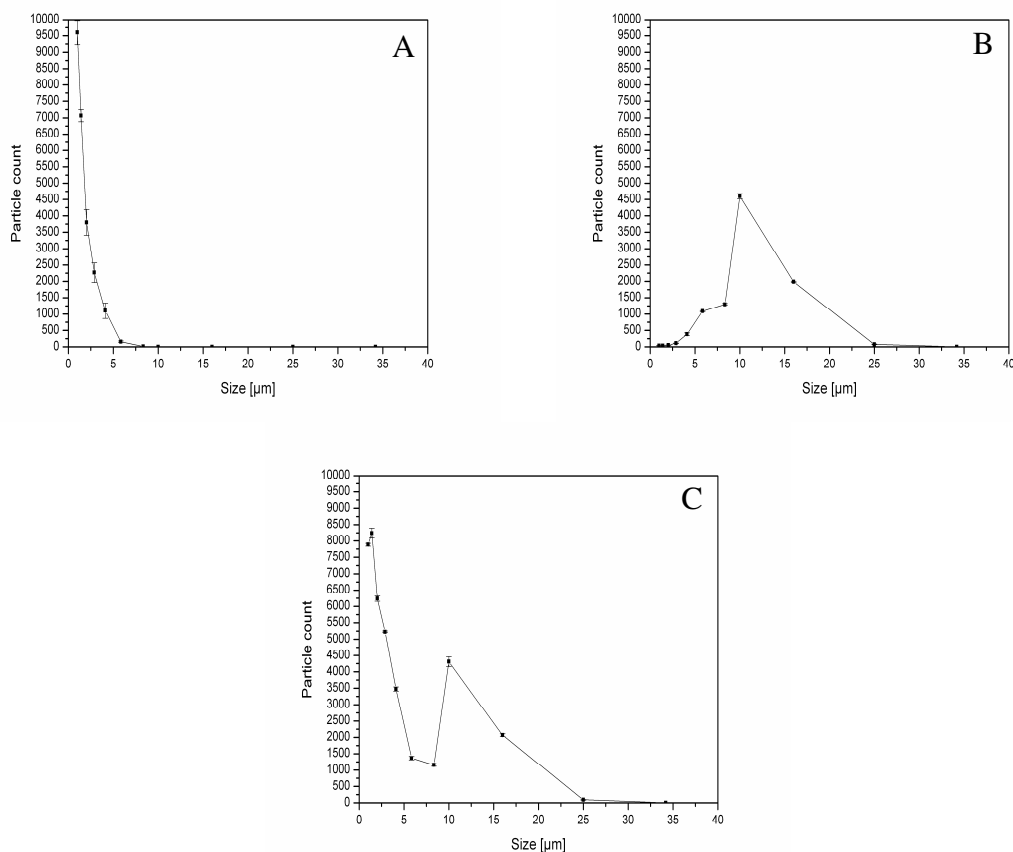


Figure 7-2 shows the SVSS-C PAMAS particle counter (LO) measurement of insulin: a) amorphous insulin aggregates, b) insulin crystals, c) mixture of amorphous insulin aggregates and insulin crystals.

Table 7-1 Mean size and polydispersity index (PDI) of the SVSS-C PAMAS particle counter (LO) of amorphous insulin aggregates and insulin crystals are displayed.

	Mean size (μm)	PDI
amorphous aggregates	1.64	2.13
crystals	10.24	11.66

The image-analysis-based micro flow imaging system detects particles flowing through a capillary, where the particle stream is imaged by a camera. Particle size is calculated by the image analyzing software, which also provides information about particle morphology¹¹. Besides particle count, the mean intensity of the particle is assessed. This feature gives information about the optical density and can be used as a tool to distinguish between aggregates and crystals.

In contrast to LO, assessment of particle size using MFI does not show a clear separation into two different populations. Although the mean size of the aggregates is rather small compared to the crystals, (2.92 vs. 10.63, respectively), the particle distribution is rather broad (PDI = 10.64 for the aggregates and 13.53 for the crystals) (Fig. 7-3), so that the two populations overlap in the mixture (Fig. 7-3 g). Thus, analysis of the mean intensity was used for better discrimination. The standard MFI software offers the possibility to determine the grey scale of the detected objects. The mean intensity is a dimensionless number with low values for dark objects. While amorphous precipitates show a mean intensity of approximately 801 (Fig. 7-3 b), the crystal values are around 644 (Fig. 7-3 e), indicating that the crystals appear darker in the MFI images. Using this method, two separate populations can be easily identified and quantified as shown in Figure 7-3 h.

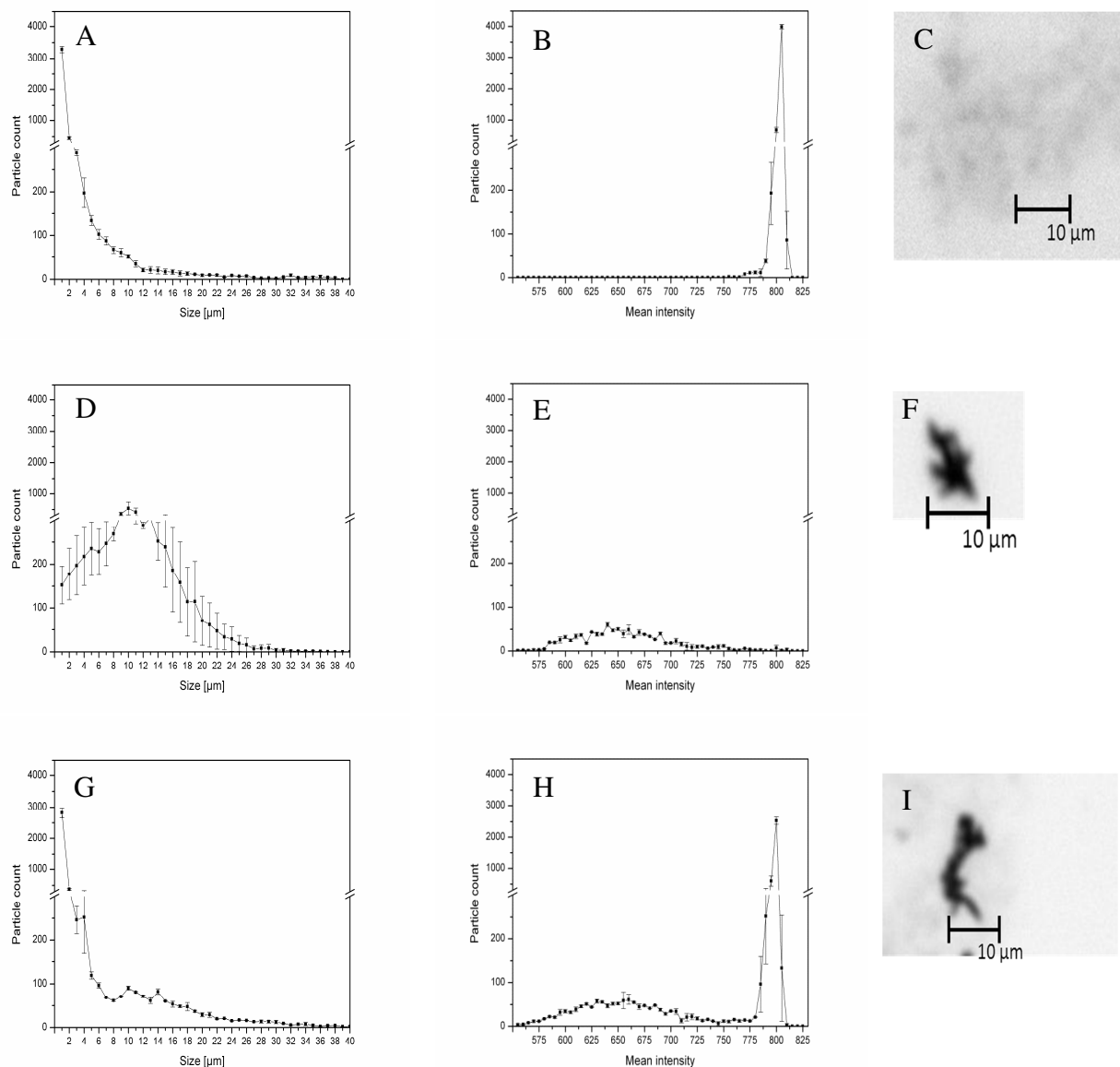


Figure 7-3 MFI size distribution measurements of A amorphous insulin aggregates, D crystalline insulin, G mixture of crystalline and amorphous insulin. Mean intensity measurements of B amorphous insulin aggregates, E crystalline insulin and H mixture of crystalline and amorphous insulin. MFI images of C amorphous insulin aggregates, F crystalline insulin, I mixture of crystalline and amorphous insulin.

Flow cytometry (FACS) was used as an additional tool for the analysis of aggregate and crystalline insulin particles. FACS measurements in the range of 0.5 – 20 μm of protein subvisible particles have already been reported¹². Results show that based on light scattering, one can identify distinct populations in FACS dot plots. While the protein crystals show relatively high side and forward scatter, the aggregates are expressed in a population with lower forward and side scatter (Fig. 7-4), allowing the identification of those impurities in the mixture (Fig. 7-4 c).

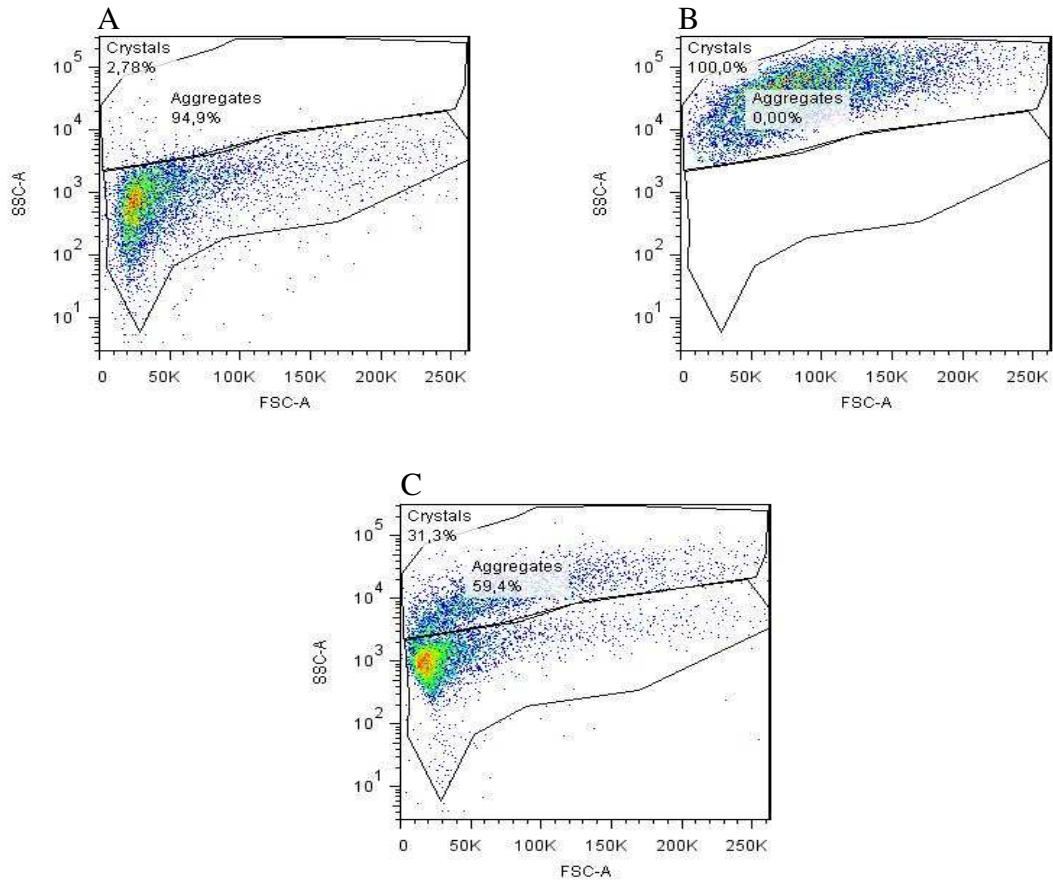


Figure 7-4 FACS dot plots of A amorphous insulin, B insulin crystals, C mixture of amorphous and crystalline insulin.

7.5 Discussion

Product quality of protein crystal suspensions is strongly dependent on reproducible production conditions. Minor changes can lead to precipitation of amorphous protein aggregates. An appropriate analytical tool should allow for the determination of the product's quality and would also quantify the degree of impurities. Microscopic techniques are often used to confirm the crystalline state. However, the accurate quantification of impurity needs the effort of using electron microscopy (including sample preparation) and non-trivial image analysis. In contrast to microscopic observations, the methods investigated in this study allow rapid quantitative analysis of product quality and are amenable for high throughput analysis, thus allowing the screening of protein crystallization conditions or monitoring crystal quality by frequent in process controls. Light obscuration was tested as a method that is commonly used in product particle analysis. This approach can size particles in the amorphous and crystalline state. LO measurements show that amorphous precipitates were in the size range of 1 - 5 μm while crystals show sizes from 4 - 25 μm (Fig. 7-2 a, b). In our experiments, differentiation between crystals and amorphous aggregates was possible based solely on particle size. However, if the particle sizes in other samples were similar or the distributions were broader, a differentiation based solely on size would have not been possible.

Meanwhile, MFI showed a larger size range for the amorphous aggregates (1 - 12 μm) and for the crystals (0.75 μm - 26 μm) compared to LO. Such differences between MFI and LO were reported previously while measuring standard polystyrene particles of different sizes and shapes¹³. One possible reason is the lower accuracy of LO for particles smaller than 2 μm . Due to the broad size distribution; identification of the crystals and amorphous aggregates based on particle size only was not possible, as both groups overlapped. However, using the mean intensity allowed the identification of two separate populations based on the fact that the crystals appeared darker than the amorphous aggregates. Possible reasons for this can be different refractive indices between the crystals and aggregates, or greater thickness (and accordingly greater path length) for the crystals, associated with larger light scattering.

FACS was also used in this study. The use of this tool was described before in context of protein aggregate analysis or contamination with silicone oil in biopharmaceutical products¹²⁻¹⁴. The flow cytometer can measure large particle numbers (up to 5000 parti-

cles/s) in a very short time frame. This single particle measurement method can analyze size ranges from 0.5 to 100 μm . To our best knowledge, this is the first reported use of flow cytometer for differentiation of protein crystals and amorphous precipitates. FACS measurements expressed as dot plots show the aggregates as a population with relatively low forward and side scatter (Fig. 7-4 a). Contrary, the oblong protein crystals show a different scattering pattern dependent on the orientation of the crystal with respect to the incident light beam, with higher forward and side scatters (Fig. 7-4 b). These results allow for qualitative and quantitative and clear discrimination between insulin crystals and amorphous precipitates.

7.6 Conclusion

The presented study shows the potential applicability of micro flow imaging and flow cytometry for the differentiation between crystalline and amorphous protein precipitates and the assessment of crystalline protein quality. MFI and FACS are rapid and reliable methods which provide quantitative statistically valuable information. To the best of our knowledge, MFI and FACS were used for the first time for determination of amorphous impurities in protein crystal suspensions. The presented tools open new possibilities in industrial early phase crystallization screening as well as large scale product quality control of crystalline biopharmaceutical products.

7.7 References

1. Yang, M.X., Shenoy, B., Disttler, M., Patel, R., McGrath, M., Pechenov, S., Margolin, A.L., *Crystalline monoclonal antibodies for subcutaneous delivery*. Proceedings of the National Academy of Sciences of the United States of America, 2003. **100**(12): p. 6934-6939.
2. Pechenov, S., Shenoy, B., Yang, M.X., Basu, S.K., Margolin, A.L., *Injectable controlled release formulations incorporating protein crystals*. Journal of Controlled Release, 2004. **96**(1): p. 149-158.
3. Jen, A., Merkle, H., *Diamonds in the Rough: Protein Crystals from a Formulation Perspective*. Pharmaceutical Research, 2001. **18**(11): p. 1483-1488.
4. Shenoy, B., Wang, Y., Shan, W., Margolin, A.L., *Stability of crystalline proteins*. Biotechnology and Bioengineering, 2001. **73**(5): p. 358-369.
5. Durbin, S., Feher, G., *Protein crystallization*. Annual Review of Physical Chemistry, 1996. **47**(1): p. 171-204.
6. Groves, M.R., Muller, I.B., Kreplin, X., Muller-Dieckmann, J., *A method for the general identification of protein crystals in crystallization experiments using a noncovalent fluorescent dye*. Acta Crystallographica Section D: Biological Crystallography, 2007. **63**(4): p. 526-535.
7. Vermant, J., Yang, H., Fuller, G.G., *Rheoptical determination of aspect ratio and polydispersity of nonspherical particles*. AIChE Journal, 2001. **47**(4): p. 790-798.
8. Basu, S.K., Govardhan, C.P., Jung, C.W., Margolin, A.L., *Protein crystals for the delivery of biopharmaceuticals*. Expert Opinion on Biological Therapy, 2004. **4**(3): p. 301-317.
9. Frokjaer, S., Hovgaard, L., *Pharmaceutical formulation development of peptides and proteins*. 1999: CRC Press.
10. McPherson, A., *Introduction to protein crystallization*. Methods, 2004. **34**(3): p. 254-265.
11. Singh, S.K., Afonina, N., Awwad, M., Bechtold-Peters, K., Blue, J.T., Chou, D., Cromwell, M., Krause, H.-J., Mahler, H.-C., Meyer, B.K., Narhi, L., Nesta, D.P., Spitznagel, T., *An industry perspective on the monitoring of subvisible particles as a quality attribute for protein therapeutics*. Journal of Pharmaceutical Sciences, 2010. **99**(8): p. 3302-3321.
12. Mach, H., Bhambhani, A., Meyer, B.K., Burek, S., Davis, H., Blue, J.T., Evans, R.K., *The use of flow cytometry for the detection of subvisible particles in therapeutic protein formulations*. Journal of Pharmaceutical Sciences, 2011. **100**(5): p. 1671-1678.

13. Mathaes, R., Winter, G., Engert, J., Besheer, A., *Application of different analytical methods for the characterization of non-spherical micro-and nanoparticles*. International Journal of Pharmaceutics, 2013.
14. Ludwig, D.B., Trotter, J.T., Gabrielson, J.P., Carpenter, J.F., Randolph, T.W., *Flow cytometry: A promising technique for the study of silicone oil-induced particulate formation in protein formulations*. Analytical Biochemistry, 2011. **410**(2): p. 191-199.

Chapter 8

8 Final summary of the thesis

mAb crystal suspensions were deemed to offer superior features compared to their solution counterparts in terms of stability and reduced viscosity enabling subcutaneous injection. Slow dissolving and stable mAb crystals would also allow the development of novel sustained release formulations. However, a wide implementation of protein crystal formulations suffers from limitations in finding suitable crystallization conditions. Such conditions would have to be biocompatible and must not result in protein degradation. Until today, a precise prediction of crystallization conditions is extremely complex and hardly to achieve and thus usually ends in extensive screening approaches. However, the opportunity to obtain stable mAb crystals formulations with superior properties compensates the effort and risk of failure.

With this in mind, a project (preliminary study - PhD thesis Stefan Gottschalk at LMU Munich) was conducted with the purpose to find suitable and biocompatible crystallization conditions for two full length IgG₁ antibodies (mAb1 and mAb2) and one antibody fragment. His aim was to develop stable crystal suspensions suitable for subcutaneous injection and for the development of sustained release formulations. Biocompatible large scale crystallization conditions were successfully determined for all three proteins. However, the formulations showed low protein crystal stability against ambient or higher temperatures which was expressed aggregates after crystal dissolution. Furthermore, Stefan Gottschalk studied the effect of vacuum drying on the stability of mAb1 crystals and investigated the applicability of the antibody crystals for sustained release formulations. The results for the drying approach were promising while no advantageous features for mAb crystals as platform for sustained release formulations could be presented.

Consequently, the feasibility of the concept to grow highly stable mAb crystals from biocompatible conditions was still arguable at the end of the preliminary study by Stefan Gottschalk. Therefore, the present study was carried out in order to prove this concept and to stabilize the crystals from the two IgG₁ antibodies by, amongst others, drying and to use the stabilized crystals as platform for sustained release formulations. The cause of aggregate formation and its origin within the crystal suspensions was also to be investigated. The project was started with a proof of concept study with a model protein for that successful crystallization was already described.

In **chapter 2**, the aforementioned model study is presented which describes a procedure to obtain a dry, stable and biologically active crystalline protein material. Lysozyme was chosen as model protein since crystallization has been successfully performed since decades and several crystalline polymorphs were known. This was desired as the stability of protein crystals was deemed to be dependent on the polymorphic form. Three different lysozyme crystals shapes (needle, octagonal, orthorhombic) were obtained in the same crystallization buffer only by variation of the crystallization agent's concentration. The polymorphs were assessed for their handling and manufacturing properties which revealed different features dependent on the crystal shape. Hot-air drying was chosen as drying technique for lysozyme crystals. During the procedure, the crystals were transferred into a volatile organic liquid and were subsequently dried in an inert gas stream of nitrogen by solvent evaporation. Freeze drying was assessed in a comparative study. However, the lysozyme crystals broke during the freeze step by volume expansion of the frozen water. An extensive solvent screening was required to realize the hot-air drying approach. Within this screening only one out of the three crystal polymorphs, the octagonal shape, was found to maintain exposure to certain ethanol and isopropanol concentrations. These solvents were identified to be ideal for the final drying step by solvent evaporation as other volatile organic solvents such as ethyl acetate induced irreversible crystal agglomeration during washing and drying. As final product after drying, a free flowing powder of octagonal lysozyme crystals was obtained which maintained its biological activity which was confirmed by a specific bioactivity assay. SE-HPLC, light obscuration, turbidity and light microscopy analysis allowed to identify isopropanol 95% as best washing liquid with respect to protein and crystal stability. In summary, a model procedure was introduced which highlighted the need for a suitable protein crystal polymorph which provides excellent features for further formulation procedures. A reasonable concept to produce dry and stable protein crystals was demonstrated. This concept should be transferred to mAb1 and mAb2 during the further course of the present study.

Chapter 3 describes the transfer of the successful drying approach for lysozyme to mAb1 and mAb2 crystals. Besides hot-air drying, the implemented (by Stefan Gottschalk) vacuum drying procedure for mAb1 crystals was used. Freeze drying was also assessed which represented a standard drying procedure for biologics. During the present study, the vacuum drying approach could not be successfully reproduced for

mAb1 crystals with respect to protein stability. The washing step with isopropanol 85% was identified to cause aggregate formation. Consequently, an extensive solvent screening like for the lysozyme crystals was performed for mAb1 and mAb2 crystals to identify more suitable washing liquids. The only washing liquid which met all requirements (crystal integrity maintained, volatile, etc.) was ethyl acetate. However, extensive washing with this liquid resulted in irreversible crystal agglomeration. A transfer of the successful drying procedure for lysozyme crystals to the mAb crystals was therefore not achieved. Finally, crystal drying by freeze drying resulted in crystal destruction during the freezing step by volume expansion of the frozen water.

Chapter 4 describes different screening approaches for mAb1 and mAb2 crystal polymorphs. Crystallization of both mAbs resulted in constant aggregate formation over time as already demonstrated by the preliminary study from Stefan Gottschalk. The unfavorable needle-like crystal morphology was deemed to provide small numbers of protein-protein interactions and thus small protein stabilization. Furthermore, one key factor during the lysozyme study was a successful screening for crystal polymorphs. For mAb1 and mAb2 crystals no polymorphs have been described so far. Several strategies were followed to grow new morphologies with enhanced features. The implementation of agitation, different crystallization temperatures, pH shifts, high hydrostatic pressure and additives was tested. However, the possibilities to alter the crystallization conditions, especially the buffer as strongest tool, were restricted to only small changes in order to maintain their biocompatibility. Unfortunately, no new crystal polymorphs could be found. Small changes in the crystal shapes were not stable under ambient conditions or were associated to aggregate formation.

High hydrostatic pressure was further tested for its feature to dissociate aggregates within mAb1 and mAb2 crystal suspensions. It could be shown that mAb aggregates can be dissociated at low pressure levels around 150 MPa. Consequently, this feature deserves attention for further studies as reduction of aggregate contents of mAb formulations was presented – with best knowledge – for the first time. Further research is required to improve complete understanding of this approach towards mAb crystallization and stability.

One essential factor to stabilize protein crystal formulations would be the knowledge about the underlying instability mechanisms. Therefore, in **chapter 5**, a study was per-

formed to investigate the cause for aggregate formation detected for mAb1 and mAb2 crystals. A large set of analytical tools which comprised among others LC-MS, SE-HPLC, light obscuration, IEF, SDS-PAGE, nephelometry and FACS was used for analysis. Two different pathways of aggregate formation were identified for the two antibodies. For mAb2, deamination was induced by the high phosphate salt concentration and low pH value of the mAb2 crystallization system. Oxidative protein degradation processes caused by PEG impurities (peroxides, formaldehyde) were identified for mAb1. A clear dependency of the level of aggregate formation on peroxides and formaldehyde was shown. A minimum level of both compounds is vital to start the crystallization. The crystallization is accompanied by aggregate formation since both, precipitation and aggregate formation, are dependent on formaldehyde induced protein linkage and oxidation. Furthermore, labelling studies enabled to localize the aggregate formation in mAb1 formulations. The results revealed that the aggregates were foremost formed in the supernatant and subsequently attached/incorporated into the crystal lattice. The crystalline state is deemed to stabilize the protein even within the harsh crystallization conditions. This was confirmed by expansion of the analytics to the in the sub-micron range more sensitive FACS device which revealed higher aggregate levels in the supernatant. A similar mechanism is assumed for mAb2. Consequently, an intrinsic protein instability in the crystalline state cannot be stated. Successful protein crystallization would consequently be dependent on suitable crystallization conditions which would allow to grow protein crystals and to maintain the protein integrity in the supernatant. This prerequisite represents the fundamental challenge during protein crystallization.

Chapter 6 addressed the question whether protein crystals are beneficial for the formulation of depots or not. In situ forming depot formulations which consisted of PLGA 502H or 755S (mAb1, mAb2), SAIB (mAb1, mAb2, lysozyme) and solid depot forms such as lipid implants (mAb1) were developed and tested for crystalline and amorphous protein. To enhance protein drug release, additives such as the pore forming sucrose or $Mg(OH)_2$ and Na_2CO_3 as pH modifiers were tested. The study was completed by investigation of the phase inversion dynamics of the PLGA depot formulations and the assessment of syringeability and depot degradation of the PLGA and SAIB depot formulations.

For the *in situ* forming depot formulations from PLGA and SAIB, a new release method was introduced. The formulation was placed on a mesh in the middle and above the bottom of the release container to enable unhindered drug diffusion to all sides. The validity of this set-up was confirmed by a higher protein release compared to depots placed on the bottom of the release container.

During the study, no superior drug release profiles of mAb crystals were found for the formulations tested. Amorphous mAb material showed superior release kinetics and higher stability towards the compounds used for depot formulation. Introduction of additives showed small effects. One mAb2 crystal formulation (30% (w/w) PLGA 502H and magnesium hydroxide) displayed enhanced release profiles compared to its amorphous counterpart.

Phase inversion studies showed detrimental results towards the literature. The slower hardened PLGA 502H showed a higher initial drug burst release. Regarding syringeability, exclusively low PLGA concentrations were found to be injectable with acceptable injection forces (10 N). Consequently, a compromise between an applicable polymer concentration enabling a desired protein drug release and the required injection force which allows for a convenient application has to be found.

The release kinetics as well as syringeability properties of SAIB were superior compared to PLGA formulations. However, the choice of a suitable carrier solvent which preserves the protein drug integrity remains crucial. mAb1 and mAb2 showed instability in the solvents used for the SAIB depot formulations (ethyl acetate, isopropanol 100%) and thus affected release profiles. Amorphous mAb1 and mAb2 showed superior release kinetics.

Vacuum dried mAb1 was used for lipid implant depot formulations and compared to amorphous mAb1. Again, the crystals did not show enhanced sustained release profiles compared to the amorphous counterpart. The amorphous mAb1 showed an optimal, constant release profile without any burst.

Notably, studies with SAIB based depot formulation which contained hot air dried lysozyme crystals, undried lysozyme crystals and freeze-dried lysozyme revealed enhanced release profiles for the dried crystalline material. The general feasibility of protein crystals to offer superior features for depot formulations was demonstrated. However, the

aforementioned studies with mAb1 and mAb2 suggested that a transfer of the results for lysozyme crystals to crystals of other proteins remains challenging.

In **chapter 7**, novel analytical approaches to distinguish between amorphous and crystalline precipitates are presented. In order to detect and quantify amorphous impurities in insulin crystal suspensions, traditional techniques like microscopy and light obscuration were compared to new analytical tools such as micro flow imaging (MFI) and flow cytometry (FACS). Superior performances were observed for the new techniques which enabled an easy and high throughput detection and quantification of amorphous aggregates besides insulin crystals. MFI and FACS were used for the first time for determination of amorphous impurities in protein crystal suspensions. These techniques allow for analysis of impurities in protein crystal suspension without microscopic examination.

In summary, the present study demonstrated that mAb1 and mAb2 crystals do not exhibit superior features compared to their amorphous and solution counterparts. However, the (at the beginning of the study) hypothesized destabilizing properties of mAb crystallization and the crystalline state could be disproved. The aggregates detected after dissolution of the mAb crystals originated in the supernatant and not from the crystals. In contrast, superior protein crystal features were shown for the model protein lysozyme for that different crystal polymorphs with different properties were presented. The best polymorph could be dried to a free flowing powder and allowed development of a depot formulation with enhanced release kinetics compared to depots containing amorphous lysozyme. This demonstrated that the concept to grow highly stable protein crystals with beneficial features remains realizable. Therefore, future studies should focus on the definition of suitable crystallization conditions from that crystal polymorphs with desired features can be grown. Furthermore, as crystallization takes place until a dynamic equilibrium is reached the crystallization conditions should not induce protein degradation in the supernatant. Crystallization conditions for therapeutic proteins are limited to biocompatible ones and thus crystals with superior features compared to liquid or amorphous states would not be reached in each case. The feasibility of the concept to grow highly stable mAb crystals from biocompatible conditions has to be proven for each single molecule.

PUBLICATIONS ASSOCIATED WITH THIS THESES

Research articles

R. Mathaes, C. Hildebrandt, G. Winter, J. Engert, A. Besheer. Quality Control of Protein Crystal Suspensions Using Microflow Imaging and Flow Cytometry. *Journal of Pharmaceutical Sciences*. 2013.

Christian Hildebrandt, Rainer Saedler, Gerhard Winter. Case study: From protein bulk crystallization towards dry protein products. *To be submitted*

Christian Hildebrandt, Lea Joos, Rainer Saedler, Gerhard Winter. The “new PEG dilemma”: PEG impurities and their paradox role in mAb crystallization. *To be submitted*

Christian Hildebrandt, Roman Mathaes, Rainer Saedler, Gerhard Winter. Extent and origin of aggregate formation in a PEG containing antibody crystal suspensions. *In preparation*

Poster presentations

G. Sax, C. Hildebrandt, W. Tian, S. Schulze, G. Winter. Delivery of drug proteins from lipid based implants, Forum Life Science, Munich, Germany, March 2011.

C. Hildebrandt, G. Winter. Lysozyme crystals of various morphology show different mechanical stability and solubility in organic solvents 8th World meeting on Pharmaceutics, Biopharmaceutics and Pharmaceutical Technology Istanbul, Turkey, March 2012.

C. Hildebrandt, G. Winter. Bulk drying of protein (lysozyme) crystals with inert drying gas 8th World meeting on Pharmaceutics, Biopharmaceutics and Pharmaceutical Technology Istanbul, Turkey, March 2012.